



# South African *Journal of Science*

volume 118  
*number 1/2*

Alignment of wetland  
restoration and alien control

Bibliometric analysis of socio-  
hydrology research in Africa

A potentially affordable,  
simple, and sustainable  
technology for point-of-use  
water treatment

WHO COP26 special report  
on climate change and health

Myths about data and  
software access in the  
Data and Cloud Policy



eISSN: 1996-7489

#### EDITOR-IN-CHIEF

Leslie Swartz   
Academy of Science of South Africa

#### MANAGING EDITOR

Linda Fick   
Academy of Science of South Africa


#### ONLINE PUBLISHING SYSTEMS ADMINISTRATOR

Nadia Grobler   
Academy of Science of South Africa

#### MARKETING & COMMUNICATION

Henriette Wagener  
Academy of Science of South Africa

#### ASSOCIATE EDITORS

Margaret Avery   
Cenozoic Studies, Iziko Museums of  
South Africa, South Africa

Priscilla Baker   
Department of Chemistry, University  
of the Western Cape, South Africa

Pascal Bessong   
HIV/AIDS & Global Health Research  
Programme, University of Venda,  
South Africa

Chrissie Boughey   
Centre for Postgraduate Studies,  
Rhodes University, South Africa


Catherine Burns   
Adler Museum of Medicine, University  
of the Witwatersrand, South Africa

Teresa Coutinho   
Department of Microbiology and  
Plant Pathology, University of Pretoria,  
South Africa

Jennifer Fitchett   
School of Geography, Archaeology  
and Environmental Studies, University  
of the Witwatersrand, South Africa

Michael Inggs   
Department of Electrical Engineering,  
University of Cape Town, South Africa

Bettine van Vuuren   
Department of Zoology, Centre  
for Ecological Genomics and  
Wildlife Conservation, University of  
Johannesburg, South Africa

Amanda Weltman   
Department of Mathematics and  
Applied Mathematics, University of  
Cape Town, South Africa

#### ASSOCIATE EDITOR

##### MENTEES

Jemma Finch   
School of Agricultural, Earth and  
Environmental Sciences, University of  
KwaZulu-Natal, South Africa

Amanda-Lee Manicum   
Department of Chemistry, Tshwane  
University of Technology, South Africa

Sandiswa Mbewana   
Department of Molecular and Cell  
Biology, University of Cape Town,  
South Africa

Sydney Moyo   
Department of Zoology and  
Entomology, Rhodes University,  
South Africa

#### EDITORIAL ADVISORY BOARD

Stephanie Burton   
Professor of Biochemistry and  
Professor at Future Africa, University  
of Pretoria, South Africa

Felix Dakora   
Department of Chemistry, Tshwane  
University of Technology, South Africa

#### Leader

African science and global opinions

Leslie Swartz ..... 1

#### Profile

Fulufhelo Nelwamondo: NRF's idealistic new leader

Michael Cherry ..... 2

#### Book Reviews

The tail wagging the dog: Tomaselli's *Contemporary Campus Life* and why we  
are overdue for introspection as academics

Elnerie W.J. Greeff ..... 4

Are South African universities disengaged from civic duty?

Jonathan Jansen ..... 5

#### Scientific Correspondence

Morphometric ('log sem') analysis of anatomical measurements of Galápagos  
finches (*Geospiza*), chimpanzees (*Pan*) and Plio-Pleistocene hominins  
(*Paranthropus*, *Australopithecus* and early *Homo*)

J. Francis Thackeray ..... 6

#### Perspective

NRF ratings and *h*-index for engineers: Are we missing the point?

Charles J. MacRobert, Theo J. Stergianos ..... 9

#### Commentaries

Driving openness – the myths about data and software access in the Data and  
Cloud Policy

Cobus Jooste ..... 12

COVID-19 recovery and the health argument for climate action. Commentary on  
the WHO COP26 special report on climate change and health

Monika dos Santos ..... 16

The SABAP2 legacy: A review of the history and use of data generated by a  
long-running citizen science project

Alan T.K. Lee, Michael Brooks, Les G. Underhill ..... 19



## Saul Dubow

Smuts Professor of Commonwealth History, University of Cambridge, UK

## Pumla Gobodo-Madikizela

Trauma Studies in Historical Trauma and Transformation, Stellenbosch University, South Africa

## Robert Morrell

School of Education, University of Cape Town, South Africa

## Catherine Ngila

Deputy Vice Chancellor – Academic Affairs, Riara University, Nairobi, Kenya

## Lungiswa Nkonki

Department of Global Health, Stellenbosch University, South Africa

## Daya Reddy

South African Research Chair – Computational Mechanics, University of Cape Town, South Africa

## Brigitte Senut

Natural History Museum, Paris, France

## Benjamin Smith

Centre for Rock Art Research and Management, University of Western Australia, Perth, Australia

## Himla Soodyall

Academy of Science of South Africa, South Africa

## Lyn Wadley

School of Geography, Archaeology and Environmental Studies, University of the Witwatersrand, South Africa

## Cherryl Walker

Department of Sociology and Social Anthropology, Stellenbosch University, South Africa

## Published by

the Academy of Science of South Africa ([www.assaf.org.za](http://www.assaf.org.za)) with financial assistance from the Department of Science & Innovation.

## Design and layout

SunBonani Media  
T: 051 444 2552  
E: [publish@sunbonani.co.za](mailto:publish@sunbonani.co.za)

## Correspondence and enquiries

[sajs@assaf.org.za](mailto:sajs@assaf.org.za)

## Copyright

All articles are published under a Creative Commons Attribution Licence. Copyright is retained by the authors.

## Disclaimer

The publisher and editors accept no responsibility for statements made by the authors.

## Submissions

Submissions should be made at [www.sajs.co.za](http://www.sajs.co.za)

## Research Articles

The alignment of projects dealing with wetland restoration and alien control: A challenge for conservation management in South Africa

*Erwin J.J. Sieben, Şerban Procheş, Aluoneswi C. Mashau, Moleseng C. Moshobane* ..... 23

Scope, trends and opportunities for socio-hydrology research in Africa: A bibliometric analysis

*Christina M. Botai, Joel O. Botai, Miriam Murambadoro, Nosipho N. Zwane, Abiodun M. Adeola, Jaco P. de Wit, Omolola M. Adisa* ..... 30

Visible light photodegradation of methyl orange and *Escherichia coli* O157:H7 in wastewater

*Sibongile M. Malunga, Nhamo Chaukura, Chiedza I. Mbiriri, Willis Gwenzi, Mambo Moyo, Alex T. Kuvarega* ..... 38

Phytochemicals and in silico investigations of Sudanese roselle

*Arwa El-Naeem, Sahar Abdalla, Ibrahim Ahmed, Gihan Alhassan* ..... 49

Characterisation of ZnO nanoparticles prepared using aqueous leaf extracts of *Chromolaena odorata* (L.) and *Manihot esculenta* (Crantz)

*Enobong R. Essien, Violette N. Atasié, Davies O. Nwude, Ezekiel Adekolurejo, Felicia T. Owoeye* ..... 56

Antiviral activity of chitosan nanoparticles for controlling plant-infecting viruses

*Ahmed Y. El Gamal, Mahmoud M. Atia, Tarek El Sayed, Mohamed I. Abou-Zaid, Mohamed R. Tohamy* ..... 64

Selection for resistance to cassava mosaic disease in African cassava germplasm using single nucleotide polymorphism markers

*Esperance D. Codjia, Bunmi Olasanmi, Paterne A. Agre, Ruth Uwugiaren, Adenike D. Ige, Ismail Y. Rabbi* ..... 73

Selected parasites of silver kob (*Argyrosomus inodorus*) (Actinopterygii: Sciaenidae) from northern Namibia

*Annette M. Amakali, Ali Halajian, Margit R. Wilhelm, Martin Tjipute, Richard Heckmann, Wilmiën Luus-Powell* ..... 80

The use of Z-scores to facilitate morphometric comparisons between African Plio-Pleistocene hominin fossils: An example of method

*J. Francis Thackeray, Ottmar Kullmer* ..... 91

## Research Letter

Possible Pleistocene hominin tracks from South Africa's west coast

*Charles W. Helm, Hayley C. Cawthra, Jan C. De Vynck, Rudolf Hattingh, Martin G. Lockley* ..... 96

## Corrigenda

Corrigendum: Aerial map demonstrates erosional patterns and changing topography at Isimila, Tanzania

*Kersten Bergstrom, Austin B. Lawrence, Alex J. Pelissero, Lauren J. Hammond, Eliwasa Maro, Henry T. Bunn, Charles M. Musiba* ..... 99

Corrigendum: Evaluating South African Weather Service information on Idai tropical cyclone and KwaZulu-Natal flood events

*Mary-Jane M. Bopape, Ezekiel Sebege, Thando Ndarana, Bathobile Maseko, Masindi Netshilema, Morne Gijben, Stephanie Landman, Elelwani Phaduli, Gift Rambuwani, Louis van Hemert, Musa Mkhwanazi* ..... 100

## Cover caption

Flower of *Hibiscus sabdariffa* L. The hibiscus is rich in phytochemicals, particularly polyphenols and anthocyanins. El-Naeem and colleagues investigated xanthine oxidase inhibition by isolated anthocyanins for development of potential novel drugs to treat diseases such as gout and hypertension.



# African science and global opinions

In late 2021, African scientists discovered a new variant of COVID-19. We should be proud and grateful, as should and is the world, to our scientists for identifying the latest variant of COVID and for choosing, correctly, to communicate this scientific information rapidly. But this important discovery led to global action not based on science. Wealthier countries closed their doors to our country and continent, implementing a travel ban. This reaction was despite the views of scientists in South Africa and recommendations from the World Health Organization. Since then, there have been other travel bans, other mistakes globally in managing the global pandemic.

This travel ban, despite evidence of spread of the Omicron variant in countries which selectively closed their borders, had potentially devastating implications for health and well-being on our continent. African scientists were exemplary in continuing to explore and report on the variant. The travel ban, which was not evidence- or science-based, has correctly been described by a group of eminent African scientists as ‘political theatre’<sup>1</sup>, and the health consequences for Africans, as these authors pointed out, had the potential to be grave, given the economic implications of travel bans. The irony of this is clear: as Africa helped in all likelihood to make the world more healthy, many in the world have helped to make Africans more sick.

What does this mean for South African and African science? Perhaps the saddest (and most obvious) observation is that the kind of reaction we saw is nothing new. We witnessed the reinscription – with potentially grave economic, personal, and health consequences – of dangerous assumptions about Africa, contagion, dirt and pollution. As our country and continent led the world in science and science communication, we again bore the brunt of the long and ongoing tail of dangerous, colonial, and non-evidence-based views. The view of Africa as a source, not of knowledge, but of pestilence and shame was a feature of much writing about our continent by social scientists and others going back centuries. Despite clear evidence of the contributions of Africa and Africans to science and knowledge<sup>2-4</sup>, Africa was once again being viewed strongly through the lens of pathology.

In South Africa, much of the focus in issues of transformation of the sciences, especially in the post-#FeesMustFall era, has been on inequality in South Africa itself, and questions of access for people formerly excluded from higher education.<sup>5-8</sup> This is appropriate and necessary, and theorists have been careful to link current issues to colonial and apartheid history. The contradictions around the early identification of the Omicron variant, however, refocus our attention on ongoing global politics and its influence on contemporary scientific practice and perceptions of science. A key feature of how African science continues to be viewed is through the lens of ‘capacity building’. There is nothing wrong with capacity building, and it is very often to be welcomed; but all too easily, talk about ‘building capacity’ reinforces stereotypes about inferior quality African science, and dependency of African scientists on the greater expertise of those in the Global North.<sup>9,10</sup> This is despite the fact that African scientists lead the world in a number of areas including HIV/Aids and ecology/conservation biology, to name just two fields.<sup>11,12</sup> It is crucial for South African science that unhelpful and inaccurate stereotypes be questioned and resisted, and that evidence is brought to bear in all discussions about what African science is and does. Unfortunately, the Omicron variant scandal shows once again how powerful stereotypes may outweigh the facts.

The *South African Journal of Science* shares with our contributors and our readership a responsibility to insist on evidence-based opinion and argument, to face difficulties and gaps where they do occur, and to attempt to rectify these, but also to question and rebut incorrect stereotypes. Within the field of studies related to COVID-19, for example,

we are planning later this year to publish a special issue on the topic, with the subheading ‘How to do social distancing in a shack?’ This focus on interdisciplinary work which takes due account of the conditions under which most people in the world live is not, we suggest, an add-on to global science. We hope that the special issue will show that considering context, placing science within the realities of the majority world, and understanding the global politics of inequality and exclusion, is at the cutting edge of good science. If we are to be decolonial in our scientific practices, we must always be clear on what the shortcomings are of what we do, but we must also be clear that Africa, and African science, need to be evaluated on their own contextual merits. Political theatre<sup>1</sup> is powerful, but it is not science or science policy.

## References

- Mendelson M, Venter F, Moshabela M, Gray G, Blumberg L, De Oliveira T, et al. The political theatre of the UK’s travel ban on South Africa. *Lancet*. 2021;398:2211–2213. [https://doi.org/10.1016/S0140-6736\(21\)02752-5](https://doi.org/10.1016/S0140-6736(21)02752-5)
- Beinart W, Dubow S. *The scientific imagination in South Africa: 1700 to the present*. Cambridge, UK: Cambridge University Press; 2021. <https://doi.org/10.1017/9781108938198>
- Gevers W. A well-told history of science in South Africa. *S Afr J Sci*. 2021;117(9/10), Art. #11967. <https://doi.org/10.17159/sajs.2021/11967>
- Ali W, Elbadawy A. Research output of the top 10 African countries : An analytical study. *COLLNET J Sci Inf Manag*. 2021;15(1):9–25. <https://doi.org/10.1080/09737766.2021.1934181>
- CMoloi K, Makgoba MW, Ogutu Miruka C. (De)constructing the #FeesMustFall campaign in South African higher education. *Contemp Educ Dialogue*. 2017;14(2):211–223. <https://doi.org/10.1177/0973184917716999>
- Trivangasi HM, Rapanyane MB, Mugambiwa SS. The toxicity of welfare state: Discourse analysis of #FeesMustFall movement in South Africa. *Afr J Peace Conflict Stud (formerly Ubuntu J Conflict Soc Transform)*. 2021;10(2):7–29. [https://hdl.handle.net/10520/ejc-aa\\_ubuntu1-v10-n2-a1](https://hdl.handle.net/10520/ejc-aa_ubuntu1-v10-n2-a1)
- Costandius E, Nell I, Alexander N, Mckay M, Blackie M, Malgas R, et al. #FeesMustFall and decolonising the curriculum: Stellenbosch University students’ and lecturers’ reactions. *S Afr J High Educ*. 2018;32(2):65–85. <https://doi.org/10.20853/32-2-2435>
- Lewis D, Hendricks CM. Epistemic ruptures in South African standpoint knowledge-making: Academic feminism and the #FeesMustFall movement. *Gender Questions*. 2017;4(1):18. <https://doi.org/10.25159/2412-8457/2920>
- Mormina M, Istratii R. ‘Capacity for what? Capacity for whom?’ A decolonial deconstruction of research capacity development practices in the Global South and a proposal for a value-centred approach [version 1; peer review: 2 approved]. *Wellcome Open Res*. 2021;6:129. <https://doi.org/10.12688/wellcomeopenres.16850.1>
- Swartz L. Building capacity or enforcing normalcy? Engaging with disability scholarship in Africa. *Qual Res Psychol*. 2018;15(1):116–130. <https://doi.org/10.1080/14780887.2017.1416801>
- Hodes R, Morrell R. Incursions from the epicentre: Southern theory, social science, and the global HIV research domain. *Afr J AIDS Res*. 2018;17(1):22–31. <https://doi.org/10.2989/16085906.2017.1377267>
- Asase A, Mzumara-Gawa TI, Owino JO, Peterson AT, Saupe E. Replacing “parachute science” with “global science” in ecology and conservation biology. *Conserv Sci Pract*. 2021; e517. <https://doi.org/10.1111/csp2.517>

## HOW TO CITE:

Swartz L. African science and global opinions. *S Afr J Sci*. 2022;118(1/2), Art. #13062. <https://doi.org/10.17159/sajs.2022/13062>





Check for updates

**AUTHOR:**

Michael Cherry<sup>1</sup>

**AFFILIATION:**

<sup>1</sup>Department of Botany and Zoology, Stellenbosch University, Stellenbosch, South Africa

**CORRESPONDENCE TO:**

Michael Cherry

**EMAIL:**

MIC@sun.ac.za

**HOW TO CITE:**

Cherry M. Fulufhelo Nelwamondo: NRF's idealistic new leader. *S Afr J Sci.* 2022;118(1/2), Art. #12965. <https://doi.org/10.17159/sajs.2022/12965>

**ARTICLE INCLUDES:**

- Peer review
- Supplementary material

**PUBLISHED:**

27 January 2022

# Fulufhelo Nelwamondo: NRF's idealistic new leader

I am slightly apprehensive about my online interview with the new Chief Executive Officer of the South African National Research Foundation (NRF), Fulufhelo Nelwamondo. On 1 April 2021 he took up office at the age of 38 – the youngest person to head the NRF.

I am apprehensive because it has taken me six months of badgering the NRF media office to set up the interview, which was postponed in July on the morning it was due to take place. I see this as symptomatic of a level of dysfunctionality that I, and many of my colleagues, have come to expect of the NRF, which has been under rudderless leadership since the end of Khotso Mokhele's 10-year term in 2006. Turning the Foundation around is going to be no mean task.

But to my pleasant surprise, Nelwamondo appears bustling with energy, despite offering no explanation for his apparent lack of enthusiasm for becoming acquainted with the readers of the SAJS.

Like a disproportionately high number of prominent South Africans, Nelwamondo hails from Venda in the Limpopo Province, where he attended the Mbilwi Senior Secondary School. He registered for an electrical engineering degree at Wits in the first year of the millennium, and stayed on to complete a doctorate under the supervision of Tshilidzi Marwala, now Rector of the University of Johannesburg.

From Wits he spent a year at Harvard as a postdoctoral fellow, before returning to the CSIR, where he worked for just under 12 years, ending up in charge of 'Next Generation Enterprises and Institutions'. This involves reducing financial wastage in government; lowering access barriers to government services, thereby contributing to increased transparency and trust in public institutions; and improving the ability of government to effectively plan and monitor programmes.

So essentially a Fourth Industrial Revolution man, and a high-flyer to boot, but his experience does not lie in the agency funding sector. Does he think this matters?

He doesn't think it does, as he says there are lots of similarities between the two organizations. Both work by using their parliamentary grant to fund core infrastructure and functions; and then use this to leverage additional funding. So he has lots of experience in leveraging funding.

The NRF, for example, has a budget of about ZAR4.5 billion, only 20% of which is derived from its parliamentary grant. And its budget has been shrinking for several years, according to Nelwamondo, before the COVID crisis of 2020. So he defends the controversial action of his predecessor, Molapo Qhobela, of discontinuing most of the incentive funding which was linked to NRF rating from 2018 onwards: 'It was unsustainable because there was no money anymore.'

I was personally unsurprised by this announcement, but I thought it was implemented inappropriately: like many researchers, I was left high and dry as it occurred in the middle of my funding cycle. But he reminds me that funding is only one component of the Foundation's four-pronged mandate. They also run the national facilities, which undertake their own research.

And they are responsible for funding bursaries to postgraduate students. These had increased, he said – the number of students funded peaked at 13 599 in 2017. But in the STEM arena at least, how do you fund postgraduate students without running expenses? Not something to which Qhobela had applied his mind, it appears.

Controversially, his predecessor also decided to abolish grant-holder bursaries with effect from 2020. This means that grant awardees have to wait until the next cycle of bursary awards in order to enrol postgrads, as the two cycles are out of sync. And their preferred candidates have to apply for postgraduate funding in their own right, for which they may or may not be successful.

Again, this was not Nelwamondo's decision, but he justifies it on the grounds that it was intended to improve transformation. In the last year of the old system (2019), 76% of postgraduates funded by the NRF were black South Africans (coloured, Indian or African, to use apartheid terms); in the first year of the new system (2020), this figure has risen to 79%. White students, who comprise 22% of bachelor's graduates nationally, now comprise 14% of NRF postgraduate bursary-holders (in 2019 they comprised 15%). The remaining 7% are foreign – down from 9% in 2019, primarily reflecting a decrease in the number of doctoral students from other African countries being funded.

The NRF could not provide data for 2021, but on the face of it, is this policy achieving its transformation goal? Nelwamondo admits that he is not sure: 'We need to look at it over the next two years and say if it's not working, let's change it. If it is working, let's see what needs to be done to improve it.'

Postgraduate student training is on the face of it an area in which his predecessor had achieved at least a modicum of success: numbers of honours students supported by the NRF increased to a peak of 4930 in 2016; and those of master's and doctoral students to 5444 and 3418, respectively, both in 2017. But by 2020, honours numbers were down 13%, master's by 21%, and doctoral by 16%. Nelwamondo says the decline in 2020, at least, reflects the fact that students are better funded under the new system.

Some of the research-based universities have stepped in to bridge the gap by increasing postgraduate bursary support. But no-one appears to have come up with alternative funding for student running expenses to compensate for the decline in incentive funding from 2018 onwards.

At the time the NRF pledged to invest the savings that would 'accrue through the revised programme model in other NRF funding interventions to benefit researchers', but it has been unclear to researchers how exactly this was done. In the same year (2018) that incentive funding was radically downscaled, it slashed the budget for its competitive support for rated researchers by 14%, and that for unrated researchers by 7%; and the number of postgraduate bursaries began to decline.

Then came COVID-19. Then NRF suffered a cut of ZAR763 million (17%) in 2020, according to Nelwamondo. In 2021, previous funding levels were restored, but because most of the NRF's programmes are multi-year in duration, the effect has been significant.

All in all, an unenviable legacy for anyone to inherit. Does he have a vision for the NRF, or a particular way in which he would like to take the Foundation forward?

Well, he'd like to focus on the innovation aspects of the research enterprise, so that the economy can grow. I get a jaded feeling – I've been hearing this since I started writing regularly about South African science in late 1989. At least since the advent of democracy, it has been a stated objective of government that research should drive innovation. But the Elon Musks and the Patrick Soon-Shiongs have fled for greener pastures.

He concurs, tempering this idealism with a sense of realism: 'We are very good at plans as South Africans. You know we fail almost at all times at execution.'

How might he succeed with his plans where others have failed then? He says that part of the solution lies in having the data at your fingertips to make decisions which can accurately predict the impact of research. And this is an area in which he has experience.



**Fulufhelo Nelwamondo, CEO of the National Research Foundation**

He also professes to have lots of energy and asserts that he will be bold in making the changes he thinks the Foundation requires. 'I think we're all scared of change. That's human nature', he says.

I confess that I am slightly disarmed by his idealism and his energy, and rather sorry that we have met only online.

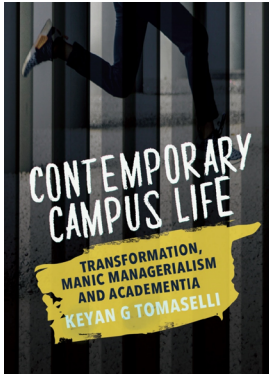




Check for updates

**BOOK TITLE:**

Contemporary campus life: Transformation, manic managerialism and academentia



**AUTHOR:**

Keyan G. Tomaselli

**ISBN:**

9781928246268 (softcover, 252 pp, ZAR350)

**PUBLISHER:**

Best Red, Cape Town, South Africa

**PUBLISHED:**

2021

**REVIEWER:**

Elnerine W.J. Greeff

**AFFILIATION:**

<sup>1</sup>Business School, University of Derby, Derby, United Kingdom

**EMAIL:**

E.Greeff@derby.ac.uk

**HOW TO CITE:**

Greeff EWJ. The tail wagging the dog: Tomaselli's *Contemporary Campus Life* and why we are overdue for introspection as academics. *S Afr J Sci.* 2022;118(1/2), Art. #12529. <https://doi.org/10.17159/sajs.2022/12529>

**ARTICLE INCLUDES:**

- Peer review
- Supplementary material

**PUBLISHED:**

27 January 2022

# The tail wagging the dog: Tomaselli's *Contemporary Campus Life* and why we are overdue for introspection as academics

Students of higher education often experience their first scholarly epiphany when they engage with ideas of communism, post-modernism or those ever-present philosophical logic exercises that are rife in the first years of postsecondary education, almost irrespective of one's course or place of study. Interesting as they are, my first moment of scholarly enlightenment was as a direct result of institutional theory. As a strategic communication academic, I am still a staunch believer in the power of institutional theory showing us what *not* to do, by helping us understand why we are doing what we are doing, within organisational settings. If you have a sense of humour while reading these theories, they have the ability to lay bare the absurdities of the bureaucratic and the inherent ridiculousness of scalable systems of productivity.

Tomaselli's *Contemporary Campus Life: Transformation, Manic Managerialism and Academentia* brings all of this vividly to life by conceptualising life and lived reality in the managerial university. It exposes how, on the ruins of the ivory tower, universities managed to build 'instrumentalist structures created by often alienating regulation and governance'. The narrative, which progresses through eleven essays, asks 'whatever happened to the publics who inhabit these symbolic, shambolic and corporeal structures' while showing how the 'public spheres that once offered agency and social imagination are fast waning'. Not being able to help yourself nodding along as you read, the book brings an awareness of how little in these structures are 'elegantly simple anymore. Policymakers always devise the most complicated solutions to address simple problems'. In this way, Tomaselli succeeds in revealing those absurdities that have academics running around in a rat race – aware but disenfranchised by the 'People of Worth' that dictate academic pursuits and endeavours.

In *Contemporary Campus Life*, Tomaselli masters the use of the weapons of the satirist – wit, sarcasm, and irony – to frame current debates 'regarding (i) the academy; (ii) the educational crisis facing South Africa; and (iii) threats to tertiary education across the world'. He does so by offering applications of the concepts of some theorists – including Martin<sup>1</sup>, Levitt and Dubner<sup>2</sup> and Harford<sup>3</sup> – but mostly through the keen eye that could only be honed through decades in academia, and a sense of humour to survive it. Tomaselli makes his stance clear:

*My narrative defamiliarizes what is taken for granted and identifies what needs to be changed for the better. Theory is not just impenetrable sentences written in a textbook, learned off by heart and the jargonised by students in exams. Rather, theory manifests in practice. Theory is explanatory and the chapters in this book connect the dots with nitty-gritty everyday illustrations from the academic experience.*

Satire, as used in this book, should not, however, be mistaken for superficiality. This approach might keep the form of the book light, but it challenges readers not to take its content lightly. Through this satire, we are asked about our own complicity in the state of academia – whether we are laughing at, with, about, or in spite of our own involvement in it. After all, as my reading into institutional theory has taught me, institutions are reflections of ourselves. *Contemporary Campus Life* asks for introspection and for us to confront the ways in which we allowed our 'self-imposed extermination' as academics and scholars; how we 'permitted our entrapment in bureaucratic structures with no soul'. Further, in unapologetic terms, the book asks about the students we are producing – products of this campus life.

Therefore, in an utterly readable style, the book raises uncomfortable but necessary topics unflinchingly, but not coldly. If a good library has something in it to offend anybody, then every library should include this book. It certainly should be compulsory reading for managers or would-be committee chairs in any academic setting because it shows how the tail is wagging the dog as academic managerialism increasingly takes root.

Through a storytelling style best characterised by that of a griot, Tomaselli confronts all academics, managers, and society at large with the idea of academentia – a term he coined in 2008. In the way that it is applied in this book, this concept is not just framed as critique, but as a call to action, a confrontation with the self, and a challenge to (self)engagement. The author clearly shows us his unique and perceptive position as culture studies and autoethnography scholar, as he articulates circumstances that he has come to know as an insider with the clarity and critical eye that one would expect from an outsider. As the book concludes, it is made clear that:

*While there is no magic bullet available in the struggle against blundering bureaucracy, understanding is the best means of navigating the terrain, and doing the best we can under the conditions in which we find ourselves. While academentia exists, the condition can be navigated, reigned in and critically examined. And making sense of it, appropriating it constructively and sometimes taming it can even be fun.*

## References

1. Martin TL. *Malice in blunderland*. New York: McGraw Hill; 1973.
2. Levitt SD, Dubner SJ. *Freakonomics: A rogue economist explores the hidden side of everything*. London: Penguin; 2006.
3. Harford T. *The undercover economist*. Oxford: Oxford University Press; 2006.

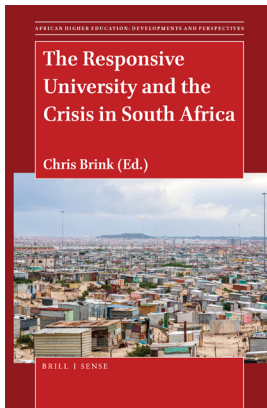
© 2022. The Author(s). Published under a Creative Commons Attribution Licence.



Check for updates

**BOOK TITLE:**

The responsive university and the crisis in South Africa



**EDITOR:**

Chris Brink

**ISBN:**

9789004465602 (hardcover, 385 pp, EUR154.00)

9789004465596 (softcover, 385 pp, EUR48.00)

9789004465619 (ebook, 385 pp, EUR154.00)

**PUBLISHER:**

Brill, Leiden, the Netherlands

**PUBLISHED:**

2021

**REVIEWER:**

Jonathan Jansen 

**AFFILIATION:**

<sup>1</sup>Department of Education Policy Studies, Stellenbosch University, Stellenbosch, South Africa

**EMAIL:**

jonathanjansen@sun.ac.za

**HOW TO CITE:**

Jansen J. Are South African universities disengaged from civic duty? *S Afr J Sci.* 2022;118(1/2), Art. #12799. <https://doi.org/10.17159/sajs.2022/12799>

**ARTICLE INCLUDES:**

- Peer review
- Supplementary material

**PUBLISHED:**

27 January 2022

# Are South African universities disengaged from civic duty?

A doorstopper of a book, the mathematician and former university vice-chancellor, Chris Brink, brings together 24 academic leaders to compose 16 chapters of more than 380 pages of writing on what he calls 'the responsive university'. Its origins lie in the editor's 'unease about universities' engagement, or lack of engagement, with civil society' (p.1).

The book is divided neatly into two equal sections of eight chapters, one global and the other South African. Its thesis is simple: the modern university faces a crisis of legitimacy in the eyes of its publics which is best addressed through a responsive university that actively engages its communities. To his credit, and unusual for edited collections, the editor Brink has a short framing introduction and a closing synthesis, which to some extent hold together the rather diverse chapter contributions.

The 'global context' section offers some rich cases of innovative and experimental instances of responsive universities, from Tufts and the University of Pennsylvania in the USA to Newcastle (UK) and a Hong Kong Polytechnic. The terrain covered is familiar to academics long engaged with the politics and policies of responsiveness, such as mandatory public service coursework embedded in all areas of study versus centre-based initiatives that encourage and incentivise outreach into communities surrounding the university.

The South African section consists of writings prepared in the heat of battle, that is, in the immediate aftermath of the student protest moment of 2015–2016 when the call for 'a free, decolonized education' echoed across the country. Perhaps inevitably, the chapters contain a mix of anguish and analysis with a good dose of normative writing about *what should be* given the wake-up call brought on by the #mustfall moment.

I have always found strange the endless exhortation for South African universities to be more responsive to their surrounding communities. Show me a single university without a school outreach programme or a law clinic or a mobile health-care facility. As the book acknowledges, the pandemic evoked a massive response from higher education institutions. The reasons for such high levels of responsiveness lies within the very nature and origins of our public universities that, unlike their Western counterparts, did not emerge from monastery cultures or ivory towers but with a strong connection to the professions and a sense of service; for example, some of our first universities started with small theology faculties endowed with a sense of outward mission long before there were schools of accounting or theoretical physics.

The problem is not that our universities are unresponsive to external or community needs; it is that their responsiveness is not intellectually and politically problematised. Two examples must suffice. Underlying much of the responsiveness to development is of the hand-out variety of outreach programmes. Responsiveness is not intellectually linked to the mainstream curriculum or programmatically included in a service-learning orientation within the broader university culture. That kind of responsiveness is a fractured business that depends almost entirely on faculty- or departmental-level initiatives that come and go with an energetic, outward-looking personality in that academic unit. Responsiveness is not, in short, conceptualised, let alone systematised, within the knowledge production (research) or knowledge exchange (teaching) functions of the South African university.

In a similar vein, South African universities are often characterised by a knee-jerk responsiveness to the pressures of the day. Put bluntly, our universities are sometimes too responsive to external or internal demands *before thinking things through*. Our forthcoming book on the decolonisation of knowledge makes this point empirically after more than 200 interviews with leading academics across 10 universities.<sup>1</sup> What happened?

On the fright occasioned by the demands for decolonisation, South African academics of all stripes declared their unthinking loyalty to the threatening new concept and proceeded to make up its meanings to fit their own capacities and ideologies; in consequence, a potentially radical concept for curriculum change was quickly and effectively defanged, to borrow from feminist scholar Sarah Ahmed.

Unsurprisingly, by the time the next fad came along, academics at places like the University of Johannesburg jumped gleefully onto the 4IR bandwagon as performance metrics changed to signal the new responsiveness. In her chapter contribution to the book, Lis Lange tries valiantly (and, in my estimation, unsuccessfully) to descriptively capture 'South African universities between decolonization and the fourth industrial revolution' (p.272).

That South African universities sit atop a serious developmental crisis inherited from colonialism and apartheid, and exacerbated by state capture and ineptitude, is not in dispute. That universities are unresponsive is, quite frankly, nonsense. Consider this: the University of Fort Hare runs the sewerage system for the broken municipality in Alice. Rhodes University in Makhanda (the former Grahamstown) is regularly faced with closure because local government there cannot maintain the water supply to the city and its main employer, a site of higher learning. Here you have a situation, mused a former vice-chancellor of this institution, where the municipality could well be the reason for institutional dysfunction.

None of these complexities about the campus-community interface are captured in the chapters of this book which are also uneven in quality, length, and focus. What the book does offer, however, is a compendium of interesting ideas about responsiveness in practice and the case for more engaged universities in other parts of the world.

## Reference

1. Jansen JD, Walters CA. The decolonization of knowledge: Radical ideas and the shaping of institutions in South Africa and beyond. Cambridge: Cambridge University Press. Forthcoming 2022.

© 2022. The Author(s). Published under a Creative Commons Attribution Licence.





**AUTHOR:**  
J. Francis Thackeray<sup>1</sup>

**AFFILIATION:**  
<sup>1</sup>Evolutionary Studies Institute,  
University of the Witwatersrand,  
Johannesburg, South Africa

**CORRESPONDENCE TO:**  
Francis Thackeray

**EMAIL:**  
mrsples@global.co.za

**HOW TO CITE:**  
Thackeray JF. Morphometric ('log sem') analysis of anatomical measurements of Galápagos finches (*Geospiza*), chimpanzees (*Pan*) and Plio-Pleistocene hominins (*Paranthropus*, *Australopithecus* and early *Homo*). S Afr J Sci. 2022;118(1/2), Art. #11913. <https://doi.org/10.17159/sajs.2022/11913>

**ARTICLE INCLUDES:**  
 Peer review  
 Supplementary material

**KEYWORDS:**  
morphometrics, Galápagos, Darwin, Finch, chimpanzee, *Pan*, hominin, Plio-Pleistocene

**PUBLISHED:**  
27 January 2022

# Morphometric ('log sem') analysis of anatomical measurements of Galápagos finches (*Geospiza*), chimpanzees (*Pan*) and Plio-Pleistocene hominins (*Paranthropus*, *Australopithecus* and early *Homo*)

## Significance:

- The 'log sem' morphometric method can be shown to be justified in the context of its use in the analysis of anatomical measurements of three sets of data: Galápagos finches (six species of *Geospiza*); two species of chimpanzees (*Pan troglodytes* and *P. paniscus*); and three hominin genera (*Australopithecus*, *Paranthropus* and early *Homo*).

A morphometric method has been used in analyses of linear measurements obtained from crania of modern hominoids<sup>1-3</sup> as well as Plio-Pleistocene hominins,<sup>1,4,5</sup> based on pairwise comparisons associated with least squares linear regression to quantify the degree of scatter around a regression line of the form  $y = mx + c$ , where  $m$  is the slope and  $c$  is the intercept. The log-transformed standard error of the  $m$ -coefficient, known as 'log sem', serves to quantify the degree of scatter around the regression line, associated with the degree of variability in shape. The effect of size is associated with the  $m$ -coefficient.

For many taxa, a mean log sem value of -1.61 has been recognised as a typical degree of intraspecific morphological variation in extant species.<sup>2,3</sup> With a standard deviation of 0.1, it has been used as a frame of reference for assessing probabilities of conspecificity when pairs of specimens are compared (e.g. Thackeray and Dykes<sup>3</sup> and Thackeray<sup>4</sup>).

In this analysis, the results of an UPGMA (unweighted pair group method with arithmetic mean) cluster analysis were obtained from log sem statistics calculated from anatomical measurements from the following three sets of data as examples of method: Galápagos finches (*Geospiza*), chimpanzees (*Pan troglodytes* and *P. paniscus*), and Plio-Pleistocene hominins (*Australopithecus africanus*, *A. sediba*, *Homo habilis*, *H. erectus*, *H. rudolfensis* and *H. naledi*). The objective was to demonstrate that the log sem statistic has biological significance, reflecting variability in shape in a diversity of taxa.

## UPGMA tree for six species of Galápagos ground finches

Using UPGMA, a log sem matrix was analysed for the six generally accepted species of ground finches, namely *Geospiza magnirostris* (MAG), *G. fortis* (FOR), *G. fuliginosa* (FUL), *G. difficilis* (DIF), *G. conirostris* (CON) and *G. scandens* (SCA).<sup>6,7</sup> The log sem matrix was based on measurements of the lengths of wing, tail, culmen, gonys, depth of bill at base, width of mandible at base, tarsus and middle toe with claw, from a database compiled by the California Academy of Sciences. Measurements were obtained from 36 specimens (an equal number of male and female specimens) resulting in more than 1200 regressions. A computer program for analysing large data sets (<https://github.com/chdwck9/professorRegressor>) was used to calculate log sem statistics.<sup>8</sup>

Figure 1 presents the resulting phenetic tree. This tree corresponds closely to a phylogeny obtained by Burns et al.<sup>9</sup> and Reaney et al.<sup>10</sup> based on genetic data.

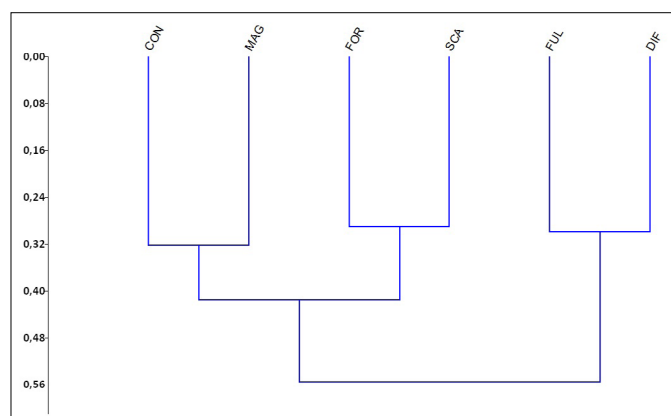


**Figure 1:** Results of a UPGMA analysis of a log sem matrix based on anatomical measurements of six species of Galápagos ground finches, namely *Geospiza magnirostris* (MAG), *G. fortis* (FOR), *G. fuliginosa* (FUL), *G. difficilis* (DIF), *G. conirostris* (CON) and *G. scandens* (SCA). The phenetic tree corresponds closely with a phylogeny presented by Burns et al.<sup>9</sup> and Reaney et al.,<sup>10</sup> based on genetic data. Measurements were obtained from the California Academy of Sciences.

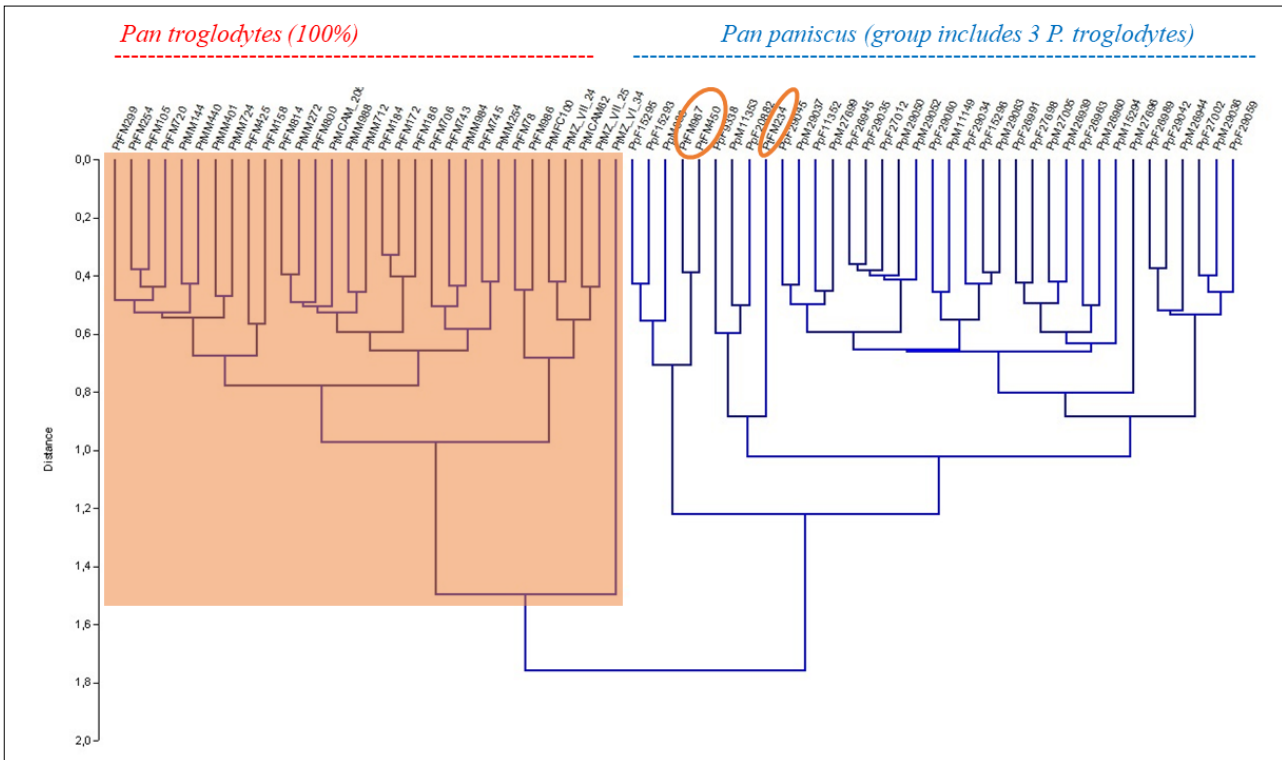


**Figure 2:** Phenetic tree obtained from UPGMA cluster analysis of log sem statistics based on pairwise linear regression analyses of cranial measurements of two chimpanzee species, *Pan troglodytes* ( $n=38$  specimens) and *P. paniscus* ( $n=38$  specimens). Measurements for specimens numbered here have been published by Gordon and Wood<sup>11</sup>. Log sem statistics generally distinguish between the two taxa.

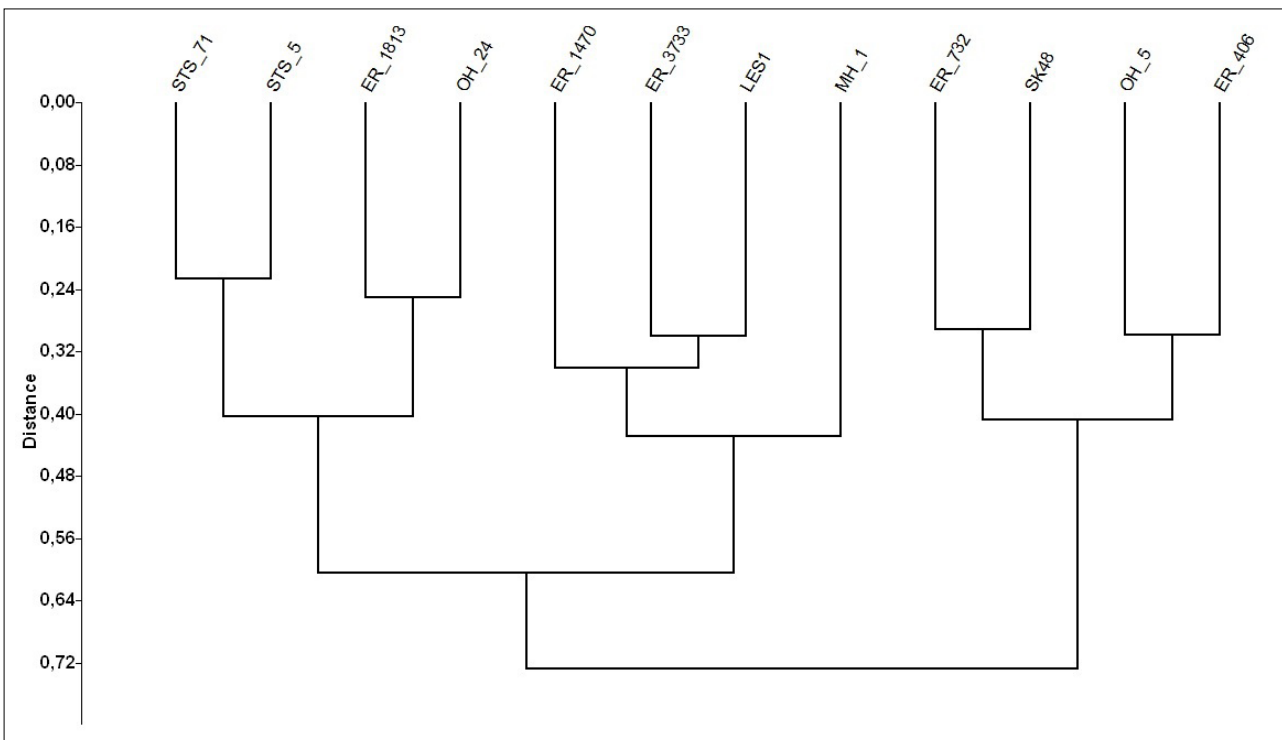


**Figure 3:** Phenetic tree obtained from UPGMA cluster analysis of log sem statistics based on pairwise linear regression analyses of cranial measurements of Plio-Pleistocene hominins, using measurements published primarily by Wood<sup>14</sup>. Three general groups are distinguished, whereby specimens attributed to *Paranthropus* are distinct from others attributed to *Australopithecus* and *Homo*. Sts 5 and Sts 71 are specimens of *Australopithecus* from Sterkfontein, South Africa. KNM-ER 1813 (Turkana Basin, Kenya) and OH 24 (Olduvai Gorge, Tanzania) have been attributed to *H. habilis* but group with *A. africanus*. KNM-ER 1470 (*H. rudolfensis*) and KNM-ER 3733 (*H. ergaster*) are both from the Turkana Basin. South African specimens LES 1 (*H. naledi*) and MH 1 (*A. sediba*) are from Rising Star and Malapa Caves, respectively. KNM-ER 406 and KNM-ER 732 are specimens of *Paranthropus boisei* from the Turkana Basin. The latter species is also represented by OH 5 from Olduvai Gorge. SK 48 represents *P. robustus* from Swartkrans, South Africa.



## UPGMA tree for two chimpanzee species

Figure 2 presents a phenetic tree obtained from UPGMA cluster analysis of log sem statistics based on pairwise linear regression analyses of *Pan troglodytes* and *P. paniscus* cranial measurements ( $n=68$  specimens, more than 4500 regressions), using measurements published as supplementary material by Gordon and Wood<sup>11</sup>. The log sem approach generally distinguishes the two taxa, reflecting robusticity of the log sem method. Although 3 out of 34 specimens attributed to *P. troglodytes* group with others attributed to the closely related *P. paniscus*, this lack of a clear boundary is consistent with genetic evidence of hybridisation between chimpanzees and bonobos within the last million years.<sup>12,13</sup>

## UPGMA tree for Plio-Pleistocene hominin specimens

Figure 3 presents a phenetic tree obtained from UPGMA cluster analysis of log sem data of the kind published by Thackeray and Odes<sup>5</sup>, generated from pairwise comparisons of Plio-Pleistocene hominin specimens attributed to *Australopithecus*, early *Homo* and *Paranthropus*, using measurements published by Wood<sup>14</sup>, with the addition of log sem data associated with *A. sediba*<sup>15</sup> and *H. naledi*<sup>16</sup>.

Specimens attributed to *A. africanus* (Sts 71 and Sts 5) from South Africa and specimens attributed to *H. habilis* (KNM-ER 1813 and OH 24) from East Africa form a group, consistent with the view that these are closely related. A log sem value of -1.51 calculated from a comparison between OH 24 and Sts 5, combined with a so-called delta log sem<sup>3</sup> value of only 0.003, points to a relatively high probability of conspecificity, despite the fact that OH 24 from Olduvai Gorge in Tanzania has generally been attributed to *H. habilis* whereas Sts 5 ('Mrs Ples' from Sterkfontein in South Africa) is accepted as a specimen representing *A. africanus*. Wood and Collard<sup>17</sup> proposed that *H. habilis* should instead be considered as *A. habilis*. Thackeray<sup>18</sup> suggested that the transition between *A. africanus* and *H. habilis* may constitute a chronospecies.

Robust australopithecines (*Paranthropus*), including specimens SK 48, OH 5, KNM-ER 406 and KNM-ER 732, are separated as a group distinct from specimens attributed to *A. africanus* and others attributed to *Homo*, including *H. ergaster* (KNM-ER 3733) and *H. rudolfensis* (KNM-ER 1470). MH 1 (*A. sediba*, described by Berger et al.<sup>15</sup> as a 'Homo-like australopith') groups with specimens attributed to *Homo*. Despite differences in age, LES 1 (*H. naledi*) groups with *H. ergaster*.

## Conclusion

The three UPGMA analyses of log sem data, calculated for Galápagos finches (*Geospiza*), chimpanzees (*Pan*) and Plio-Pleistocene hominins (*Paranthropus*, *Australopithecus* and early *Homo*) reflect groups that have biological significance, serving at the same time to demonstrate that the log sem morphometric method has merit, based on anatomical measurements using landmarks.

## Acknowledgements

This research was supported by the National Research Foundation (South Africa). I am grateful to the late Sue Dykes, Richard Dykes, Caitlin Schrein and Julien Benoit for their roles in the use of the log sem morphometric method. Anatomical measurements of Darwin's finches used in this study are from collections of *Geospiza* in the California Academy of Sciences, with the assistance of Moe Flannery. I thank Peter and Rosemary Grant, Arkhat Abzhanov, Ashley Reaney, Jack Dumbacher, Bob Zink, Tim Crowe, Marine Cazenave, Clément Zanolli, Peter Knox-Shaw and an anonymous reader for comments and encouragement in relation to this study. I dedicate this paper to Sue Dykes.

## References

1. Thackeray JF, Bellamy CL, Bellars D, Bronner G, Bronner L, Chimimba C, et al. Probabilities of conspecificity: Application of a morphometric technique to modern taxa and fossil specimens attributed to *Australopithecus* and *Homo*. *S Afr J Sci*. 1997;93:195–196.
2. Thackeray JF. Approximation of a biological species constant? *S Afr J Sci*. 2007;103:489.

3. Thackeray JF, Dykes S. Morphometric analyses of hominoid crania, probabilities of conspecificity and an approximation of a biological species constant. *HOMO J Comp Hum Biol*. 2016;67(1):1–10. <http://doi:10.1016/j.jchb.2015.09.003>
4. Thackeray JF. Alpha and sigma taxonomy of *Pan* (chimpanzees) and Plio-Pleistocene hominin species. *S Afr J Sci*. 2018;114(11/12), Art. #a0291. <https://doi.org/10.17159/sajs.2018/a0291>
5. Thackeray JF, Odes E. Morphometric analysis of early Pleistocene African hominin crania in the context of a statistical (probabilistic) definition of a species. *Antiquity*. 2013;87. <http://antiquity.ac.uk/projgall/thackeray335/>
6. Grant PR, Grant BR. How and why species multiply: The radiation of Darwin's finches. Princeton, NJ: Princeton University Press; 2008. <https://doi.org/10.1515/9781400837946>
7. Grant PR, Grant BR. 40 years of evolution: Darwin's finches on Daphne Major Island. Princeton, NJ: Princeton University Press; 2014. <https://doi.org/10.1515/9781400851300>
8. Dykes SJ, Dykes RD. 'Professor Regressor': A computer programme for rapid processing of large sets of data for pairwise regression analyses in palaeontological contexts. *Palaeontol Afr*. 2015;49:53–59. <https://wiredspace.wits.ac.za/handle/10539/17371>
9. Burns KJ, Shultz AJ, Title PO, Mason NA, Barker FK, Klicka J, et al. Phylogenetics and diversification of tanagers (Passeriformes: Thraupidae), the largest radiation of Neotropical songbirds. *Mol Phylogenet Evol*. 2014;75:41–77. <https://doi.org/10.1016/j.ympev.2014.02.006>
10. Reaney AM, Bouchenak-Khelladi Y, Tobias JA, Abzhanov A. Ecological and morphological determinants of evolutionary diversification in Darwin's finches and their relatives. *Ecol Evol*. 2020;10(24):14020–14032. <https://doi.org/10.1002/ece3.6994>
11. Gordon AD, Wood BA. Evaluating the use of pairwise dissimilarity metrics in paleoanthropology. *J Hum Evol*. 2013;65:465–477. <https://doi.org/10.1016/j.jhevol.2013.08.002>
12. De Manuel M, Kuhlwillm M, Frandsen P, Sousa VC, Desai T, Prado-Martinez J, et al. Chimpanzee genomic diversity reveals ancient admixture with bonobos. *Science*. 2016;354(6311):477–481. <https://doi.org/10.1126/science.aag2602>
13. Thackeray JF, Schrein CM. A probabilistic definition of a species, fuzzy boundaries and 'sigma taxonomy'. *S Afr J Sci* 2017;113(5/6), Art. #a0206. <https://doi.org/10.17159/sajs.2017/a0206>
14. Wood BA. Koobi Fora Research Project. Volume 4: Hominid cranial remains. Oxford: Clarendon Press; 1991.
15. Berger LR, De Ruiter DJ, Churchill SE, Schmid P, Carlson KJ, Dirks PHGM, et al. *Australopithecus sediba*: A new species of *Homo*-like australopith from South Africa. *Science*. 2010;328:195–204. <https://doi.org/10.1126/science.1184944>
16. Berger LR, Hawks J, De Ruiter DJ, Churchill SE, Schmid P, Deleuzene LK, et al. *Homo naledi*, a new species of the genus *Homo* from the Dinaledi Chamber, South Africa. *eLife*. 2015;4, e09560, 35 pages. <https://elifesciences.org/articles/09560>
17. Wood BA, Collard M. The changing face of the genus *Homo*. *Evol Anthropol*. 1999;8:195–207. [https://doi.org/10.1002/\(SICI\)1520-6505\(1999\)8:6<195::AID-EVAN1>3.0.CO;2-2](https://doi.org/10.1002/(SICI)1520-6505(1999)8:6<195::AID-EVAN1>3.0.CO;2-2)
18. Thackeray JF. *Homo habilis* and *Australopithecus africanus*, in the context of a chronospecies and climatic change. In: Runge R, editor. Changing climates, ecosystems and environments within arid southern Africa and adjoining regions. Palaeoecology of Africa 33. Leiden: CRC Press; 2015. p. 53–58.

**AUTHORS:**Charles J. MacRobert<sup>1</sup>   
Theo J. Stergianos<sup>1</sup> **AFFILIATION:**<sup>1</sup>Department of Civil Engineering,  
Stellenbosch University, Stellenbosch,  
South Africa**CORRESPONDENCE TO:**

Charles MacRobert

**EMAIL:**

macrobert@sun.ac.za

**HOW TO CITE:**MacRobert CJ, Stergianos TJ. NRF  
ratings and *h*-index for engineers: Are  
we missing the point? *S Afr J Sci.*  
2022;118(1/2), Art. #12260. <https://doi.org/10.17159/sajs.2022/12260>**ARTICLE INCLUDES:**

- Peer review
- Supplementary material

**KEYWORDS:**bibliometrics, Hirsch's *h*-index, NRF  
rating, research administration**PUBLISHED:**

27 January 2022

# NRF ratings and *h*-index for engineers: Are we missing the point?

**Significance:**

- For the few rated engineers, NRF ratings show a close correlation with *h*-index.
- Publication of journal articles and the citation thereof may be poor indicators of engineering research impact.

**Introduction**

Polanyi<sup>1</sup> showed how scientific progress relies on a system of 'mutual control', or simply the means by which 'scientists keep watch over each other' to prevent resources being grossly wasted. In our present context, two ways in which this 'mutual control' is exercised is through peer-reviewed ratings from the South African National Research Foundation (NRF) and Hirsch's bibliometric *h*-index.<sup>2</sup>

Application for an NRF rating requires individuals to prepare portfolios. These portfolios are peer reviewed and individuals are given an A-rating (leading international researchers), B-rating (internationally acclaimed researchers) or C-rating (established researchers). The subsidiary ratings for young researchers are not considered here. Whilst guidelines for what can be included in these portfolios have been tailored to specific disciplines, emphasis across all disciplines is placed on peer-reviewed journal papers.<sup>3</sup> Other outputs (e.g. confidential reports of applied research for industry in engineering) require considerably more justification and are therefore assessed with greater subjectivity. Nevertheless, this subjectivity is perhaps the main advantage of the NRF-rating system as reviewers can assess individuals holistically and in context.<sup>4</sup>

Hirsch's *h*-index (where *h* is the number of publications cited *h* times) is significantly easier to obtain as it is based purely on bibliometrics. The *h*-index is advantageous as it measures the impact of a body of work better than relying on total publications or total citations. Although *h*-indices are based on a formula, they can differ based on the database used. For instance, Google Scholar *h*-indices tend to be higher than Scopus *h*-indices, as the former's database is generated by an algorithm scouring the web, whereas the latter is based on a smaller curated database. The main disadvantage of the *h*-index is that it is a metric that does not consider the context of a researcher, which can both unduly inflate an individual's *h*-index or fail to capture an individual's impact.<sup>4</sup>

Despite differences, it is unsurprising that a relationship exists between the two metrics. Johnson<sup>4</sup> compared 614 NRF-rated biological scientists to their respective *h*-indices in 2020 and found fairly distinct ranges of *h*-index associated with each NRF rating. In 2013, Fedderke<sup>5</sup> also found a significant statistical relationship between NRF ratings and *h*-index for 1932 scholars across various disciplines, including engineering. Nevertheless, it is considered worthwhile reassessing this relationship for engineers as citation practices are rapidly changing<sup>4</sup> and engineering faculties increasingly emphasise research, particularly in promotion criteria.

**Method**

Following the same methodology as Johnson<sup>4</sup>, the latest NRF ratings (23 March 2021) were downloaded from the NRF website ([www.nrf.ac.za](http://www.nrf.ac.za)) and Scopus *h*-indices were obtained for individuals listing 'Engineering sciences' as one of their primary disciplines (accessed over 16/17 August 2021). Sub-disciplines were not considered, as it was questionable whether this would add significantly to the debate; however, future work may want to consider this aspect. Unlike in Johnson<sup>4</sup>, differences between *h*-index and NRF rating were tested using a single factor ANOVA test. Similarities between engineers and biologists were tested using two-sample *t*-tests assuming equal variance. Pearson correlation was used to test whether *h*-index increased with time from date of rating.

**Results**

The latest NRF ratings (23 March 2021) included 385 rated individuals with 'Engineering sciences' as one of their primary disciplines. In the 2020 study<sup>4</sup>, a total of 644 rated scientists listed 'Biological sciences' as a primary discipline. In the latest ratings, 'Biological sciences' researchers are the most rated (18%), followed closely by 'Social sciences' also at 18%; the rest of the top five are 'Humanities' at 16%, 'Health sciences' at 12% and Engineering at 9%.

Figure 1 depicts ranges of *h*-index for each of the three main NRF ratings for both biologists and engineers. It is clear that, similarly to biologists, *h*-indices for engineers fall into distinct ranges for each rating ( $F(2, 301) = 81$ ,  $p < 0.001$ ). Johnson suggested *h*-index norms for biologists were about 5–20 for C-ratings, 20–40 for B-ratings and  $>40$  for A-ratings.<sup>4</sup> These *h*-index norms are shown in Figure 1 by green shading and the percentage of individuals falling within these norms is indicated above these bars. While the majority of engineers also fell within these norms, a number of A- and B-rated engineers fell below the suggested norms. Consequently, in all cases, the mean *h*-index, per rating, was statistically lower for engineers than for biologists ( $p < 0.05$  in all three cases). This difference was 19 for A-ratings, 5 for B-ratings and 4 for C-ratings.

Johnson<sup>4</sup> reported significant differences in *h*-index, per rating, with time since rating. However, our analysis of biologists showed a weak relationship between *h*-index and time since rating, with  $r = 0.2$  for A-ratings,  $r = 0.04$



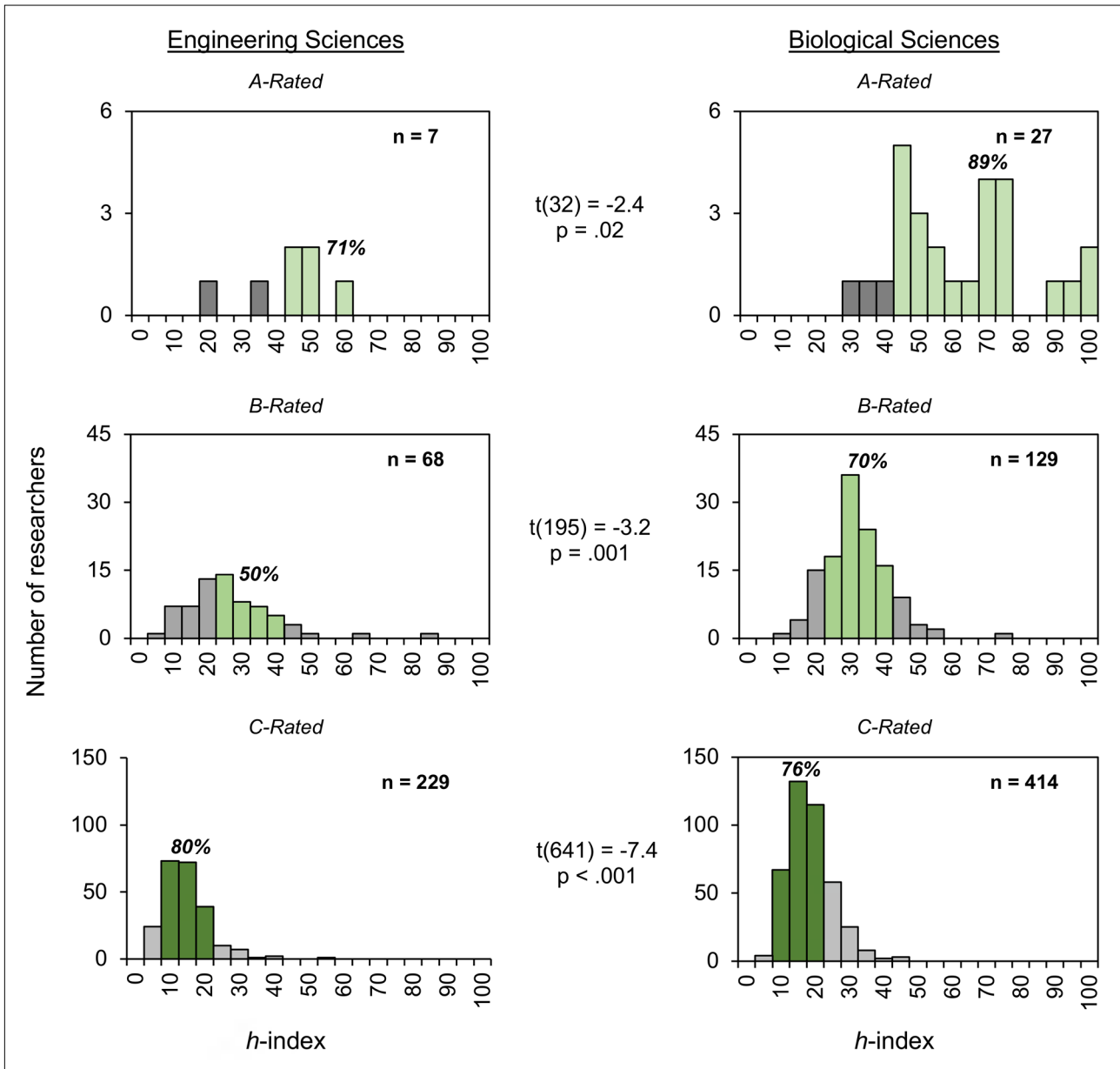


Figure 1: Distribution of Scopus *h*-index per NRF rating for engineering sciences and biological sciences (data for biological sciences from Johnson<sup>4</sup>).

for B-ratings and  $r = 0.2$  for C-ratings. For engineers, the relationship between *h*-index, per rating, and time since rating was not significantly better, with  $r = 0.4$  for A-ratings,  $r = 0.2$  for B-ratings and  $r = 0.2$  for C-ratings.

## Discussion

A striking result was how few engineers were rated. Ascertaining whether this result reflects vastly different numbers of individuals in these fields is difficult. Estimating this from the number of graduates in each field is problematic. Firstly, disciplines are not similarly captured, and, secondly, scientists, whether studying humans or nature, are far more likely to do research compared to engineers who typically enter applied engineering fields. Considering the number of academics in each field is also problematic as scientific research is often not university-bound. Engineering faculties also focus on producing engineers and academics may not feel an equal need to create knowledge compared to those in more pure fields. While a more detailed study could be undertaken, we hope this discrepancy is not due to higher student to academic ratios in engineering, or fewer research-active engineers, or engineering research

being inferior, but that it reflects fewer engineers applying for rating. This may change particularly as university promotion criteria increasingly prioritise research and academics seek to demonstrate their worth.

The low number of rated engineers raises the question, Are engineers missing out? NRF ratings are a means of allocating public resources to research and engineers may well be missing out. However, engineering research being more applied, is more likely to obtain private funding as the commercial utility is clearer. Consequently, the question we rather focus on is: Are we missing the point? Returning to Polanyi, scientific worth is a function of three factors, which vary with domain: exactitude, systematic importance and intrinsic interest of the subject matter.<sup>1</sup> While engineering may be deficient in the first two factors, it adequately makes up with 'intrinsic interest', especially for the layperson. Nevertheless, engineering researchers need to be kept in check, so we now consider whether an NRF rating or an *h*-index is the correct measure.

A key driver of engineering research is developing methods for practising engineers to solve problems.<sup>6</sup> While dissemination of these methods is done in journals, dissemination is more often via conferences, standards, guidelines and trade magazines (so-called grey literature). While tracking

grey literature has been attempted<sup>7-9</sup>, doing so is largely impractical. Tracking engineering research within real-world engineering is almost impossible as outputs (i.e. designs, reports and drawings) are 'invisible' to the public and rarely use standardised referencing conventions. Research-active engineers may therefore feel it is impossible to show research impact within the guidelines suggested for rating. The strong correlation between NRF ratings and *h*-indices will likely reinforce this perception.

As alluded to in the previous paragraph, the users of engineering research ought to be practising engineers. There is a growing body of work that shows that journal papers are a poor means of knowledge transfer between academia and the applied world, particularly within engineering.<sup>10,11</sup> Practising engineers are also contributing less to journals – either by way of original research or by discussion – compared to decades past.<sup>12</sup> Consulting co-workers and supervisors is favoured<sup>13</sup>, with some suggesting that it is only as problem complexity increases that journal articles are considered<sup>14</sup>. However, it is more likely that textbooks are referred to than original research papers. Increasingly, engineers are also turning to social media for information.<sup>15</sup> Fraser et al.<sup>10</sup> contend, and show within Australian engineers, that this lack of trust in journals is due to a perceived research–practice gap. That is, research by academics is perceived to have little or no practical relevance. Fraser et al.<sup>10</sup> argue that the measure of engineering research impact should be the practical use of research. Interestingly, medical practitioners are shown to have a much higher view of journal publications<sup>10</sup>, suggesting medical researchers are much better at articulating the practical significance of their work.

Research-active engineers seemingly face a dilemma of demonstrating the worth of their research. Much engineering research ends up in grey literature, which is hard to index and track. It is also questionable whether high *h*-indices reflect practising engineers using cited research, given evidence that practising engineers rarely consider journals and the 'invisible' nature of engineering outputs. NRF ratings, in principle, seem the better metric as they take a more holistic view of engineers, but guidance documents emphasise peer-reviewed journal articles and in practice show close agreement to bibliometric patterns present in other disciplines.

Engineers strive to be pragmatic and propose solutions to all problems. In our view, research-active engineers should be able to demonstrate a close relationship with practising engineers. They should show how they are actively approached by industry to solve complex problems and show how they have solved these problems. Solving problems is fundamentally what research is all about.<sup>16</sup> Complex problems are rarely tackled alone and teams of peers contribute and critique each other along the way. Engineers should demonstrate how they are striving to bring about knowledge transfer, not simply through traditional media (e.g. trade magazines, courses and discussion) but also through digital platforms. Altmetrics are increasingly able to track research impact across digital platforms.<sup>17</sup> Peer-reviewed journal articles remain a key way to formalise research, but impact needs to be measured through more than just citations. Citations in textbooks, guidelines and standards should receive emphasis. Industry recognition through invited lectures, prizes and fellowship to voluntary associations should also be heavily weighted as these provide evidence of peer review and standing. In our view, basing an engineer's research impact on a few well-cited papers is a simplification of what is entailed in engineering research.

## Acknowledgements

Chris James helped shape views expressed in this paper and reviewed a draft.

## Competing interests

We have no competing interests to declare.

## References

1. Polanyi M. The tacit dimension. Chicago, IL: University of Chicago Press; 2009.
2. Hirsch JE. An index to quantify an individual's scientific research output. *Proc Natl Acad Sci USA*. 2005;102(46):16569–16572. <https://doi.org/10.1073/pnas.0507655102>
3. South African National Research Foundation. Key research areas and types of research outputs [document on the Internet]. c2020 [cited 2021 Sep 01]. Available from: [https://www.nrf.ac.za/sites/default/files/documents/11\\_Key%20Research%20Areas%20and%20Types%20of%20Research%20Outputs\\_Rating%20Call%202021\\_Sep%202020.pdf](https://www.nrf.ac.za/sites/default/files/documents/11_Key%20Research%20Areas%20and%20Types%20of%20Research%20Outputs_Rating%20Call%202021_Sep%202020.pdf)
4. Johnson SD. Peer review versus the *h*-index for evaluation of individual researchers in the biological sciences. *S Afr J Sci*. 2020;116(9/10), Art. #8700. <https://doi.org/10.17159/sajs.2020/8700>
5. Fedderke JW. The objectivity of national research foundation peer review in South Africa assessed against bibliometric indexes. *Scientometrics*. 2013;97(2):177–206. <https://doi.org/10.1007/s11192-013-0981-0>
6. Poulos HG. Simplicity – a desirable end-point of geotechnical research. *Ground Engineering*. 1982;15(7).
7. Cooper K, Marsolek W, Riegelman A, Farrell S, Kelly J. Grey literature: Use, creation, and citation habits of faculty researchers across disciplines. *J Librariansh Inf Sci*. 2019;7(1), eP2314. <https://doi.org/10.7710/2162-3309.2314>
8. Musser L. Preserving the digital record of science and engineering: The challenge of new forms of grey literature. *Issues Sci Technol Librariansh*. 2016;83. <https://doi.org/10.5062/F4251G69>
9. Stephen McMinn H, Fleming K. Tracking the use of engineering conference papers: Citation influence of the Stapp Car Crash Conference. *Collection Building*. 2011;30(2):76–85. <https://doi.org/0.1108/01604951111127443>
10. Fraser K, Tseng T-LB, Deng X. The ongoing education of engineering practitioners: How do they perceive the usefulness of academic research? *Eur J Eng Educ*. 2018;43(6):860–878. <https://doi.org/10.1080/03043797.2018.1450847>
11. Fothergill A. Knowledge transfer between researchers and practitioners. *Nat Hazards Rev*. 2000;1(2):91–98. [https://doi.org/10.1061/\(ASCE\)1527-6988\(2000\)1:2\(91\)](https://doi.org/10.1061/(ASCE)1527-6988(2000)1:2(91))
12. James CS. Editorial. *Proc Inst Civil Eng-Wat Manag*. 2010;163(5):217–218. <https://doi.org/10.1680/wama.2010.163.5.217>
13. Anderson CJ, Glassman M, McAfee R, Pinelli T. An investigation of factors affecting how engineers and scientists seek information. *J Eng Technol Manag*. 2001;18(2):131–155. [https://doi.org/10.1016/S0923-4748\(01\)00032-7](https://doi.org/10.1016/S0923-4748(01)00032-7)
14. Leckie GJ, Pettigrew KE, Sylvain C. Modeling the information seeking of professionals: A general model derived from research on engineers, health care professionals, and lawyers. *Libr Q*. 1996;66(2):161–193. <https://www.jstor.org/stable/4309109>
15. Murphy G, Salomone S. Using social media to facilitate knowledge transfer in complex engineering environments: A primer for educators. *Eur J Eng Educ*. 2013;38(1):70–84. <https://doi.org/10.1080/03043797.2012.742871>
16. Cross H. *Engineers and ivory towers*. New York: McGraw-Hill; 1952.
17. Wikipedia. Altmetrics [webpage on the Internet]. No date [cited 2021 Sep 01]. Available from: <https://en.wikipedia.org/wiki/Altmetrics>



# Driving openness – the myths about data and software access in the Data and Cloud Policy

**AUTHOR:**  
Cobus Jooste<sup>1</sup>

**AFFILIATION:**  
<sup>1</sup>Consolidoc Postdoctoral Fellow,  
Department of Mercantile Law,  
Stellenbosch University, Stellenbosch,  
South Africa

**CORRESPONDENCE TO:**  
Cobus Jooste

**EMAIL:**  
cobusjooste@gmail.com

**HOW TO CITE:**  
Jooste C. Driving openness – the  
myths about data and software  
access in the Data and Cloud Policy.  
S Afr J Sci. 2022;118(1/2), Art.  
#12124. [https://doi.org/10.17159/  
sajs.2022/12124](https://doi.org/10.17159/sajs.2022/12124)

**ARTICLE INCLUDES:**  
 Peer review  
 Supplementary material

**KEYWORDS:**  
law, data protection, policy, data,  
software, intellectual property,  
copyright

**PUBLISHED:**  
27 January 2022

## Significance:

- This article responds to the highly controversial recently published Draft National Policy on Data and Cloud and the related stakeholder commentary from a cyberlaw perspective. Selected issues regarding the ownership of scientific data, databases and processing software, within the intellectual property law framework, are summarised. The law on issues regarding computer science and software engineering, specifically decompilation and digital rights management, are discussed insofar as these matters are implicated in the Data and Cloud Policy. A call to conduct a rights audit is issued to those whose scientific research activity relies on controlled data access and/or those who have a proprietary interest in the economic value of data.

## Introduction

There is no doubt that access to information is fundamental to scientific, cultural and economic progress, but it is not, as some would have it, a recent symptom of the Fourth Industrial Revolution.<sup>1,2</sup> The opportunity to rely on the work of others has been a cornerstone of legal development since, at least, as early as 1710 when the first Copyright Act in the world was published. Since then, a substantial body of intellectual property and neighbouring laws has developed to address the tension between the public interest in access to information and the private interests in controlling the dissemination of their work or the use of their ideas.<sup>3</sup>

Therefore, it is worrying to note that, when dealing with the two most valuable manifestations of knowledge (namely data and software), the South African government seems unaware of the existence of private rights. In the recently published Draft National Policy on Data and Cloud (the Data Policy), the Ministry of Communications and Digital Technologies states ‘it remains unclear how data generated through intellectual activities of varying degrees and types would be correctly categorised in terms of intellectual property rights’<sup>1</sup> and suggests, incorrectly, that there is no policy applicable to the ownership of data.<sup>1</sup>

Labouring under this misapprehension, the Data Policy proposes to provide universal access to data by, inter alia, consolidating all publicly funded data centres into a single, state-owned entity, nationalising all data generated in the country and establishing an open data platform to control access to all the data held by this entity.<sup>1</sup> The Data Policy’s primary goal is to concentrate power over data in the state and seeks to localise data processing by creating widespread reliance on state-owned data and cloud infrastructure.

The Data Policy is indeed an alarming document and has met with substantial opposition. For the purpose of this article, the focus is on selected issues regarding the future of private ownership of software and data and the ability to control access thereto. This is done by addressing a number of myths espoused in the Data Policy, from a cyberlaw perspective.

## Myth 1: Data is inherently valuable

The Data Policy waxes lyrical about data as the ‘new oil’ and declares data to be ‘the infrastructure for the digital economy’ because ‘the greatest advantage of data is the value it generates after it is processed into information and knowledge.’<sup>1</sup> This view is problematic on two fronts. First, it implies that data need only be processed in order to extract economic value. Second, it implies that those who hold data collections are in a position to exploit the data at will. In other words, the Data Policy relies on the myth that data is a mineable commodity with inherent potential value.

### Value is in the application of knowledge

In reality, data are simply digitally represented information and have no more inherent value than the contents of a dictionary or a list of phone numbers. The value of data per se is nil, and so too is the *potential* value of data. The value of data lies in the *application* of knowledge obtained from processed data – often described as a data value chain.<sup>4</sup> This is the reason why data are used as a commodity. Those who invest in data determine the value according to their possible application and the commercial benefit that may be derived from using the knowledge they have gained.<sup>2</sup>

Furthermore, data cannot be imbued with inherent value. Even when great skill and advanced analytical methodology are applied to data, the value is created in, and derived from, the results of those efforts. In these cases, the commercial or other value of the data exists only because of the results facilitated.<sup>2</sup> Consider, for example, two very different databases: a database containing the shopping habits of customers and a database containing the blood glucose level of patients. In isolation, each database may be used to create value through application. The first may aid advertisers in their targeted marketing efforts, assist retailers to make informed decisions about stock purchases or product placement, or help manufacturers to decide on product design or factory retooling. In all of these cases, the economic value lies in the cost savings or increase in turnover made possible as a result of the knowledge gained from the processed and interpreted data. The data itself, even after processing, are not responsible for the value. The second database is the same. Consisting of protected and sensitive information, its utility is restricted but it may be useful to medical research for any number of applications. In these cases,





the value depends on the results of the research. It may be directly economic, such as subsidy for published research output, or indirect, in the form of attracting future grants. Once again, the value is derived from the knowledge that was created from the data, not from the knowledge contained in the data.

Into this picture one may add so-called big data – the massification and concentration of data to extract value from the combination of a variety of data points. Thus, for example, by combining the two databases, one may determine a possible correlation between eating habits and blood glucose level. This statistic might be useful to medical aid providers when designing healthy living incentives or to pharmaceutical manufacturers or foodstuff producers when making decisions on product development. In all these cases, the value of the data is second hand – it is derived from the amendments made to current business strategy.

### ***The law is purpose and outcome focused***

Once this is understood, the fallacy in the Data Policy's approach is laid bare. From a cyberlaw perspective, data are treated as information – they have no inherent value. For this reason, the range of legal measures applicable to data depend on what the data may be (or may not be) used for or, in other cases, how the investment in processing the data, or creating knowledge from the data, should be repaid. The law recognises that the value of data is downstream, as are the threats to society.<sup>5</sup> As scholars have pointed out when considering the status of intellectual property, 'the constitutional conception of property, according to which the focus falls on the function that the alleged property has in society rather than the traditional, pre-constitutional conceptions of property'<sup>6</sup> is the basis for the manner in which the law, specifically intellectual property law, regulates the protection of information.

That is why the law operates as a data steward – it facilitates the value chain by balancing competing interests *in context* when it restricts human activity. The context of each data regulation will differ (e-commerce, evidence, crime, taxation, property, etc.) and, therefore, the law seeks to restrict everything that is necessary, but nothing more, in a delicate weighing exercise.<sup>5</sup> A plethora of statutes, judgements and common law provisions govern individual use cases. Some data law scholars criticise the sheer volume of legal measures applicable to ownership of information for being contrary to the sharing norms of scientific research.<sup>7</sup> For this reason, a global data policy which seeks to inculcate value into data itself will never survive legal critique unscathed.

### ***The law restricts the application***

The same holds true for the ability to extract value from data at will. The Data Policy is under the impression that those who amass data are free to manipulate it. Once again, this is at odds with the legal reality. Even those who hold data are seldom free to apply it for any purpose or at their own discretion, because data stewardship is a matter of combined legal measures.<sup>4</sup> Depending on the nature of the information, a volume of legal (including ethical, environmental, security and regulatory) *approvals* must be sought before information, whether in data format or not, may be processed. This administrative burden is so complex that it often accounts for a large portion of the resource investment in data processing. The Data Policy seems to neglect this fact and appears to convey that data sovereignty may be achieved merely through physical, local control.<sup>4,5</sup>

## **Myth 2: Data ownership is unclear**

Of major concern is the Data Policy's manifest ignorance of the law regarding ownership of information. It assumes that possession is really nine tenths of the law, and that data are somehow a unique asset that exists independently from the information represented. Therefore, the Data Policy enviously refers to a strange creature it calls 'mega technological digital companies [...] operational in selected countries' which, in their opinion, unfairly monopolise the (fantastical) inherent value in data. This myth is wrong-footed on both counts.

## ***Most data are owned by someone***

First, data ownership is not a question the law is concerned about – ownership vests in the information as it is expressed, whether it is data or not. As some notable legal scholars point out: 'few people have information; instead, what most people actually have is data'<sup>8</sup>.

Therefore, the ownership of information is addressed by a variety of statutes, key among which is the Copyright Act. There are good reasons why copyright law is implicated directly where data are concerned. First, a large volume of the information contained in data is subject to copyright protection. Second, electronic communications operate by way of copying data, which means that the exclusivity of the right to make reproductions is always at stake.<sup>8</sup>

If the data consist of individual expressions of human intellectual endeavour, such as literary, musical or artistic works, films, broadcasts or computer programs, each data set (or even each data point), will automatically be owned by someone.<sup>9</sup> Because copyright law does not impose a merit test, it does not matter if the data point is meaningless.<sup>9,10</sup> Similarly, copyright protection has been held to vest in minute works (such as individual phrases or lines of code). Therefore, provided that a data point qualifies as a fit type of work, it may be individually protected. In many cases, data samples will be considered a literary work because it is a form of 'writing'<sup>9</sup> consisting of numerical values or symbolic language<sup>11</sup>, but the same data may also qualify for protection as another type of work.

If the data points do not meet the threshold for protection as individual works (with individual owners), they may nevertheless be protected as a compilation<sup>11</sup> (with a single or joint owners) in a database. Ownership of the database vests in the person(s) who applied their mind to the selection and arrangement of information, regardless of where that information came from or whether it was lawfully obtained.<sup>8</sup> That is why, in South Africa, even the most mundane database may qualify for copyright protection.<sup>9,11</sup> All that is required to vest ownership is a sufficient, qualitatively small, effort in selecting and arranging the data. This effort does not have to be unique, novel, creative or in any way distinguishable from other databases, as long as it is clear that the selection and arrangement is the result of the author's own judgement, skill and labour.<sup>10</sup>

In practice, many databases consist of data collected by sensors, monitors, gauges or other electronic or technological means. In other cases, large volumes of data are produced automatically during the operation of a computer program. This has led some commentators to suggest that most databases will not qualify for copyright protection because they lack a human author.<sup>12</sup> This view is incorrect. The Copyright Act makes it clear that ownership in a computer-generated work, including individual works, compilations or databases,<sup>9</sup> will vest in the person who made the arrangements necessary to create the work.<sup>13</sup> The Supreme Court of Appeal<sup>10</sup> confirmed this and held that if the work has no human author, it is protected as a computer-generated work. If a human was involved in the creative process, it is protected as a computer-assisted work.<sup>10</sup>

The identity of the person who is vested with the rights in the work (data or database), is a factual question. It is determined, primarily, with reference to the first ownership rule.<sup>9</sup> Accordingly, the person who is identified, by law, as the author of the work will be the first owner of all the rights in that work.

There are, however, some cases where copyright will not vest in the information and it is, therefore, not subject to ownership. This would be the case where the work is not substantial enough, or is too commonplace, to qualify as a fit type of work. The most common example is statistical personal information. This is the reason why social media service providers insist that they do not own a user's data, because the user does not have a property right in their personal information. This fact does not prevent ownership from vesting in the database itself, but the use of that data will be restricted by the scope of authorisation granted by the data subject.

### **Data are transferrable property**

Second, the law deals with data ownership as a matter of *intellectual property*. This means the law recognises the immaterial/intangible nature of the rights but has, nevertheless, incorporated it under the existing legal framework applicable to tangible property. Contrary to the view of some commentators on the Data Policy, copyright is movable property<sup>14</sup> and is protected against expropriation<sup>14</sup> in terms of section 25 (the property clause) of the Constitution<sup>6,15</sup>.

Furthermore, the law acknowledges that this kind of property exists simultaneously everywhere in the world and also nowhere in the physical world. Internationally, copyright protection operates by way of the principle of national treatment.<sup>9</sup> This means the nature and scope of the owner's entitlement is determined according to the rules applicable in the country where the data are exploited<sup>9</sup> and will exist independently and simultaneously in all relevant countries of the world<sup>7</sup>. That means, in legal terms, data cannot be moved from one country to another.<sup>4</sup> Its storage location may change, but even if the data are entirely deleted in one country, the legal ownership in that country remains valid. However, to exploit the taxation potential of intellectual property, the South African Treasury has declared that any change in owner (by assignment) from a national to a foreigner, will amount to an export of capital and will therefore trigger foreign exchange control clearance.<sup>9</sup> This means that, if the Data Policy succeeds in forcing localisation of data, it will also trap that information in South Africa. This will likely have a devastating impact on foreign investment in research and development. This is one example of what commentators call the 'unintended and perverse consequences' of using the 'blunt tool' of data localisation.<sup>5</sup> Other commentators add that 'measures which introduce policy uncertainty or otherwise disincentivise investment must be avoided'<sup>16</sup> or else it will imperil South Africa's ability to compete on the African continent.

### **Myth 3: Controlling infrastructure allows control of data**

The Data Policy is devoted to establishing local data processing 'infrastructure' as a combination of physical data storage/processing facilities and cloud services. Nowhere does it consider the fact that infrastructure consists of hardware *and software*. Without the appropriate computer programs in place to use the data, it is impossible to derive any downstream value from the data. This means the policy fails to recognise a number of substantial legal barriers to achieving its goal of promoting access.

### **Local access requires local software maintenance and development**

A significant spin-off industry from the data economy is the creation and maintenance of database-related software. To be effective, these computer programs must handle large volumes of data and do so securely and reliably. All three factors pose substantial risks to the integrity of the data, the service, the data subject and an array of third parties. Therefore, the stability of data processing infrastructure has become big, lucrative, business<sup>4</sup> and it is a software-based issue. Very few database controllers will assume the cost and risks associated with in-house software and prefer to rely on proven solutions. In Africa, that means imported solutions, i.e. software copyright licences.

For many new entrants to the data market, the software licensing costs are prohibitive. Providing access to the data along with access to the software will not solve the problem of 'opportunity costs'.<sup>14</sup> On the contrary, it will exponentially increase the licence cost, because the programs will have to be sub-licensable, and will transfer that cost to the taxpayer. Commentary on the policy suggests that 'this policy will add unnecessary operational burdens on the shoulders of smaller businesses and make their growth yet more uncertain and difficult'<sup>17</sup> while others demonstrate that the policy will increase economic risks by, inter alia, impacting negatively on enterprise productivity, global market access and manufacturing<sup>18</sup>.

### **Home grown infrastructure is unlikely**

The only alternative is locally produced database software. To design such programs afresh is simply not feasible and the local software industry will have to learn from existing programs. However, the law currently prohibits access to the knowledge contained in computer program code. It is impossible to legally decompile a computer program in order to understand how it works.<sup>19</sup> A proposal to permit decompilation, by way of section 19B of the Copyright Amendment Bill 2017, is currently under re-consideration. However, even if this problematic provision becomes law, it will only permit decompilation in order to create an interoperable program. The proposed exception expressly prohibits creating a functionally equivalent program. Furthermore, any knowledge gained from decompilation may not be shared with anyone for any purpose. That means each program developer must incur the same substantial cost associated with decompilation before they may begin developing any database-applicable program and, even then, the result of their efforts may not be substantially similar to the program on which it was based.

### **Digital rights management criminalises access**

While copyright law provides wide and strong protection for data and databases, it does not address the cybersecurity concerns associated with digital information. Therefore, the vast majority of data and databases is protected by layers of electronic security measures, ranging from the most basic (such as passwords, biometric user authentication, watermarking and usage logging) to the extreme (an array of data and communication encryption and real-time monitoring). However, these measures are of lesser value to the data controller if there is no punishment for a transgression.<sup>20</sup>

This aspect is dealt with by another area of law, namely anti-circumvention protection or digital rights management (DRM) provisions<sup>19</sup> contained in section 86 of the *Electronic Communications and Transactions Act 25 of 2002* and set to be replaced by the more extensive provisions in chapter 2 part 1 of the *Cybercrimes Act 19 of 2020*. The DRM provision *criminalises* the act of accessing a computer program or the medium on which it is stored, if permission has not been granted or the scope of use exceeds the extent of authorisation. Using, or being in possession of, a computer program designed or adapted primarily to access data or a computer program is also a crime.<sup>8</sup> The Copyright Amendment Bill creates additional offences when the electronic means which identify the owner or prevent access or copying of the work are tampered with. This double layer of protection over software, coupled with the decompilation limitation, impedes the development of local database software.

The majority of DRM provisions are attempts, based on foreign law, to address piracy and an array of cybercrimes and are not per se unwelcome.<sup>21</sup> However, the manner in which these provisions are drafted is often draconian and pose a barrier to participation in the digital economy.<sup>20</sup> DRM law simply means that *prior* authorisation to access data must be obtained, and this permission may be withheld unless a fee is paid. This cost is in addition to the copyright licensing fee but, unlike copyright infringement, DRM infringement is a crime.

Consequently, to make government's dream of open access to data possible, it will have to amend DRM law to decriminalise certain use cases (creating significant risk) or incur the cost of obtaining permission on behalf of its intended users. What government will do if permission is refused is a worrying, but not unlikely, eventuality.

### **Conclusion**

The relationship between the law and data is a complex one. Unfortunately, the Data and Cloud Policy's ignorance of the most basic legal principles indicates an alarming disregard for private ownership and postulates a future where very little data will be safeguarded by the law to the extent it is now. Fortunately, government policy is not law and, as this article shows, many things will have to change in order to implement the policy goals. That is why every data stakeholder, in particular those who rely on the downstream value in research and development, should undertake an intellectual property rights audit as a matter of urgency. It may well be wise to divert from current strategy to safeguard their interests.

## Acknowledgements

This article was prepared with financial support from the Vice-Rector: Research, Innovation and Postgraduate Studies, Stellenbosch University.

## Competing interests

I declare that I have no competing interests. I provided research input to the author of one of the reports, published by the Mandela Institute of the University of the Witwatersrand and cited in this article, in my personal capacity.

## References

1. Draft National Policy on Data and Cloud. Government Gazette No 44389 Notice 306 (1 April 2021).
2. Beylveld A. Data protection in Kenya, Nigeria and South Africa in the 2020s and Beyond. Policy Brief 01. Johannesburg: Mandela Institute, University of the Witwatersrand; 2021.
3. World Intellectual Property Organisation (WIPO). Overview of the international protection of copyright and related rights: From the Berne Convention for the Protection of Literary and Artistic Works to the WIPO Copyright Treaty and the WIPO Performances and Phonograms Treaty WIPO/CR/DAM/05/8. Proceedings of the WIPO National Seminar on Copyright and Related Rights for Lawyers and Judges; 2005 April 27–28; Damascus, Syria. Geneva: International Bureau of WIPO; 2005. p. 1–19.
4. De la Chapelle B, Porciuncula L. We need to talk about data: Framing the debate around free flow of data and data sovereignty. Paris: Internet and Jurisdiction Policy Network; 2021.
5. Van der Berg S. Data protection in South Africa: The potential impact of data localisation on South Africa's Project of Sustainable Development. Policy Brief 02. Johannesburg: Mandela Institute, University of the Witwatersrand; 2021.
6. Shay RM, Van der Walt A. Constitutional analysis of intellectual property. *PER*. 2014;17:52–85. <https://doi.org/10.4314/pej.v17i1.02>
7. Reichman JH, Okediji RL. When copyright law and science collide: empowering digitally integrated research methods on a global scale. *Minn Law Rev*. 2012;96:1362–1480.
8. Van der Merwe DP, Roos A, Pistorius T, Eiselen GTS, Nel SS. Information and Communications Technology Law. 2nd ed. Johannesburg: LexisNexis; 2016. p. 1–49, p. 1362–1480.
9. Dean OH. Handbook of South African Copyright Law. 14th ed. Johannesburg: Juta Law Publishers; 2012.
10. Haupt t/a Softcopy v Brewers Marketing Intelligence (Pty) Ltd and Others 4 SA 458 (SCA). 2006.
11. Blignaut H. Copyright. In: Dean OH, Dyer A, editors. Dean & Dyer introduction to intellectual property law. Cape Town: Oxford University Press; 2014. p. 1–76.
12. Research ICT Africa. Written submission in response to the proposed National Data and Cloud Policy [document on the Internet]. c2021 [cited 2021 Sep 03]. Available from: [https://researchictafrica.net/wp-content/uploads/2021/06/RIA\\_Submission\\_DATA\\_and\\_Cloud\\_Policy.pdf](https://researchictafrica.net/wp-content/uploads/2021/06/RIA_Submission_DATA_and_Cloud_Policy.pdf)
13. Tong L-A. Case Comment: Copyright and computer programs, computer-generated works and databases in South Africa. *Eur Intellect Property Rev*. 2006;28:625–628.
14. Du Bois M. Intellectual property rights and the Constitution. In: Dean OH, Dyer A, editors. Dean & Dyer introduction to intellectual property law. Cape Town: Oxford University Press; 2014. p. 466–491.
15. Dean OH. The case for the recognition of intellectual property in the Bill of Rights. *J Contemp Roman Dutch Law*. 1997;60:105–119.
16. Internet Service Providers' Association. Submissions on the Proposed National Data and Cloud Policy. [document on the Internet]. c2021 [cited 2021 Sep 03]. Available from: <https://ispa.org.za/wp-content/uploads/2021/06/ISPA-Submission-Proposed-Data-and-Cloud-Policy-20210601.pdf>
17. Free Market Foundation Rule of Law Project. Submission to the Department of Communications and Digital Technologies on the National Data and Cloud Policy [document on the Internet]. c2021 [cited 2021 Sep 03]. Available from: <https://www.freemarketfoundation.com/dynamicdata/documents/20210611-submission-on-national-data-and-cloud-policy-2021.pdf>
18. Global Data Alliance. Comments to the Republic of South Africa on The Proposed Data and Cloud Policy [document on the Internet]. c2021 [cited 2021 Sep 03]. Available from: <https://globaldataalliance.org/wp-content/uploads/2021/07/05122021gdasafrdatacloud.pdf>
19. Jooste C. Copyright law and the Internet. In: Papadopoulos S, Snail S, editors. *Cyberlaw@SA*. 4th ed. Pretoria: Van Schaik; 2021. p. 181–258.
20. Samuelson P. Intellectual property and the digital economy: Why the anti-circumvention regulations need to be revised. *Berkeley Technol Law J*. 1999;14:5–10. <https://doi.org/10.1145/318536.318538>
21. Jooste C, Karjiker S. Intellectual property law in the digital environment (EIP law). In: Dean OH, Dyer A, editors. Introduction to intellectual property law. Cape Town: Oxford University Press; 2014. p. 390–465.





**AUTHOR:**  
Monika dos Santos<sup>1</sup>

**AFFILIATION:**  
<sup>1</sup>Department of Psychology,  
University of South Africa, Pretoria,  
South Africa

**CORRESPONDENCE TO:**  
Monika dos Santos

**EMAIL:**  
dsantmml@unisa.ac.za

**HOW TO CITE:**  
Dos Santos M. COVID-19 recovery  
and the health argument for climate  
action. Commentary on the WHO  
COP26 special report on climate  
change and health. *S Afr J Sci.*  
2022;118(1/2), Art. #12860. <https://doi.org/10.17159/sajs.2022/12860>

**ARTICLE INCLUDES:**  
 Peer review  
 Supplementary material

**KEYWORDS:**  
climate change, health, COVID-19,  
COP26, sustainable development

**PUBLISHED:**  
27 January 2022

# COVID-19 recovery and the health argument for climate action. Commentary on the WHO COP26 special report on climate change and health

## Significance:

- Critical climate change and health action needs to be considered globally post the COVID-19 pandemic.
- The WHO Climate Change and Health Special Report outlines 10 priority recommendations to be considered by nations and adopted at COP26.
- The special report provides South Africa with the opportunity to consider how the priority recommendations can be implemented locally.

The World Health Organization (WHO)'s release of the *COP26 Climate Change and Health Special Report: The Health Argument for Climate Action*<sup>1</sup> outlines critical action that needs to be considered by politicians, scientists, corporations and civil society, post the COVID-19 pandemic. The report was prepared in advance of the Conference of Parties (COP) meeting that was held in Glasgow in November 2021, and strives to significantly advance the call for global and local climate-smart healthcare.

Climate change is the largest and most singular danger confronting humankind, with vulnerable and disadvantaged communities progressively and most disproportionately at risk as natural ecologies become less stable.<sup>2,3</sup> Increasingly recurrent extreme and life-threatening climatic events, such as droughts and heatwaves, hurricanes and flooding, kill thousands and dislocate millions of people, whilst at the same time threaten fragile healthcare systems and facilities when they are most needed. Climatic changes are further jeopardising food security and increasing food-, water- and vector-borne diseases, such as dengue and malaria, whilst adversely impacting on mental health. Reaching the Paris Agreement targets will save millions of human lives annually due to improved air quality, diet, and physical activity, for example. Nonetheless, most current climate decision-making practices do not account for these health co-benefits and their economic impacts.<sup>2</sup> An unmitigated increase in the health impacts of climate change, and the existing health aftermaths of delayed and erratic responses of nations worldwide, evidence a distinct need for fast-tracked interventions which position the health of individuals and the planet as priorities.<sup>4</sup> As poorer populations are most defenceless against climate-induced health impacts, demand for healthcare access will also intensify in significance in South Africa and elsewhere.<sup>5</sup>

To avoid the looming health crises, global warming needs to be restricted to under 1.5 °C, while human health and equitable healthcare access need to be centrally placed in all climate change mitigation and adaptation activities. Moreover, the COVID-19 health crisis has clearly indicated the magnitude and significance of listening to the health and medical community and incorporating their views in strategic planning. It has also highlighted the inequitable impacts of such a worldwide threat. All nations need to set ambitious national climate commitments if they are to sustain a healthy and green recovery from the pandemic. Furthermore, the origins of many worldwide health crises are interlinked with the annihilation of entire ecosystems and biodiversity loss, the climate crisis, and, in particular, findings from a comparative risk assessment on the global burden of disease, indicate that air pollution causes 13 deaths per minute globally.<sup>6</sup> Lowering air pollution to WHO-recommended levels, as an example, would cut the total sum of worldwide mortalities from air pollution, which is estimated to be seven million people per year, by 80%, while simultaneously significantly limiting the greenhouse gas emissions which fuel climate change.<sup>2,7</sup> Minimising food losses, together with modifications in production approaches, has also been shown to be a pivotal means of increasing food security, while simultaneously decreasing stress on the earth.<sup>8</sup> A transition to more wholesome plant-based diets, as aligned with WHO recommendations, can also significantly cut global emissions and subsequently safeguard more resilient food systems, as well as prevent up to 5.1 million diet-related deaths a year by 2050.<sup>2</sup> Addressing air pollution and shifting today towards the direction of sustainable food systems will thus not only assist in addressing the climate crisis, but will simultaneously also improve everybody's health.

The 2021 United Nations Climate Change Conference (COP26) in Glasgow is critical in terms of current and future global climate action, and decisions made there will have sweeping significance for the long-term health of communities. As the *Lancet Countdown 2020 Report* concludes: no continent, nation, or society is resistant to the health consequences of the climate crisis.<sup>4</sup>

WHO has called on governments to pledge to more ambitious climate action and to a healthy recovery from COVID-19. To accomplish this, the WHO COP26 climate change and health special report collects health arguments on what the world needs to do, and by which means, to tackle the climate crisis.<sup>1</sup> The special report provides distinct resolutions from both the health community and policymakers. It strives to ensue representivity from across sectors, districts, and population groups, and particularly that of the expressions of the medical community. It is necessary for nations to set ambitious national climate commitments and goals if they are to advance a health and green recovery from the COVID-19 pandemic.<sup>1</sup> The WHO report was presented simultaneously as an open letter, signed by over two thirds of the international health workforce, with 300 organisations acting on behalf of at least 45 million medical doctors and other health professionals internationally, calling for heads of state and other COP26 country representatives to step up climate action. The letter stipulates the following demands<sup>2</sup>:

© 2022. The Author(s). Published  
under a Creative Commons  
Attribution Licence.



- *We call on all nations to update their national climate commitments under the Paris Agreement to commit to their fair share of limiting warming to 1.5 °C; and we call on them to build health into those plans;*
- *We call on all nations to deliver a rapid and just transition away from fossil fuels, starting with immediately cutting all related permits, subsidies and financing for fossil fuels, and to completely shift current financing into development of clean energy;*
- *We call on high income countries to make larger cuts to greenhouse gas emissions, in line with a 1.5 °C temperature goal;*
- *We call on high income countries to also provide the promised transfer of funds to low-income countries to help achieve the necessary mitigation and adaptation measures;*
- *We call on governments to build climate resilient, low-carbon, sustainable health systems; and*
- *We call on governments to also ensure that pandemic recovery investments support climate action and reduce social and health inequities.*

WHO's COP26 special report reflects consensus statements from the international health community on key actions that governments need to take in order to address the climate crisis, rebuild ecosystems, and safeguard health. It proposes 10 priority recommendations for governments to adopt in order to amplify the health benefits of addressing climate change in a number of sectors, thus avoiding the worst health impacts of the climate crisis. The following recommendations provide concrete examples of actions that, with the correct backing, can be scaled up quickly in order to preserve both health and the environment<sup>1</sup>:

1. **Commit to a healthy recovery.** This goal strives to commit to a healthy, green and just recovery post COVID-19. The next couple of months and years will provide a critical window in which to align climate change and health goals. Furthermore, the pandemic has also provided the world with an opportunity to build toward the future in a better fashion which is both green and more equitable. Climate and health goals need to be aligned, commitment needs to be made for a fossil-free recovery, the world needs to prevent and prepare for the next pandemic, health needs to be included in all policies, and, lastly, there needs to a commitment to global vaccine equity.
2. **Our health is not negotiable.** Health and social justice need to be placed at the heart of the United Nations Framework Convention on Climate Change (UNFCCC) climate talks. In order to achieve this goal, the 1.5 °C gap needs to be closed in order to survive, the scaling up of finance for vulnerable countries needs to be mobilised in order to tackle climate change, support for adaptation and resilience efforts needs to be stepped up, and the finalisation of the Paris Agreement Rulebook needs to take place.
3. **Harness the health benefits of climate action.** Climate interventions with the largest health and socio-economic gains need to be prioritised. In order to do this, health co-benefits of climate action need to be identified and measured at all levels of governance and maximised, everyone's right to health needs to be honoured, and the science of health and climate change should be bolstered.
4. **Build health resilience to climate risks.** Climate resilient and environmentally sustainable health systems and facilities need to be built and health adaptation and resilience across sectors supported. This will require iterative health vulnerability and adaptation assessments, the development and implementation of evidence-based adaptation plans for health and the health sector, strengthening climate resilience and environmental sustainability of health systems and facilities, addressing the lack of financing for health and adaptation resilience, and, lastly, protecting health

and advancing climate justice by implementing health-promoting interventions in other sectors.

5. **Create energy systems that protect and improve climate and health.** A just and inclusive transition to renewable energy to save lives from air pollution, particularly from coal combustion, needs to be undertaken. Energy poverty in households and healthcare facilities needs to be ended. Investing in clean solutions for household energy needs to be pursued, and powering the health sector with clean energy, and ensuring a just transition for workers and communities transitioning out of the fossil fuel sector, need to be prioritised.
6. **Reimagine urban environments, transport and mobility.** The promotion of sustainable, healthy urban design and transport systems, with improved land use, access to green and blue public spaces, and priority for walking, cycling and public transport, needs to be prioritised. In order to achieve this goal, the phasing out of internal combustion engines needs to take place as well as the reduction of private car use; walking, cycling and ventilated public transport needs to be prioritised, and the creation of people-centred cities needs to be pursued.
7. **Protect and restore nature as the foundation of our health.** We need to protect and restore natural systems which constitute the foundation for healthy lives, sustainable food systems, and livelihoods. Action points here include ending our destruction and degradation of nature, protecting and restoring the ecosystems that we all depend on, recognising the interconnections between human, animals and ecosystem health, promoting nature-based solutions and nature-based recovery, protecting people and planet by implementing a new global biodiversity framework.
8. **Promote healthy, sustainable and resilient food systems.** The promotion of sustainable and resilient food production geared towards more affordable and nutritious diets will deliver on both climate and health outcomes. Harmful and discriminatory agricultural subsidies, such as those supporting the meat and dairy industry (which contributes significantly to the rise in global greenhouse gases) and only large-scale farmers, should be removed to support a just agricultural transition which supports sustainable food systems and local small-scale farming. This transition will in turn mainstream biodiversity for nutrition and health.
9. **Finance a healthier, fairer and greener future to save lives** by transitioning towards a well-being economy, which needs to be actioned by: stopping the funding of pollution, closing the health finance gap, ensuring that public finance does no harm, and providing debt relief to vulnerable nations.
10. **Listen to the health community and prescribe urgent climate action.** Include the healthcare communities' voices in planning for climate change. Action also needs to be taken to mobilise and support the health community on climate action by training the health workforce to respond to climate change, taking climate action in the healthcare sector, enabling health professional advocacy on climate change and health, and lastly by protecting the health of future generations.

The special report emphasises that individual health can be protected by transformational acts in every sector, including the engineering, energy, transport, urban design, nature, food systems and finance sectors. It points to the potential for public health co-benefits of climate change interventions to offset their costs, and provides South Africa with the opportunity to reflect and carefully consider how priority recommendations may be implemented locally.<sup>1</sup>

## References

1. World Health Organization (WHO). COP26 Special report on climate change and health: The health argument for climate action. Geneva: WHO; 2021.



2. World Health Organization (WHO). WHO's 10 calls for climate action to assure sustained recovery from COVID-19: Global health workforce urges action to avert health catastrophe [news release]. 2021 October 11. Available from: <https://www.who.int/news/item/11-10-2021-who-s-10-calls-for-climate-action-to-assure-sustained-recovery-from-covid-19>
  3. Dos Santos M. Climate change, the fourth industrial revolution and sustainable development in Africa. *Africa Insight*. 2020;49:4.
  4. Romanello M, McGushin A, Di Napoli C, Drummond P, Hughes N, Jamart L, et al. The 2021 report on the Lancet Countdown on health and climate change: Code red for a healthy future. *Lancet*. 2021;398(10311):1619–1662. [https://doi.org/10.1016/S0140-6736\(21\)01787-6](https://doi.org/10.1016/S0140-6736(21)01787-6)
  5. Dos Santos M, Howard D, Kruger P, Banos A, Kornik S. Climate change and healthcare sustainability in the Agincourt sub-district, Kruger to Canyons Biosphere Region, South Africa. *Sustainability*. 2019;11, 2. <https://doi.org/10.3390/su11020496>
  6. Amnuaylojaroen T, Parasin N. The association between COVID-19, air pollution, and climate change. *Front Public Health*. 2021;6, 9. <https://doi.org/10.3389/fpubh.2021.662499>
  7. World Health Organization. Air pollution [webpage on the Internet]. c2021 [cited 2021 Oct 29]. Available from: [https://www.who.int/health-topics/air-pollution#tab=tab\\_1](https://www.who.int/health-topics/air-pollution#tab=tab_1)
  8. Kosseva MR, Webb C. Food industry wastes: Assessment and recuperation of commodities. Amsterdam: Academic Press; 2020.
-





#### AUTHORS:

Alan T.K. Lee<sup>1,2,3</sup>   
Michael Brooks<sup>2</sup>  
Les G. Underhill<sup>4,5</sup>

#### AFFILIATIONS:

<sup>1</sup>Centre for Functional Biodiversity, School of Life Sciences, University of KwaZulu-Natal, Pietermaritzburg, South Africa

<sup>2</sup>FitzPatrick Institute of African Ornithology, Department of Biological Sciences, University of Cape Town, Cape Town, South Africa

<sup>3</sup>BirdLife South Africa, Isdell House, Johannesburg, South Africa

<sup>4</sup>Department of Biological Sciences, University of Cape Town, Cape Town, South Africa

<sup>5</sup>Biodiversity and Development Institute, Cape Town, South Africa

#### CORRESPONDENCE TO:

Alan Lee

#### EMAIL:

alan.lee@birdlife.org.za

#### HOW TO CITE:

Lee ATK, Brooks M, Underhill LG. The SABAP2 legacy: A review of the history and use of data generated by a long-running citizen science project. *S Afr J Sci.* 2022;118(1/2), Art. #12030. <https://doi.org/10.17159/sajs.2022/12030>

#### ARTICLE INCLUDES:

Peer review

[Supplementary material](#)

#### KEYWORDS:

citizen science, South Africa, bird atlas, ornithology, database

#### PUBLISHED:

27 January 2022

# The SABAP2 legacy: A review of the history and use of data generated by a long-running citizen science project

#### Significance:

- The Second Southern African Bird Atlas Project (SABAP2) – initiated in 2007 – is one of the region's longest-running citizen science programmes and collects spatial and temporal data on birds.
- Data from the project are publicly available and used extensively by environmental impact assessment practitioners, conservationists, authors, protected area managers, scientists and the general public.
- The project is the template for other established projects that now operate across the continent, collectively now falling under the 'African Bird Atlas Project' umbrella.
- We show that since the initiation of SABAP2, there has been a three-fold increase in publications, with over 150 papers that can be attributed to SABAP2.
- The contribution of citizen scientists to the published scientific domain has been enormous.

One of the largest citizen science projects in Africa is the Second Southern African Bird Atlas Project (SABAP2). SABAP2 is a follow-up project of the Southern African Bird Atlas Project (now labelled SABAP1). The primary data collection period for the first bird atlas project was 1987 to 1991; it incorporated data from as far back as 1980, and in some regions included data until 1993, assembling a total of 7.2 million records of bird distribution.<sup>1</sup> SABAP1 generated the *Atlas of Southern African Birds* in two volumes.<sup>2</sup> Harrison et al.<sup>3</sup> demonstrated that the SABAP1 database had become a valuable resource to four main user constituencies: environmental consultants, conservationists, research scientists, and birders. Academic research output (theses and papers) was summarised by Underhill<sup>4</sup>; most of the 102 papers and 19 postgraduate theses listed had been based on SABAP1 data.

The 'second' atlas project, SABAP2, was launched in 2007 and was ongoing in 2021. There is currently no planned end to the project, as the database is recognised as providing useful information in a changing world.<sup>5</sup> The BirdMap data collection protocol has been extended into Nigeria and Kenya, including bespoke websites and data curation, with data collected through these projects falling under the umbrella of the 'African Bird Atlas Project'.<sup>6,7</sup> The SABAP2 data are already extensively used: in scientific publications to inform conservation management; species conservation assessments; and in environmental impact assessments. We summarise this use here.

The initial principal aim of the bird atlas projects was to produce avian range maps from the sightings of volunteers contributing bird lists from various geographic locations.<sup>2</sup> However, the systematic data collection protocol allows an investigation of a wide variety of conservation and academic questions.<sup>8</sup> Today, the continued strength of the project is the easy calculation of relative abundance, which is possible due to multiple lists contributed for each sampling area. Global range maps are recently better visualised using the eBirds global database, which taps into a much larger citizen science contributor database<sup>9</sup>, although, for the southern African subregion, SABAP2 is still the best source of distributional information given the data vetting processes in place to check data quality.<sup>10</sup> Indeed, SABAP2 lists can be exported into eBird data for submission to that database through the BirdLasser bird recording software.<sup>11</sup> Due to the long-term undertaking of SABAP2, it is also becoming increasingly important for evaluation of population trend analyses.<sup>12</sup>

The objectives of this paper are to describe the background to the SABAP2 database and examine the use of the data in the publication record.

## African Bird Atlas Project description

SABAP2 and the BirdMap protocol were the foundations of the African Bird Atlas Project. This project is now the umbrella for country-specific citizen science projects that collect bird list data submitted by the bird watching community using the 'BirdMap' protocol. The African Bird Atlas Project encourages and facilitates participation through birding (birdwatching) communities through three established projects, each with their own websites. Apart from SABAP2, the Kenya Bird Map Project manages a core team that focuses on collecting data across Kenya (<http://kenya.birdmap.africa/>)<sup>6</sup>, and the same for the Nigeria Bird Atlas Project (<http://nigeria.birdmap.africa/>)<sup>7</sup> in conjunction with the A.P. Leventis Ornithological Research Institute. There are start-ups in other African countries (Liberia, Ghana, Sierra Leone, Cameroon, Uganda, and Malawi, among others).

Data in the form of spatially and temporally explicit bird lists are collected by volunteer 'citizen scientists' from diverse backgrounds: both professional ornithologists and amateur birders. Participation is entirely voluntary; participants register with SABAP2, Nigeria Bird Atlas Project or Kenya Bird Map to receive their unique 'Citizen Science' membership number, which allows them to keep track of their data. Each project has a website interface where volunteers can plan their atlas activities and keep track of their own data submissions.

### *BirdMap protocol*

African Bird Atlas Project data collection follows a simple protocol.<sup>8</sup> Lists are collected within a geographical pentad, which is a grid cell on a map corresponding to five geographical minutes of latitude north-south and

5-minute by 5-minutes of longitude east–west. Where lists meet the minimum survey requirements of 2 hours birding effort and attempts to reach all accessible habitats, they are marked as ‘Full Protocol’, and ‘Ad-hoc Protocol’ otherwise. Each full protocol list represents a minimum of 2 hours active birding in a pentad, up to a maximum of 5 days, after which a new list may be started by the observer who initiated the list. The number of new species added every hour is recorded. Initially, various observers contributed to a single list; it is now more common to have individuals compiling their own lists due to the gamification of the current submission software (BirdLasser).<sup>11</sup>

### A brief history of the African Bird Atlas Projects

The first South African Bird Atlas Project (SABAP1) took place from 1986 to 1997, with data collection representing the period 1987 to 1992. The initiative was based out of the Avian Demography Unit (now retired) at the University of Cape Town, building on various regional atlas projects conducted prior to this period.<sup>13,14</sup> The methods and protocol are outlined in detail in *The Atlas of Southern African Birds*.<sup>2</sup> In essence, the birding community of southern Africa was encouraged to collect their sightings of birds in a standardised format by compiling their lists per quarter degree grid cell geographic areas (QDGC, (approximately 27 km long (north–south) and 23 km wide (east–west)); but larger half degree grid cells in Botswana). Volunteers were sent introductory materials, including an instruction booklet and printed checklists. Lists were compiled by hand and sent to the University of Cape Town for data checking, entry, and upload.

SABAP1 gathered 7.2 million peer-reviewed distribution records for 932 bird species in the southern African sub-region, contributed by more than 5000 birdwatchers.<sup>3</sup> It covered six southern African countries (Botswana, Lesotho, Namibia, South Africa, Swaziland, and Zimbabwe). Mozambique was excluded due to the civil war in that country at that time. It was the first time a biological survey had been attempted on anything like that scale in Africa. Indeed, SABAP1 remains one of the largest completed projects of its kind, even globally.<sup>3</sup> The resulting published atlas volumes contained contributions by 62 authors and seven editors.<sup>3</sup>

The second atlas project (SABAP2) was directed as of 2006 by Les Underhill at the Animal Demography Unit. Data collection started in 2007 and is ongoing. SABAP2 is currently managed by the FitzPatrick Institute of African Ornithology. The data collection protocol was similar to that used for SABAP1, but at a finer spatial and temporal resolution – using pentads (5 × 5 geographical minutes: there are nine pentads in a QDGC) and recording species over at most 5-day periods, compared to monthly lists in SABAP1. There was also an attempt to standardise the minimum time effort for a list to count towards estimates of species reporting rates (2 hours and effort to cover all major habitats for lists to qualify as ‘full protocol’ lists). In addition, species were to be reported in the order sighted, on the assumption that more common species will appear earlier on species lists and rare species generally recorded last, on average.<sup>10</sup>

By 2009, the second full year of SABAP2, citizen scientists were submitting c. 17 000 checklists per year to the project; this remained stable until 2014. In 2015, a combination of the initiation of a series of Citizen Scientist Days and the introduction of mobile apps, especially BirdLasser, resulted in an increase in the rate of submission of checklists to c. 30 000 per year (Table 1). There was a decrease in submissions in 2020 due to the COVID-19 pandemic.

### Citizen scientists and their contributions

In August 2021 there were 3106 registered contributors to the African Bird Atlas Projects, with those registered with SABAP2 representing the majority of these: 2501 observers, followed by Kenya (348), Nigeria (196) and others (61). However, it is rare to have more than 850 observers contributing full protocol checklists in any one year to SABAP2 (Table 1). Many of the registered observers with SABAP2 are inactive: 448 registered SABAP2 users have submitted just one checklist. On the other hand, others have been involved through both SABAP1 and SABAP2: for instance, Dawie de Swardt (affiliated with the

**Table 1:** Annual SABAP2 milestones for coverage of South Africa, Lesotho and eSwatini in terms of the total number of contributing observers, with the total number of checklists contributed and the number of pentads. Percentage coverage is based on a potential 17 444 pentads for this geographical region.

Year	Checklists	Observers	Pentads	Cumulative pentads	Coverage (%)
2007	1916	264	953	953	5.5
2008	9791	457	3164	3409	19.5
2009	17 372	558	4759	5993	34.4
2010	18 419	615	5353	8170	46.8
2011	17 563	585	5418	9809	56.2
2012	16 460	551	5084	10 928	62.6
2013	15 393	565	4391	11 537	66.1
2014	17 868	618	4784	12 314	70.6
2015	22 196	719	4916	12 912	74
2016	26 159	859	4999	13 402	76.8
2017	26 435	861	4898	13 706	78.6
2018	25 244	811	4612	14 009	80.3
2019	22 107	805	4282	14 181	81.3
2020	14 425	692	3746	14 313	82.1
<b>Average</b>	<b>17 953</b>	<b>640</b>	<b>4383</b>		

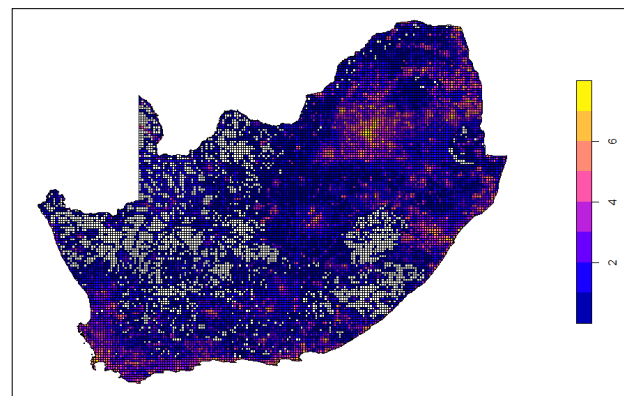


**Figure 1:** A coverage map of South Africa, Lesotho and eSwatini, indicating the numbers of cards per pentad. Colours are based on the log of the number of checklists for each pentad. Grey pentads have no full protocol cards. Urban and proximate areas are well covered, while Lesotho, the far Eastern Cape and Northern Cape are generally poorly covered.

National Museum in Bloemfontein, but atlas contributor in his private capacity<sup>15</sup>) was involved in Regional Atlas Committees for both.

At the end of 2020, the number of full protocol checklists was 251 348 and ad-hoc checklists was 165 885. The majority came from relatively few prolific contributors, with 68 observers having contributed more than 1000 checklists. The top 20 contributors are acknowledged in [Supplementary table 1](#). However, some of the most valuable data comes from occasional contributors who submit just a handful of checklists from out-of-the-way places.

Branded to gainfully use time in a safe yet meaningful manner, as well as ‘contributing to science’, the nourishing effects on emotional well-being and mental health have been highlighted as benefits of birding ‘with a cause’.<sup>16</sup> Volunteers in SABAP2 were satisfied and exhibited behaviours suggesting they act as advocates for the programme.<sup>17</sup> Atlasers (the term used to describe contributors to the African Bird Atlas Project) travel large distances to contribute to the atlas, often engaging with landowners on bird conservation issues.<sup>3</sup>

Of great value to the project in terms of data generation, and also to atlas participants who gain a sense of camaraderie, are ‘atlas bashes’. These can be once-off expeditions to target remote regions or encourage systematic repeated data collection over a defined geographical region, for example, the ‘Four Degrees region of Greater Gauteng: the challenge to obtain at least 11 checklists in 576 pentads’.<sup>18</sup> The systematic atlasing coordinated by Johan van Rooyen in Stilbaai is a further exemplary case of how to maximise coverage with a small team of people.<sup>19</sup>

## Data availability

Publicly available data can be obtained for species or locations (pentads) via the project websites (<http://sabap2.birdmap.africa/>) or via an R package *rabm* (<https://github.com/davidclarance/rabm>). For locations, this includes species lists at various temporal intervals (total, annual, monthly), allowing examination of trend data and annual patterns of occurrence. Species occurrence data are available either as reporting rates in pentads, allowing broadscale distribution modelling, or can be obtained including null counts, which allows for better modelling of factors influencing occurrence. Species reporting rate data are also available as geoJSON files, which can be used in GIS software. A comparison of SABAP2 vs SABAP1 reporting rates is also available. Bespoke data products are also available by arrangement with the project coordinators.

## Examining output and trends in publications referring to SABAP

Given the lack of a centrally citable resource for use of the SABAP2 database, tracking use and output from the available database is extraordinarily difficult because the data are free to download in various formats with no registration or declaration of use required. For instance, a set of the SABAP2 data has been shared with the GBIF global biodiversity database, which is used by global ecologists to model broad biological or ecological questions using multiple data channels. That set of the data alone had been cited 43 times as of 3 June 2021 according to the database description landing page (<https://www.gbif.org/dataset/906e6978-e292-4a8b-9c39-adf6bb0f3323>).

A set of publications brought to the attention of project coordinators is available on the project website (<http://sabap2.birdmap.africa/media/bibliography#pgcontent>). This set is based on the initial bibliography of peer-reviewed articles, theses and semi-scientific papers that make substantial use of the SABAP data.<sup>4</sup> As of 1 June 2021, the website contained 201 documents, including both peer-reviewed articles and non-peer reviewed newsletters or reports.

To perform as comprehensive a survey as possible of wider use and recognition, we used the ‘Publish or Perish’ software<sup>20</sup> to implement a keyword search based on search terms ‘SABAP’, ‘Southern African Bird Atlas’ and ‘SABAP2’ through the Google Scholar search engine, excluding patents and citations. Searches were saved as .csv files and imported into R<sup>21</sup> for further data cleaning and analysis. Attempts to search by the previously mentioned GBIF DOI were also attempted but returned no results.

Search results were manually scanned for relevance. The ‘SABAP’ search term alone returned 1190 results; however, as ‘sabap’ has alternative meanings in other languages, many results were not relevant. After excluding these, combining search results across search terms, and excluding repeated and irrelevant results, 717 documents and publications – representing a mix of books, html documents, 145 environmental impact assessments, and peer-reviewed articles – referred to the atlas projects.

Of 275 identified peer-reviewed articles, 186 were published after 2006, corresponding with the SABAP2 period. Separating articles that merely refer to SABAP rather than make use of the data was harder to gauge. For instance, the two articles with the greatest citations referred to research related to SABAP,<sup>22,23</sup> but did not make use of the data. Of the 717 articles, 94 specifically mention SABAP2 in either title or abstract. However, many articles which made use of SABAP2 data (including all the GBIF articles) did not mention this in the title or abstract.<sup>24,25</sup> As a minimum estimate based on the above filters, SABAP2 data alone has contributed to at least 150 peer-reviewed articles, and likely many more.

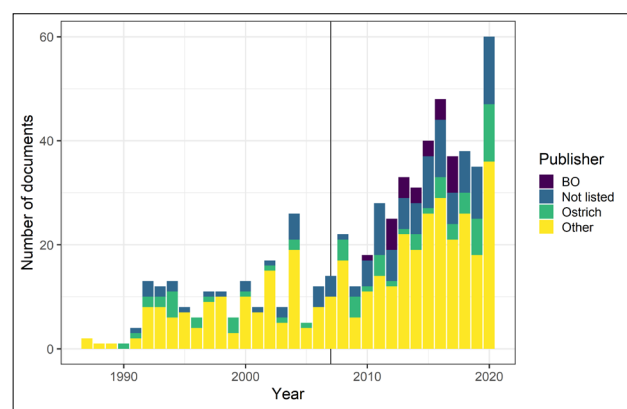
In addition, the atlas projects are often referred to in publications specifically on the growing field of citizen science research: these publications do not actually use SABAP data (e.g. Wright et al.<sup>17</sup>). Many of the articles that refer to the atlas project or use the data are in themselves highly influential (Supplementary table 2).

Plotting the temporal pattern of publication data from the Google Scholar search results reveals a linear increase in publications per year from the initiation of SABAP2 in 2007, until about 2015, and a tripling of research output compared to the period before this associated with SABAP1 (Figure 2). In both 2016 and 2020, more than 40 articles referred to the atlas projects; these articles were associated with a series in *Biodiversity Observations* (2016) and a special issue of *Ostrich* on the theme of citizen science.<sup>26</sup>

## A recipe for value and success

The SABAP2 project has been a success due to a mutually beneficial triumvirate of three organisations: South African National Biodiversity Institute (SANBI; a governmental organisation), University of Cape Town (UCT; academic institution) and BirdLife South Africa (a non-governmental organisation). SANBI initially sponsored the project, implementing the database vision of Les Underhill at the Animal Demography Unit of UCT, with the mobilisation of the key data contributors (birders) encouraged by BirdLife South Africa. Currently, the African Bird Atlas Project provides extraordinary value at no cost to data users. The entire project is run essentially on volunteers, both citizens and professionals, contributing time, money and resources. Provisional estimates suggest that the value of the in-kind contributions by citizen scientists exceeds ZAR40 million per year – more than 25 times the cost of maintaining the core team which runs the project.

In 2021 there were essentially two salaried positions at UCT: the database manager and a communications officer. After Les Underhill’s retirement, the institutional support of the FitzPatrick Institute at UCT has been critical to maintaining the project, which provides the administrative envelope for delivering the current features. The partnership with BirdLife



BO = *Biodiversity Observations*; ‘Not listed’ represents missing data for titles or publisher, usually associated with web documents and reports.

**Figure 2:** The number of documents from Google Scholar search results per year that directly refer to SABAP or the atlas in the title or keywords. The vertical line indicates the initiation of SABAP2 in 2007.





South Africa, which salaries a position which carries the role of SABAP2 coordinator, among other roles, has been critical for maintaining momentum in data contributions through continued promotion and training. Financing for the database manager position was partly through SANBI for 18 years, supplemented by private donations, and contributions from the FitzPatrick Institute since 2020. In addition, the entire data submission pathway via BirdLasser software is independently funded by Lejint Inc.<sup>11</sup>

Here we have quantified academic use of the database, but the value extends into many more dimensions that are harder to quantify: social, economic and cultural. On a day-to-day basis, the data are used for an extraordinary cross section of purposes, from planning holidays to informing industrial development. BirdLife South Africa has used the data in a number of projects: the Important Bird Area Directory,<sup>27</sup> the 2015 Red List Assessment<sup>28</sup>, current environmental impact assessment site-screening tools, and within BirdLife South Africa to motivate for research projects.

Given the value of this project, and the ethos of open data (conditional for early SANBI support), the support of this position through government institutions makes sense – this is after all an area where citizen science taxpayers would be happy to see their money spent. Nonetheless, project funding has been a constant source of struggle for almost the entire history of the project. SANBI's annual investment has resulted in a product worth millions of rands because of the money spent by atlasers. If ever there was proof of the value of the project, both to local conservation and to informing a wide spectrum of global scientific research, this review reveals the extraordinary publication output from the SABAP2. Needless to say, this output is also only the tip of the iceberg in terms of the potential of this extensive and impressive database.

## Acknowledgements

We thank all contributors, both citizens and scientists, and funders of the African Bird Atlas Projects. We also thank Ernst Retief and Dawie de Swardt for comments on draft versions of the manuscript.

## Competing interests

M.B. is employed by the FitzPatrick Institute to manage the African Bird Atlas Project databases.

## References

- Harrison JA, Underhill LG. Introduction and methods. In: Harrison JA, Allan DA, Underhill LG, Herremans M, Tree AJ, Parker V, et al., editors. The atlas of southern African birds Vol 1: Non-passerines. Johannesburg: BirdLife South Africa; 1997. p. xliii–lxv.
- Harrison JA, Allan DG, Underhill LG, Herremans M, Tree AJ, Parker V, et al. The atlas of southern African birds (Vol 1 & 2). Johannesburg: BirdLife South Africa; 1997.
- Harrison JA, Underhill LG, Barnard P. The seminal legacy of the southern African bird atlas project. *S Afr J Sci*. 2008;104(3–4):82–84.
- Underhill LG. Bibliography: Research papers and postgraduate theses which have been largely dependent on data from the Southern African Bird Atlas Projects. *Biodivers Obs*. 2016;7(43):1–13.
- Barnard P, Altwegg R, Ebrahim I, Underhill LG. Early warning systems for biodiversity in southern Africa – How much can citizen science mitigate imperfect data? *Biol Conserv*. 2017;208:183–188. <https://doi.org/10.1016/j.biocon.2016.09.011>
- Kung'u G, Jackson CH. Kenya Bird Map: Achievements from January 2014 to December 2016. *Biodivers Obs*. 2017;8(30):1–6.
- Tende T, Ivande S, Ottoson U. Nigeria Bird Atlas Project: How far so far? Progress report August 2016. *Biodivers Obs*. 2016;7(50):1–3.
- Underhill LG, Brooks M, Loftie-Eaton M. The Second Southern African Bird Atlas Project: Protocol, process, product. *Vogelwelt*. 2017;137:64–70.
- Sullivan BL, Wood CL, Iliff MJ, Bonney RE, Fink D, Kelling S. eBird: A citizen-based bird observation network in the biological sciences. *Biol Conserv*. 2009;142(10):2282–2292. <https://doi.org/10.1016/j.biocon.2009.05.006>
- Harebottle DM, Smith N, Underhill LG, Brooks M. Southern African bird atlas project 2: Instruction manual. Cape Town: Animal Demography Unit, University of Cape Town; 2007.
- Lee ATK, Nel H. BirdLasser: The Influence of a Mobile App on a Citizen Science Project. *Afr Zool*. 2020;55(2):155–160. <https://doi.org/10.1080/15627020.2020.1717376>
- Brown M, Arendse B, Mels B, Lee ATK. Bucking the trend: The African black oystercatcher as a recent conservation success story. *Ostrich*. 2019;90(4):327–333. <https://doi.org/10.2989/00306525.2019.1679904>
- Parker V. Statistical analysis of bird atlas data from Swaziland [MSc thesis]. Cape Town: University of Cape Town; 1995.
- Parker V. Modelling the distribution of bird species in Swaziland in relation to environmental variables. *Ostrich*. 1996;67(3–4):105–110. <https://doi.org/10.1080/00306525.1996.9639693>
- De Swardt DH. 2925BD Hagesdam – SABAP1 and SABAP2 compared. Vol. 3. *Biodivers Obs*. 2012;3:109–122.
- Rose S, Suri J, Brooks M, Ryan PG. COVID-19 and citizen science: Lessons learned from southern Africa. *Ostrich*. 2020;91(2):188–191. <https://doi.org/10.2989/00306525.2020.1783589>
- Wright DR, Underhill LG, Keene M, Knight AT. Understanding the motivations and satisfactions of volunteers to improve the effectiveness of citizen science programs. *Soc Nat Resour*. 2015;28(9):1013–1029. <https://doi.org/10.1080/08941920.2015.1054976>
- Ainsley J. The SABAP2 “Four Degrees Blue” project: The challenge to obtain at least 11 checklists in 576 pentads. *Biodivers Obs*. 2016;7(39):1–7.
- Van Rooyen J. Systematic atlasing in Hessequa – moving from mapping to monitoring. *Biodivers Obs*. 2018;9(10):1–13. <https://doi.org/10.15641/bo.v9i0.508>
- Harzing AW. Publish or perish [software on the Internet]. c2007. Available from: <https://harzing.com/resources/publish-or-perish>
- R Core Team. R: A language and environment for statistical computing. Vienna: R Foundation for Statistical Computing; 2021. Available from: <https://www.R-project.org/>
- Bibby CJ, Burgess ND, Hillis DM, Hill DA, Mustoe S. Bird census techniques. Elsevier; 2000.
- Gotway CA, Young LJ. Combining incompatible spatial data. *J Am Stat Assoc*. 2002;97(458):632–648. <https://doi.org/10.1198/016214502760047140>
- Van der Niet T, Pirie MD, Shuttleworth A, Johnson SD, Midgley JJ. Do pollinator distributions underlie the evolution of pollination ecotypes in the Cape shrub *Erica plukenetii*? *Ann Bot*. 2014;113(2):301–316. <https://doi.org/10.1093/aob/mct193>
- Gula J, Weckerly F, Sundar KG. The first range-wide assessment of saddle-billed stork *Ephippiorhynchus senegalensis* distribution. *Ostrich*. 2019;90(4):347–357. <https://doi.org/10.2989/00306525.2019.1696900>
- Harebottle DM. The value of citizen science projects to African ornithology. *Ostrich*. 2020;91(2):139–140. <https://doi.org/10.2989/00306525.2020.1783851>
- Marnewick MD, Retief EF, Theron NT, Wright DR, Anderson TA. Important bird and biodiversity areas of South Africa. Johannesburg: BirdLife South Africa; 2015.
- Taylor MR, Peacock F, Wanless RM. The 2015 Eskom red data book of birds of South Africa, Lesotho and Swaziland. Johannesburg: BirdLife South Africa; 2015.

**AUTHORS:**

Erwin J.J. Sieben<sup>1</sup>   
 Šerban Procheş<sup>1</sup>   
 Aluoneswi C. Mashau<sup>2</sup>   
 Moleseng C. Moshobane<sup>2,3</sup>

**AFFILIATION:**

<sup>1</sup>School of Agricultural, Earth, and Environmental Sciences, University of KwaZulu-Natal, Durban, South Africa  
<sup>2</sup>National Herbarium, South African National Biodiversity Institute (SANBI), Pretoria, South Africa  
<sup>3</sup>Department of Biology, Sefako Makgatho Health Sciences University, Pretoria, South Africa

**CORRESPONDENCE TO:**

Erwin Sieben

**EMAIL:**

siebene@ukzn.ac.za

**DATES:**

**Received:** 22 June 2021

**Revised:** 10 Sep. 2021

**Accepted:** 13 Sep. 2021

**Published:** 27 Jan. 2022

**HOW TO CITE:**

Sieben EJJ, Procheş S, Mashau AC, Moshobane MC. The alignment of projects dealing with wetland restoration and alien control: A challenge for conservation management in South Africa. *S Afr J Sci.* 2022;118(1/2), Art. #11540. <https://doi.org/10.17159/sajs.2022/11540>

**ARTICLE INCLUDES:**

- Peer review
- Supplementary material

**DATA AVAILABILITY:**

- Open data set
- All data included
- On request from author(s)
- Not available
- Not applicable

**EDITOR:**

Teresa Coutinho

**KEYWORDS:**

invasive species, Expanded Public Works Programme, ecological restoration, revegetation, wetland plants

**FUNDING:**

Water Research Commission (project K5/1980)



# The alignment of projects dealing with wetland restoration and alien control: A challenge for conservation management in South Africa

An inventory of wetland vegetation across the country generated a list of the most common invasive alien plants across South Africa. Many of the plants on that list do not correspond with the priorities in the programmes for alien control across the country, as they are not listed on a government produced list that guides the priorities for alien control. We explore the reasons for this situation. We argue that because wetlands are such important parts of the landscape, invasive aliens in wetlands are of special concern, and there should be more alignment between alien control programmes and wetland rehabilitation programmes. This alignment starts by considering the full number of species that form a threat to wetland habitats, but also considers which pesticides to use, erosion and recolonisation in wetlands, planting indigenous vegetation after aliens have been removed, and strategising by working from upstream to downstream. Existing alien control programmes for specific grasses (some relatively new to the country and in the phase of early detection) and floating aquatic plants may guide how to tackle the invasions of grasses and forbs that have been established in South African wetlands for an extended period of time.

**Significance:**

- Wetlands have a distinct set of alien invasive plants that affect their ecology and functioning and many of these plants are not listed as priorities in alien control programmes.
- Many restoration projects have an element of removing invasive plants and revegetating. Wetland restoration and alien control need to be integrated to preserve water resources.

## Introduction

Two of the biggest conservation challenges that South Africa faces are the control of invasive alien plants and the prevention of the loss of wetland resources against land degradation. The government invests heavily in programmes that address these challenges while employing large numbers of low-skilled workers in public works programmes.<sup>1,2</sup> These programmes profess to pursue the same goals, which are the protection of biodiversity and enhancement of ecosystem services, which, in the context of a semi-arid country, revolve for a large part around protecting the condition of water resources. It is therefore surprising to find that there is little alignment between the programmes that aim to restore wetland habitats and those that remove invasive alien plants from them as most of the species that are targeted for alien control do not correspond with the invasive species that are commonly found in wetlands. Therefore, many of the invasive species that particularly affect wetland ecosystems are considered to have a low priority in alien control programmes.

Many invasive plant species are known to thrive in habitats that are regularly disturbed, such as riverbanks, which are naturally subject to regular flooding and removal of vegetation, and rivers also aid in the dispersal of seeds.<sup>3</sup> Rivers and their immediate environments are often among the worst invaded parts of a landscape,<sup>4</sup> and many of the efforts in alien control have focused on these areas. Therefore, there is an awareness of the connection between drainage networks and alien invasion, but this has not yet translated into systematic on-site control of invasive aliens in wetlands, when we recognise wetlands as distinct habitats within the drainage network, that are different from riverbanks. Invasive aliens growing along riverbanks are known to use excessive amounts of water and this is one of the reasons for their systematic removal from important catchments. They have their own dynamics; and guidelines for managing invasive alien plants in these areas are well developed.<sup>5,6</sup>

Wetlands in this study are defined as any terrestrial area where water is present at or close to the surface area for at least part of the year, the depth of which is never higher than 6 m.<sup>7</sup> This definition includes seepages, rivers, shallow lakes and saline pans, which are all areas that are inundated for extended periods of time and this inundation represents the main stress on vegetation. However, riverbanks are high-energy disturbance-prone environments that often do not get inundated for prolonged times and therefore not all riparian corridors can be regarded as wetlands. Wetlands are limited in extent but have a disproportionate role in many landscape-level ecosystem processes, often being referred to as the ‘kidneys of the landscape’ with reference to their role in biogeochemical cycles.<sup>8</sup> Invasions in these parts of the landscape should therefore be regarded as having high consequences for the landscape as a whole, even though the invaded areas may be limited in size due to the restrictions imposed by the size of the wetland. There are specific groups of plants that thrive in wetland environments that are defined as such, and these are not necessarily the same species as those that thrive on riverbanks.

When biological invasions take place in wetland environments, it should be a priority to understand what impact they have on wetland functioning and on the broader water cycle in the surrounding landscape. Wetlands are positioned in such a way in the landscape that it is nearly certain that invasions in them will have high social and ecological consequences<sup>9</sup>, and this has implications for strategic planning around invasions in wetlands<sup>1</sup>. Species that are capable of surviving and establishing in a wetland environment need to have a certain number of morphological and physiological adaptations, but many of the traits required for this survival are also traits that

benefit the invasiveness of organisms (clonal growth, large numbers of light seeds, high rate of resource capture<sup>10</sup>) and it is therefore expected that there will be a subset of the invasive species in South Africa that is particularly successful in invading wetland habitats. It also means that combating alien invasives in these habitats must not affect indigenous species with similar properties.

In this paper, we provide an overview of the problem of alien invasive species and how in particular they affect wetland ecosystems, with regard to species composition and ecological restoration. We focus on which species are mostly problematic in wetland habitats, speculate on why they may have been neglected in alien eradication programmes, and discuss some general problems that we have to face when dealing with invasion in wetland habitats.

## Species that invade wetland habitats

Within the group of plants that have invaded South Africa so far, a limited number of species have created such problems that they have been prioritised for clearing and targeted for alien control.<sup>11</sup> Which species are included on the list of invasive species targeted to this effect, represents a critical decision within every integrated plan for control of invasives.<sup>12,13</sup> Legislation around alien control in South Africa's natural ecosystems is provided by the *National Environmental Management: Biodiversity Act No. 10 of 2004* (NEMBA). The invasive species that are targeted for alien control programmes are listed in the NEMBA legislation, whereby the species are categorised in different classes, with different strategies to prevent their further spread and their eventual eradication.<sup>14</sup> If wetland species are well represented on this NEMBA list, we would expect the majority of the most common alien invaders in wetlands to feature prominently on this list, as widespread occurrence of an alien invader is a suitable indicator for the level of threat that they pose.

The National Wetlands Vegetation Database provided the data on which this assessment of invasion of wetland habitats by invasive aliens is based.<sup>15</sup> Firstly, the most common invasive species in wetlands are listed and ranked in Table 1. Here it can be clearly seen that many of the most common species in this database are not listed in the NEMBA list of species. When all alien plant species (whether invasive or not) found in the wetlands of South Africa are cross-referenced with the NEMBA list for prioritisation for alien control, it appears that only a fraction of the invasive alien species in wetlands are listed as priorities for eradication and that this fraction is independent of their frequency of occurrence (Table 2). This can be tested with a chi-square test and it appears that the likelihood of a species to be found in wetlands and the likelihood for a species to be listed on NEMBA are independent of each other and therefore that the most important wetland invasive alien species are underrepresented when it comes to priorities in alien control.

## Discussion

Species that are regularly found invading in wetland habitats have been largely overlooked in strategic planning around invasive plants. Exploring the reasons why such species are not targeted in alien control programmes and the difficulties that are faced when clearing wetlands of invasive species, may lead to an improvement in the overall management of invasive aliens and valuable water resources in the country.

The reasons why wetland invasive aliens do not feature very highly on the NEMBA list may partially be linked to properties of the plants themselves, but also to properties of the invaded habitats, the wetlands. The criteria that are used to list which invasive alien species are prioritised in national legislation are given by Nel et al.<sup>16</sup> and Moshobane et al.<sup>17</sup> It is worth looking more closely at the specific aspects of wetland plants that may create hurdles for the implementation of alien control in wetlands. Prioritisation in alien control considers the feasibility of success and these aspects may prevent action on alien control in wetlands as the risk of a poor return on investments is considered too high. Nevertheless, it is worth explaining the possible reasons explicitly, before looking at potential solutions of how to deal with the frequent occurrence of alien invasion in wetland habitats.

### **(1) Focus on ecosystem transformers creates a bias against herbaceous plants**

Alien invaders that are known as 'transformers' change the landscape and the potential for humans to benefit from certain ecosystem services.<sup>18-20</sup> Because larger species have a proportionally larger impact on ecosystem processes,<sup>21</sup> it may seem to make sense to particularly focus on invasive species that produce high biomass such as trees and shrubs. Indeed, woody trees and shrubs often receive special attention in invasive biology<sup>22</sup> and many of the more aggressive invasive alien plants are known to have a woody habit.<sup>23,24</sup> These species also have an impact on local hydrology because of their deep taproots.

Many of the problematic plants in wetlands are herbaceous plants that can produce significant biomass although this is less obvious than with trees and shrubs, as they expand horizontally via rhizomes. Wetlands are naturally often dominated by clonal plants, especially those propagating by means of fragmentation (many aquatic plants) and those propagating by means of rhizomes.<sup>25</sup> This is probably because sexual reproduction requires germination, which is particularly problematic in anoxic environments. This means that alien invaders that have such means of propagation can be successful as invaders in wetlands. Whether they are alien or indigenous, clonally propagating species may often lead to monodominance.<sup>26</sup> In this case, grasses, especially, have been recognised as an important category of potentially invasive species<sup>27</sup> and species listed for eradication should be more inclusive of them<sup>28</sup>. Grasses of the genus *Paspalum* L. may have been overlooked because of their generally low stature and low biomass but represent true problems for wetland ecosystems.<sup>29</sup>

### **(2) Focus on invaders of recent wave of globalisation creates a bias against species from older waves of invasion**

When invasive alien species are targeted for eradication, it is done generally because there is a fear that they will still expand and grow in extent, forming a threat to existing pristine ecosystems. Therefore, they tend to be species that have been brought in by the most recent wave of globalisation, in the last 50 or 100 years. However, human trade and traffic on an intercontinental scale has already been taking place for more than 500 years.<sup>30</sup> Species that have been introduced in earlier periods within Europe or the Middle East are generally known as archaeophytes.<sup>31,32</sup> But also, in other parts of the world, many species have been present long enough to have established and it is quite possible that some species are ignored as alien invaders simply because the landscape is already saturated with them.<sup>33</sup> They have occupied all their potential niches, and have stable populations that are no longer growing.

For many herbaceous wetland species in South Africa, the majority of local conservation practitioners are not aware of the fact that these species are alien, or their status is regarded as ambiguous (EJJS personal observation). It can be very difficult to establish whether a species has been part of a 'natural' jump dispersal event, or whether human traffic facilitated the process.<sup>34</sup> These introduced species may already have been present before extensive records of native biodiversity became established. But even in the long term, they may still pose problems as they change genetically and become better adapted to their new environment.<sup>35</sup> In South Africa, some widespread wetland species in this category that are locally dominant are *Carex acutiformis* Ehrh. and *Juncus inflexus* L. It is not known which indigenous plant communities they have replaced, as these are clonal dominants that cover the entire surface in their area of occurrence.

### **(3) Focus on transformed landscapes creates a bias against species that are capable to invade natural habitats slowly**

Most invader species are being noticed because they tend to become dominant in certain areas over a very short period and become dominant in their local landscapes. These tend to be the landscapes that are close to urban centres, from where most invasions are starting.<sup>36</sup> But it is also possible that species start to spread geographically without



**Table 1:** Alien species prominent in wetland habitats ranked according to their frequency in the National Wetlands Vegetation Database<sup>15</sup>

Rank	Species	Fraction of wetland plots	Legal category	Growth form / functional type	Wetness zone
1	<i>Paspalum dilatatum</i> Poir.	9.43%		Tufted graminoid	S,T
2	<i>Verbena bonariensis</i> L.	4.94%	1b	Perennial forb	T
3	<i>Conyza albida</i> Spreng.	2.93%		Annual	T
4	<i>Juncus effusus</i> L.	2.93%		Tufted graminoid	P,S
5	<i>Cirsium vulgare</i> (Savi) Ten.	2.91%	1b	Rosette	S,T
6	<i>Persicaria lapathifolia</i> (L.) Gray	2.84%		Annual	S,T
7	<i>Paspalum distichum</i> L.	2.83%		Mat graminoid	P,S
8	<i>Paspalum urvillei</i> Steud.	2.83%		Tufted graminoid	S,T
9	<i>Oenothera rosea</i> L'Hér. ex Aiton	2.62%		Perennial forb	T
10	<i>Verbena brasiliensis</i> Vell.	2.24%	1b	Perennial forb	T
11	<i>Conyza bonariensis</i> (L.) Cronquist	2.13%		Annual	T
12	<i>Hypochaeris radicata</i> L.	2.11%		Rosette	T
13	<i>Tagetes minuta</i> L.	2.05%		Annual	T
14	<i>Veronica anagallis-aquatica</i> L.	1.94%		Annual	P,S
15	<i>Juncus inflexus</i> L.	1.87%		Tufted graminoid	S
16	<i>Carex acutiformis</i> Ehrh.	1.77%		Mat graminoid	P
17	<i>Alternanthera sessilis</i> (L.) DC.	1.73%		Perennial forb	P
18	<i>Cyperus esculentus</i> L.	1.70%		Tufted graminoid	S,T
19	<i>Bidens pilosa</i> L.	1.49%		Annual	T
20	<i>Xanthium strumarium</i> L.	1.44%	1b	Annual	T
21	<i>Lolium perenne</i> L.	1.40%		Mat graminoid	T
22	<i>Schkuhria pinnata</i> (Lam.) Cabrera	1.39%		Annual	T
23	<i>Senecio inaequidens</i> DC.	1.25%		Perennial forb	T
24	<i>Spergularia media</i> (L.) C. Presl.	1.21%		Annual	S,T
25	<i>Paspalum vaginatum</i> Sw.	1.09%		Mat graminoid	S
26	<i>Ageratum houstonianum</i> Mill.	1.09%	1b	Annual	S,T
27	<i>Ciclospermum leptophyllum</i> (Pers.) Eichler	1.07%		Annual	T
28	<i>Chenopodium album</i> L.	1.06%		Annual	S,T
29	<i>Amaranthus hybridus</i> L. s. <i>hybridus</i>	0.80%		Annual	T
30	<i>Alternanthera nodiflora</i> R.Br.	0.75%		Annual	P,S
31	<i>Pennisetum clandestinum</i> Chiov.	0.71%	1b	Mat graminoid	S,T
32	<i>Gamochaeta pennsylvanica</i> (Willd.) Cabrera	0.69%		Annual	T
33	<i>Acacia mearnsii</i> De Willd.	0.68%	2	Shrub	T
34	<i>Acacia saligna</i> (Labill.) H.L. Wendl.	0.66%	1b	Shrub	T
35	<i>Physalis viscosa</i> L.	0.61%		Perennial forb	T
36	<i>Bidens bipinnata</i> L.	0.59%		Annual	T
37	<i>Medicago laciniata</i> (L.) Mill.	0.57%		Annual	T
38	<i>Conyza canadensis</i> (L.) Cronquist	0.57%		Annual	T

T, temporary wet; S, seasonally wet; P, permanently wet



**Table 2:** Different categories of alien species in terms of their frequency of occurrence and the number of species that are NEMBA listed. The frequency of species found that are also listed on NEMBA does not differ significantly between rare and common species ( $\chi^2 = 2.67$ , d.f. = 4,  $p=0.18$ ), which means that the NEMBA list does not effectively capture the most frequent species in wetlands.

	No. of species not listed on NEMBA	No. of species listed on NEMBA	Total number of species
Very rare (less than 0.18% of plots)	126	64	190
Rare (0.18–0.32% of plots)	15	5	20
Infrequent (0.32–0.52% of plots)	17	5	22
Occasional (0.52–1.5% of plots)	15	5	20
Frequent (1.5–10% of plots)	14	4	18
Total	187	83	270

attaining high-density local populations.<sup>37</sup> Compared to heavily disturbed landscapes, few alien plants can invade natural habitats, but many landscapes are subject to small-scale disturbances that can create local niches for invasive aliens, for example by means of subtle fire or grazing regime changes.<sup>38</sup> If the plant does not attain high densities and affect local ecosystem functioning in immediately obvious ways, it is likely to go unnoticed and ignored in eradication plans. Therefore, if a species is capable of invading natural or semi-natural ecosystems with minimum disturbance, it might mean that it is quietly spreading and might have delayed effects that may become evident only after environmental change takes place.

This scenario may be a problem in wetland species as these species always have the potential to start spreading clonally within their habitat as time proceeds. Even when populations do not easily disperse towards other wetlands, they may still form extensive populations within a single wetland. This leads to some species having very extensive but mainly local populations. Some invasive alien grasses that appear in large wilderness areas, such as the Drakensberg in South Africa, may appear in this category; an example is the grass *Deschampsia cespitosa* (L.) P.Beauv.<sup>39</sup> Even so, these species may impact such a wetland to such an extent that its functioning within the catchment as a whole is compromised and eventually seeds or clonal fragments can spread further downstream.

### Unique problems associated with working in wetland habitats

An additional reason that many wetlands are neglected in terms of alien eradication programmes is to be found in the difficulties in working in wetland environments. Wetlands that are inward-draining, in particular, form sinks in the landscape (sinks for sediments, nutrients, propagules and eventually also for herbicides and other pollutants that may be used in combating aliens). This property of wetlands not only makes them very vulnerable to invasion, but also means that combating aliens in a wetland is a delicate matter that has the potential to lead to high concentrations of toxicants in the wetland and eventually to ecosystem collapse. It may be that manual control and the active planting of indigenous vegetation is the only remedy that helps in keeping wetlands free of invasive aliens.

We focus here on four aspects of control of alien invasions that we think play an important role for alien control in wetlands and that should be taken into consideration when aligning wetland conservation with control of invasive aliens.

### (1) The choice of herbicides

The first issue that needs to be considered in combating aliens in wetlands is the use of herbicides. The challenge with the control of alien plants in wetlands with herbicides is due to the vulnerability or susceptibility of these aquatic environments. Around the world, the use of herbicides is highly regulated, and in South Africa specifically, the use of herbicides for control of weeds and invasive plants must be consistent with provisions in NEMBA and the *Fertilizer, Farm Feeds, Agricultural Remedies and Stock Remedies Act (Act No. 36 of 1947)*. The latter dictates that anyone using herbicides needs to have a valid Pest Control Operators Licence. Additionally, the pesticides that are used must be registered for use in aquatic environments by the Australian Pesticides & Veterinary Medicines Authority. All intended clearing activities should be outlined in the control plans which should be drawn up according to the guidelines required in Section 76 of NEMBA.<sup>40</sup>

Herbicides can be safely used in wetlands to protect the ecosystem from their negative effects, but only if they are applied correctly.<sup>41</sup> There are a number of characteristics that need to be considered when herbicides are applied in wetlands. For example, herbicides should have a low volatility at all temperatures in order to reduce the potential for spray drift.<sup>42</sup> They also should have a low water solubility, in order to reduce the potential for leaching to places of groundwater recharge or surface runoff.<sup>41,43,44</sup> Furthermore, the herbicides should have a low eco-toxicity and a low half-life, so that they cannot accumulate in the wetland, as many wetlands are inward-draining and would be ecological sinks.

Currently in South Africa there are no registered herbicides for use to control *Paspalum dilatatum* in terrestrial wetlands. However, some of the recommended herbicides for the control of this species are thiencazabone-methyl, foramsulfuron, halosulfuron-methyl, fluzafop and monosodium methanearsonate combined with foramsulfuron.<sup>45-47</sup> The study by Henry et al.<sup>45</sup> has shown nearly 90% control of *Paspalum dilatatum* by multiple applications of monosodium methanearsonate with foramsulfuron during the summer season.

### (2) Replanting indigenous vegetation after alien control

Many wetlands occur in key points in the landscape, and within South Africa, they are often very susceptible to erosion. Gully erosion is very common in wetlands and the removal of vegetation should therefore be accompanied by replanting of indigenous vegetation. The indigenous plants chosen for this purpose play an important role in the functioning of the restored ecosystem, in terms of holding the soil together, preventing erosion and preventing the establishment of new invasive alien plants. For this reason, it is important to select species that are viable and competitive in the environment in which they are planted, and that are suited to the hydrology and the substrate of the site in question. An in-field experiment in Wakkerstroom (Mpumalanga, South Africa) showed that an indigenous species such as *Cyperus fastigiatus* Rottb. can be suitable for preventing erosion cutbacks to proceed, even though the often-used species *Vetiveria zizanioides* L. is more effective in retaining soils in place when planted densely.<sup>48</sup> This last species is not indigenous but it has also been shown to be not invasive and is very effective in holding soils together on steep slopes.<sup>49</sup> However, in the long term, rhizomatous species that are local may be more effective in preventing both erosion and re-colonisation by invasive alien species. For this reason, it is important to have a good idea of reference conditions in the area and to choose species from the indigenous species pool that have suitable properties for this intended purpose (which are mostly rhizomatous species).

### (3) Working downstream to prevent the spread of propagules

Many wetlands are part of a drainage system and alien invasions would spread through the wetland from the upper to the lower sections. Therefore, removal of invasive aliens should start in the upper parts of any river catchment working downstream to prevent new infestations.<sup>50</sup> Before the removal of alien invaders is attempted in a wetland, and resources are spent on that particular wetland, an assessment needs to be made on the state of the catchment upstream of that wetland.

**Table 3:** A list of emerging invasive grasses in wetlands that may become more widespread in the near future

Grass species	Habitat invaded	Challenges	Management	References
<i>Glyceria maxima</i> (Hartm.) Holmb.	Wetlands, so far only recorded in Boston-Bulwer-Underberg area in KwaZulu-Natal	Spreads rapidly through thick rhizomes, clogging waterways, and possibly has toxic effects on livestock	Listed under NEMBA Category 1b. Control through fire or chemicals	Fish et al. <sup>39</sup> , Visser et al. <sup>27</sup> , Mugwedi <sup>51</sup>
<i>Phalaris aquatica</i> L. and <i>P. arundinacea</i> L.	Wetlands in cooler regions at high altitudes	Stands are shade-tolerant and competitive, even under drought conditions	When detected early, it can be removed physically. Herbicides that have been used are amitrole-T (3-amino-1,2,4-triazole ammonium thiocyanate), glyphosate (N-[phosphonomethyl]glycine) and dalapon (2,2-dichloro propionic acid). Recommended in conjunction with prescribed burning. Not yet listed under NEMBA and no risk analysis available.	Visser et al. <sup>27</sup> , Lyons <sup>52</sup>
<i>Coix lacryma-jobi</i> L.	Coastal areas of KwaZulu-Natal, especially in wetlands associated with streams	Utilised culturally as a food crop and ornamentally in beads and necklaces. Forms dense populations that can block streams.	Not yet listed under NEMBA and no risk analysis available	Fish et al. <sup>39</sup>
<i>Cortaderia selloana</i> (Schult. & Schult.f.) Asch. & Graebn.	Widespread in South Africa in seasonally wet habitats	Originally established to control soil erosion and as an ornamental	Listed under NEMBA Category 1b. Seedlings and small plants can be removed by pulling and digging.	Fish et al. <sup>39</sup>
<i>Alopecurus arundinaceus</i> Poir.	Stable population exists in Wakkerstroom wetland in Mpumalanga	Possibly overlooked where it has found since the 1960s (according to misidentified herbarium specimen in John Bews herbarium)	Not yet listed under NEMBA and no risk analysis available	Fish et al. <sup>39</sup>

**Table 4:** Most important invasive floating aquatic plants

Species	Habitat invaded	Challenges	Management	References
<i>Azolla filiculoides</i> Lam.	Sometimes rivers, mostly on dams, throughout South Africa	Fast clonal reproduction on the water surface	Listed as Category 1 on NEMBA list. It can be subjected to biological control with the weevil <i>Stenopelmus rufinasus</i> , Gyllenhal.	Cook <sup>53</sup>
<i>Salvinia molesta</i> D.S. Mitchell	Dams and pools in warm regions, mostly in eutrophic conditions	Fast clonal reproduction on the water surface. No sexual reproduction in South Africa.	Listed as Category 1 on NEMBA list. Biological control by means of the weevil <i>Cyrtobagous singularis</i> Hustache.	Cook <sup>53</sup> , Motitsoe et al. <sup>54</sup>
<i>Pistia stratiotes</i> L.	Dams and pools in warm regions of the country. Originally from tropical Africa. May be tolerant of slightly brackish water.	Berries produced that may be dispersed by birds	Listed as Category 1 on NEMBA list	Cook <sup>53</sup> , Coetzee et al. <sup>55</sup>
<i>Pontederia crassipes</i> Mart.	Dams and rivers in warm regions of the country. Juvenile stage submerged.	It can occur in heavily polluted water where it can remove heavy metals and purify the water.	Listed as Category 1 on NEMBA list. Biological control is feasible with weevils of the genus <i>Neochetina</i> .	Opande et al. <sup>56</sup> , Jafari <sup>57</sup> , Martinez Jimenez and Gomez Balandra <sup>58</sup>

#### (4) Restoring hydrology of the wetland

The main focus of wetland restoration is the adjustment of hydrology of a wetland system so that flooding regime and hydroperiod are restored to the natural situation. In some cases, this aim intersects with the presence of invasive alien species in the wetland, for example when those alien species absorb excessive amounts of water or when invasion has followed a drying period of the wetland. Manipulating the hydrology of wetlands through rewetting, dispersion of flow or plugging erosion gullies should make the wetland more suitable for indigenous vegetation. However, the removal of the invasive aliens should help accelerate the natural recruitment process.

#### Specific problems arising from some groups of invasive alien species

Lastly, we focus on two categories of invaders in wetlands and their removal: alien grasses and alien floating aquatics. Both groups are underrepresented in the National Wetlands Vegetation Database – the grasses because they are mostly recent invasions that are not yet very widely spread across the country, and the floating aquatic plants because they mostly invade farm dams and other artificial waterbodies that are underrepresented in the National Wetlands Vegetation Database. However, the practice of combating these alien species may inform ways in which other invasive species in wetlands, that have often not been considered, may be targeted as well.

### Alien grasses

With alien grasses, it is very important to set up an early detection programme, as several grasses have been recorded in recent years that appear to cause problems on other continents. It has become clear that many grasses may remain undetected in wetlands just because many environmental practitioners are not familiar with them.<sup>27</sup> A number of recent finds of wetland invasive alien grasses in South Africa are listed in Table 3.

### Alien floating aquatics

A second group of water plants that are often targeted for eradication are floating aquatic plants. There are four species that create problems in southern Africa. It is well established that floating aquatic plants create drastic changes to the underwater environment as they affect the light regime in the water column. The advantage of floating aquatic plants is that it is relatively easy to remove them mechanically, and, for most of them, there are biological control agents available in the form of weevils that graze on them. Submerged aquatic plants are much less of a problem in South Africa and most often only on a local scale, some examples being *Egeria densa* Planchon and *Myriophyllum aquaticum* (Velloso) Verdcourt. The four most troublesome floating aquatics are listed in Table 4.

Especially in the case of floating aquatic species, the removal of the aliens often triggers the recovery of the natural ecosystem. Consequently, the removal of invasive aliens should be regarded as an integral part of the restoration of natural ecosystems. This brings us back to the programmes for wetland restoration. Many of the wetland restoration works that have been carried out involve digging and may result in clear open areas that are subject to natural recruitment. If it is difficult and expensive to clear alien invasions in wetlands after they take place and it is difficult to control which plants enter a site, it may be a good idea to pre-empt alien invasion in wetlands by planting indigenous vegetation as a part of the restoration measures taken. Many of the species that enter a wetland after restoration are annuals and ruderal species, but eventually later-successional species may become more perennial aliens that are very difficult to remove.

In conclusion, alien invasion in wetland habitats is of particular concern and should be addressed as a distinct problem in ecosystem management. This has a bearing on both alien control programmes and wetland restoration programmes and if synergy between such programmes takes place, they will benefit the mandate of both. As South Africa faces an uncertain future with a water crisis looming, the alignment of these programmes is crucial if we want to obtain the goal of recovering the ecological functioning of wetlands, which are critical ecosystems that form an integral part of our ecological infrastructure.

### Acknowledgements

We thank Ingrid Nänni, Sebataolo Rahlao, Umesh Bahadur, John Wilson and Farai Tererai for fruitful discussions that inspired the writing of this manuscript. The findings of the BSc Honours projects of Kimberley Moodley and Karmigan Naicker formed an important part of the conclusions that were discussed in the manuscript. We also thank the Water Research Commission (project K5/1980) for sponsoring the development of the National Wetlands Vegetation database that lies at the base of these findings.

### Competing interests

We have no competing interests to declare.

### Authors' contributions

E.J.J.S.: Conceptualisation, data collection, data analysis, writing – the initial draft, writing – revisions, project management. Ş.P.: Conceptualisation, writing – the initial draft, writing – revisions. A.C.M.: Writing – revisions. M.C.M.: Writing – revisions.

### References

1. Van Wilgen BW, Forsyth GG, Le Maitre DC, Wannenburg A, Kotzé JDF, van den Berg E, Henderson L. An assessment of the effectiveness of a large, national-scale invasive alien plant control strategy in South Africa. *Biol Conserv.* 2012;148:28–38. <https://doi.org/10.1016/j.biocon.2011.12.035>
2. Hassan R, Mahlathi S. Evaluating the environmental and social net-worth of controlling alien plant invasions in the Inkomati catchment, South Africa. *Water SA.* 2020;46:54–65. <https://doi.org/10.17159/wsa/2020.v46.i1.7881>
3. Galatowitsch S, Richardson DM. Riparian scrub recovery after clearing of alien invasive trees in headwater streams of the Western Cape, South Africa. *Biol Conserv.* 2005;122:509–521. <https://doi.org/10.1016/j.biocon.2004.09.008>
4. Meek CS, Richardson DM, Mucina L. A river runs through it: Land-use and composition of vegetation along a riparian corridor in the Cape Floristic Region, South Africa. *Biol Conserv.* 2010;143:156–164. <https://doi.org/10.1016/j.biocon.2009.09.021>
5. Holmes PM, Richardson DM, Esler KJ, Witkowski ETF, Fourie S. A decision-making framework for restoring riparian zones degraded by invasive alien plants in South Africa: Review article. *S Afr J Sci.* 2005;101:553–564.
6. Holmes PM, Esler KJ, Richardson DM, Witkowski ETF. Guidelines for improved management of riparian zones invaded by alien plants in South Africa. *S Afr J Bot.* 2008;74:538–552. <https://doi.org/10.1016/j.sajb.2008.01.182>
7. Finlayson CM, Van der Valk AG. Wetland classification and inventory: A summary. *Vegetatio.* 1995;118:185–192. <https://doi.org/10.1007/BF00045199>
8. Schlesinger WH, Bernhardt ES. *Biogeochemistry: An analysis of global change.* Waltham: Academic Press; 2013.
9. Bacher S, Blackburn TM, Essl F, Genovesi P, Heikkilä J, Jeschke JM, et al. Socio-economic impact classification of alien taxa (SEICAT). *Methods Ecol Evol.* 2018;9:159–168. <https://doi.org/10.1111/2041-210X.12844>
10. Moor H, Rydin H, Hylander K, Nilsson MB, Lindborg R, Norberg J. Towards a trait-based ecology of wetland vegetation. *J Ecol.* 2017;105:1623–1635. <https://doi.org/10.1111/1365-2745.12734>
11. Kumschick S, Bacher S, Dawson W, Heikkilä J, Sendek A, Pluess T, et al. A conceptual framework for prioritization of invasive alien species for management according to their impact. *NeoBiota.* 2012;15:69–100. <https://doi.org/10.3897/neobiota.15.3323>
12. Veitch CR, Clout MN. Turning the tide: The eradication of invasive species: Proceedings of the International Conference on Eradication of Invasive Invasives; 2001 February 19–23; Auckland, New Zealand. Gland: IUCN; 2002.
13. Pyšek P, Richardson DM, Rejmánek M, Webster GL, Williamson M, Kirschner J. Alien plants in checklists and floras: Towards better communication between taxonomists and ecologists. *Taxon.* 2004;53:131–143. <https://doi.org/10.2307/4135498>
14. Henderson L. Alien weeds and invasive plants. Pretoria: Plant Protection Research Institute; 2001.
15. Sieben EJJ, Mtshali H, Janks M. National Wetland Vegetation Database: Classification and analysis of wetland vegetation types for conservation planning and monitoring. Pretoria: Water Research Commission; 2014.
16. Nel JL, Richardson DM, Rouget M, Mgidi TN, Mdzeke N, Le Maitre DC, et al. A proposed classification of invasive alien plant species in South Africa: Towards prioritizing species and areas for management action: Working for water. *S Afr J Sci.* 2004;100:53–64.
17. Moshobane MC, Mukundamago M, Adu-Acheampong S, Shackleton R. Development of alien and invasive taxa lists for regulation of biological invasions in South Africa. *Bothalia.* 2019;49:1–12. <https://doi.org/10.4102/abc.v49i1.2361>
18. Weidenhamer JD, Callaway RM. Direct and indirect effects of invasive plants on soil chemistry and ecosystem function. *J Chem Ecol.* 2010;36:59–69. <https://doi.org/10.1007/s10886-009-9735-0>
19. Vilà M, Espinar JL, Hejda M, Hulme PE, Jarošík V, Maron JL, et al. Ecological impacts of invasive alien plants: A meta-analysis of their effects on species, communities and ecosystems. *Ecol Lett.* 2011;14:702–708. <https://doi.org/10.1111/j.1461-0248.2011.01628.x>



20. Corbin JD, D'Antonio CM. Gone but not forgotten? Invasive plants' legacies on community and ecosystem properties. *Invasive Plant Sci Manag.* 2012;5:117–124. <https://doi.org/10.1614/IPSM-D-11-00005.1>
21. Grime JP. Benefits of plant diversity to ecosystems: Immediate, filter and founder effects. *J Ecol.* 1998;86:902–910. <https://doi.org/10.1046/j.1365-2745.1998.00306.x>
22. Richardson DM, Rejmánek M. Trees and shrubs as invasive alien species – A global review. *Divers Distrib.* 2011;17:788–809. <https://doi.org/10.1111/j.1472-4642.2011.00782.x>
23. Van Kleunen M, Dawson W, Maurel N. Characteristics of successful alien plants. *Mol Ecol.* 2015;24:1954–1968. <https://doi.org/10.1111/mec.13013>
24. Van Kleunen M, Dawson W, Schlaepfer D, Jeschke JM, Fischer M. Are invaders different? A conceptual framework of comparative approaches for assessing determinants of invasiveness. *Ecol Lett.* 2010;13:947–958. <https://doi.org/10.1111/j.1461-0248.2010.01503.x>
25. Song Y-B, Yu F-H, Keser LH, Dawson W, Fischer M, Dong M, et al. United we stand, divided we fall: A meta-analysis of experiments on clonal integration and its relationship to invasiveness. *Oecologia.* 2013;171:317–327. <https://doi.org/10.1007/s00442-012-2430-9>
26. Sieben EJJ, Le Roux PC. Functional traits, spatial patterns and species associations: What is their combined role in the assembly of wetland plant communities? *Plant Ecol.* 2017;218:433–445. <https://doi.org/10.1007/s11258-017-0701-6>
27. Visser V, Wilson JRJ, Canavan K, Canavan S, Fish L, Maitre DL, et al. Grasses as invasive plants in South Africa revisited: Patterns, pathways and management. *Bothalia.* 2017;47:1–29. <https://doi.org/10.4102/abc.v47i2.2169>
28. Gaertner M, Biggs R, te Beest M, Hui C, Molofsky J, Richardson DM. Invasive plants as drivers of regime shifts: Identifying high-priority invaders that alter feedback relationships. *Divers Distrib.* 2014;20:733–744. <https://doi.org/10.1111/ddi.12182>
29. Nkuna KV, Visser V, Wilson JRJ, Kumschick S. Global environmental and socio-economic impacts of selected alien grasses as a basis for ranking threats to South Africa. *Neobiota.* 2018;41:19–65. <https://doi.org/10.3897/neobiota.41.26599>
30. Robertson RT. The three waves of globalization: A history of a developing global consciousness. London: Zed Books; 2003.
31. Weeda EJ. The role of archaeophytes and neophytes in the Dutch coastal dunes. *J Coast Conserv.* 2010;14:75–79. <https://doi.org/10.1007/s11852-009-0079-2>
32. Aronson J, Aronson TB, Patzelt A, Knees SG, Lewis GP, Lupton D, et al. Paleorelicts or archaeophytes: Enigmatic trees in the Middle East. *J Arid Environ.* 2017;137:69–82. <https://doi.org/10.1016/j.jaridenv.2016.11.001>
33. Stohlgren TJ, Pyšek P, Kartesz J, Nishino M, Pauchard A, Winter M, et al. Widespread plant species: Natives versus aliens in our changing world. *Biol Invasions.* 2011;13:1931–1944. <https://doi.org/10.1007/s10530-011-0024-9>
34. Le Roux JJ, Strasberg D, Rouget M, Morden CW, Koordom M, Richardson DM. Relatedness defies biogeography: The tale of two island endemics (*Acacia heterophylla* and *A. koa*). *The New Phytol.* 2014;204:230–242. <https://doi.org/10.1111/nph.12900>
35. Sorte FAL, Pyšek P. Extra-regional residence time as a correlate of plant invasiveness: European archaeophytes in North America. *Ecology.* 2009;90:2589–2597. <https://doi.org/10.1890/08-1528.1>
36. McLean P, Gallien L, Wilson JRJ, Gaertner M, Richardson DM. Small urban centres as launching sites for plant invasions in natural areas: Insights from South Africa. *Biol Invasions.* 2017;19:3541–3555. <https://doi.org/10.1007/s10530-017-1600-4>
37. Liebhold A, Bascompte J. The Allee effect, stochastic dynamics and the eradication of alien species. *Ecol Lett.* 2003;6:133–140. <https://doi.org/10.1046/j.1461-0248.2003.00405.x>
38. Lake JC, Leishman MR. Invasion success of exotic plants in natural ecosystems: The role of disturbance, plant attributes and freedom from herbivores. *Biol Conserv.* 2004;117:215–226. [https://doi.org/10.1016/S0006-3207\(03\)00294-5](https://doi.org/10.1016/S0006-3207(03)00294-5)
39. Fish L, Mashau AC, Moeaha MJ, Nembudani MT. Identification guide to southern African grasses. An identification manual with keys, descriptions and distributions. *Strelitzia.* Vol. 36. Pretoria: South African National Biodiversity Institute; 2015.
40. South African Department of Environment, Forestry and Fisheries. National Environmental Management: Biodiversity Act No. 10 of 2004: Alien and Invasive Species Lists. *Government Gazette.* 2020;43726:31–104.
41. Donald DB, Cessna AJ, Farenhorst A. Concentrations of herbicides in wetlands on organic and minimum-tillage farms. *J Env Qual.* 2018;47:1554–1565. <https://doi.org/10.2134/jeq2018.03.0100>
42. Bereswill R, Strelake M, Schulz R. Risk mitigation measures for diffuse pesticide entry into aquatic ecosystems: Proposal of a guide to identify appropriate measures on a catchment scale. *Integr Environ Assess Manag.* 2014;10:286–298. <https://doi.org/10.1002/ieam.1517>
43. Elliott JA, Cessna AJ. Transport of two sulfonylurea herbicides in runoff from border dyke irrigation. *J Soil Water Conserv.* 2010;65:298–303. <https://doi.org/10.2489/jswc.65.5.298>
44. Cessna AJ, McConkey BG, Elliott JA. Herbicide transport in surface runoff from conventional and zero-tillage fields. *J Environ Qual.* 2013;42:782–793. <https://doi.org/10.2134/jeq2012.0304>
45. Henry GM, Yelverton FH, Burton MG. Dallisgrass (*Paspalum dilatatum*) control with foramsulfuron in Bermudagrass turf. *Weed Technol.* 2007;21:759–762. <https://doi.org/10.1614/WT-06-163.1>
46. Elmore M, Brosnan J, Mueller T, Horvath B, Kopsell D, Breeden G. Seasonal application timings affect dallisgrass (*Paspalum dilatatum*) control in tall fescue. *Weed Technol.* 2013;27(3):557–564. <https://doi.org/10.1614/wt-d-13-00007.1>
47. Johnston CR, Henry GM. Dallisgrass (*Paspalum dilatatum*) control with thiencarbazone-methyl, foramsulfuron, and halosulfuron-methyl in bermudagrass turf. *Hortic Sci.* 2016;51:754–756. <https://doi.org/10.21273/HORTSCI.51.6.754>
48. Sieben EJJ, Kotze DC, Noffke M. Erosion control in wetlands. *Veld & Flora.* 2007;93(2):106–107.
49. Banerjee R, Goswami P, Lavania S, Mukherjee A, Lavania UC. Vetiver grass is a potential candidate for phytoremediation of iron ore mine spill dumps. *Ecol Eng.* 2019;132:120–136. <https://doi.org/10.1016/j.ecoleng.2018.10.012>
50. Foxcroft LC, Rouget M, Richardson DM. Risk assessment of riparian plant invasions into protected areas. *Conserv Biol.* 2007;21:412–421. <https://doi.org/10.1111/j.1523-1739.2007.00673.x>
51. Mugwedi LF. Invasion ecology of *Glyceria maxima* in KZN rivers and wetlands [MSc dissertation]. Johannesburg: University of the Witwatersrand; 2012.
52. Lyons KE. Element stewardship abstract for *Phalaris arundinacea*. The nature conservancy [webpage on the Internet]. c1998 [2021 Feb 18]. Available from: <http://tncweeds.ucdavis.edu/esadocs/docmnts/phalaru.html>
53. Cook CDK. Aquatic and wetland plants of southern Africa. Leiden: Backhuys Publishers; 2005.
54. Motitsoe SN, Coetzee JA, Hill JM, Hill MP. Biological control of *Salvinia molesta* D.S. Mitchell drives aquatic ecosystem recovery. *Diversity.* 2020;12:204. <https://doi.org/10.3390/d12050204>
55. Coetzee JA, Langa SDF, Motitsoe SN, Hill MP. Biological control of water lettuce, *Pistia stratiotes* L., facilitates macroinvertebrate biodiversity recovery: A mesocosm study. *Hydrobiologia.* 2020;847:3917–3929. <https://doi.org/10.1007/s10750-020-04369-w>
56. Opande GO, Onyango JC, Wagai SO. Lake Victoria: The water hyacinth (*Eichhornia crassipes* [Mart.] Solms), its socio-economic effects, control measures and resurgence in the Winam gulf. *Limnologia.* 2004;34:105–109. [https://doi.org/10.1016/S0075-9511\(04\)80028-8](https://doi.org/10.1016/S0075-9511(04)80028-8)
57. Jafari N. Ecological and socio-economic utilization of water hyacinth (*Eichhornia crassipes* Mart Solms). *J Appl Sci Environ Manag.* 2010;14:43–49. <https://doi.org/10.4314/jasem.v14i2.57834>
58. Martinez Jimenez M, Gomez Balandra MA. Integrated control of *Eichhornia crassipes* by using insects and plant pathogens in Mexico. *Crop Protect.* 2007;26:1234–1238. <https://doi.org/10.1016/j.cropro.2006.10.028>





# Scope, trends and opportunities for socio-hydrology research in Africa: A bibliometric analysis

## AUTHORS:

Christina M. Botai<sup>1</sup>   
Joel O. Botai<sup>1,2,3</sup>   
Miriam Murambadoro<sup>1,4</sup>  
Nosipho N. Zwane<sup>1</sup>   
Abiodun M. Adeola<sup>1,5</sup>   
Jaco P. de Wit<sup>1</sup>  
Omolola M. Adisa<sup>2</sup>

## AFFILIATIONS:

<sup>1</sup>South African Weather Service, Pretoria, South Africa  
<sup>2</sup>Department of Geography, Geoinformatics and Meteorology, University of Pretoria, Pretoria, South Africa  
<sup>3</sup>Department of Information Technology, Central University of Technology, Bloemfontein, South Africa  
<sup>4</sup>Global Change Institute, University of the Witwatersrand, Johannesburg, South Africa  
<sup>5</sup>Institute for Sustainable Malaria Control, University of Pretoria, Pretoria, South Africa

## CORRESPONDENCE TO:

Christina Botai

## EMAIL:

christina.botai@weathersa.co.za

## DATES:

Received: 06 Aug. 2020

Revised: 02 Aug. 2021

Accepted: 02 Aug. 2021

Published: 27 Jan. 2022

## HOW TO CITE:

Botai CM, Botai JO, Murambadoro M, Zwane NN, Adeola AM, De Wit JP, et al. Scope, trends and opportunities for socio-hydrology research in Africa: A bibliometric analysis. *S Afr J Sci.* 2022;118(1/2), Art. #8742. <https://doi.org/10.17159/sajs.2022/8742>

## ARTICLE INCLUDES:

- Peer review
- [Supplementary material](#)

## DATA AVAILABILITY:

- Open data set
- All data included
- On request from author(s)
- Not available
- Not applicable

## EDITORS:

Yali Woyessa   
Jennifer Fitchett

## KEYWORDS:

bibliometric, VOSviewer, Web of Science, Scopus, socio-hydrology, Africa

## FUNDING:

None

Socio-hydrology research is concerned with the understanding of how humanity interacts with water resources. The purpose of this study was to assess the disparity between global and African trends as well as developments in the research domain of socio-hydrology. From the viewpoint of a multitude of research themes, multi-author collaborations between African and international researchers and the number of publications produced globally, the results reveal that the field of socio-hydrology is still underdeveloped and yet nascent. At a global level, the USA, China, and the Netherlands have the highest number of scientific publications, while in Africa, South Africa dominates, although these scientific publications are significantly much lower than the global output. The output of scientific publications on socio-hydrology research from Africa increased from 2016, with significant output reached in 2019. Water management and supply, hydrological modelling, flood monitoring as well as policies and decision-making, are some of the dominant themes found through keywords co-occurrence analysis. These main keywords may be considered as the foci of research in socio-hydrology. Although socio-hydrology research is still in the early stages of development in Africa, the cluster and emerging themes analysis provide opportunities for research in Africa that will underpin new frontiers of the research agenda encompassing topics such as the (1) impacts of climate change on socio-hydrology; (2) influence of socio-hydrology on water resources such as surface water and groundwater; (3) benefits of socio-hydrological models on river basins and (4) role of socio-hydrology in economic sectors such as agriculture. Overall, this study points to a need to advance socio-hydrology research in Africa in a bid to address pressing water crises that affect sustainable development as well as to understand the feedback mechanisms and linkages between water resources and different sectors of society.

## Significance:

- The field of socio-hydrology is still under-researched in Africa.
- Limited research could be attributed to a lack of expertise, resources and data limitations.
- Socio-hydrology research is likely to be strengthened through collaborations between Africa and other developed countries.
- Existing gaps present opportunities to advance socio-hydrology research in Africa.

## Introduction

For decades, the increased interactions between humans and the environment on a broader scale have significantly intensified impacts on societal development, particularly through the co-evolution between society and water systems.<sup>1</sup> Impacts of human interventions on the ecosystem are often manifested in, for example, landscape changes, accelerated mass wasting, pollution, over-abstraction of natural resources including water, and climate change. This problem is exacerbated due to the present industrial, geo-politised, religious, as well as socio-cultural activities that are highly dependent on water resources.<sup>2</sup> These interdependencies are referred to as the Water-Energy-Food-Ecosystems Nexus.<sup>3</sup> This Nexus is mediated by policy decisions relevant to water resource management and planning for societal benefit. Such interrelated decisions are significantly influential to both water resources and society's responses, undoubtedly due to the coupling and feedback mechanisms that exist between water systems and societal behaviour.<sup>4</sup> The relationship between water systems and society is described by different authors, for example, as 'system of mutual interaction',<sup>5</sup> 'hydrosociology',<sup>6,7</sup> 'hydro-social'<sup>8</sup> and recently 'socio-hydrology',<sup>9</sup> and has emerged as a research field of interest, attracting both hydrologists and social scientists.

Nowadays, the term 'socio-hydrology', which was coined by Sivapalan et al.,<sup>9</sup> is considered a novel subject matter, that is duly concerned with the science of people and water, and specifically aimed at understanding the ever-changing processes and co-evolution of the coupled human-water systems.<sup>4</sup> Society, in general, forms part of hydrological systems, including the water cycle. As a result, the two-way research efforts on the inherent impacts on humanity and water provide a holistic understanding of long-term progressions and can therefore lead to effective support for water resource management and planning.<sup>10</sup> Several socio-hydrological research studies focusing on various themes have been reported in the literature. These research themes include the conceptualisation and theoretical framework of the subject matter for the benefit of water resource management, planning and sustainability,<sup>11-15</sup> socio-hydrological dynamics and modelling,<sup>1</sup> power relations and political governance.<sup>13,16</sup> Despite such incredible development in socio-hydrology, as evident from the proliferation of the research publications, the socio-hydrology scholar-practitioner footprint in Africa is still nascent. Contributions that socio-hydrology research bring forth, particularly towards better water resource management and planning,

© 2022. The Author(s). Published under a Creative Commons Attribution Licence.

especially across developing countries, in a changing world, need to be well documented and appreciated. To achieve this, there is a need to understand the current state of research through scientific mapping of the social research patterns and trends as well as the existing gaps in this emergent discipline. The current contribution, therefore, theoretically and empirically advances, through investigating and documenting the progression of socio-hydrology (hereafter the term is also used to include hydrosocial) research in Africa, based on bibliometric analysis.

## Data and methods

The data analysed in this study were retrieved from the Web of Science and Scopus databases. These databases are considered to have a comprehensive archive of the scientific literature and have been widely used, particularly for the analysis of scientific publications.<sup>17</sup> The search strings were: “socio-hydrological\* research” or “studies”, “socio-hydrological\* modelling” or “models”, “socio-hydrological\* systems” or “dynamics”, “socio-hydrological\* resilience”, “sociohydrologic\* dynamics” or “models”, “hydro-socio\* research” or “studies” and “human-water\* interaction” or “relationships.” Each search string was placed in a separate row, with the added rows joined by the OR logical, implying that the search outcome displays documents based on the first topic [OR] the second topic, and so on. The quotation marks were included in each search so as to confine the search conditions, thereby ensuring the robustness of the search outcomes. In addition, the term “Africa”, was added in the search with an AND condition in order to search published documents that were limited to the African continent.

In the current analysis, the documents were retrieved for the period 2000–2019. Additionally, different types of documents were retrieved for the analysis, including articles, reviews, conference proceedings (or papers) and book chapters. The data – 556 and 29 documents for global and Africa, respectively (Supplementary table 1) – were used to conduct a bibliometric analysis, focusing on mapping socio-hydrological research at a global scale as well as for Africa.

The bibliometric analysis was carried out by using bibliometrix R package<sup>18</sup> in conjunction with an open-source software program, VOSviewer<sup>19</sup>. Bibliometric analysis is one of the tools used to study/represent/display the structural and dynamic aspects of scientific research, through a scientific mapping approach.<sup>20</sup> This approach is based on analysing quantitative information of published scientific articles from the bibliographic database.<sup>20</sup> Through bibliometric analysis, general development of scientific output – including performance patterns of dominant authors, key journals, leading countries and collaborative institutions involved in the publication of scientific articles within a specific research discipline – can be identified and assessed.<sup>21</sup> Other essential information that can be derived from the bibliometric analysis includes emerging research themes, research directions<sup>22</sup>,

leading research topics and research gaps in a specific research field.<sup>23</sup> Bibliometric analysis methods have been applied to various studies, focusing on different fields of scientific research, for instance, in e-government,<sup>24-26</sup> tourism,<sup>27,28</sup> safety culture,<sup>29</sup> education systems,<sup>30</sup> policy,<sup>31</sup> biochar,<sup>32,33</sup> ecosystem services,<sup>34</sup> water resources,<sup>35</sup> and socio-hydrology.<sup>36</sup>

The scientific mapping of socio-hydrology research undertaken in this study assessed the following: (1) annual publication growth and trends; (2) leading countries in the subject matter; (3) country representation and collaboration in the socio-hydrology body of knowledge; (4) keywords frequency and co-occurrence; (5) emerging themes and (6) direct citation. The authors’ keywords and keywords-plus (extracted from the titles of the cited references) were used to assess the frequency of occurrence of the keywords. According to Omerzel,<sup>20</sup> words that frequently co-occur in a cluster of documents are closely related and represent a network of themes within a field of research (in this case, socio-hydrology research).

A thematic map was used to assess the evolution of themes or topics in the socio-hydrology research field. The thematic map was sub-divided into four quadrants: the upper-right quadrant indicates the motor themes (hot topics); themes appearing in the upper-left quadrant are considered very specialised topics; and topics in the lower-right and lower-left quadrants are termed basic themes and emerging/disappearing themes, respectively.<sup>37</sup> Furthermore, direct citation network analysis was conducted to track the historical development of a scientific breakthrough in the socio-hydrology research field, including emerging research topics, technologies and trends.<sup>38,39</sup> The VOSviewer software program was used to map and visualise the bibliometric network of countries’ collaboration and keywords co-occurrence.

## Results

### Scientific publication output and growth trend

Figure 1 depicts the annual distribution of the 29 and 556 research documents published in Africa and globally from 2000 to 2019. The results show that the number of scientific publications on socio-hydrology conducted globally remained limited between 2000 and 2008. An increase in the number of scientific publications is observed from 2009, with a significant annual increase in the number of scientific publications observed from 2014. The number of published scientific documents peaked in 2019 ( $n=142$ ), translating to an approximately 21% average annual growth rate for that period.

In contrast to global studies, research studies in Africa appear to be very scarce, with some of the years showing no productivity. On average, only one article was published in Africa between 2004 and 2014. This excludes the years that had no publications – 2005, 2007, 2008

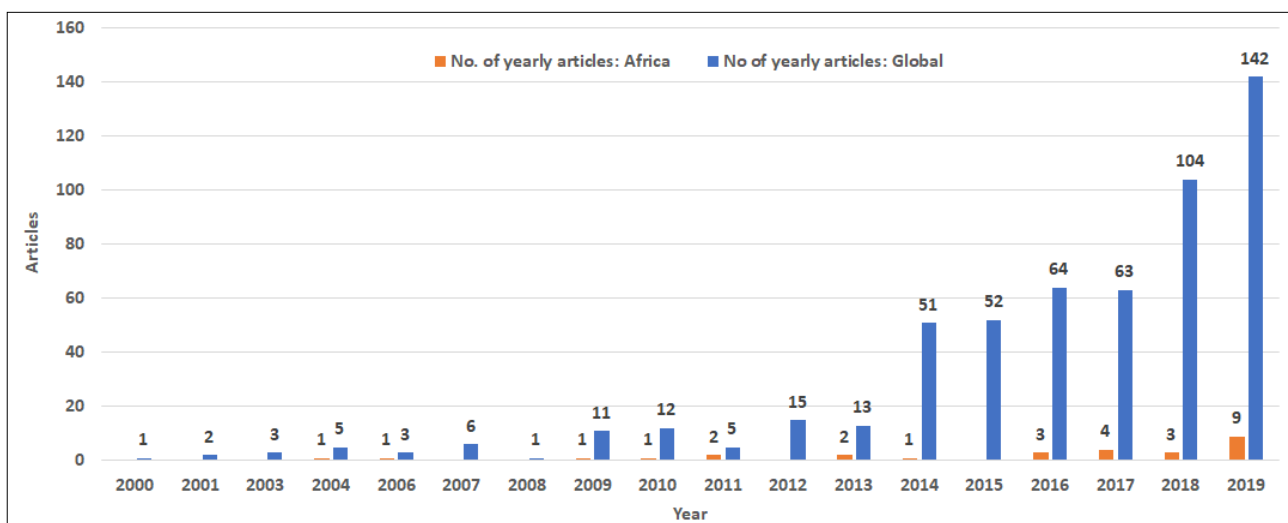


Figure 1: Annual scientific publication output, globally and from Africa.

and 2012. As shown in Figure 1, a slight increase in annual scientific publications is observed from 2016 and reached a peak in 2019 ( $n=9$ ). Scientific publications in Africa showed an approximately 4.4% average annual growth rate.

### Leading countries in scientific publications on socio-hydrology

Numerous countries have contributed to the publication of scientific articles on socio-hydrology research at a global scale (Figure 2). The published articles were either a product of multi-country publications (MCP) or single country publications (SCP). Of the 556 global documents assessed, there were 1396 and 109 authors of multi- and single-authored documents. The USA is the most productive country with 81 (16 MCP and 65 SCP) articles, followed by China (35, with 10 MCP and 25 SCP), the Netherlands (28 with 8 MCP and 20 SCP), Germany (27 with 5 MCP and 22 SCP) and the UK (26 with 5 MCP and 21 SCP). The ranking of the countries is based on the affiliation of the first author. In Africa, the 29 scientific documents were co-authored by 138 researchers under MCPs, with only 8 researchers publishing under the SCP category. The USA leads in scientific publications, with 7 articles (6 SCP and 1 MCP), followed by the Netherlands (5; 1 SCP and 4 MCP), Germany (4; 1 SCP and 3 MCP) and South Africa (4; 3 SCP and 1 MCP) and the UK (3; 2 SCP and 1 MCP). While the study focuses on Africa, the leading countries could be publishing scientific articles emanating from collaborative projects. Overall, most of the scientific papers in Africa were SCP, while only 14% of the output were MCP.

### Countries' collaboration networks

The collaboration mapping of 66 countries resulted in six clusters (Figure 3). Approximately 1216 lines connected the countries; for better visualisation, only 400 lines representing the strongest links between

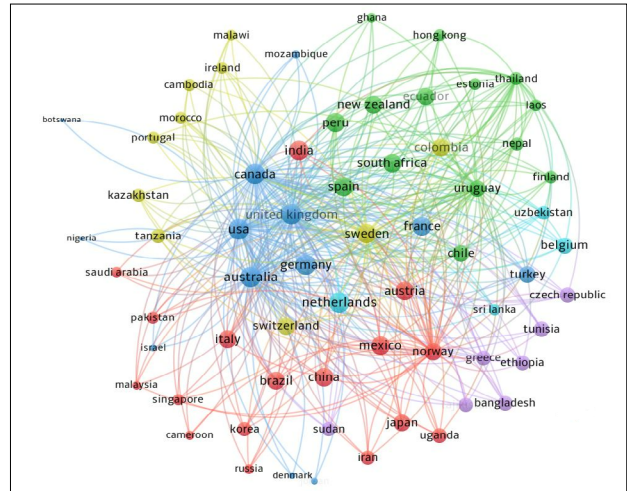


Figure 3: Countries' network collaboration at the global scale.

countries are displayed. The USA (63), Australia (63), Canada (62) and the UK (62) and Germany (62) had the most country collaborations in the dark blue cluster. The most collaborative countries in the red cluster were India (57), Austria (55), Mexico (54), China (54), Italy and Brazil (both with 52 links). Spain (57), Peru (56), South Africa (54), and New Zealand (52) showed significant collaborations in the green cluster. The main collaborative countries in the yellow cluster were Sweden (57), Colombia (51), Switzerland (48), Tanzania (34), Morocco (24), and Malawi (21). The pink and light blue clusters contain few countries with dominant collaborations by Czech Republic (39) and Ethiopia (37) as well as the Netherlands (64) and Belgium (44), respectively. While the network of African countries is not exhaustive, South Africa, Uganda, Tanzania, Morocco, Senegal, Cameroon, Nigeria, Botswana, Ghana, Mozambique, Sudan, are some of the countries publishing socio-hydrology research in the region.

### Keywords co-occurrence analysis

The keywords (approximately 100 for global scale) were grouped into four clusters and are represented by circle shapes in different colours and sizes (Figure 4a). The red cluster reflects on different themes that address important issues within socio-hydrology research. These themes include maintenance of water reservoirs (e.g. surface water, groundwater, and aquifers) and the impacts of climate variability and change on water resources (climate change, drought, anthropogenic effect, irrigation systems, water availability/demand/allocation and seasonal variation). In addition, the red cluster highlights issues relating to governance and stakeholder participation, climate research (through modelling), sustainable development, resilience, and decision-making. Keywords appearing in the yellow cluster are related to water resource management/supply/quality. The green cluster covers planning and innovation concepts such as hydrological modelling/simulation, water planning, conceptual framework, interdisciplinary approach, floodplain, nature–society relations, resource allocation, and uncertainty analysis. The blue cluster consists of policy and environmental management related words. These themes include environmental policy, risk assessment, land use, ecosystems, agriculture, streamflow, rivers and urbanisations.

Keywords co-occurrence analysis for Africa resulted in three clusters (Figure 4b). Hydrological modelling and climate change themes dominated in the green cluster. The red cluster brings to the fore water resource and management issues, with keywords such as hydrology, catchment modelling, integrated approach, and runoff. Agriculture is the central theme in the yellow cluster, connecting with water, food supply and irrigation systems. Rivers dominate in the blue cluster, connecting with river basin, and households within the same cluster as well as with other keywords in the green and red clusters.

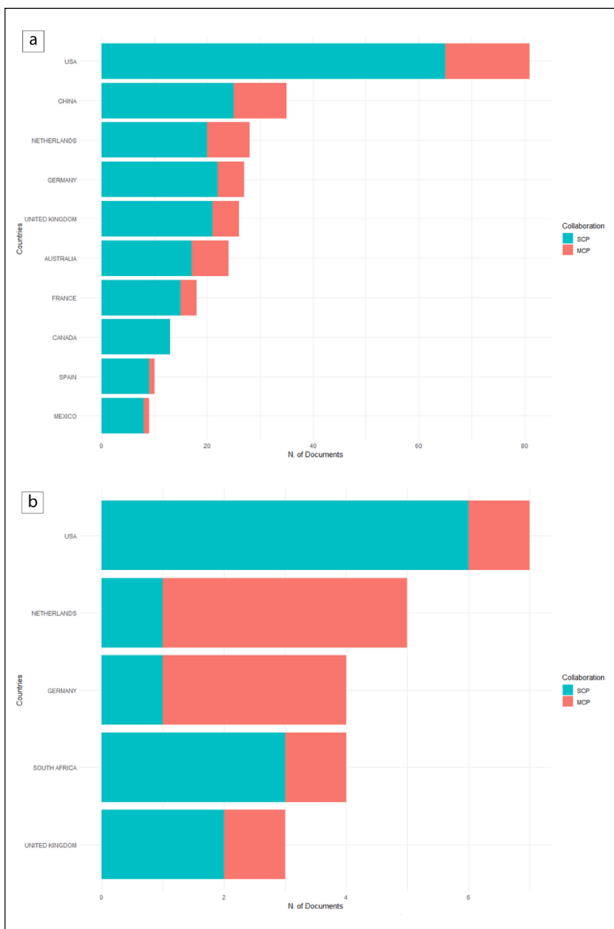


Figure 2: Most productive countries in regard to socio-hydrology research output, (a) globally and (b) in Africa.







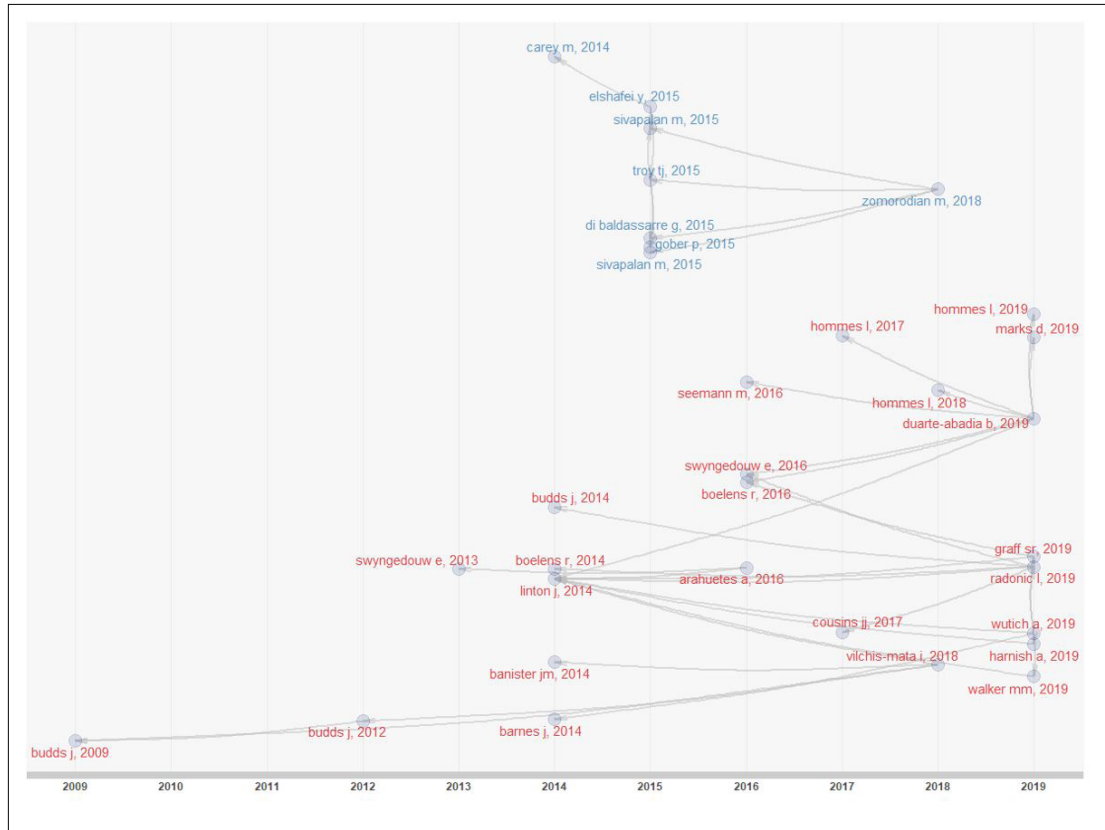


Figure 6: Historical direct citation network of hydrosocial research.

## Discussion

### *Salient features of socio-hydrology research in Africa*

Socio-hydrology has become a prominent field of science aimed at understanding the dynamics and co-evolution of human–water interactions.<sup>9</sup> This field of research has evolved over the years, seemingly, under synonyms such as hydrosociology<sup>6</sup>, hydro-social<sup>8</sup> and ecohydrosolidarity,<sup>49</sup> among others. In this study, we investigated the current body of knowledge and the nature of socio-hydrology research at the global scale as well as in Africa. Socio-hydrology research slowly emerged in 2000, with only one scientific article reported globally. On average, only 13% of articles were released between 2000 and 2011, taking into account the years that had no published output (i.e. 2002 and 2005). Socio-hydrology research gained momentum from 2014, resulting in approximately 79% of the published scientific articles being produced between 2015 and 2019. This great progression suggests that the scientific community globally are paying greater attention to and are advancing socio-hydrology research. In Africa, socio-hydrology research progressed at a minimal rate between 2004 and 2014. However, there is evidence of growing interest in the socio-hydrology research domain among researchers. This assertion is corroborated by the significant growing trend in research publications from Africa between 2016 and 2019.

The current study illustrates that socio-hydrology research has established social structures. In this regard, there is an overwhelming collaboration among countries at the global scale, as evidenced by about 1396 authors involved in multi-country authorship of published scientific documents. However, collaboration between countries in Africa is still lacking. The observed extent of collaboration patterns in the African domain is mostly between developed countries with the necessary expertise, resources, and funding measures. This is also evident from the topmost countries contributing to socio-hydrology research output both globally and in Africa. For instance, the USA is the topmost leading country in published scientific articles at both global and African scales. None of the African countries appears in the list of top ten most

productive countries at a global scale. South Africa is the only country appearing in the top five list at a regional scale. There is, therefore, a need for African countries to expand collaboration between developing countries so that the benefit of socio-hydrology research can be attained in the region. The most significant benefits of such collaborations would include knowledge sharing, and access to advanced technologies such as socio-hydrological models to support the management and planning of water resources, including transboundary resources in the context of a changing climate.

The scope of topics and methods used in socio-hydrology is also still very limited. The results reported in this study indicate that research in socio-hydrology has expanded over the years, with two main emerging areas of research practices: the development of a conceptual framework that also highlighted limitations of hydrological modelling and integrative studies that guide policy and practice in water resource planning and management. The latter have taken a holistic approach to study the coupled human and hydrological systems on human and environmental factors (e.g. increased population growth, water governance, environmental management, and climate).<sup>50</sup> Overall, through direct citation analysis, we posit that the hydrosocial research theme considered by researchers along the two clusters emerged as a concept, and then transitioned into a theoretical framework and tool with practical policy applications in water resources planning and management.

Thematic analysis indicated that research on topics such as water security and hydropower are well established at a global scale. This is especially true in countries such as Colombia and Mexico. There is, however, a need for more research on important cross-cutting topics such as drought, resilience to environmental stressors (associated with, for example, climate change), water governance and hydro-social territories. Emerging topics on water resource management, climate change and health have been undertaken mostly in China. The present analysis also points to global research that has been conducted on specialised topics such as water resource management, politics, flood system dynamics and energy. Meanwhile, the focus in Africa has been on the application of socio-hydrology research to river basins, households

and food supply. Consequently, there is a need to expand this work to further support other nexus sectors such as biodiversity and energy.

The keywords co-occurrence analysis on research done to date on the African continent brought forth topical issues such as catchments, water resources, runoff, rivers and river basins. From a global perspective, co-occurrence analysis brought to the fore water management, water supply, water resources, water conservation, groundwater and irrigation as hot topics. Additionally, the thematic analysis shows that climate change research is an emerging topic that is still nascent in the context of socio-hydrology research at both the global and African scales. However, given the vulnerability of Africa to current and future changes in climate perpetuated by social, economic, and political factors, there is a need to augment this research to enhance the resilience of socio-ecological systems in the region.<sup>51</sup>

### **Opportunities and gaps in socio-hydrology research in Africa**

From a global perspective, socio-hydrology research points to some gaps and opportunities for future research. Wesselink et al.<sup>19</sup> highlighted the benefits of combining both social and hydrological science approaches so as to strengthen both research domains rather than antagonistically question their fundamental assumptions. Their study suggests that the siloed and water-centric approaches cannot adequately capture the everyday realities of water. These realities manifest as complex systems and therefore require integrative approaches to ensure that water users at the community level also contribute to water governance. Nevertheless, governance of hydro-social systems is complex, hence there is a need to establish more effective communication pathways to navigate through conflicting stakeholder priorities and interests. Water demand and environmental management mechanisms such as payment for environmental services can lead to further marginalisation of poor communities' livelihood strategies.<sup>52</sup> Similarly, there is an opportunity to address social and environmental injustice when responding to projected changes in climate. However, initiatives would require that governance actors have a good understanding of how to incorporate the coupled nature of various location- and context-specific human-water interactions and embrace the uncertainties that are part of the process.<sup>53-55</sup>

More so, Page et al.<sup>56</sup> illustrated that there is a need to develop an integrative water research methodology to appreciate the impacts and necessity of desalination within complex hydro-socio-technical systems in countries, especially those currently faced with water scarcity. Furthermore, studies on the multidimensional change in watershed processes resulting from the change in forest cover in tropical regions of Africa illustrate that there are still knowledge gaps on how different types of forest transitions affect low flows and the socio-hydrological links. Therefore, research is required to provide a better understanding of the subject matter and guide policy development within the different tropical regions to integrate concepts and methods as informed by the most recent research.<sup>57</sup>

The bibliometric assessment in this study has demonstrated the diversity of research themes that are linked to socio-hydrology as shown in global studies. It has also highlighted opportunities for Africa to also explore relevant established and emerging concepts to ensure that the knowledge generated can guide policy and yet also transition it to practice in order to achieve sustainable development within the African context.<sup>58,59</sup> The identified emerging research topics in Africa have the potential to contribute to the sustainability of socio-ecological systems and improved human well-being. Such topics include socio-hydrology and its links to energy, health, politics, land governance in communal areas, transboundary water resources as well as climate change related extreme weather events such as floods and droughts.

### **Conclusion**

A bibliometric analysis was conducted to evaluate the nature of socio-hydrology research as well as salient features, such as developmental patterns, research collaborations, keywords co-occurrence and emerging

themes within the subject matter, at a global scale and, specifically, across the African continent. While socio-hydrology research at a global scale began to show an increasing trend two decades ago, gaining momentum in 2014, the scientific publications on socio-hydrology in the African continent only emerged in 2016. The sparing extent of social networks of socio-hydrology research point to the need to collaboratively expand and enhance the research domain in the region. Notwithstanding the apparent developed conceptual structures inherent in the socio-hydrology research domain, developed countries continue to harbour the intellectual structures. This is, undoubtedly, duly supported by the inherent well-established social structures: the collaborative networks. From this perspective, socio-hydrology scholarship on the African continent is, sadly, in its infancy, yet growing. Recognising the inherent pathways of socio-hydrology scholarship, several emerging research topics were identified, and if pursued, we argue, will immensely expand socio-hydrology research on the African continent. Some of these research themes, we opine, include (1) the impacts of climate change on socio-hydrology systems; and (2) the influence of socio-hydrology interactions on the Water-Energy-Food Nexus; and (3) the applications of system dynamic modelling for advancing the understanding of the complex coupled socio-hydrology dynamics.

### **Acknowledgements**

We thank the anonymous reviewers for providing constructive and comprehensive comments that helped to improve the quality of the manuscript.

### **Competing interests**

We have no competing interests to declare.

### **Authors' contributions**

C.M.B.: Conceptualised the study, analysed data, crafted the original draft, and finalised the manuscript. J.O.B.: Conceptualised the study, wrote the scripts, discussed the results, and edited and approved the manuscript. M.M.: Crafted the introduction, discussed the results and edited the manuscript. N.N.Z.: Acquired data, discussed the results and edited the manuscript. A.M.A.: Discussed the results and edited the manuscript. J.Pd.W.: Prepared the study area map and discussed the results. O.M.A.: Discussed the results and edited the manuscript. All authors read the final manuscript and approved the submission.

### **References**

1. Liu Y, Tian F, Hu H, Sivapalan M. Socio-hydrologic perspectives of the co-evolution of humans and water in the Tarim River Basin, Western China: The Taiji-Tire model. *Hydro Earth Syst Sci*. 2014;18:1289–1303. <https://doi.org/10.5194/hess-18-1289-2014>
2. Food and Agriculture Organization of the United Nations (FAO). The state of the world's land and water resources for food and agriculture (SOLAW) – Managing systems at risk. Rome / London: FAO / Earthscan; 2011.
3. Leck H, Conway D, Bradshaw M, Rees J. Tracing the Water-Energy-Food Nexus: Description, theory and practice. *Geogr Compass*. 2015;9(8):445–460. <https://doi.org/10.1111/gec3.12222>
4. Blair P, Buytaert W. Modelling socio-hydrological systems: A review of concepts, approaches and applications. *Hydro Earth Syst Sci Discussions*. 2015;12:8761–8851. <https://doi.org/10.5194/hess-20-443-2016>
5. Falkenmark M. Water and mankind: A complex system of mutual interaction. *Ambio*. 1977;6:3–9. <https://www.jstor.org/stable/4312233>
6. Falkenmark M. Main problems of water use and transfer of technology. *GeoJournal*. 1979;3:435–443. <https://doi.org/10.1007/BF00455982>
7. Sivakumar B. Socio-hydrology: Not a new science, but a recycled and reworded hydrosociology. *Hydro Process*. 2012;26:3788–3790. <https://doi.org/10.1002/hyp.9511>
8. Swyngedouw E. The political economy and political ecology of the hydro-social cycle. *J Contemp Water Res Educ*. 2009;142:56–60. <https://doi.org/10.1111/j.1936-704X.2009.00054.x>



9. Sivapalan M, Savenije HHG, Blöschl G. Socio-hydrology: A new science of people and water. *Hydrol Process*. 2012;26:1270–1276. <https://doi.org/10.1002/hyp.8426>
10. Pande S, Sivapalan M. Progress in sociohydrology: A meta-analysis of challenges and opportunities. *WIREs Water*. 2017;4(4), e1193. <https://doi.org/10.1002/wat2.1193>
11. Di Baldassarre G, Kooy M, Kemerink JS, Brandimarte L. Towards understanding the dynamic behaviour of floodplains as human-water systems. *Hydrol Earth Syst Sci*. 2013;17:3235–3244. <https://doi.org/10.5194/hess-17-3235-2013>
12. Di Baldassarre G, Viglione A, Carr G, Kuil L, Salinas JL, Blöschl G. Sociohydrology: Conceptualising human-flood interactions. *Hydrol Earth Syst Sci*. 2013;17:3295–3303. <https://doi.org/10.5194/hess-17-3295-2013>
13. Elshafei Y, Sivapalan M, Tonts M, Hipsey MR. A prototype framework for models of socio-hydrology: Identification of key feedback loops and parameterisation approach. *Hydrol Earth Syst Sci*. 2014;18:2141–2166. <https://doi.org/10.5194/hess-18-2141-2014>
14. Wutich A, Beresford M. The economic anthropology of water. *Econ Anthropol*. 2019;6:168–182. <https://doi.org/10.1002/sea2.12153>
15. Wilfong M, Pavao-Zuckerman M. Rethinking stormwater: Analysis using the hydrological cycle. *Water*. 2020;12:1273. <https://doi.org/10.3390/w12051273>
16. Chang H, Thiers P, Netusil NR, Yeakley JA, Rollwagen-Bollens G, Bollens SM, et al. Relationships between environmental governance and water quality in a growing metropolitan area of the Pacific Northwest, USA. *Hydrol Earth Syst Sci*. 2014;18:1383–1395. <https://doi.org/10.5194/hess-18-1383-2014>
17. Yang L, Chen Z, Liu T, Gong Z, Yu Y, Wang J. Global trends of solid waste research from 1997 to 2011 by using bibliometric analysis. *Scientometrics*. 2013;96:133–146. <https://doi.org/10.1007/s11192-012-0911-6>
18. Aria M, Cuccurullo C. Bibliometric: An R-tool for comprehensive science mapping analysis. *J Inform*. 2017;11:959–975. <https://doi.org/10.1016/j.joi.2017.08.007>
19. Wesselink A, Kooy M, Warner J. Socio-hydrology and hydrosocial analysis: Toward dialogues across disciplines. *WIREs Water*. 2017;4, e1196. <https://doi.org/10.1002/wat2.1196>
20. Omerzel DG. A systematic review of research on innovation in hospitality and tourism. *Int J Contemp Hosp M*. 2016;28(3):516–558. <https://doi.org/10.1108/IJCHM-10-2014-0510>
21. Li W, Zhao Y. Bibliometric analysis of global environmental assessment research in a 20-year period. *Environ Impact Assess Rev*. 2015;50:158–166. <https://doi.org/10.1016/j.eiar.2014.09.012>
22. Wang B, Pan S-Y, Ke R-Y, Wang K, Wei Y-M. An overview of climate change vulnerability: A bibliometric analysis based on Web of Science database. *Nat Hazards*. 2014;74:1649–1666. <https://doi.org/10.1007/s11069-014-1260-y>
23. Gall M, Nguyen KH, Cutter SL. Integrated research on disaster risk: is it really integrated? *Int J Disaster Risk Reduct*. 2015;12:255–267. <https://doi.org/10.1016/j.ijdrr.2015.01.010>
24. Dias GP. A decade of Portuguese research in e-government: Evolution, current standing and ways forward. *Int J Electron Gov*. 2016;12(3):201. <http://dx.doi.org/10.1504/EG.2016.078415>
25. Dias GP. Bibliometric analysis of Portuguese research in e-government. *Proc Tech*. 2014;16:279–287. <https://doi.org/10.1016/j.protcy.2014.10.093>
26. Ajibade P, Mutula SM. Bibliometric analysis of citation trends and publications on e-government in southern African countries: A human-computer interactions and IT alignment debate. *Libr Philos Pract*. 2019, Art. #2234. Available from: <https://digitalcommons.unl.edu/libphilprac/2234/>
27. Corte VD, Del Gaudio G, Sepe F, Sciarelli F. Sustainable tourism in the open innovation realm: A bibliometric analysis. *Sustainability*. 2019;11(21), Art. #6114. <https://doi.org/10.3390/su11216114>
28. Naruetharadhol P, Gombsombut N. A bibliometric analysis of food tourism studies in Southern Asia. *Cogent Bus Manag*. 2020;7, Art. #1733829. <https://doi.org/10.1080/23311975.2020.1733829>
29. Van Nunen K, Li J, Reniers G, Ponnet K. Bibliometric analysis of safety culture research. *Safety Sci*. 2018;108:248–258. <https://doi.org/10.1016/j.ssci.2017.08.011>
30. Cortes PD, Rodrigues R. A bibliometric study on “education for sustainability”. *Braz J Sci Technol*. 2016;3:1–17. <https://doi.org/10.1186/s40552-016-0016-5>
31. Virani A, Wellstead AM, Howlett M. Where is the policy? A bibliometric analysis of the state of policy research on medical tourism. *Glob Health Res Policy*. 2020;5:19. <https://doi.org/10.1186/s41256-020-00147-2>
32. Ahmed ASF, Vanga S, Raghavan V. Global bibliometric analysis of the research in biochar. *J Agri Food Inf*. 2018;19(3):228–236. <https://doi.org/10.1080/10496505.2017.1403328>
33. Arfaoui A, Ibrahim K, Trabelsi F. Biochar application to soil under arid conditions: A bibliometric study of research status and trends. *Arab J Geosci*. 2019;12:45. <https://doi.org/10.1007/s12517-018-4166-2>
34. Zhang X, Estoque RC, Xie H, Murayama Y, Ranagalage M. Bibliometric analysis of highly cited articles on ecosystem services. *PLoS ONE*. 2019;14(2), e0210707. <https://doi.org/10.1371/journal.pone.0210707>
35. Zhu Z, Jiang Ji-T, Han Ch-L, Gao S, He K, Zhao H, et al. A bibliometrics review of water footprint research in China: 2003–2018. *Sustainability*. 2019;11:5082. <https://doi.org/10.3390/su11185082>
36. Xu L, Gober P, Wheeler HS, Kajikawa Y. Reframing socio-hydrological research to include a social science perspective. *J Hydrol*. 2018;563:76–83. <https://doi.org/10.1016/j.jhydrol.2018.05.061>
37. Cobo MJ, López-Herrera AG, Herrera-Viedma E, Herrera F. An approach for detecting, quantifying, and visualizing the evolution of a research field: A practical application to the fuzzy sets theory field. *J Informetr*. 2011;5(1):146–166. <https://doi.org/10.1016/j.joi.2010.10.002>
38. Garfield E, Sher IH, Torpie RJ. The use of citation data in writing the history of science. Technical report. Philadelphia, PA: Institute for Scientific Information; 1964.
39. Shibata N, Kajikawa Y, Takeda Y, Matsushima K. Comparative study on methods of detecting research fronts using different types of citation. *J Am Soc Inf Sci Tec*. 2009;60(3):571–580. <https://doi.org/10.1002/asi.20994>
40. Budds J. Contested H<sub>2</sub>O: Science, policy and politics in water resources management in Chile. *Geoforum*. 2009;40(3):418–430. <https://doi.org/10.1016/j.geoforum.2008.12.008>
41. Budds J, Hinojosa L. Restructuring and rescaling water governance in mining contexts: The co-production of waterscapes in Peru. *Water Altern*. 2012;5(1):119–137. <http://oro.open.ac.uk/32484/>
42. Barnes J, Alatout S. Water worlds: Introduction to the Special issue of Social Studies of Science. *Soc Stud Sci*. 2012;42:483–488. <https://doi.org/10.1177/0306312712448524>
43. Vilchis-Mata I, Garrocho C, Delgado CD. Adaptive dynamic model for sustainable decision making in the urban hydrosocial cycle in Mexico. *Rev Geogr Norte Gd*. 2018;71:59–90. <https://doi.org/10.4067/S0718-34022018000300059>
44. Carey M, Baraer M, Mark BG, French A, Bury J, Young KR, et al. Toward hydro-social modeling: Merging human variables and the social sciences with climate-glacier runoff models (Santa River, Peru). *J Hydrol*. 2014;518:60–70. <https://doi.org/10.1016/j.jhydrol.2013.11.006>
45. Sivapalan M. Debates-perspectives on socio-hydrology: Changing water systems and the “tyranny of small problems” – Socio-hydrology. *Water Resour Res*. 2015;51:4795–4805. <https://doi.org/10.1002/2015WR017080>
46. Troy TJ, Pavao-Zuckerman M, Evans TP. Debates-perspectives on socio-hydrology: Socio-hydrologic modeling: Tradeoffs, hypothesis testing, and validation. *Water Resour Res*. 2015;51:4806–4814. <https://doi.org/10.1002/2015WR017046>
47. Elshafei Y, Coletti JZ, Sivapalan M, Hipsey MR. A model of the socio-hydrologic dynamics in a semiarid catchment: Isolating feedbacks in the coupled human-hydrology system. *Water Resour Res*. 2015;51:6442–6471. <https://doi.org/10.1002/2015WR017048>
48. Zomorodian M, Lai SH, Homayounfar M, Ibrahim S, Fatemi SE, El-Shafie A. The state-of-the-art system dynamics application in integrated water resources modeling. *J Environ Manage*. 2018;1(227):294–304. <https://doi.org/10.1016/j.jenvman.2018.08.097>
49. Falkenmark M. Ecohydro solidarity – Towards better balancing of humans and nature. *Waterfront*. 2009(2):4–5. Available from: <http://dlc.dlib.indiana.edu/dlc/handle/10535/5164>



50. Sivapalan M, Blöschl G. Time scale interactions and the coevolution of humans and water. *Water Resour Res.* 2015;51:6988–7022. <https://doi.org/10.1002/2015WR017896>
51. Nhemachena C, Hassan R. Determinants of African farmers' strategies for adapting to climate change: Multinomial choice analysis. *Afr J Agric Resour Econ.* 2008;2(1):83–104.
52. Rodriguez-de-Francisco JC, Boelens R. PES hydrosocial territories: De-territorialization and re-patterning of water control arenas in the Andean highlands. *Water Int.* 2016;41(1):140–156. <https://doi.org/10.1080/02508060.2016.1129686>
53. Nikkels M, Kumar S, Meinke H. Adaptive irrigation infrastructure – linking insights from human-water interactions and adaptive pathways. *Curr Opin Env Sust.* 2019;40:37–42. <https://doi.org/10.1016/j.cosust.2019.09.001>
54. Di Baldassarre G, Viglione A, Carr G, Kuil L, Yan K, Brandimarte L, et al. Debates-perspectives on socio-hydrology: Capturing feedbacks between physical and social processes. *Water Resour Res.* 2015;51:4770–4781. <https://doi.org/10.1002/2014WR016416>
55. Wessels M, Veldwisch GJ, Kujawa K, Delcarme B. Upsetting the apple cart? Export fruit production, water pollution and social unrest in the Elgin Valley, South Africa. *Water Int.* 2019;44(2):188–205. <https://doi.org/10.1080/02508060.2019.1586092>
56. Page A, Langarudi S, Forster-Cox S, Fernald A, Liu G. A dynamic hydro-socio-technical policy analysis of transboundary desalination development. *J Environ Account Manag.* 2019;7:87–114. <https://doi.org/10.5890/JEAM.2019.03.007>
57. Sharachchandra L. Watershed services of tropical forests: From hydrology to economic valuation to integrated analysis. *Curr Opin Env Sust.* 2009;1:148–155. <https://doi.org/10.1016/j.cosust.2009.10.007>
58. Adams EA, Kuusaana ED, Ahmed A, Campion BB. Land dispossessions and water appropriations: Political ecology of land and water grabs in Ghana. *Land Use Policy.* 2019;87:104068. <https://doi.org/10.1016/j.landusepol.2019.104068>
59. Sow S, de Vlas SJ, Stelma F, Vereecken K, Gryseels B, Polman K. The contribution of water contact behavior to the high *Schistosoma mansoni* infection rates observed in the Senegal River Basin. *BMC Infect Dis.* 2011;11:198. <https://doi.org/10.1186/1471-2334-11-198>



**AUTHORS:**

Sibongile M. Malunga<sup>1</sup>  
 Nhamo Chaukura<sup>2</sup>   
 Chiedza I. Mbiriri<sup>3</sup>  
 Willis Gwenzi<sup>4</sup>  
 Mambo Moyo<sup>5</sup>  
 Alex T. Kuvarega<sup>6</sup>

**AFFILIATIONS:**

<sup>1</sup>Chemistry Department, Bindura University of Science Education, Bindura, Zimbabwe  
<sup>2</sup>Department of Physical and Earth Sciences, Sol Plaatje University, Kimberley, South Africa  
<sup>3</sup>Department of Biological Sciences, Bindura University of Science Education, Bindura, Zimbabwe  
<sup>4</sup>Biosystems and Environmental Engineering Research Group, Department of Soil Science and Agricultural Engineering, University of Zimbabwe, Harare, Zimbabwe  
<sup>5</sup>Department of Chemical Technology, Midlands State University, Gweru, Zimbabwe  
<sup>6</sup>Nanotechnology and Water Sustainability Research Unit, College of Engineering, Science and Technology, University of South Africa, Johannesburg, South Africa

**CORRESPONDENCE TO:**

Nhamo Chaukura

**EMAIL:**

nhamo.chaukura@spu.ac.za

**DATES:**

**Received:** 28 Apr. 2021

**Revised:** 16 Sep. 2021

**Accepted:** 21 Sep. 2021

**Published:** 27 Jan. 2022

**HOW TO CITE:**

Malunga SM, Chaukura N, Mbiriri CI, Gwenzi W, Moyo M, Kuvarega AT. Visible light photodegradation of methyl orange and *Escherichia coli* O157:H7 in wastewater. S Afr J Sci. 2022;118(1/2), Art. #10938. <https://doi.org/10.17159/sajs.2022/10938>

**ARTICLE INCLUDES:**

- Peer review
- Supplementary material

**DATA AVAILABILITY:**

- Open data set
- All data included
- On request from author(s)
- Not available
- Not applicable

**EDITOR:**

Jennifer Fitchett

**KEYWORDS:**

catalysis, environmental remediation, pollution, porous materials, wastewater, zeolite

**FUNDING:**

None



© 2022. The Author(s). Published under a Creative Commons Attribution Licence.

# Visible light photodegradation of methyl orange and *Escherichia coli* O157:H7 in wastewater

Water pollution due to dyes and pathogens is problematic worldwide, and the disease burden is higher in low-income countries where water treatment facilities are usually inadequate. Thus the development of low-cost techniques for the removal of dyes and pathogens in aquatic systems is critical for safeguarding human and ecological health. In this work, we report the fabrication and use of a photocatalyst derived from waste from coal combustion in removing dyes and pathogens from wastewater. Higher TiO<sub>2</sub> loading of the photocatalyst increased the removal efficiency for methyl orange (95.5%), and fluorine-doping improved the disinfection efficacy from 76% to 95% relative to unmodified material. Overall, the work effectively converted hazardous waste into a value-added product that has potential in point-of-use water treatment. Future research should focus on upscaling the technique, investigating the fate of the potential of the photocatalysts for multiple reuse, and the recovery of TiO<sub>2</sub> in treated water.

**Significance:**

- The study provides a pathway for the fabrication of a value-added product from coal fly ash waste.
- The use of the proposed nanocomposite material for wastewater treatment represents a potentially affordable, simple, and sustainable technology for point-of-use water treatment.

## Introduction

Dyes such as methyl orange and methylene blue are used in printing, pharmaceuticals and research laboratories, but the textile industry remains one of the most polluting industries that use dyes due to the large quantities of effluents discharged.<sup>1</sup> The World Bank estimates that the textile dyeing industry contributes 20% of all industrial wastewater pollution globally.<sup>2</sup> Azo dyes account for up to 70% of all textile dyes produced, and hence constitute a major component (2–20%) of wastewater effluents discharged from textile industries.<sup>3,4</sup> Due to their intricate aromatic molecular structure and synthetic origin, dyes and pigments are mostly non-biodegradable.<sup>1</sup> Consequently, they cause water pollution, even at very low concentrations. Moreover, dyes decrease light penetration and thus reduce photosynthesis in aquatic plants.<sup>5</sup> Dyes may also contain toxic metals, either within their structure or through complexation in the environment. Hence, their removal in wastewater has been a subject of interest in recent years.

The presence of coliforms, in particular *Escherichia coli*, in water indicates faecal contamination; therefore *E. coli* is one of the most common and important indicator organisms of water safety. Some strains, of which O157:H7 is representative, cause sporadic outbreaks of severe food and waterborne disease. *E. coli* produces a shiga toxin which can cause severe enteric infection, resulting in diarrhoea, haemorrhagic colitis, and haemolytic-uremic syndrome in humans.<sup>6</sup> One key factor in reducing or eliminating such diseases lies in providing safe water, especially to isolated communities where centralised water supplies are limited.

Methods currently used for the removal of dyes include chemical coagulation, biodegradation, flocculation, precipitation, reverse osmosis, photocatalysis, adsorption, ionising and gamma radiation.<sup>7</sup> Recent developments in nanotechnology have led to the use of carbon-based and metal oxide nanocomposites to remove organic compounds.<sup>8,9</sup> However, these techniques have high capital and maintenance costs, and produce secondary pollutants through the generation of sludge, while oxidation processes may produce metabolic products that pose public health risks.<sup>10</sup> Greener and more cost-effective methods such as dye solubilisation using natural surfactants or biosurfactants have been recently proposed.<sup>11,12</sup> However, the methods work only with ionic dyes such as Congo Red, and their efficiency with non-ionic surfactants is limited.<sup>11</sup> Furthermore, wastewater treatment plants are not adequately equipped to remove dyes, especially where they are based on conventional methods. Therefore, there is need to develop innovative wastewater treatment technologies which are economically feasible, easy to operate and maintain, effective, and which allow for materials to be recovered and reused.<sup>13</sup>

Zeolites, which are aluminosilicate materials, are one of the most extensively used adsorbents due to their high contaminant removal efficiency arising from a large surface area.<sup>14</sup> The cost of natural zeolites is high, and becomes even higher when synthetic compounds are used. Fly ash (FA), a solid residue from the combustion of coal, is produced in large quantities in several developing countries, where it is stockpiled or disposed of in non-engineered landfills. Such poor disposal practices pose human and ecological health risks, and pollution due to discharged FA has been documented.<sup>15</sup> Globally, attempts have been made to convert FA into value-added products such as synthetic zeolites.<sup>16</sup> Thus, the overall environmental footprint and cost of FA-based zeolites is lower than that of natural zeolites or those developed from the precursors.

Advanced oxidation processes are a recent technology in the treatment of wastewater.<sup>17</sup> Of all the advanced oxidation processes, semiconductor photocatalysts are an interesting option in removing dyes because they can completely mineralise dyes at room temperature and pressure, via oxidation using light energy, and they can withstand the toxicity of dyes.<sup>18</sup> Among the photocatalysts, TiO<sub>2</sub> is most commonly used because it is cheap, non-toxic, thermodynamically and photo-chemically stable, works over a wide pH range, and its band edges are aligned to the redox potential of water.<sup>17</sup> Consequently, a number of studies have investigated photodegradation

using TiO<sub>2</sub>-based nanoparticles.<sup>8,19,20</sup> The application of unmodified TiO<sub>2</sub> as a photocatalyst is limited by its wide band gap (3.2 eV), electron-hole recombination, and low absorption of visible light.<sup>8</sup> The high band gap in TiO<sub>2</sub> results in a reduction of photo-efficiency. Accordingly, dopants such as C, N, and F have been introduced to narrow the band gap.

TiO<sub>2</sub>-zeolite nanocomposites have been studied for the removal of dyes in industrial effluent.<sup>5,21</sup> Zeolites can be cheaply obtained from FA. The conversion of FA into zeolites, and their subsequent use for contaminant removal, minimises the health risks associated with poor disposal of FA, while providing novel materials for wastewater treatment. The capacity of zeolites to remove contaminants can be enhanced by coupling to photocatalysts to produce hybrid materials, so that adsorption occurs on the zeolite while the photocatalyst degrades the pollutant.<sup>21,22</sup> In this study, we sought to improve the photo-efficiency of TiO<sub>2</sub> photocatalysts by using low-cost zeolites as support structures for doped TiO<sub>2</sub> in the photodegradation of methyl orange (MO) and *E. coli* in aqueous solution using a custom-made photocatalytic reactor. Although MO and *E. coli* do not always coexist in the natural aquatic environment, this work proves the case of the removal of organic compounds and pathogenic organisms. Most previous research has demonstrated the photodegradation of either a model dye compound or a model pathogen species separately. Moreover, they use photocatalysts synthesised from commercial reagents, which are expensive. Because it uses waste feedstock for the synthesis of photocatalysts, and mimics solar radiation in the photodegradation process, this is an affordable and sustainable innovative approach with immense potential in point-of-use water-treatment devices. Although the TiO<sub>2</sub> photocatalysts are likely to persist and cause pollution in treated water, their recovery was not investigated in this study. Specifically, the study aimed at: (1) synthesising a low-cost photocatalyst derived from fly ash, TiO<sub>2</sub>, and fluorine, and (2) evaluating the photocatalytic behaviour of the materials in the degradation of MO and *E. coli*.

## Materials and methods

### Ethical considerations

Before carrying out this work, ethical clearance was provided based on the proposed handling of hazardous chemicals and data generation, processing, and storage. This ensured safe procedures were followed

in handling chemicals and other potentially hazardous materials. The handling and disposal of *E. coli* was according to strict procedures that prevented contamination. Permission was obtained prior to sampling FA from a local power plant. Protocols for data generation, processing, storage, and sharing were followed to ensure integrity and validity of the findings.

### Materials

Chemical reagents used included titanium (IV) isopropoxide (TTIP) (97%), 2-propanol (99.7%), formic acid (85%), NaOH (98%), trifluoroacetic acid (purity >97%), MO (85%) and HCl (30–33%). All the chemicals were of analytical reagent grade purchased from either Sigma-Aldrich, Merck, or Glassworld (Berlin, Germany). Except in the study of the degradation of *E. coli* where Ringer's solution was used, deionised water was used to prepare solutions. FA was obtained from Harare Thermal Power Station, and *E. coli* 0157:H7 was obtained from Sigma-Aldrich. A custom-made photocatalytic reactor was fabricated from 5-m-long light emitting diode strips (60 LED/m, 4.8 W, 12 V DC, luminous flux 360 lm/m, and colour temperature 3000 K) wrapped around a 1-L glass beaker and held in place using tape (Figure 1). Preliminary tests conducted using TiO<sub>2</sub> and methylene blue dye showed that the intensity of the light output can be tuned to the desired level by controlling the luminance. In this work, white light at 80% luminance was used for all experiments.

### Preparation of photocatalysts

#### TiO<sub>2</sub>

The sol-gel method was used to prepare TiO<sub>2</sub> nanoparticles with TTIP as a precursor. Briefly, TTIP (10 mL) was dissolved in 2-propanol (50 mL) and stirred to get a homogeneous solution. Under continuous stirring, formic acid (10 mL) was added dropwise for 60 min to hydrolyse the mixture. The resulting TiO<sub>2</sub> sol was left to age for 24 h at room temperature. The dry TiO<sub>2</sub> gel was placed in a muffle furnace and calcined at 450–500 °C for 3 h.

#### Zeolitic fly ash

Zeolites were synthesised from FA via hydrothermal synthesis using NaOH to produce zeolite fly ash (ZFA).<sup>23</sup> Zeolitic materials have been prepared previously from the same FA using a similar method and

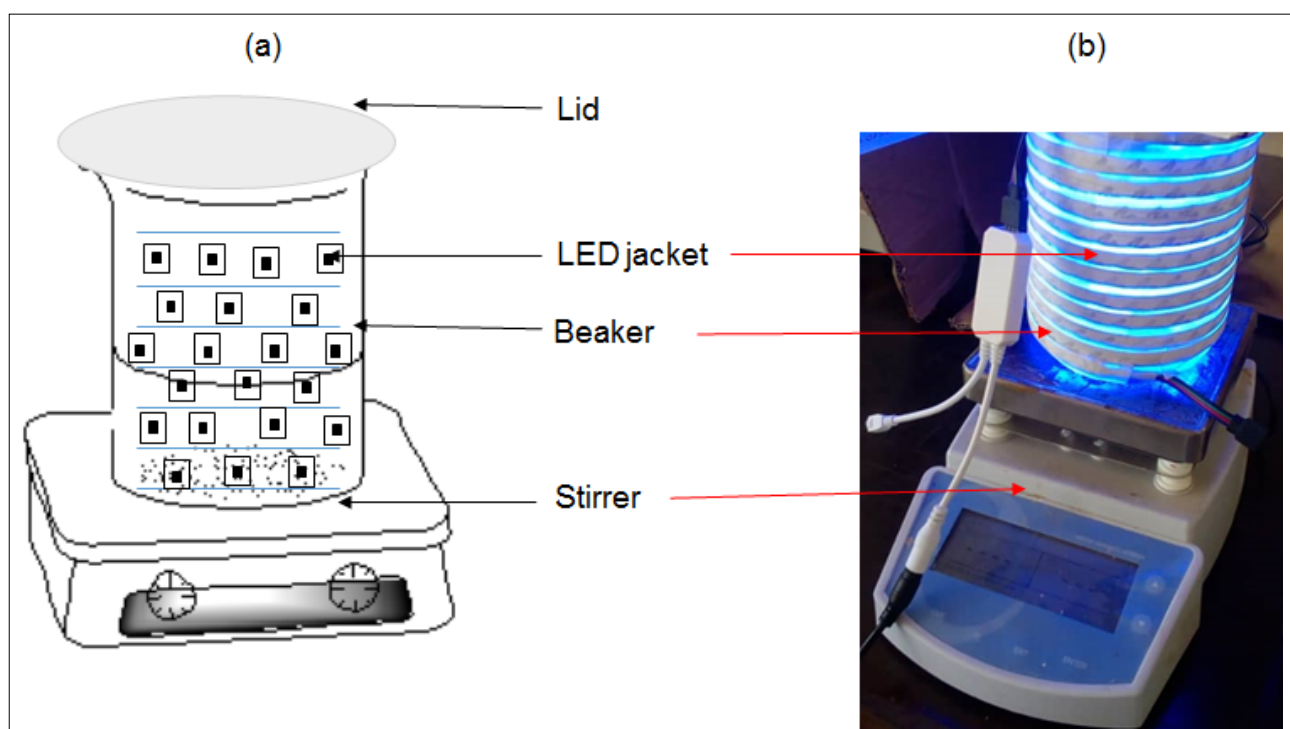


**Figure 1:** The custom-made photocatalytic reactor showing (a) the sketch, and (b) the digital image of the reactor.

successfully used to remove metals in acid mine drainage.<sup>24</sup> In brief, FA was dried in an oven at 70 °C. NaOH pellets were added to the dry FA in the ratio 1:12 (w/w), and the mixture was ground and mixed thoroughly. The mixture was fused at 550–600 °C for 1 h in a muffle furnace, after which it was cooled and ground again. To the resulting powder was added deionised water (400 mL) and this mixture was stirred at room temperature overnight. This mixture was then placed in an oven to cure at 55 °C for 4 days to allow crystallisation to occur. The solid was separated from the liquid phase by filtration using No. 1 Whatman filter paper. The resulting ZFA was washed twice with distilled water, dried in an oven at 80 °C for 12 h, and milled to pass through a 250- $\mu$ m sieve.

### TiO<sub>2</sub>-ZFA nanocomposites

A one-pot acid catalysed sol-gel synthesis method was used to prepare TiO<sub>2</sub>-ZFA nanocomposites. In this method, ZFA of particle size 75  $\mu$ m and mass 24.5 g was added to 2-propanol (50 mL), followed by 30 min of stirring at 40 °C. Different volumes of TTIP (Table 1) were added to the mixture to give 5%, 7% and 10% TiO<sub>2</sub> (w/w) followed by stirring for a further 30 min. Then formic acid (10 mL) was added dropwise under continuous stirring for 30 min until a white sol-gel was observed. This sol-gel was allowed to age for 24 h at room temperature and then dried in an oven at 80 °C for 10 h. The sample was then ground to pass through a 250- $\mu$ m sieve, and calcined at 450 °C for 4 h in a muffle furnace.

Table 1: Preparation of TiO<sub>2</sub>-ZFA photocatalysts

Sample	TTIP (mL)	2-propanol (mL)	Formic acid (mL)	ZFA (g)
5% TiO <sub>2</sub> -ZFA	5	50	10	24.5
7% TiO <sub>2</sub> -ZFA	7	50	10	24.5
10% TiO <sub>2</sub> -ZFA	10	50	10	24.5

### F-doped TiO<sub>2</sub> and F-doped TiO<sub>2</sub>-ZFA photocatalysts

F-doped TiO<sub>2</sub> (F-TiO<sub>2</sub>) was prepared using a two-step sol-gel method.<sup>25</sup> Specifically, TTIP (10 mL) was dissolved in 2-propanol (50 mL) and vigorously stirred for 10 min to make solution A. Trifluoroacetic acid (0.5 mL) was mixed with 2-propanol (30 mL), formic acid (10 mL), deionised water (10 mL) and HCl (3 mL) and continuously stirred for 30 min to make solution B. This solution was added dropwise to solution A and continuously stirred for 30 min until a white sol-gel was observed. The sol-gel was aged for 24 h, oven-dried overnight at 50 °C, ground to pass through a 250- $\mu$ m sieve, and calcined at 450 °C for 4 h in a muffle furnace. F-doped TiO<sub>2</sub>-ZFA (F-TiO<sub>2</sub>-ZFA) was prepared in the same way except the precursor was TiO<sub>2</sub>-ZFA, and CF<sub>3</sub>CO<sub>2</sub>H was used instead of formic acid.

### Characterisation of photocatalysts

#### pH<sub>zpc</sub> and ash content

The pH<sub>zpc</sub> was used as a proxy for surface charge, and it was determined to elucidate the solid-liquid interfacial charge interactions between the photocatalysts and MO molecular surfaces.<sup>26</sup> Determination of pH<sub>zpc</sub> was performed following the pH-drift method.<sup>27</sup> The ash content was determined from the mass difference before and after igniting the samples at 750 °C for 4 h.

#### Fourier transform infrared spectroscopy

To determine the surface functional groups on the photocatalysts, infrared spectra were recorded using a Fourier transform infrared (FTIR) spectrometer (Analytical® Technologies Limited, Infra 3000A, India). The samples were prepared using the KBr pellet method with a sample/KBr ratio of 1:40 to allow the samples to be infrared transparent. The spectra were recorded using 32 scans in the range 4000–400 cm<sup>-1</sup> with a resolution of 4.

### Diffuse reflectance UV-Vis spectroscopy

Diffuse reflectance spectroscopy UV-Vis spectra of the photocatalysts were measured using a UV-Vis near-infrared spectrophotometer<sup>22</sup> (Lambda 650S, PerkinElmer, Johannesburg, South Africa) equipped with deuterium and tungsten lamps as the UV-Vis near-infrared radiation sources. The reflectance (*R*) for each sample was measured in the range 250–800 nm using the 150-mm sphere reflectance method. A slit width of 4 mm, a 0.2-s photomultiplier response, and reflectance blank of BaSO<sub>4</sub> were used. From the UV-Vis data, an absorption coefficient was obtained in the form of the Kubelka–Munk function  $[F(R)]^{25,28}$ , which was used to predict reflectance based on radiation transfer (Equation 1):

$$F(R) = \frac{(1-R)^2}{2R} \quad \text{Equation 1}$$

Using the equation of Tauc (Equation 2), the band gap ( $E_g$ ) for the different photocatalysts was estimated.<sup>29</sup> Values of  $E_g$  were determined at the point of the horizontal intercept from plots of  $[\hbar\nu \times F(R)]^{1/n}$  against  $\hbar\nu$ .

$$(\hbar\nu \times F(R))^{1/n} = A(\hbar\nu - E_g)^n, \quad \text{Equation 2}$$

where  $h$  is Planck's constant ( $6.626 \times 10^{-34}$ ),  $\nu$  is frequency of radiation,  $c$  is the speed of light ( $3.0 \times 10^8$  m/s),  $n$  is the numerical value of electronic transitions and is equal to 2 for TiO<sub>2</sub>.

### Surface morphology and crystallinity of the photocatalysts

Scanning electron microscopy (SEM) was used to obtain information on the surface morphology of the photocatalysts.<sup>15</sup> Micrographs were obtained from a SEM microscope (Tescan, Vega 3, Brno, Czech Republic). Samples were prepared by placing powdered samples on an adhesive carbon tape stuck to a sample holder and then sputter-coating with 15  $\mu$ m gold film; samples were observed under a microscope at 50  $\mu$ m magnification. The crystallinity of the photocatalysts was measured using a powder X-ray diffraction spectrometer<sup>19,22</sup> (D2 Phaser, Bruker, Billerica, MA, USA) fitted with a Cu X-ray source at 1.5418 Å, and operated in the continuous position-sensitive detector fast-scan mode.

### Preparation of MO solutions and *E. coli* contaminated water

A 100 mg/L stock solution of synthetic wastewater was prepared by dissolving a known mass of MO dye in deionised water. From this, working solutions (1, 2, 3, 4, 5 mg/L) were prepared by serial dilution. *E. coli* 0157:H7, a commonly used indicator organism, was selected as the model microorganism representing potentially pathogenic organisms occurring in water and wastewaters. The initial concentration of *E. coli* in the synthetic wastewater was  $3.8 \times 10^8$  CFU/mL; the concentration was enumerated initially and at hourly intervals for 3 h thereafter.<sup>30</sup> HiCrome™ *E. coli* agar, a selective medium that allows for the growth of *E. coli*, and nutrient agar for subsequent enumeration, were used. *E. coli* cell cultures were made to the sixth dilution using Ringer's solution, and the cultures were plated on duplicate nutrient agar plates for each dilution. The agar plates were then incubated at 37 °C for 48 h.

### Evaluation of the photocatalytic activity of photocatalysts

Photodegradation experiments were performed using a custom-made photocatalytic reactor to evaluate the effect of contact time on the photodegradation process. The kinetics of the photodegradation of MO were studied using F-doped photocatalysts owing to their superior photocatalytic properties. The photodegradation studies were carried out using 100 mL of synthetic wastewater at 25 °C, at pH 7.2, a photocatalyst dosage of 500 mg, a dye concentration of 2 mg/L, and contact time of -60, 0, 60, and 120 min in a 150 mL beaker, following a variation of the method reported by Mukonza et al.<sup>25</sup> To eliminate the interference of leftover photocatalyst in absorbance readings, a blank experiment of distilled water and photocatalyst was set up. All samples were stirred in the dark for 1 h under room temperature ( $25 \pm 1$  °C) to attain absorption equilibria before being irradiated with visible light in the photocatalytic reactor.



The concentrations of MO before ( $C_0$ ) and after ( $C_t$ ) photodegradation experiments were determined based on UV-Vis absorbance spectra. Samples (4 mL) were drawn at 1 h intervals using a 10-mL syringe and filtered through a 0.45- $\mu$ m filter. The aliquots were centrifuged and the residual concentration of MO in the supernatant was measured at 460 nm using a UV-Vis spectrophotometer (Spectroquant® Pharo 300). The dye removal ( $r$ ) was computed using Equation 3<sup>31</sup>:

$$r = \frac{C_0 - C_t}{C_0} \times 100 \quad \text{Equation 3}$$

The order of reaction for the photocatalytic degradation of MO was confirmed using the linearised Langmuir–Hinshelwood model (Equation 4)<sup>29</sup>:

$$\ln\left(\frac{C_0}{C_t}\right) = k_{app} t, \quad \text{Equation 4}$$

where  $k_{app}$  is the apparent reaction rate constant.

### Evaluation of the antimicrobial activity of the photocatalysts

To determine the individual effects of visible light irradiation and adsorption on the photodegradation of *E. coli*, experiments were conducted in triplicate under the following conditions: (1) in the presence of photocatalysts under dark conditions, (2) in the absence of photocatalysts under light irradiation, (3) in the absence of photocatalysts under dark conditions and (4) in the presence of catalysts and light irradiation. To reduce growth before assaying, water samples were refrigerated at <4 °C. Monitoring *E. coli* numbers was indicative of the quality of the wastewater and the efficacy of the disinfection process. From these data, the disinfection rate was calculated using Equation 3. Samples from disinfection experiments were plated on nutrient agar in duplicate, and incubated at 37 °C for 48 h. Thereafter, colonies were counted and viable cell concentrations determined.<sup>32</sup>

### Data analysis

One-way analysis of variance (ANOVA) was used to determine the individual effects of the photocatalysts and experimental factors on MO and *E. coli* removal after testing the data for normality and homogeneity of variance. Data that violated the ANOVA assumptions were either transformed or analysed using non-parametric statistical tests. Regression analysis was used to test the degree of fit of kinetic models to the experimental data based on the coefficient of determination. All statistical analyses were done at a probability level ( $p$ ) of 0.05 using SPSS statistical software.

### Study limitations

The limitations of this work were: (1) the removal of MO and *E. coli* from synthetic wastewater samples rather than real wastewater, and (2) evaluation of pollutant removal at laboratory scale. Hence, the following could not be adequately addressed in the current study: (1) potential interactions among contaminants, and (2) effects of typical concentrations occurring in wastewaters. Moreover, no experimental work was conducted to investigate regeneration potential.

## Results and discussion

### Characteristics of TiO<sub>2</sub>-ZFA and F-TiO<sub>2</sub>-ZFA nanocomposites

#### pH<sub>zpc</sub> and ash content of photocatalyst

While TiO<sub>2</sub> had no significant effect on the pH<sub>zpc</sub>, all the F-doped TiO<sub>2</sub> photocatalysts shifted towards lower pH<sub>zpc</sub> as the TiO<sub>2</sub> content increased (Table 2). For the photocatalysts, a high pH<sub>zpc</sub> is associated with a positive surface charge, while low pH<sub>zpc</sub> is associated with a negative surface charge.<sup>26</sup> Surface charge affects the agglomeration of the nanoparticles and their stability in suspension, with a more negative surface charge leading to less particle agglomeration.<sup>26</sup> The results showed that the ash content significantly ( $p=0.05$ ) decreased with dopant loading. The ash content of TiO<sub>2</sub> was lowest, while ZFA had the highest ash content.

Generally, ash content is an indication of the amount of inorganic material bound in the physical structure of the nanocomposites.<sup>22</sup> The ash content for TiO<sub>2</sub>-ZFA photocatalysts was not significantly different ( $p>0.05$ ), and averaged 85%, whereas F-TiO<sub>2</sub>-ZFA photocatalysts averaged 72%. As expected, the presence of ZFA increases ash content, suggesting a high load of inorganic elements.

**Table 2:** Physico-chemical parameters of the photocatalysts

Photocatalyst	pH <sub>zpc</sub>	Ash (%)
TiO <sub>2</sub>	7.5±0.1	5±1
ZFA	7.0±0.1	98±3
5% TiO <sub>2</sub> -ZFA	8.1±0.2	89±2
7% TiO <sub>2</sub> -ZFA	8.1±0.1	85±2
10% TiO <sub>2</sub> -ZFA	8.2±0.1	82±3
10% F-TiO <sub>2</sub> -ZFA	6.6±0.1	76±1
20% F-TiO <sub>2</sub> -ZFA	6.4±0.1	72±2
30% F-TiO <sub>2</sub> -ZFA	6.1±0.1	69±1
100% F-TiO <sub>2</sub>	5.4±0.1	10±1

### Surface functional groups

The FTIR spectra for ZFA and TiO<sub>2</sub>-ZFA resemble those for zeolites (Figure 2). The broad peaks at ~3400 cm<sup>-1</sup> were attributed to -OH vibrations of silanol groups (Si-OH), which are formed from the interaction of -Si groups in the ZFA with water molecules.<sup>7</sup> The small peaks at ~1600 cm<sup>-1</sup> are characteristic of the -OH bending vibrations in water molecules linked to zeolite particles.<sup>1</sup> All spectra for the F-doped photocatalysts showed broad O-H stretching peaks in the range 3200–3500 cm<sup>-1</sup>, which were ascribed to adsorbed moisture. The presence of the O-H functional groups enhances the photocatalytic activity because holes generated under irradiation trap O-H groups to produce OH• radicals, which reduce electron-hole recombination.<sup>5</sup> The intensities of the O-H bond peak increased with increasing F-TiO<sub>2</sub> loading, suggesting possible higher photocatalytic activity for the 30% F-TiO<sub>2</sub> than for photocatalysts at lower TiO<sub>2</sub> loadings. Sharp Ti-O-Si peaks were observed between 900 cm<sup>-1</sup> and 1000 cm<sup>-1</sup>. Similar peaks were reported in a previous study, and were attributed to the Ti-O-Si bonds formed when Ti was introduced into the ZFA structure.<sup>33</sup> However, another study attributed the peaks to the Al-O-Al or Si-O-Si bonds found in the AlO<sub>4</sub> and SiO<sub>4</sub> tetrahedra in the ZFA structure.<sup>21</sup> The ZFA-doped photocatalysts are expected to have both these functional groups. The C=O stretch in the range 1760–1690 cm<sup>-1</sup> suggests the presence of some residual CF<sub>3</sub>CO<sub>2</sub>H used for doping the material.<sup>34</sup> The broad symmetrical peak around 750 cm<sup>-1</sup> was ascribed to the Ti-O-Ti bond, while the peak at 1100 cm<sup>-1</sup> suggests the presence of the Ti-O-C bond. The presence of the Ti-O-C peak shows some chemical bonding interactions between the TiO<sub>2</sub> nanoparticles and the ZFA.<sup>1</sup> Comparing spectra for TiO<sub>2</sub>-ZFA and F-TiO<sub>2</sub>-ZFA shows F-doping increased the intensities of all the O-H peaks, suggesting F-doping potentially enhances photocatalytic activity.<sup>19</sup> The peak at 2347 cm<sup>-1</sup> only appears in F-doped samples, and points to traces of residual C-C=O groups from TTIP precursors and solvents used during synthesis. The C-F bond around 1400 cm<sup>-1</sup> confirms the presence of F in the F-TiO<sub>2</sub>-ZFA photocatalysts, and thus successful F-doping.<sup>34</sup>

### Surface morphology

The surface morphology of TiO<sub>2</sub>, ZFA, TiO<sub>2</sub>-ZFA and F-TiO<sub>2</sub>-ZFA was characterised by heterogeneous and rough surfaces (Figure 3). Aggregates of TiO<sub>2</sub> nanoparticles showed characteristic dispersed near-spherical particles with a rash-like appearance (Figure 3a).<sup>1,22,32</sup> ZFA showed larger particles than TiO<sub>2</sub> with irregular-shaped edges (Figure 3b). Particles in the nanocomposite photocatalysts were of different irregular shapes with a broad size distribution (Figure 3c, d). After being introduced into the photocatalyst, particles of ZFA formed



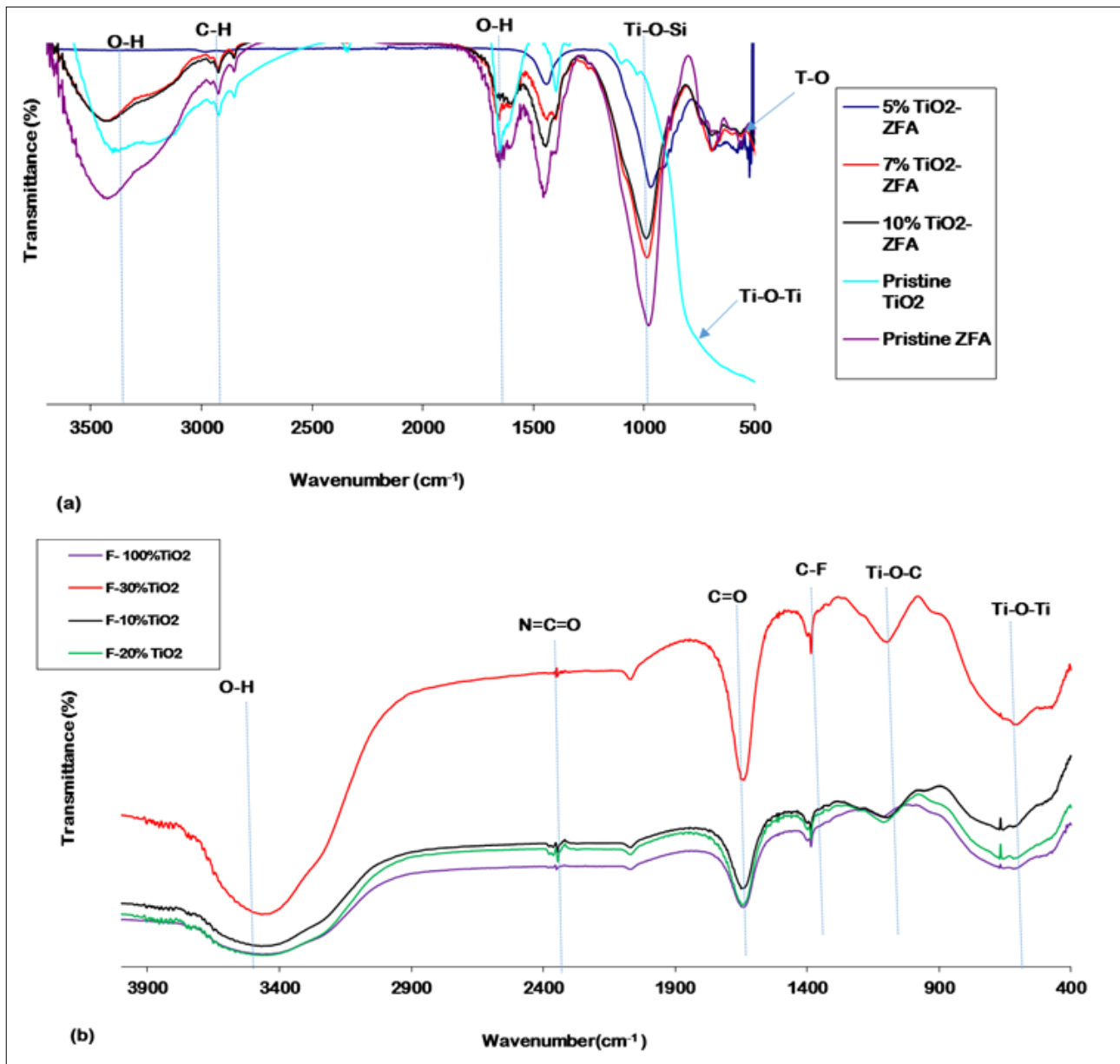


Figure 2: Fourier transform infrared spectra for  $\text{TiO}_2$ , ZFA and  $\text{TiO}_2$ -ZFA photocatalysts, F- $\text{TiO}_2$ , and F- $\text{TiO}_2$ -ZFA photocatalysts.

plate-like units with an irregular and rough surface with numerous microsized cavities (Figure 3c). The estimated average sizes of the  $\text{TiO}_2$ -ZFA and F- $\text{TiO}_2$ -ZFA particles were in the range of several hundred nanometres. This big particle size could be due to the presence of the microsized ZFA particles. Images of  $\text{TiO}_2$ -ZFA and F- $\text{TiO}_2$ -ZFA show  $\text{TiO}_2$  nanoparticle agglomerates embedded onto ZFA particles (Figure 3c, d). Because of the smaller quantity of  $\text{TiO}_2$  relative to ZFA, most of the  $\text{TiO}_2$  particles were covered and hidden under the ZFA particles. The SEM images suggest the  $\text{TiO}_2$  nanoparticles were immobilised on the external surface of the ZFA particles and not in the pore structures and voids of the ZFA particles.<sup>32</sup> From these images, it is clear that the morphology of the precursors was transformed through the modification via synthesis. Overall, the surface morphologies of the photocatalysts are suitable for the photodegradation of MO subsequent to adsorption, and provide a heterogeneous surface for accommodating *E. coli*.

### Crystallinity of the photocatalysts

Unmodified  $\text{TiO}_2$  showed X-ray diffraction peaks at  $2\theta = 25^\circ$ ,  $38^\circ$ , and  $48^\circ$ , which are characteristic of the anatase phase (Figure 4).<sup>5</sup> The spectra for ZFA showed multiple crystalline and amorphous

regions. This is expected from the wide range of organic carbon and metal compounds that constitute FA.<sup>19,35</sup> These characteristics were inherited by  $\text{TiO}_2$ -ZFA, which showed an increased crystallinity owing to the presence of  $\text{TiO}_2$ . The organic matter in the photocatalyst nanocomposite is beneficial for adsorption along with zeolitic porous properties, while the  $\text{TiO}_2$  is key to the photocatalytic properties.<sup>5</sup>

### Photoactive properties

Diffuse reflectance spectroscopy UV-Vis spectra showed the photoactive properties of the various photocatalysts (Figure 5a, b). Compared to those for  $\text{TiO}_2$  and F- $\text{TiO}_2$ , the spectra for the F- $\text{TiO}_2$ -ZFA photocatalysts have absorbance in the visible light region and a red shift. For  $\text{TiO}_2$ , the band gap was estimated to be 3.2 eV, which was within the 3.0–3.2 eV range reported in the literature.<sup>36</sup> For F- $\text{TiO}_2$ , there was a slight shift in the band gap energy to 2.8 eV, which is comparable to the 2.75 eV reported in previous studies.<sup>19</sup> F- $\text{TiO}_2$ -ZFA samples showed a 63–72% decrease in band gap relative to  $\text{TiO}_2$ , while  $\text{TiO}_2$ -ZFA samples showed a 31–38% band gap narrowing (Table 3). In summary, increasing the dopant loading into the  $\text{TiO}_2$  led to a decrease in the band gap energies. F- $\text{TiO}_2$ -ZFA

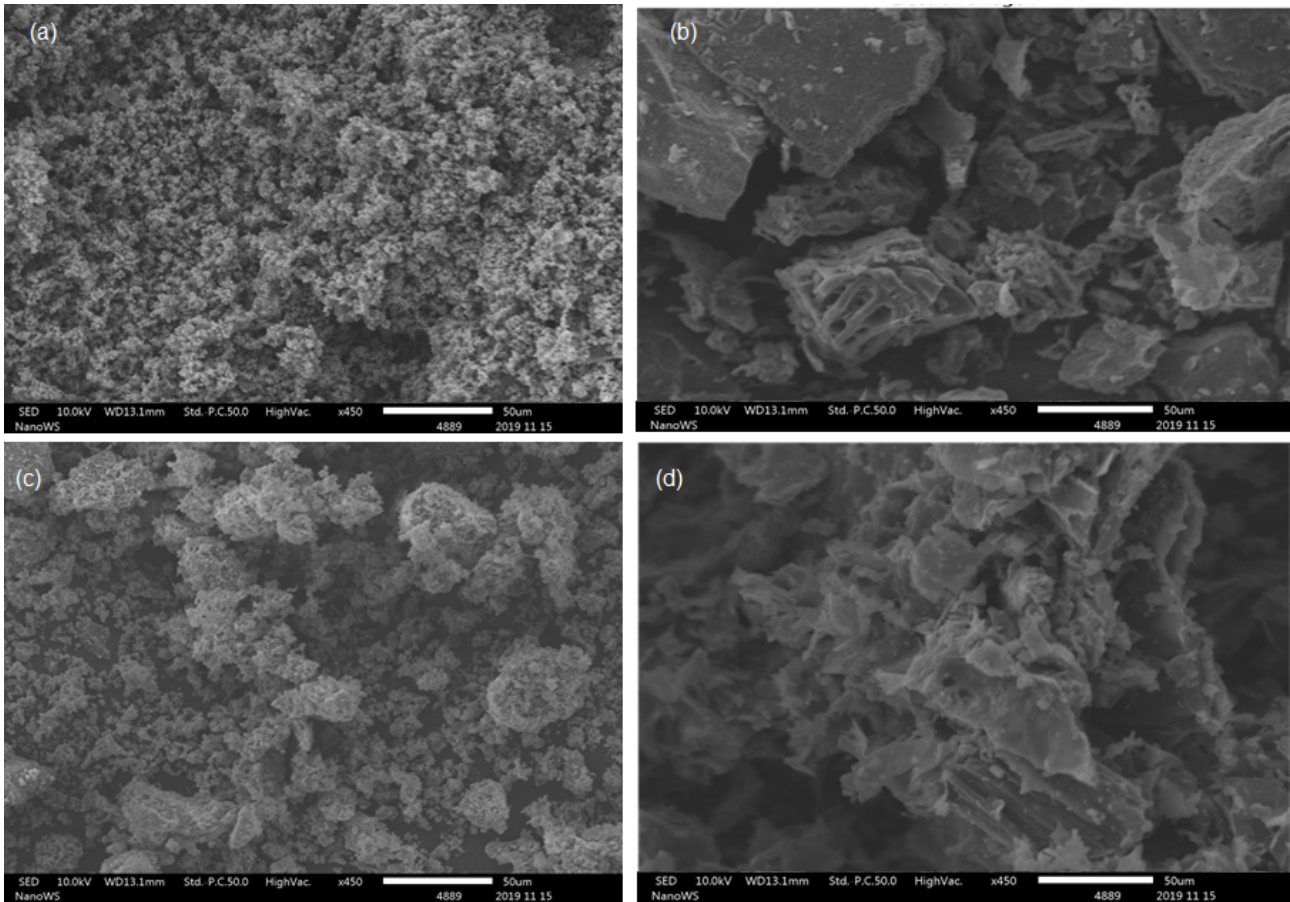


Figure 3: Scanning electron microscopy images for (a)  $\text{TiO}_2$ , (b) ZFA, (c) 10%  $\text{TiO}_2$ -ZFA, and (d) 30% F- $\text{TiO}_2$ -ZFA.

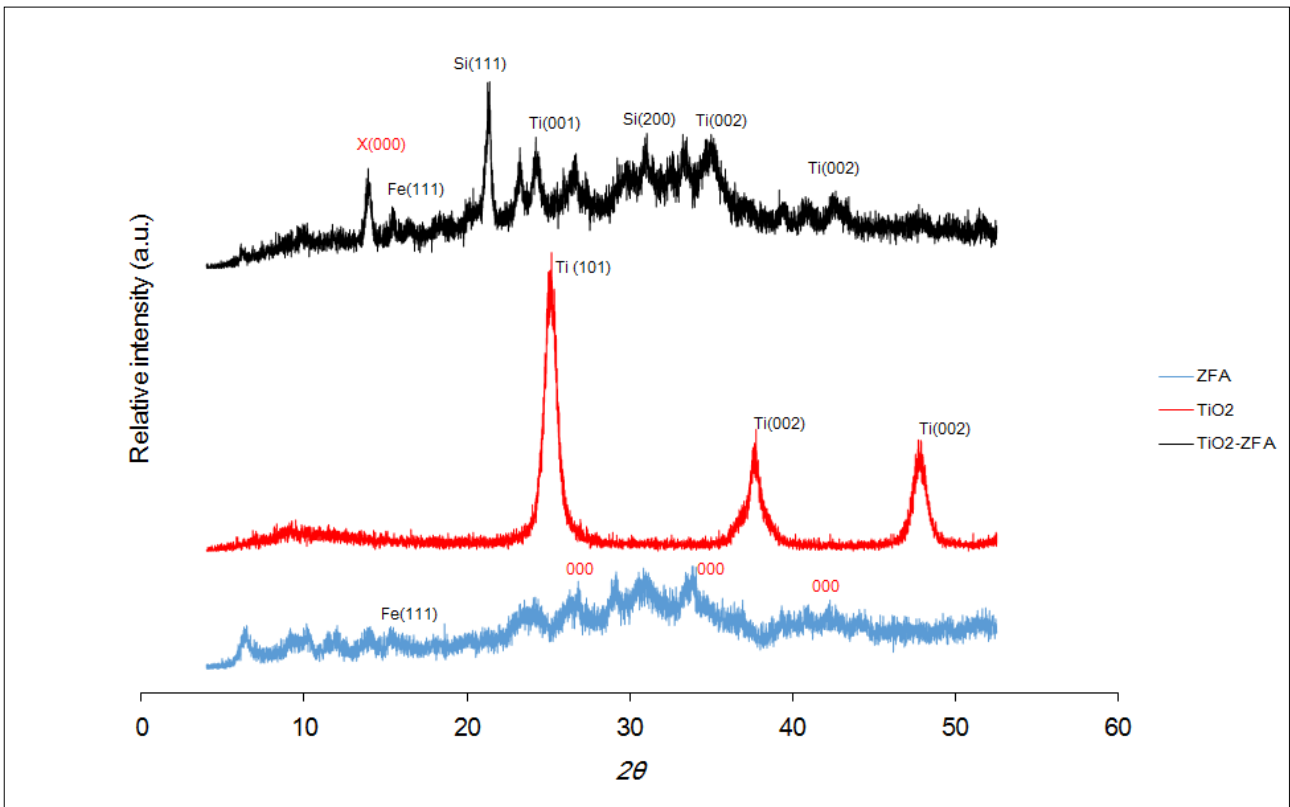
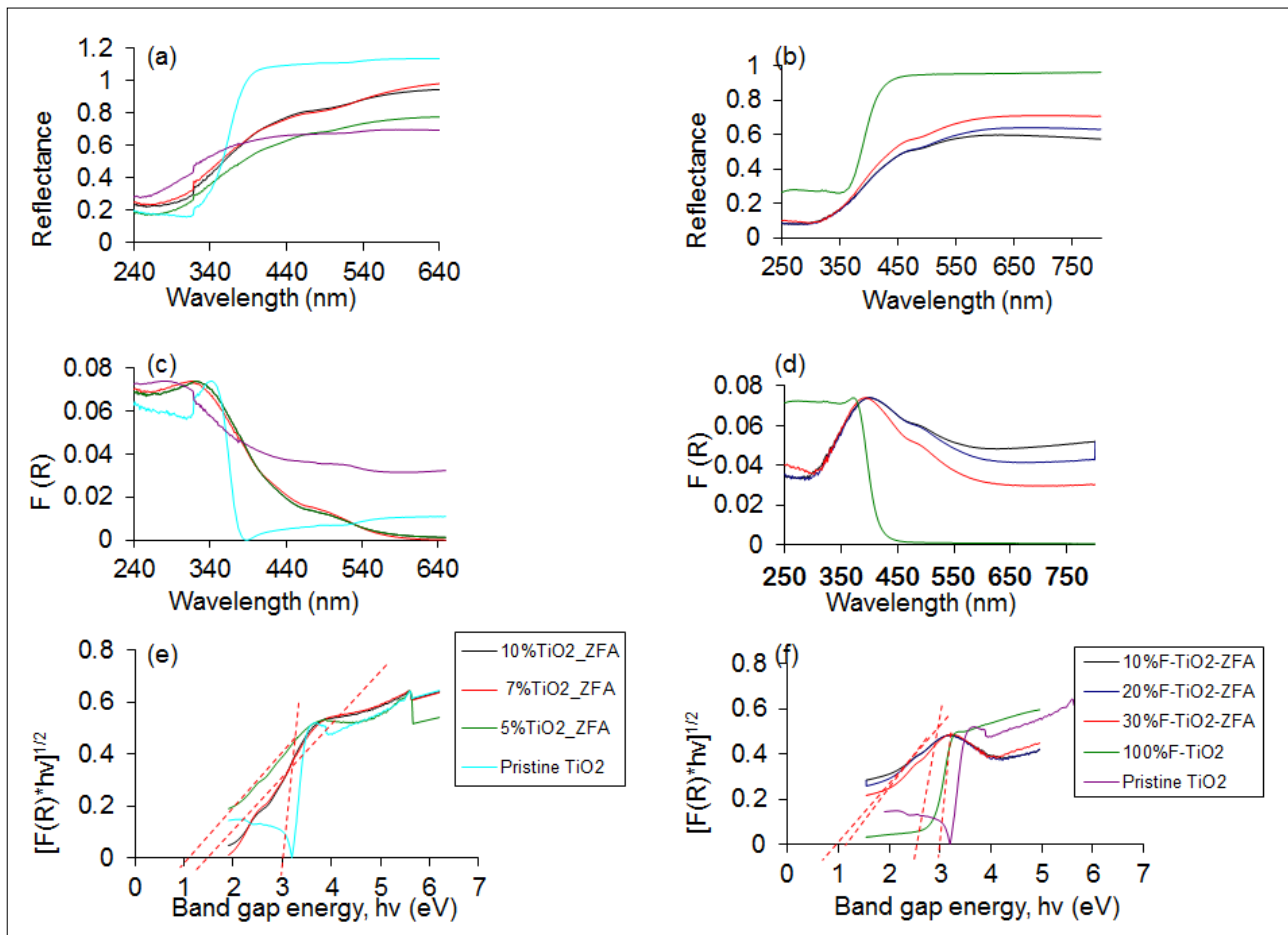


Figure 4: X-ray diffraction spectra for  $\text{TiO}_2$ , ZFA, and 10%  $\text{TiO}_2$ -ZFA.



**Figure 5:** Diffuse reflectance UV-Vis spectra for (a)  $\text{TiO}_2$ , 5–7%  $\text{TiO}_2$ -ZFA and (b)  $\text{TiO}_2$ , 10–30%  $\text{TiO}_2$ -ZFA. Kubelka–Munk function plots for (c)  $\text{TiO}_2$ , 5–7%  $\text{TiO}_2$ -ZFA and (d)  $\text{TiO}_2$ , 10–30%  $\text{TiO}_2$ -ZFA. Tauc plots for (e)  $\text{TiO}_2$ , 5–7%  $\text{TiO}_2$ -ZFA and (f)  $\text{TiO}_2$ , 10–30%  $\text{TiO}_2$ -ZFA.

samples showed increased absorption intensities extending to the near-infrared region of the electromagnetic spectrum (Figure 5a, b). This increase is due to the narrowing of the band gap caused by introduction of ZFA and F. Although the intention of using ZFA was as an immobiliser for  $\text{TiO}_2$  nanoparticles, Tauc plots show that ZFA also reduced the band gap for  $\text{TiO}_2$ . During calcination, some of the constituents of ZFA, such as carbon, may become potential  $\text{TiO}_2$  dopants. It thus appears that the  $\text{TiO}_2$  in F- $\text{TiO}_2$ -ZFA samples was co-doped, hence the significant narrowing of the band gap. Given its off-white colour, ZFA will absorb in the entire visible region, thus enhancing the visible light absorption of the nanocomposite. Similar findings were observed for F and Sm co-doped  $\text{TiO}_2$  nanocomposites.<sup>25</sup> The absorption edge for  $\text{TiO}_2$ -ZFA was also red-shifted into the visible light region of the electromagnetic spectrum. The introduction of ZFA and F introduced impurities, which in turn introduced intra-band gap energy states between the valence band and conduction band of  $\text{TiO}_2$ . The radius of the F anion (131 pm) is smaller than that of the  $\text{O}^{2-}$  (140 pm), hence it is possible that F occupies substitutional doping sites, replacing  $\text{O}^{2-}$  and resulting in a 2p energy sub-state above the valence band.<sup>20</sup> In contrast, the radii of tetrahedral  $[\text{SiO}_4]^{4-}$  and  $[\text{AlO}_4]^{5-}$  in ZFA is much bigger than that of  $\text{O}^{2-}$ , and more likely to occupy the interstitial doping sites.<sup>37</sup>

### Kinetics of the photodegradation of MO

Unmodified  $\text{TiO}_2$  had the least photocatalytic activity, and the fractional degradation of MO was the lowest (13.5%) (Figure 6a). The rate of degradation was fast in the first 60 min for all the doped photocatalysts. Beyond 60 min, there was a slight decrease in degradation. Hence optimum visible light irradiation time appears to be 60–120 min. Previous research reported that  $\text{TiO}_2$ -based photocatalysts are a good choice for the degradation of organic dyes such as Rhodamine B and methyl orange.<sup>8,20</sup>

**Table 3:** Indirect band gap energy estimates and calculated absorption wavelengths for different  $\text{TiO}_2$ -ZFA and F- $\text{TiO}_2$ -ZFA samples

Sample	Indirect band gap (eV)	*Estimated $\lambda$ (nm) $\left(\lambda = \frac{h}{E_g}\right)$
Pristine $\text{TiO}_2$	3.2	387.5
5% $\text{TiO}_2$ -ZFA	2.2	563.6
7% $\text{TiO}_2$ -ZFA	2.0	620.0
10% $\text{TiO}_2$ -ZFA	2.0	620.0
10% F- $\text{TiO}_2$ -ZFA	0.9	1377.8
20% F- $\text{TiO}_2$ -ZFA	0.9	1377.8
30% F- $\text{TiO}_2$ -ZFA	1.2	1033.3
100% F- $\text{TiO}_2$	2.8	442.9

The photocatalytic degradation of MO using 100% F- $\text{TiO}_2$  was 52% higher than  $\text{TiO}_2$ . This is possibly a result of the band gap narrowing for the 100% F- $\text{TiO}_2$ , which is more aligned to absorption of radiation in the visible region than  $\text{TiO}_2$ . The order of the degradation was:  $\text{TiO}_2$  (13.5%) < 100% F- $\text{TiO}_2$  (56%) < 10% F- $\text{TiO}_2$ -ZFA (59.5%) < 20% F- $\text{TiO}_2$ -ZFA (69%) < 10%  $\text{TiO}_2$ -ZFA (88%) < 30% F- $\text{TiO}_2$ -ZFA (95.5%) (Figure 6a). In general, reducing the F-loading in the photocatalysts resulted in diminished photocatalytic activity, possibly due to increasing band gap energy. Previous studies have reported that the introduction of F into  $\text{TiO}_2$  results in an increase in photocatalytic activity due to the

reduction of the band gap.<sup>25</sup> Fluorine substitution has been reported to reduce the electron-hole recombination rate due to the charge compensation between F and Ti<sup>4+</sup>.<sup>38</sup> Moreover, F-doping also creates oxygen vacancies that serve as active sites for the formation of OH• radicals, which in turn enhance photoactivity.<sup>39</sup>

The photocatalytic degradation of MO is a pseudo-first-order reaction as confirmed by the linear transforms of  $\ln(A_t/A_0)$  against  $t$  ( $0.80 < r^2 < 0.93$ ) from which rate constants were computed (Figure 6b). The photocatalyst 30% F-TiO<sub>2</sub>-ZFA had the highest apparent pseudo-first-order rate constant ( $k_{app}$ ) of  $11.9 \times 10^{-3} \text{ min}^{-1}$  compared to  $8 \times 10^{-3} \text{ min}^{-1}$  for 20% F-TiO<sub>2</sub>-ZFA and  $5.3 \times 10^{-3} \text{ min}^{-1}$  for 10% F-TiO<sub>2</sub>-ZFA. The rate constant for TiO<sub>2</sub> was the lowest at  $2.5 \times 10^{-3} \text{ min}^{-1}$ . The degradation rate increased with higher catalyst loading, indicative of the corresponding increases in the available catalytic and adsorption sites, resulting in more MO molecules being adsorbed and degraded. Previous studies have shown that F-TiO<sub>2</sub> has a higher rate constant ( $43.3 \times 10^{-3} \text{ min}^{-1}$ ) compared to TiO<sub>2</sub> ( $4.2 \times 10^{-3} \text{ min}^{-1}$ ).<sup>38</sup>

The difference in performance of the photocatalysts may be because of the difference in band gaps. The band gap for 10% TiO<sub>2</sub>-ZFA (2.0 eV) was more aligned to absorption in the visible light range used in the study compared to the band gap for 10% F-TiO<sub>2</sub>-ZFA (0.9 eV). Dopants may have different effects on the trapping of electrons and holes because of the different positions of the dopants in the TiO<sub>2</sub> crystal lattice.<sup>40</sup> Increasing the content of dopants in TiO<sub>2</sub> introduces defect states which promote electron-hole recombination.<sup>41</sup> Overall, optimising photocatalyst loading is important because it facilitates maximum photocatalytic activity while avoiding unnecessary wastage of photocatalyst.

### Photodegradation of *E. coli*

Because of their superior performance in the photodegradation of MO, the 10% TiO<sub>2</sub>-ZFA and 30% F-TiO<sub>2</sub>-ZFA photocatalysts were used to remove *E. coli* from water. In the absence of a photocatalyst and in the presence of visible light, 21% disinfection was achieved after 180 min (Figure 7a,b). This can be attributed to photolysis from visible light causing the lysis of the bacterial cells. Previous studies have shown that visible light photolysis alone has a small effect on bacterial inactivation, while the experiment in the dark has been reported to result in no inactivation.<sup>42</sup> The intensity of the LED lights on the photocatalytic reactor may have helped increase the disinfection by photolysis. A disinfection rate of 95% occurred after 3 h of irradiation, while 10% TiO<sub>2</sub>-ZFA showed 76% disinfection within 3 h (Figure 7b). This may be due to the higher photocatalytic activity of the co-doped F-TiO<sub>2</sub>-ZFA photocatalyst, compared to the singly doped TiO<sub>2</sub>-ZFA photocatalyst. Disinfection under visible light was enhanced by the presence of a photocatalyst compared to that in the absence of a photocatalyst. In the presence of a

photocatalyst, OH• radicals are formed and released, and these weaken the bacterial cell integrity, leading to loss of cell respiration, and ultimately death.<sup>32</sup> In the presence of a photocatalyst and in the absence of visible light, 37% disinfection was achieved using 30% F-TiO<sub>2</sub>-ZFA compared to 29% for 10% TiO<sub>2</sub>-ZFA. This disinfection is possibly caused by phagocytosis by the photocatalysts as well as the antimicrobial activity of F and TiO<sub>2</sub> nanoparticles, which cause disintegration of the bacterial cell membrane.<sup>43</sup> For the control experiments in the absence of both light and photocatalyst, a mere 3% disinfection was achieved in 180 min. The disinfection could possibly be due to: (1) the absence of a nutrient source for survival of the bacteria, or (2) the antimicrobial activity of nanoparticles. Previous studies have shown that solar energy alone is an effective disinfectant<sup>44</sup>, although it requires prolonged exposure. In summary, co-doped 30% F-TiO<sub>2</sub>-ZFA has more effective antimicrobial properties due to its higher photocatalytic activity.

### Possible photodegradation mechanisms

The photodegradation results show that the photocatalytic efficacy increased in the order: TiO<sub>2</sub> < TiO<sub>2</sub>-ZFA < F-TiO<sub>2</sub>-ZFA. It can thus be deduced that both F and ZFA enhance the photocatalytic properties of TiO<sub>2</sub>, possibly via the formation of a hetero-junction between F and TiO<sub>2</sub>, and ZFA and TiO<sub>2</sub>, which facilitate electron-hole pair separation.<sup>9</sup> Previous studies have reported that F-doping of TiO<sub>2</sub> improved electron trapping, which reduced electron-hole recombination.<sup>8,25</sup> The photodegradation mechanism of MO and *E. coli* using TiO<sub>2</sub>-ZFA and F-TiO<sub>2</sub>-ZFA can thus be conjectured (Box 1). Upon visible light irradiation, TiO<sub>2</sub> produces electrons and holes, which are respectively entrapped in the photocatalyst and react with H<sub>2</sub>O to produce reactive radicals.<sup>8,29</sup> The degradation of MO and *E. coli* is affected by the hydroxyl free radicals to produce by-products and dead biomass, respectively. The degradation mechanism of pathogenic microorganisms can be studied by monitoring the optical density of treated water or by gene expression analyses, and evaluating morphological transformations of cell membranes using microscopy techniques.<sup>45,46</sup> On exposure to light, electron/hole pairs are generated on the photocatalyst surface, leading to a series of reactions facilitated by OH• radicals. These radicals attack *E. coli* cytoplasmic membranes, causing lipid peroxidation and oxidising the intracellular components, consequently leading to cell death.<sup>45,47</sup>

### Conclusion

We investigated the photocatalytic activity and antimicrobial efficacy of TiO<sub>2</sub>-ZFA and F-TiO<sub>2</sub>-ZFA photocatalysts derived from residues from the combustion of coal. The key findings are:

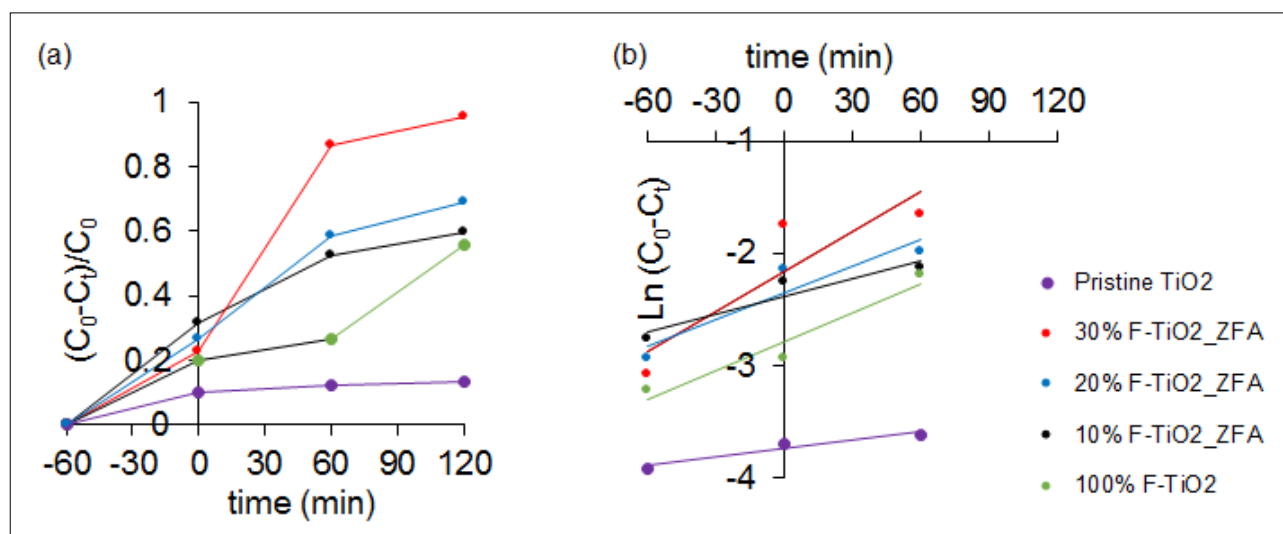
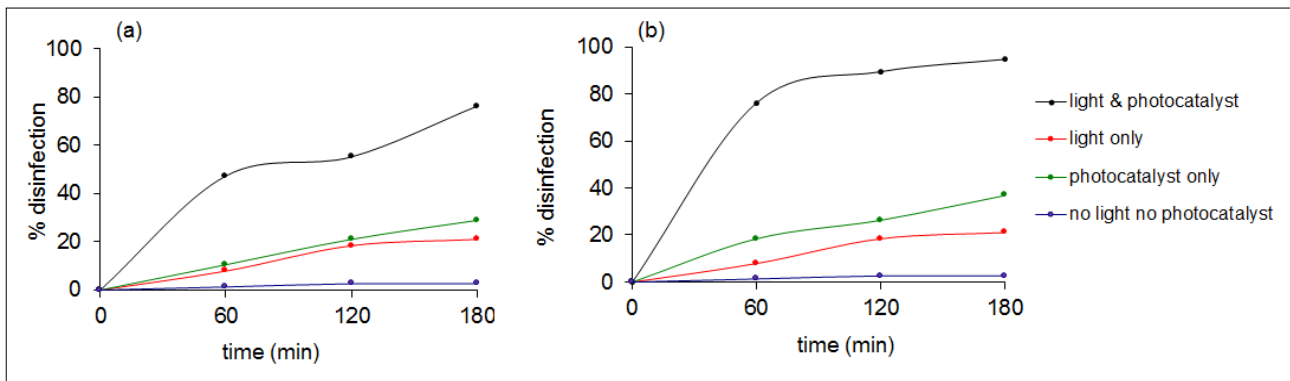
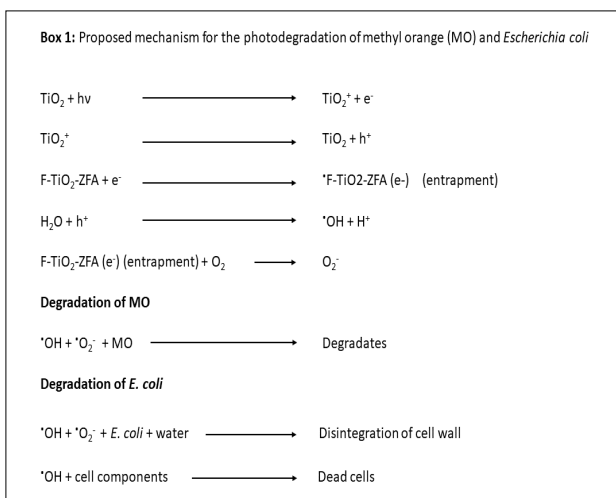


Figure 6: (a) Photodegradation of MO, and (b) pseudo-first-order kinetics using TiO<sub>2</sub> and F-doped photocatalysts.





**Figure 7:** Disinfection studies using average initial viable cell concentration of  $3.8 \times 10^8$  CFU/mL under visible light irradiation of 3 h using (a) 10%  $\text{TiO}_2$ -ZFA photocatalyst or (b) 10% F- $\text{TiO}_2$ -ZFA photocatalyst.



1. FTIR data revealed that F- $\text{TiO}_2$ -ZFA photocatalysts had a high content of  $\text{OH}^*$  groups on the surface, which improve the photocatalytic activity of the photocatalysts.
2. F-doped and  $\text{TiO}_2$ -ZFA photocatalysts showed a 63–72% and 31–38% decrease in the band gap of  $\text{TiO}_2$ , respectively.
3. F- $\text{TiO}_2$ -ZFA photocatalysts had higher disinfection efficacy (95%) than  $\text{TiO}_2$ -ZFA (76%).
4. MO photodegradation followed pseudo-first-order kinetics.

The performance of photocatalysts was attributed to a combination of the band narrowing effects of the F and ZFA dopants, as well as the adsorption capabilities of the ZFA. The conversion of coal fly ash to photocatalysts has the potential to reduce the environmental impacts associated with the disposal of coal fly ash, while providing novel materials for applications in water and wastewater treatment. In addition, being derived from waste, the material is likely to have lower cost and a reduced environmental footprint relative to commercially available materials. Detailed cost and life-cycle analyses will, however, be useful. Because the technique uses visible light, which is a major component of sunlight, point-of-use devices based on this technique have potential for use in isolated communities. However, large-scale application of this technology is still hindered by the very small particle size of the  $\text{TiO}_2$  which poses a challenge for its post-use recovery. A combination of centrifugation, decantation and filtration could be used to recover the nanocomposite in treated water. Because the nanoparticles are usually highly dispersed in aqueous solution, this could limit their recovery and increase the cost of treatment. Besides, the additional processes could increase the cost of the treatment technique. Hence, further studies should investigate up-scaling the technique, investigating the fate of the

potential of the photocatalysts for multiple reuse, and the recovery of  $\text{TiO}_2$  in treated water. Optimisation studies based on tools such as response surface methodology are also required to develop the best combination of operating conditions. There is also need to investigate methods for the safe disposal of the spent photocatalysts and adsorbents, including their potential use in novel construction materials. Besides using the photocatalysts/adsorbents in free granular form, scope also exists to develop point-of-use water-treatment devices relying on photocatalysis for water disinfection. Recent work involving the development of e-DRINK, a photo-electrocatalytic device for rapid water disinfection, points to the possibility to develop such point-of-use systems. Besides antimicrobial activity, such point-of-use devices should also be tested for their capacity to remove emerging contaminants such as antimicrobials, pharmaceuticals, and pesticides.

## Acknowledgements

We are grateful for the technical support from Harare Polytechnic.

## Competing interests

We have no competing interests to declare.

## Authors' contributions

S.M.M.: Data collection and treatment; manuscript draft writing. N.C.: Conception, supervision, manuscript writing and reviewing. C.I.M.: Supervision, manuscript writing. W.G.: Manuscript writing, reviewing. M.M.: Manuscript writing, materials characterisation. A.T.K.: Manuscript writing, materials characterisation.

## References

1. Visa M, Chelaru AM. Hydrothermally modified fly ash for heavy metals and dyes removal in advanced wastewater treatment. *Appl Surf Sci*. 2014;303:14–22. <https://doi.org/10.1016/j.apsusc.2014.02.025>
2. Kant R. Textile dyeing industry and environmental hazard. *Nat Sci*. 2012;4:22–26. <https://doi.org/10.4236/ns.2012.41004>
3. Ghaly AE, Ananthashanka R, Alhattab M, Ramakrishnan VV. Production, characterization and treatment of textile effluents: A critical review. *J Chem Eng Process Technol*. 2014;5:1–18. <https://doi.org/10.4172/2157-7048.1000182>
4. Hao O, Hao OJ, Kim H, Chiang P. Decolorization of wastewater. *Crit Rev Environ Sci Technol*. 1999;30(4):449–505. <https://doi.org/10.1080/10643380091184237>
5. Duta A, Visa M. Simultaneous removal of two industrial dyes by adsorption and photocatalysis on a fly-ash- $\text{TiO}_2$  nanocomposite. *J Photochem Photobiol A*. 2015;306:21–30. <https://doi.org/10.1016/j.jphotochem.2015.03.007>
6. Martorelli L, Albanese A, Vilte D, Cantet R, Bentancor A, Zolezzi G, et al. Shiga toxin-producing *Escherichia coli* (STEC) O22:H8 isolated from cattle reduces *E. coli* O157:H7 adherence *in vitro* and *in vivo*. *Vet Microbiol*. 2017;208:8–17. <https://doi.org/10.1016/j.vetmic.2017.06.021>



7. Rondina DJG, Ymbong DV, Cadutdut MJM, Nalasa JRS, Paradero JB, Mabayo VIF, et al. Utilization of a novel activated carbon adsorbent from press mud of sugarcane industry for the optimized removal of methyl orange dye in aqueous solution. *Appl Water Sci.* 2019;9:181. <https://doi.org/10.1007/s13201-019-1063-0>
8. Mousli F, Chaouchi A, Jouini M, Maurel F, Kadri A, Chehimi MM. Polyaniline-grafted RuO<sub>2</sub>-TiO<sub>2</sub> heterostructure for the catalysed degradation of methyl orange in darkness. *Catalysts.* 2019;9(7):578. <https://doi.org/10.3390/catal9070578>
9. Zarei M, Bahrami J, Zarei M. Zirconia nanoparticle-modified graphitic carbon nitride nanosheets for effective photocatalytic degradation of 4-nitrophenol in water. *Appl Water Sci.* 2019;9:175. <https://doi.org/10.1007/s13201-019-1076-8>
10. Gwenzi W, Chaukura N. Organic contaminants in African aquatic systems: Current knowledge, health risks and future research directions. *Sci Total Environ.* 2018;619–620:1493–1514. <https://doi.org/10.1016/j.scitotenv.2017.11.121>
11. Pal A, Grain A, Chowdhury D, Mondal MH, Saha B. A comparative spectral study on the interaction of organic dye Congo-Red with selective aqueous micellar media of CPC, rhamnolipids and saponin. *Tenside Surf Det.* 2020;57(5):401–407. <https://doi.org/10.3139/113.110700>
12. Mondal MH, Malik S, Saha B. Characterization of pyrene solubilization in selective micellar media of novel bio-degradable natural surfactant saponin (extracted from soap nut) and conventional surfactant SDBS in presence and absence of common salt NaCl. *Tenside Surf Det.* 2017;54(5):378–384. <https://doi.org/10.3139/113.110519>
13. Nhapi I, Gijzen HJ. Wastewater management in low-income countries in the context of sustainability. *Water Policy.* 2004;6(6):501–517. <https://doi.org/10.2166/wp.2004.0033>
14. Sivalingam S, Sen S. An ultra-fast non-conventional waste management protocol to recycle of industrial fly ash into zeolite X. *Environ Sci Pollut Res Int.* 2018;26(34):34693–34701. <https://doi.org/10.1007/s11356-018-3664-9>
15. Koshy N, Singh DN. Fly ash zeolites for water treatment applications. *J Environ Chem Eng.* 2016;4:1460–1472. <http://dx.doi.org/10.1016/j.jece.2016.02.002>
16. Taunov Z, Tsakiridis PE, Mikhalovsky SV, Inglezakis VJ. Synthetic coal fly ash-derived zeolites doped with silver nanoparticles for mercury (II) removal from water. *J Environ Manage.* 2018;224:164–171. <https://doi.org/10.1016/j.jenvman.2018.07.049>
17. Yahya N, Aziz F, Jamaludin NA, Mutalib MA, Ismail AF, Salleh WNW, et al. A review of integrated photocatalyst adsorbents for wastewater treatment. *J Environ Chem Eng.* 2018;6(6):7411–7425. <https://doi.org/10.1016/j.jece.2018.06.051>
18. Liu J, Wang Y, Ma J, Peng Y, Wang A. A review on bidirectional analogies between the photocatalysis and antibacterial properties of ZnO. *J Alloy Compd.* 2019;783:898–918. <https://doi.org/10.1016/j.jallcom.2018.12.330>
19. Todorova N, Giannakopoulou T, Vaimakis T, Trapalis C. Structure tailoring of fluorine-doped TiO<sub>2</sub> nanostructured powders. *Mat Sci Eng B-Adv.* 2008;152:50–54. <https://doi.org/10.1155/2008/534038>
20. Li J, Liang N, Jin X, Zhou D, Li H, Wu M, et al. The role of ash content on bisphenol A sorption to biochars derived from different agricultural wastes. *Chemosphere.* 2017;171:66–73. <https://doi.org/10.1016/j.chemosphere.2016.12.041>
21. Chong MN, Tneu ZY, Poh PE, Jin B, Aryal R. Synthesis, characterisation and application of TiO<sub>2</sub>-zeolite nanocomposites for the advanced treatment of industrial dye wastewater. *J Taiwan Inst Chem Eng.* 2014;50:288–296. <https://doi.org/10.1016/j.jtice.2014.12.013>
22. Li C, Sun Z, Ma R, Xue Y, Zheng S. Fluorine doped anatase TiO<sub>2</sub> with exposed reactive (001) facets supported on porous diatomite for enhanced visible-light photocatalytic activity. *Micropor Mesopor Mat.* 2017;243:281–290. <https://doi.org/10.1016/j.micromeso.2017.02.053>
23. Chang HL, Shih WH. A general method for the conversion of fly ash into zeolites as ion exchangers for cesium. *Ind Eng Chem Res.* 1998;37:71–78. <https://doi.org/10.1021/ie970362o>
24. Gwenzi W, Chaukura N, Noubactep C, Mukome FN. Biochar-based water treatment systems as a potential low-cost and sustainable technology for clean water provision. *J Environ Manage.* 2017;197:32–749. <https://doi.org/10.1016/j.jenvman.2017.03.087>
25. Mukonza SS, Nxumalo EN, Mamba BB, Mishra AK. Enhanced solar light photodegradation of brilliant black bis-azo dye in aqueous solution by F, Sm<sup>3+</sup> co-doped TiO<sub>2</sub>. *IOP Conf Ser Mater Sci Eng.* 2017;195:012006. <https://doi.org/10.1088/1757-899X/195/1/012006>
26. Kausar A, Naeem K, Hussain T, Nazli Z, Bhatti HN, Jubeen F, et al. Preparation and characterization of chitosan/clay composite for direct Rose FRN dye removal from aqueous media: Comparison of linear and non-linear regression methods. *J Mater Res Technol.* 2019;8(1):1161–1174. <https://doi.org/10.1016/j.jmrt.2018.07.020>
27. Ferro-Garcia MA, Rivera-Utrilla J, Bautista-Toledo I, Moreno-Castilla C. Adsorption of humic substance on activated carbon from aqueous solutions and their effect on the removal of Cr(III) ions. *Langmuir.* 1998;14(7):1880–1886. <https://doi.org/10.1021/la970565h>
28. Kortüm G, Braun W, Herzog G. Principles and techniques of diffuse reflectance spectroscopy. *Angew Chem Int Edit.* 1963;2(7):333–341. <https://doi.org/10.1002/anie.196303331>
29. Rosman N, Salleh WNW, Aziz F, Ismail AF, Harun Z, Bahri SS, et al. Electrospun nanofibers embedding ZnO/Ag<sub>2</sub>CO<sub>3</sub>/Ag<sub>2</sub>O heterojunction photocatalyst with enhanced photocatalytic activity. *Catalysts.* 2019;9:565. <https://doi.org/10.3390/catal9070565>
30. Yan Y, Zhou X, Lan J, Li Z, Zheng T, Cao W, et al. Efficient photocatalytic disinfection of *Escherichia coli* by N-doped TiO<sub>2</sub> coated on coal fly ash cenospheres. *J Photochem Photobiol A.* 2018;367:355–364. <https://doi.org/10.1016/j.jphotochem.2018.08.045>
31. Hassan MA, Nemr AE, Madkour FF. Testing the advanced oxidation processes on the degradation of Direct Blue 86 dye in wastewater. *Egypt J Aquat Res.* 2017;43(1):11–19. <https://doi.org/10.1016/j.ejar.2016.09.006>
32. Sreeja S, Shetty VK. Photocatalytic water disinfection under solar irradiation by Ag-TiO<sub>2</sub> core-shell structured nanoparticles. *Sol Energy.* 2017;157:236–243. <https://doi.org/10.1016/j.solener.2017.07.057>
33. Ricchiardi G, Damin A, Bordiga S, Lamberti C, Spano G, Rivetti F, et al. Vibrational structure of titanium silicate catalysts. A spectroscopic and theoretical study. *J Am Chem Soc.* 2001;123:11409–11419. <https://doi.org/10.1021/ja010607v>
34. Larkin P. General outline and strategies for IR and Raman spectral interpretation. In: Larkin P, editor. *Infrared and Raman spectroscopy: Principles and spectral interpretation.* Elsevier; 2011. p. 117–133.
35. An C, Yang S, Huang G, Zhao S, Zhang P, Yao Y. Removal of sulfonated humic acid from aqueous phase by modified coal fly ash waste: Equilibrium and kinetic adsorption studies. *Fuel.* 2016;165:264–271. <https://doi.org/10.1016/j.fuel.2015.10.069>
36. Ndlangamandla NG, Kuvarega AT, Msagati TAM, Mamba BB, Nkambule TTI. A novel photodegradation approach for the efficient removal of natural organic matter (NOM) from water. *Phys Chem Earth.* 2018;106:97–106. <https://doi.org/10.1016/j.pce.2018.05.011>
37. Busca G. Catalytic materials based on silica and alumina: Structural features and generation of surface acidity. *Prog Mater Sci.* 2019;104:215–249. <https://doi.org/10.1016/j.pmatsci.2019.04.003>
38. Umadevi M, Parimaladevi R, Sangari M. Synthesis, characterisation and photocatalytic activity of fluorine doped TiO<sub>2</sub> nanoflakes synthesized using solid state reaction method. *Spectrochim Acta A Mol Biomol Spectrosc.* 2014;120:365–369. <https://doi.org/10.1016/j.saa.2013.10.046>
39. Li FB, Li XZ, Ao CH, Lee SC, Hou MF. Enhanced photocatalytic degradation of VOCs using Ln<sup>3+</sup>-TiO<sub>2</sub> catalysts for indoor air purification. *Chemosphere.* 2005;59(6):787–800. <https://doi.org/10.1016/j.chemosphere.2004.11.019>
40. Manusamy S, Aparna RSI, Prasad RGSV. Photocatalytic effect of TiO<sub>2</sub> and the effect of dopants on degradation of brilliant green. *Sustain Chem Process.* 2013;1:4. <https://doi.org/10.1186/2043-7129-1-4>
41. Ozawa K, Emori M, Yamamoto S, Yukawa R, Yamamoto S, Hobaru R, et al. Electron-hole recombination time at TiO<sub>2</sub> single-crystal surfaces: Influence of surface band bending. *J Phys Chem Lett.* 2014;5(11):1953–1957. <https://doi.org/10.1021/jz500770c>



42. Booshehri AY, Polo-Lopez MI, Castro-Alferez M, Pengfie-He Rong X, Rong W, Malato S, et al. Assessment of solar photocatalysis using Ag/BiVO<sub>4</sub> at pilot solar compound parabolic collector for inactivation of pathogen in well water and secondary effluents. *Catalysis*. 2017;281(1):124–134. <https://doi.org/10.1016/j.cattod.2016.08.016>
  43. Wang L, Hu C, Shao L. The antimicrobial activity of nanoparticles: Present situation and prospects for the future. *Int J Nanomedicine*. 2017;12:1227-1249. <https://doi.org/10.2147/IJN.S121956>
  44. Pichel N, Vivar M, Fuentes M. The problem of drinking water access: A review of disinfection technologies with an emphasis on solar treatment methods. *Chemosphere*. 2019;218:1014-1030. <https://doi.org/10.1016/j.chemosphere.2018.11.205>
  45. Alafif ZO, Anjum M, Ansari,MO, Kumar R, Rashid J, Madkour M, Barakat MA. Synthesis and characterization of S-doped-rGO/ZnS nanocomposite for the photocatalytic degradation of 2-chlorophenol and disinfection of real dairy wastewater. *J Photochem Photobiol A Chem*. 2019;377:190–197. <https://doi.org/10.1016/j.jphotochem.2019.04.004>
  46. Li Y, Zhao J, Zhang G, Zhang L, Ding S, Shang E, et al. Visible-light-driven photocatalytic disinfection mechanism of PB-BiFeO<sub>3</sub>/rGO photocatalyst. *Water Res*. 2019;161:251–261 <https://doi.org/10.1016/j.watres.2019.06.011>
  47. Arellano U, Asomoza M, Ramírez F. Antimicrobial activity of Fe–TiO<sub>2</sub> thin film photocatalysts. *J Photochem Photobiol A Chem*. 2011;222:159–165. <https://doi.org/10.1016/j.jphotochem.2011.05.016>
-



Check for updates

#### AUTHORS:

Arwa El-Naeem<sup>1</sup>  
Sahar Abdalla<sup>1</sup>   
Ibrahim Ahmed<sup>1</sup>  
Gihan Alhassan<sup>2</sup>

#### AFFILIATIONS:

<sup>1</sup>Department of Chemistry, University of Khartoum, Khartoum, Sudan  
<sup>2</sup>Department of Botany, University of Khartoum, Khartoum, Sudan

#### CORRESPONDENCE TO:

Sahar Abdalla

#### EMAIL:

sahar.abdalla@uofk.edu

#### DATES:

Received: 07 Mar. 2021

Revised: 15 June 2021

Accepted: 21 June 2021

Published: 27 Jan. 2022

#### HOW TO CITE:

El-Naeem A, Abdalla S, Ahmed I, Alhassan G. Phytochemicals and in silico investigations of Sudanese roselle. *S Afr J Sci.* 2022;118(1/2), Art. #10383. <https://doi.org/10.17159/sajs.2022/10383>

#### ARTICLE INCLUDES:

- Peer review
- Supplementary material

#### DATA AVAILABILITY:

- Open data set
- All data included
- On request from author(s)
- Not available
- Not applicable

#### EDITORS:

Teresa Coutinho   
Salmima Mokgehele

#### KEYWORDS:

roselle, polyphenols, anthocyanins, gout, xanthine oxidase

#### FUNDING:

None

# Phytochemicals and in silico investigations of Sudanese roselle

We analysed four different Sudanese roselle samples for their potential as novel xanthine oxidase (XO) inhibitors. Phytochemical screening showed the presence of polyphenols, flavonoids, organic acids, saponins and sterols in all samples. Liquid chromatography with tandem mass spectrometry (LC-MS/MS) was used to identify and characterise five anthocyanins in all samples: cyanidin-3-glucoside (cy-3-glu), delphinidin-3-sambubioside (dp-3-sam), cyanidin-3-rhamnoside (cy-3-rhm), delphinidin-3-rhamnoside (dp-3-rhm) and pelargonidin-3-glucoside (pg-3-glu). Identification of cy-3-rhm, dp-3-rhm and pg-3-glu confirmed the selectivity and sensitivity of LC-MS as a powerful technique for identifying anthocyanins. In silico studies of the identified anthocyanins were performed to explore their promising inhibitory activity toward XO. Interactions between the ligand and the enzyme were via the H-bond, and hydrophobic ( $\pi$ -alkyl,  $\pi$ -sigma and alkyl) and/or electrostatic ( $\pi$ -cation) bonds. Inhibition of the anthocyanins was compared with that of topiroxostat, a commercial drug for hyperuricaemia. Dp-3-rhm was the most active inhibitor with a binding energy of ca. -10.90 kcal/mol compared to topiroxostat's binding energy of ca. -8.60 kcal/mol. The good inhibition results obtained from anthocyanins toward XO suggest their application as a drug candidate to treat gout and other diseases related to the activity of XO.

#### Significance:

- Sudanese roselle is rich in phytochemicals, particularly polyphenols and anthocyanins. The isolated anthocyanins in this study were explored as novel potential XO inhibitors. Further pharmacological and clinical studies are necessary for the development of new potential anthocyanin drugs to treat gout and other diseases related to XO increased activity such as hypertension.

## Introduction

*Hibiscus sabdariffa* L. – commonly known as roselle, hibiscus and karkade – is an annual or perennial plant that grows in tropical and subtropical regions of the world including Sudan.<sup>1-3</sup> Its calyces are characterised by a sour taste, brilliant red colour, and pleasant aroma that gives the plant its commercial importance.<sup>3,4</sup>

Roselle, like other plants, possesses phytochemical compounds such as tannins, saponins, glycosides, phytosterols, minerals, organic acids, and antioxidants like polyphenols, flavonoids, and vitamins.<sup>2,4,5</sup> These compounds occur naturally in different parts of the plants and they are characterised by their protective and preventive properties against several diseases.<sup>6</sup>

The calyces of roselle are rich in anthocyanin pigments; anthocyanins are water-soluble plant pigments responsible for providing the colours to almost all plant tissues.<sup>7-9</sup> In various plant tissues, anthocyanins vary in amount and type according to composition and chemical structures.<sup>7</sup> Plants containing anthocyanin extracts may have up to 10 different anthocyanins in addition to other flavonoids.<sup>10</sup> All anthocyanins share a basic common structure of glycosylated anthocyanidin as illustrated in Figure 1. The aglycone part (anthocyanidin) is a polyhydroxy or a polymethoxy derivative of 2-phenyl-benzopyrylium or flavylium salt.<sup>7,8</sup> All identified anthocyanins are based on six major anthocyanidins: cyanidin, delphinidin, pelargonidin, peonidin, petunidin, and malvidin.<sup>7-9</sup>

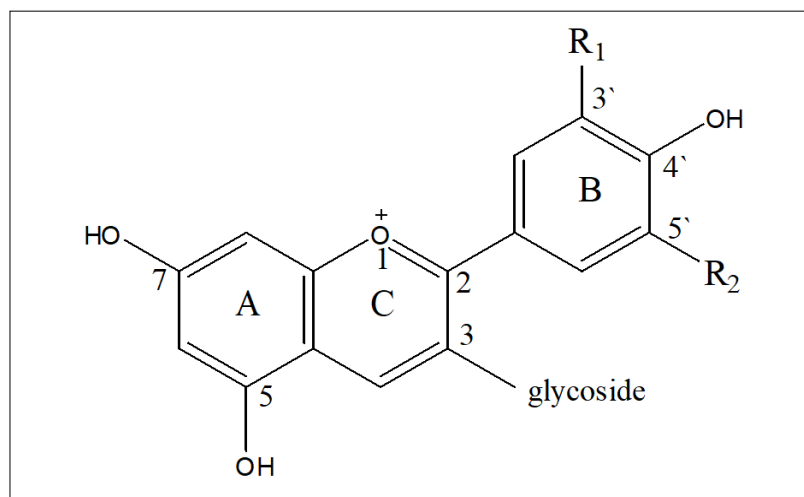


Figure 1: General structure of anthocyanins.

© 2022. The Author(s). Published under a Creative Commons Attribution Licence.



Identification of anthocyanins is usually carried out using chromatographic, spectrophotometric and capillary electrophoresis analytical methods.<sup>3,9</sup> The most commonly used technique is hyphenated liquid chromatography–mass spectrometry (LC-MS), as it is the most efficient due to its high selectivity and sensitivity.<sup>9</sup>

The red colour of roselle calyces is attributed to the presence of: dp-3-sam, cy-3-sam, dp-3-glu and cy-3-glu anthocyanins.<sup>5</sup> Dp-3-sam and cy-3-sam anthocyanins are responsible for the reddish-violet colour of roselle.<sup>3,11</sup>

Characterisation of anthocyanins is essential due to their numerous curative and preventive properties which make them potential pharmacological and therapeutic agents.<sup>8,12</sup> Dp-3-sam and cy-3-sam are considered to be antihypertensive, antioxidant, and hypocholesterolaemic. There is a correlation between the antioxidant activity and the intensity of the red colour of the calyces.<sup>13</sup> Anthocyanins play an indirect role as antioxidants by inhibiting some enzymes such as lipoxygenases, nicotine amide adenine dinucleotide phosphate (NADPH) oxidase and xanthine oxidase (XO).<sup>7,14</sup>

In the present work, we put special emphasis on the inhibition of XO by anthocyanins. XO belongs to the molybdenum protein family of enzymes. Structurally, XO is composed of two identical monomers. Each monomer contains one molybdenum atom, one of the flavin adenine dinucleotides, and two iron-sulfur (2Fe-S) centres of the ferredoxin type including two separated substrate-binding sites, i.e. the purine binding site and the flavin adenine dinucleotides cofactor site; both binding sites are vulnerable to inhibitors.<sup>15</sup> To our knowledge, XO is a highly versatile enzyme, which is widely distributed among different animal kingdom species.<sup>16</sup> Furthermore, XO catalyses the metabolic conversion of purine bases to uric acid<sup>15,16</sup> to produce superoxide radicals as well as

hydrogen peroxide reactive oxygen species<sup>15</sup>. Thus, an increase in the activity of the enzyme leads to accumulation of uric acid and reactive oxygen species<sup>15,17</sup>, and results in several diseases. For example, hyperuricaemia and gout are the main chronic diseases associated with increased activity of XO, as well as several diseases including, but not limited to: hypertension, metabolic syndrome, cardiovascular disease, diabetes, obesity, cancer and hyperlipidaemia.<sup>15-17</sup>

The well-known traditional uses of roselle for treating hypertension as well as some other diseases, encouraged us to examine the inhibitory effect of anthocyanins in roselle towards XO by aid of molecular docking in the current work. The structures of the compounds obtained from the LC-MS analysis that used docking ligands are illustrated in Figure 2.

To validate the inhibitory activity of the anthocyanin ligands towards XO, we compared their activity with that of topiroxostat, the standard drug for treatment of hyperuricaemia. The structure of topiroxostat is represented in Figure 3.

## Experimental

### Sample preparation

A total of four dried samples of roselle calyces, including both red and white calyces, were collected from different parts of Sudan. After selection, each sample was cleaned from agricultural residues and ground to a fine powder using an electrical grinder (Monolex, France); the powder was well homogenised, packed in polyethylene bags, and stored at room temperature (20–30 °C).

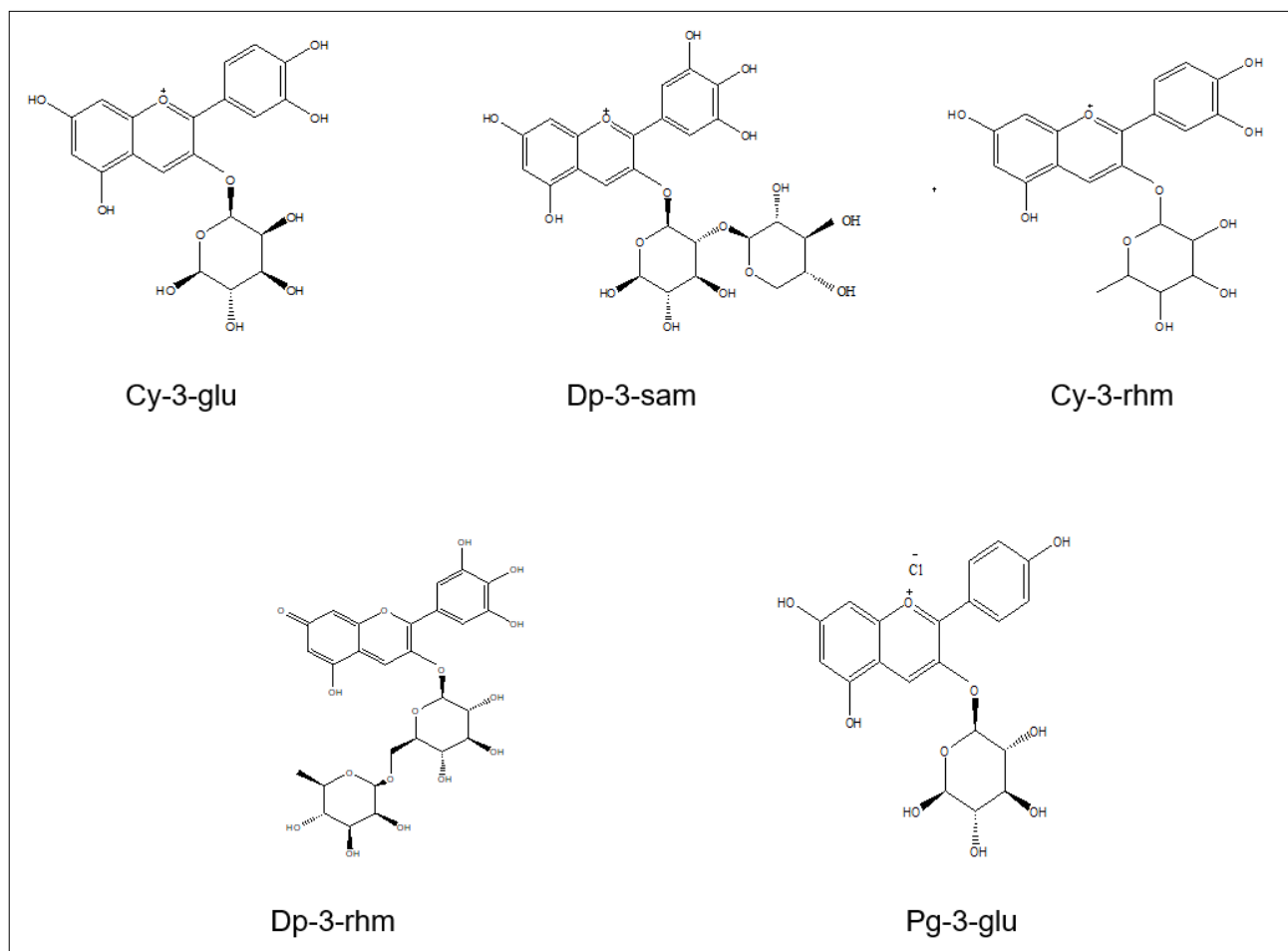


**Figure 2:** Chemical structures of the anthocyanin ligands.

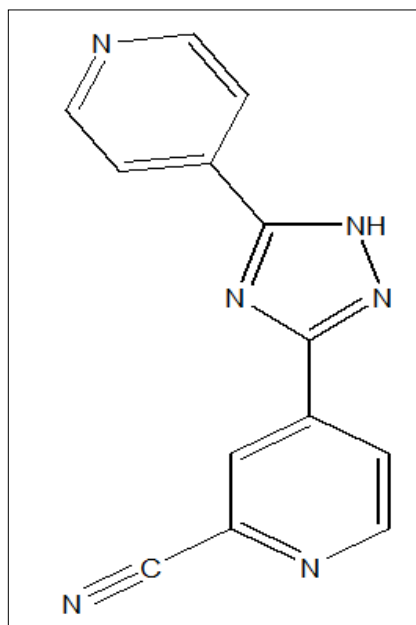


**Figure 3:** The chemical structure of topiroxostat (FYX-051).

### Chemicals

All chemicals were of analytical grade except those used in LC-MS analysis which were HPLC-grade.

### Phytochemical screening

#### Preparation of extracts

The extract was prepared according to Wrolstad et al.'s<sup>18</sup> alternative protocol with some modifications in the purification step. The purification was established by simple liquid-liquid extraction using an organic non-polar solvent (petroleum ether) and (0.01% (v/v) HCl) acidified methanol to remove water-insoluble impurities. The desired layer was reserved, the solvent was evaporated using a rotatory evaporator (Heidolph Laborota 4000 efficient HB digital, Germany) and allowed to air dry for 3–4 h. The attained gummy extract was used for all the phytochemical qualitative and quantitative analyses after dissolving in 1–2 cm<sup>3</sup> methanol for each qualitative test.

#### Preliminary screening

Qualitative analysis was carried out according to methods described by Harborne<sup>10</sup> and Sofowara<sup>19</sup> via simple test tube tests. These are the test for polyphenols (FeCl<sub>3</sub> test), test for flavonoids (AlCl<sub>3</sub> test), test for sterols (H<sub>2</sub>SO<sub>4</sub> test), test for saponins (Frothing test), and test for anthraquinones (KOH test).

#### Thin-layer chromatography

An amount of 10 mg from the gummy powdered extract of each of the samples was dissolved in 1 cm<sup>3</sup> of methanol and, using a capillary tube, spots were made from each sample extract on an aluminium sheet of pre-coated silica gel thin-layer chromatography plates, then elution was carried out in a covered thin-layer chromatography chamber using the mobile phase of a mixture of chloroform and methanol (7:3 v/v) according to Harborne<sup>10</sup>. The procedure was repeated on two other plates.

After performing the elution, plates were examined immediately in daylight, then sprayed with chemical reagents and visualised under a UV lamp (at 365 nm). Bromocresol green was the spray reagent employed for detection of organic acids, while AlCl<sub>3</sub> was used for detection of flavonoids.<sup>20</sup>

### Quantitative analysis

Total phenolic content was measured using Folin–Ciocalteu's reagent as described by Wolfe et al.<sup>21</sup> Total flavonoid and total anthocyanin contents were measured according to Shanmukha et al.<sup>22</sup> and Pacôme et al.<sup>6</sup>, respectively.

For total phenolic and flavonoid contents, absorbance was measured at 765 nm and 510 nm, respectively, against a reagent blank using a Jenway 7205 UV/Vis double-beam spectrophotometer. The concentrations of phenolics and flavonoids in the test sample were determined and expressed as gram equivalent of gallic acid (g GAE) and quercetin per gram of air-dried extract (g ADE), using a standard calibration plot for each individually. All measures were performed in duplicate.

### Determination of total anthocyanins

Total anthocyanin content was measured at an absorbance of 530 nm using a Jenway 7205 UV/Vis spectrophotometer against the blank; total anthocyanin content was estimated as cyanidin-3-glucoside at 530 nm using a molar extinction coefficient of 26 900 L/mol/cm and molar mass (449 g/mol) and was expressed as cyanidin-3-glucoside (g cy-3-glu)/(100 g of air-dried extract).<sup>6</sup>

### LC-MS/MS identification

Anthocyanin extraction was carried out using 250 cm<sup>3</sup> acidified methanol by Soxhlet apparatus<sup>2</sup> at a temperature of 50–55 °C. The extract was purified by simple liquid/liquid extraction after reducing the extract volume using the rotatory evaporator (Heidolph Laborota 4000 efficient HB digital, Germany).

Anthocyanins were identified in the purified sample extracts using LC-MS/MS with a UPLC-Q-TOF-MS (XEVO-G2 QTOF YCA119, Waters, using Acquity UPLC HS T3 (100 × 2.1 mm, 1.8 μm; Waters) column maintained at 45 °C in a column oven in the LC-MS Laboratory, Beijing University of Chemical Technology BUCT, China. The analysis was carried out according to the method described by Cahliková et al.<sup>23</sup> with some modifications. The conditions of the chromatographic run were as follows: 0–1 min: 90% A and 10% B, 1–5 min: 85% A and 15% B, 5–10 min: 40% A and 60% B, 10–13 min: 0% A and 100%B, 13–15 min: 90% A and 10% B. Gradient mobile phase composed of water acidified with 0.1% formic acid (solvent A) and acetonitrile (solvent B). The flow rate and sample injection volume were 0.4 cm<sup>3</sup>/min and 3.00 μL, respectively.

The ion source of the quadrupole time-of-flight (Q-TOF) detector was set at the positive electrospray ionisation polarity mode. The optimum conditions of the Q-TOF system, performed in the resolution mode, were: capillary voltage: +3.000 kV, ion source temperature: 100 °C, extractor: 4.0 V; RF lens: 0.3 V, mass range m/z: 50 to 2000 Da, nitrogen as the desolvation gas at a flow rate of 800 L/h and at a temperature of 400 °C. Nitrogen was used also as the cone gas (20 L/h), and argon as the collision gas. The cone voltage, collision energy, and well time were carefully optimised for each compound and transition individually (cone voltage set at 4/30 V, collision energy set finally at 6 eV). The software used for the MS control and data gathering was Mass Lynx 4.1.

### Molecular docking

Molecular docking is a method used to screen for the ability of specific small compounds (ligands) to fit into a previously identified therapeutic target (the receptor; usually a protein enzyme).<sup>24,25</sup> Several docking programs can be used: AutoDock Vina, GOLD, and MOE-Dock are top ranked with the best scores.<sup>25</sup> We used the AutoDock Vina program<sup>26</sup> for the docking of anthocyanin ligands to the active site of the XO enzyme, after performing the required preparations.

First, the protein crystal structure and ligand 3D structures were downloaded from RCSB Protein Data Bank<sup>27</sup> (1FIQ PDB code) and PubChem online databases<sup>28</sup>, respectively. Then the suitable binding site of the protein was obtained using Chimera software<sup>29</sup> and the ligands were converted via Open Babel software<sup>30</sup> from SDF format to pdbqt. Thereafter, using autodock tools<sup>31</sup>, all water molecules in the protein

pdb file were removed, hydrogen atoms were added, and the grid box dimensions were set, then the file saved as pdbqt. Ligands were prepared by detecting torsions for each structure and saved as a pdbqt file. The AutoDock Vina order was then created after preparing the configuration files. The process was repeated for each docking trial for all ligands.

### Data analysis

The obtained (out.pdbqt) file for each ligand was visualised using discovery studio<sup>32</sup> and pymol<sup>33</sup> visualisation programs.

## Results and discussion

### Phytochemical screening

#### Qualitative analysis

Our results show that roselle is rich in phytochemicals, especially anthocyanins, in agreement with the results of previous studies.<sup>3-5</sup> The general screening of some phytochemical constituents detected the presence of polyphenols, flavonoids, saponins, and sterols, and an absence of anthraquinones. Although the different roselle types had similar phytochemical constituents, the red type exhibited higher contents of polyphenols and flavonoids than the white type. Table 1 reports the phytochemical screening tests for four samples of roselle.

The sour taste of roselle is due to the presence of organic acids.<sup>3,4</sup> Flavonoids, particularly the anthocyanins, are the compounds that give roselle its importance and its colour.<sup>3-5</sup> To investigate the presence of organic acids and flavonoids, thin layer chromatography was performed and the results are shown in Table 2.

The presence of different organic acids is confirmed by spots at different  $R_f$  values. In contrast, similar types of flavonoids are separated at equal  $R_f$  values for all samples. Therefore, it is worth mentioning that the solvent system used, i.e. chloroform: methanol 7:3, is suitable for separation of organic acids but not the best for separation of flavonoids. Our finding of the presence of phytochemical compounds in roselle is in good agreement with previous investigations.<sup>2,5,6,34</sup>

#### Quantitative analysis

Result of the quantitative analysis of polyphenols, flavonoids, and anthocyanins in roselle are presented in Table 3. Anthocyanins have the lowest concentration among the three measured phytochemical groups, followed by flavonoids and then polyphenols. All samples show high polyphenolic and flavonoid contents and therefore express the antioxidant character of roselle, in agreement with Riaz et al.<sup>5</sup>

Sample 1 (light red colour) has the lowest phenolic and flavonoid contents of all the samples, while Sample 3 (brown-white colour) has the lowest anthocyanin content. Sample 4 has the highest phenolic content, but lower anthocyanin content and Sample 2 (dark red), which is characterised by its brilliant violet-red extract, has the highest flavonoid and anthocyanin contents.

**Table 1:** Phytochemical screening tests

Constituents	Reagents	Observation	Samples			
			1	2	3	4
Polyphenols	FeCl <sub>3</sub>	Samples 1 and 2: dark green Samples 3 and 4: light green	++ve	++ve	+ve	+ve
Flavonoids	AlCl <sub>3</sub>	Samples 1 and 2: blue Samples 3 and 4: yellow	++ve	++ve	+ve	+ve
Anthraquinones	KOH	Yellow	-ve	-ve	-ve	-ve
Sterols	CHCl <sub>3</sub> and H <sub>2</sub> SO <sub>4</sub>	Reddish violet	+ve	+ve	+ve	+ve
Saponins	Boiled H <sub>2</sub> O	Formation of frothing persisted on warming	+ve	+ve	+ve	+ve

**Table 2:** Thin layer chromatography results

Constituents	Spray reagent	Observation
*Flavonoids	AlCl <sub>3</sub>	Bright yellow spots under 365 nm wavelength
*Organic acids	Bromocresol green	Yellow spots in blue background under daylight

\*Chloroform: methanol 7:3 mixture solvent system

In contrast to the above-mentioned qualitative test of polyphenols and flavonoids, the red samples show lower values of polyphenols and flavonoids than the white samples in the quantitative test. The red colour affects the colour intensity in the qualitative tests, appearing higher than the actual amount, whereas the quantitative analysis gives the exact concentrations of polyphenols and flavonoids.

Our findings show that Sudanese roselle is rich in polyphenols and flavonoids and the total anthocyanin content is high<sup>3</sup> compared to Egyptian<sup>4</sup> and Abidjan<sup>6</sup> roselle.

#### LC-MS/MS Identification of anthocyanins

LC-Q-TOF-MS identification of anthocyanins revealed the presence of five anthocyanin types in all samples. The formulae and molecular weights of the identified compounds match the theoretical molecular weight values of anthocyanins obtained from PubChem.<sup>28</sup> Table 4 presents the chemical formulae, and the measured and theoretical values of the molecular weights of the identified anthocyanins.

The presence of five anthocyanin types in our results confirms the validity of the LC-MS technique as the most powerful and suitable technique for analysing anthocyanins, due to its high sensitivity and selectivity. These findings are in accordance with studies considering Sudanese roselle using the same technique which identified dp-3-rhm<sup>23,35</sup>, cy-3-rhm<sup>23,35</sup>, and pg-3-glu anthocyanins<sup>35</sup>. However, these anthocyanins were not identified in Abidjan roselle analysed using non-hyphenated HPLC.<sup>6,36</sup> Analysis of Sudanese roselle using thin-layer chromatography expressed the presence of two anthocyanins: dp-3-sam and cy-3-sam.<sup>3</sup>

#### Molecular docking

The inhibition property of the five obtained anthocyanins was tested against XO. According to our docking results, all obtained anthocyanins manifested strong inhibitory activity toward XO, superior to the standard drug (topiroxostat). All ligands exhibited low binding energies, ranging from -10.9 to -9.6 kcal/mol. The binding energies are shown in Table 5.

The variation of the binding energy values can be directly related to the anthocyanin types, i.e. anthocyanins with different glucoside, or different position or type of substituent group. This finding supported the idea that different anthocyanins result in different molecular fittings into a binding

**Table 3:** Quantitative analysis of polyphenol, flavonoid, and anthocyanin contents (in g/g%) in methanolic extracts of roselle

Phytochemical group	Contents in (g/g%)						
	1	2	3	4	Ref [3]	Ref [4]	Ref [6]
Polyphenols	6.77±0.19	9.81±0.49	6.98±0.07	13.15±0.42	–	3.70	0.74
Flavonoids	2.12±0.03	8.70±0.06	6.24±0.03	8.23±0.34	–	–	0.35
*Anthocyanins	0.32±0.02	1.03±0.03	0.043±0.00	0.09±0.02	(0.97,1.0)** and 0.001***	0.622	1.65

Values are means of duplicate determinations ( $n = 2$ ) ± standard deviation  
 \*Total anthocyanins measured as cyanidin-3-glucoside; \*\*red samples, \*\*\*white samples

**Table 4:** Liquid chromatography quadrupole time-of-flight mass spectrometry (LC-Q-TOF-MS) identification

Measured $m/z$	Theoretical $m/z$	Chemical formula	Name of the identified compound
449.1084	449.388	$C_{21}H_{21}O_{11}^+$	Cy-3-glu
597.1456	597.502	$C_{26}H_{29}O_{16}^+$	Dp-3-sam
595.1663	595.530	$C_{21}H_{21}O_{10}^+$	Cy-3-rhm
611.1612	610.521	$C_{27}H_{30}O_{16}^+$	Dp-3-rhm
433.415	433.389	$C_{21}H_{21}O_{10}^+$	Pg-3-glu

**Table 5:** Binding energies of the anthocyanin–XO and topiroxostat–XO complexes

Docked ligand	Binding energy (kcal/mol)
Dp-3-rhm	-10.90
Dp-3-sam	-10.50
Cy-3-rhm	-10.30
Pg-3-glu	-9.60
Cy-3-glu	-9.50
Topiroxostat	-8.60

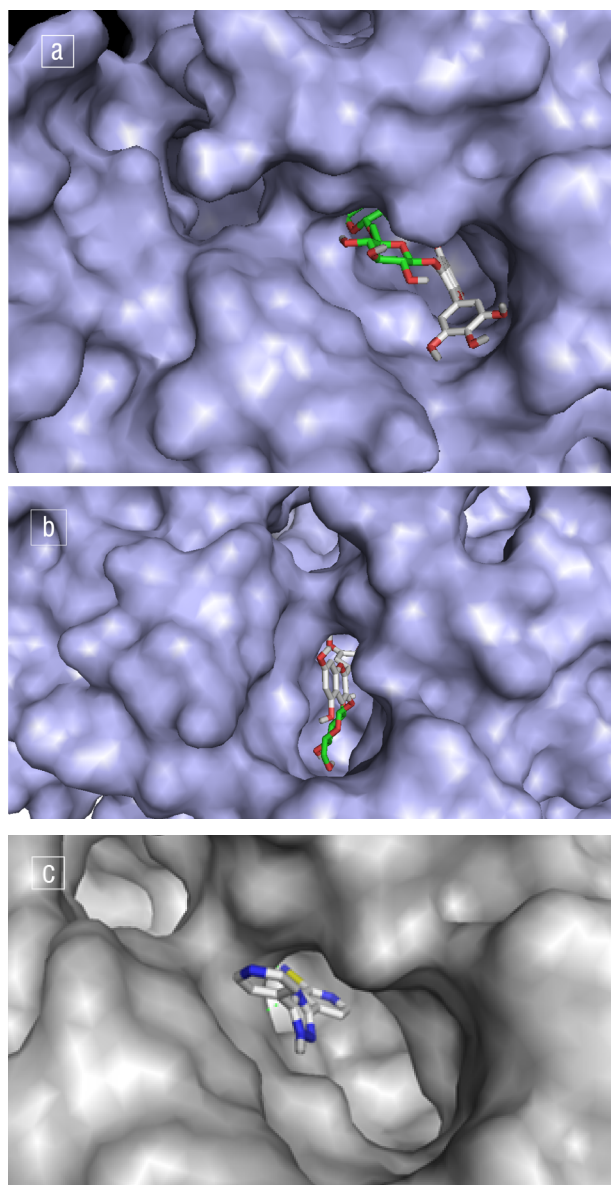
site.<sup>7</sup> Fittings of dp-3-rhm, cy-3-glu and topiroxostat into the binding site are shown in Figure 4.

The small values of the binding energy may be due to the presence of free hydroxyl groups in the ligand structures that are available to involve in hydrogen bonds, as proposed by Wallace et al.<sup>14</sup> The source of these hydroxyl groups is either one or more anthocyanidin rings (B and/or C) or glucoside moiety. For instance, Figure 4 illustrates the binding of the hydroxyl cy-3-glu.

In addition to the binding of the OH group via H-bonds, the  $\pi$ -system of the rings contributes to the interaction and enhances the inhibition of XO. The interaction is either hydrophobic ( $\pi$ -alkyl,  $\pi$ -sigma and alkyl) or electrostatic ( $\pi$ -cation). Figure 5 exhibits the different interactions in cy-3-glu.

The amino acid residues' binding sites THR354 and ARG394 are bonded to topiroxostat with a hydrogen bond of length 2.78 Å, and carbon hydrogen bond of length 3.55 Å. THR354 and ARG394 are bonded with dp-3-sam by hydrogen bonds of lengths 2.16 Å and 2.42 Å. THR354 interacts with cy-3-rhm and dp-3-rhm by 2.12 Å and 2.27 Å hydrogen bonds, respectively.

Different basic structures between topiroxostat and the anthocyanins allow different bindings. Topiroxostat, illustrated in Figure 2, lacks


**Figure 4:** Fittings of (a) dp-3-rhm, (b) cy-3-glu and (c) topiroxostat into the flavin adenine dinucleotide binding site in xanthine oxidase inhibition.

glucoside moiety and substituted hydroxyl groups which constitute the most important moieties in the binding interactions of anthocyanins.

Dp-3-rhm obtains the most stable conformer with a binding energy of ca -10.9 kcal/mol; whereas the complex with the highest binding energy of ca. -9.50 kcal/mol is cy-3-glu, which has a lower binding energy than topiroxostat (-8.6 kcal/mol).



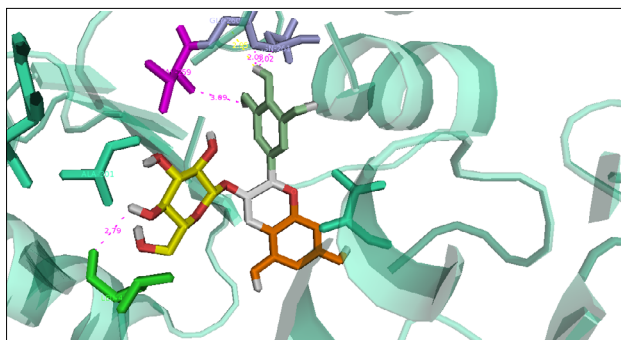


**Figure 5:** Cy-3-glu docking binding interactions through hydroxyl groups.

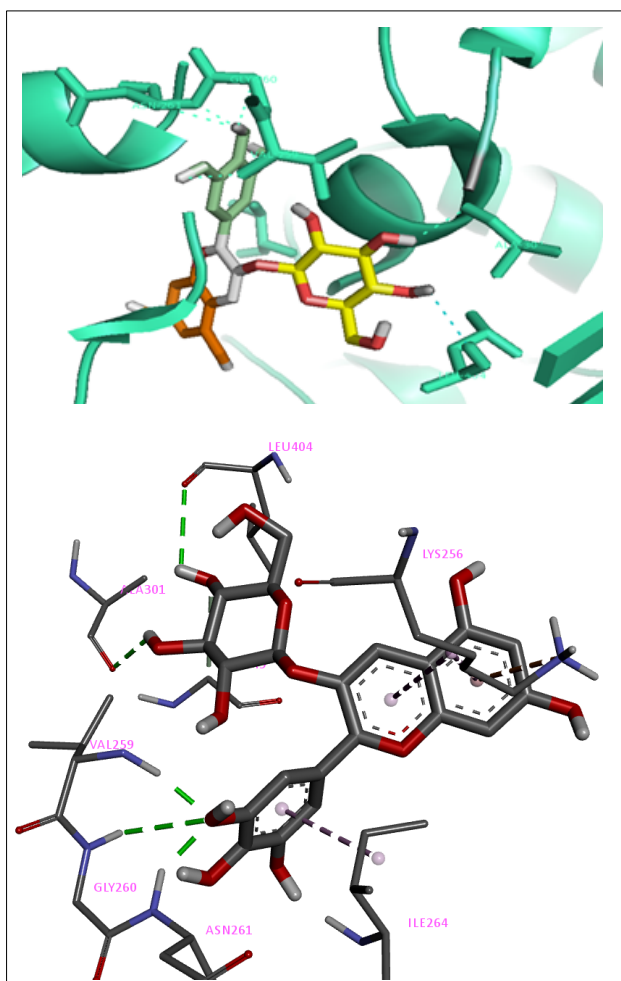


**Figure 6:** The different interactions: H-bonds  $\pi$ -alkyl,  $\pi$ -sigma and alkyl hydrophobic and electrostatic in cy-3-glu anthocyanin. Bonds are represented by dashed lines; classical H-bonds are in green; C-H bonds in grey,  $\pi$ -sigma dark violet,  $\pi$ -cation orange,  $\pi$ -alkyl violet, and alkyl faint violet.

According to Kostić et al.<sup>15</sup>, the absence of a hydroxyl group in the anthocyanins at C-3 position, as shown in Figure 1, is the main factor influencing the inhibitory activity of all anthocyanins.

Dp-3-rhm is characterised over other ligands by the presence of hydroxyl groups at C-5 and C-7 and a double bond between C-2 and C-3. These are essential requirements for its high inhibitory activity toward XO, as reported by Kostić et al.<sup>15</sup>

The strong inhibitory activity of the anthocyanin ligands towards XO suggests the use of anthocyanins as components of potential drugs as superior to the standard hyperuricaemia drug, topiroxostat. The interactions of ligands and topiroxostat toward the enzyme are given in Figure 7.

## Acknowledgements

We thank the LC-MS Laboratory, Beijing University of Chemical Technology, China, for the identification analysis via LC-MS/MS. We also thank Dr Sed Ahmed Osman, El-Neelain University, Khartoum, Sudan.

## Competing interests

We have no competing interests to declare.

## Authors' contributions

A.E-N.: Conceptualisation, formulation or evolution of overarching research goals and aims; methodology development and design; chemical and computational experiments and analysis; data collection; sample preparation and analysis; data analysis; writing – the initial draft (including substantive translation); validation. S.A.: Conceptualisation, formulation or evolution of overarching research goals and aims; writing – revisions; project management; student supervision. I.A.: Project management; student supervision. G.A.: Phytochemistry.

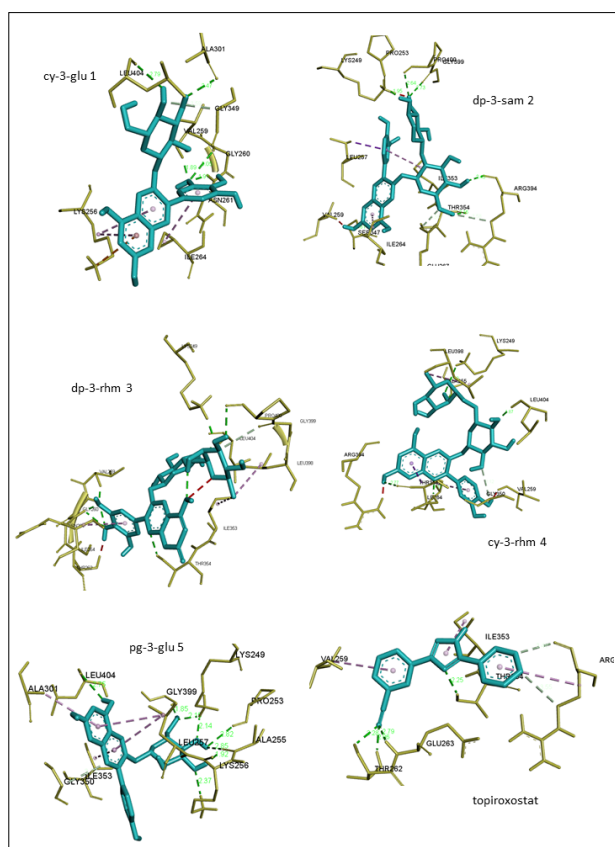


**Figure 7:** Binding interactions of the ligands cy-3-glu 1, dp-3-sam 2, dp-3-rhm 3, cy-3-rhm 4, pg-3-glu 5 and topiroxostat. Hydrogen bonds between the binding amino acid residues at the flavin adenine dinucleotides binding site and ligands. The ligand structures are shown in light blue, amino acid residues in pale yellow, and classical H-bonds are in green.

## References

1. Mohamed BB, Sulaiman AA, Dahab AA. Roselle (*Hibiscus sabdariffa* L.) in Sudan, cultivation and their uses. *Bull Env Pharmacol Life Sci.* 2012;1:48–54.
2. Okereke CN, Iroka FC, Chukwuma MO. Phytochemical analysis and medicinal uses of *Hibiscus sabdariffa*. *Int J Herb Med.* 2015;2:16–19.
3. AL-Shoosh WGAA. Chemical composition of some roselle (*Hibiscus sabdariffa*) genotypes [thesis]. Khartoum: University of Khartoum; 1997.
4. Abou-Arab AA, Abu-Salem FM, Abou-Arab EA. Physico-chemical properties of natural pigments (anthocyanin) extracted from roselle calyces (*Hibiscus sabdariffa*). *J Am Sci.* 2011;7:445–456.
5. Riaz G, Chopra RA. Review on phytochemistry and therapeutic uses of *Hibiscus sabdariffa* L. *Biomed Pharmacother.* 2018;102:575–586. <https://doi.org/10.1016/j.biopha.2018.03.023>
6. Obouayeba AP, Djyh NB, Diabate S, Djaman AJ, N'Guessan JD, Kone M, et al. Phytochemical and antioxidant activity of roselle (*Hibiscus sabdariffa* L.) petal extracts. *Res J Pharm Biol Chem Sci.* 2014;5:1454.
7. Zia-Ul-Haq M, Riaz M, Saad B. Anthocyanins and human health: Biomolecular and therapeutic aspects. Cham: Springer International Publishing; 2016. <https://doi.org/10.1007/978-3-319-26456-1>
8. Hirsch GE, Martins LAM. Anthocyanins: Chemical features, food sources and health benefits. In: *Handbook of anthocyanins*. New York: Nova Science Publishers; 2015. p. 227–248.
9. Welch CWuQ, Simon J. Recent advances in anthocyanin analysis and characterization. *Curr Anal Chem.* 2008;4:75–101. <https://doi.org/10.2174/157341108784587795>
10. Harborne JB. *Phytochemical methods: A guide to modern techniques of plant analysis*. 3rd ed. London: Chapman and Hall; 1998.
11. Ingrid HM, Jaka, Santoso H. Natural red dyes extraction on roselle petals. *IOP Conf Ser Mater Sci Eng.* 2016;162:012029. <https://doi.org/10.1088/1757-899X/162/1/012029>
12. Kong JM, Chia LS, Goh NK, Chia TF, Brouillard R. Analysis and biological activities of anthocyanins. *Phytochemistry.* 2003;64:923–933. [https://doi.org/10.1016/S0031-9422\(03\)00438-2](https://doi.org/10.1016/S0031-9422(03)00438-2)
13. Hopkins AL, Lamm MG, Funk JL, Ritenbaugh C. *Hibiscus sabdariffa* L. in the treatment of hypertension and hyperlipidemia: A comprehensive review of animal and human studies. *Fitoterapia.* 2013;85:84–94. <https://doi.org/10.1016/j.fitote.2013.01.003>
14. Wallace TC. Anthocyanins in cardiovascular disease prevention. In: *Handbook of anthocyanins in health and disease*. London: Taylor and Francis; 2014. p. 165–198.
15. Kostić DA, Dimitrijević DS, Stojanović GS, Palić IR, Đorđević AS, Ickovski JD. Xanthine oxidase: Isolation, assays of activity, and inhibition. *J Chem.* 2015;2015:1–8. <https://doi.org/10.1155/2015/294858>
16. Umamaheswari M, Madeswaran A, Asokkumar K, Sivashanmugam T, Subhadradevi V, Jagannath P. Discovery of potential xanthine oxidase inhibitors using in silico docking studies. 2011;3:240–247. <https://doi.org/10.3329/bjp.v7i1.10007>
17. Gliozzi M, Malara N, Muscoli S, Mollace V. The treatment of hyperuricemia. *Int J Cardiol.* 2016;213:23–27. <https://doi.org/10.1016/j.ijcard.2015.08.087>
18. Wrolstad RE, Acree TE, Decker EA, Penner MH, Reid DS, Schwartz SJ. Pigments and colorants. In: *Handbook of food analytical chemistry*. Hoboken, NJ: John Wiley and Sons; 2004. p. 1–69. <https://doi.org/10.1021/ja059701s>
19. Sofowara A. Screening plants for bioactive agents. In: *Medicinal plants and traditional medicine in Africa*. Ibadan: Spectrum Books Ltd; 1993. p. 134–156.
20. Jork H, Funk W, Fischer W, Wimmer H. Physical and chemical detection methods: Fundamentals. In: *Thin-layer chromatography: Reagents and detection methods*. Weinheim: VCH; 1990.
21. Wolfe K, Wu X, Liu RH. Antioxidant activity of apple peels. *J Agric Food Chem.* 2003;51:609–614. <https://doi.org/10.1021/jf020782a>
22. Shanmukha I, Patel J, Settee RS. Spectroscopic determination of total phenolic and flavonoid contents of *Sesbani afrandiflora* (Linn) flower. *Am J Pharm Tech Res.* 2012;2:399–405.
23. Cahlíková L, Ali BH, Havlíková L, Ločárek M, Siatka T, Opletal L, et al. Anthocyanins of *Hibiscus sabdiffera* calyces from Sudan. *Nat Prod Commun.* 2015;10:77–79. <https://doi.org/10.1177/1934578X1501000120>
24. Bisht N, Singh BK. Role of computer aided drug design in drug development and drug discovery. *Int J Pharm Sci Res.* 2018;9:1405–1415.
25. Pagadala NS, Syed K, Tuszynski J. Software for molecular docking: a review. *Biophys Rev.* 2017;9:91–102. <https://doi.org/10.1007/s12551-016-0247-1>
26. Trott O, Olson AJ. AutoDock Vina: Improving the speed and accuracy of docking with a new scoring function, efficient optimization, and multithreading. *J Comput Chem.* 2010;31:455–461. <https://doi.org/10.1002/jcc.21334>
27. Berman HMJ, Westbrook J, Feng Z, Gilliland GTN, Bhat GTN, Weissig H, et al. The Protein Data Bank. *Nucleic Acids Res.* 2000;28:235–242.
28. Kim S, Chen J, Cheng T, Gindulyte A, He J, He S, et al. PubChem 2019 update: Improved access to chemical data. *Nucleic Acids Res.* 2019;47:1102–1109. <https://doi.org/10.1093/nar/gky1033>
29. Pettersen EF, Goddard TD, Huang CC, Couch GS, Greenblatt DM, Meng EC, et al. UCSF Chimera – a visualization system for exploratory research and analysis. *J Comput Chem.* 2004;25:1605–1612. <https://doi.org/10.1002/jcc.20084>
30. O'Boyle NM, Banck M, James CA, Morley C, Vandermeersch T, Hutchison GR. Open Babel: An open chemical toolbox. *J Chem Inf.* 2011;3:33. <https://doi.org/10.1186/1758-2946-3-33>
31. Sanner MF. Python: A programming language for software integration and development. *J Mol Graphics Mod.* 1999;17:57–61.
32. Diego S. Dassault Systèmes BIOVIA, Discovery Studio Visualizer,, 2016.
33. The PyMOL Molecular Graphics System, Version 1.2r3pre, Schrödinger, LLC.
34. Salem MZM, Olivares-Pérez J, Salem AZM. Studies on biological activities and phytochemicals composition of *Hibiscus* species – A review. *Life Sci J.* 2014;5:1–8.
35. Alamin YK. Physicochemical study of *Hibiscus sabdariffa* L. (Karkade) genotypes [thesis]. Khartoum: University of Khartoum; 2012.
36. Obouayeba AP, Okoma KM, Diarrassouba M, Diabaté S, Kouakou TH. Phytochemical characterisation and antioxidant activity of *Hibiscus sabdariffa* (Malvaceae) calyx extracts. *JAAS.* 2015;3:39–46.

**AUTHORS:**

Enobong R. Essien<sup>1</sup>   
Violette N. Atasie<sup>1</sup>   
Davies O. Nwude<sup>1</sup>  
Ezekiel Adekolurejo<sup>1</sup>  
Felicia T. Owwoeye<sup>1</sup>

**AFFILIATION:**

<sup>1</sup>Department of Chemical and Food Sciences, Bells University of Technology, Ota, Nigeria

**CORRESPONDENCE TO:**

Enobong Essien

**EMAIL:**

reggiessien@gmail.com

**DATES:**

**Received:** 27 May 2021

**Revised:** 25 Sep. 2021

**Accepted:** 27 Sep. 2021

**Published:** 27 Jan. 2022

**HOW TO CITE:**

Essien ER, Atasie VN, Nwude DO, Adekolurejo E, Owwoeye FT. Characterisation of ZnO nanoparticles prepared using aqueous leaf extracts of *Chromolaena odorata* (L.) and *Manihot esculenta* (Crantz). S Afr J Sci. 2022;118(1/2), Art. #11225. <https://doi.org/10.17159/sajs.2022/11225>

**ARTICLE INCLUDES:**

Peer review

Supplementary material

**DATA AVAILABILITY:**

Open data set

All data included

On request from author(s)

Not available

Not applicable

**EDITOR:**

Teresa Coutinho

**KEYWORDS:**

cost-effective technique, eco-friendliness, zinc oxide nanoparticles, *Chromolaena odorata*, *Manihot esculenta*

**FUNDING:**

None



# Characterisation of ZnO nanoparticles prepared using aqueous leaf extracts of *Chromolaena odorata* (L.) and *Manihot esculenta* (Crantz)

Plant-mediated routes for synthesising metal oxide nanoparticles are gaining tremendous attention due to the benefits of the technique: simplicity, cost-effectiveness, and eco-friendliness. We compared the properties of zinc oxide nanoparticles (ZnONPs) made from aqueous leaf extracts of *Chromolaena odorata* and *Manihot esculenta*, both of which are abundant on the African continent. The phytochemical composition of the extracts was first assessed using gas chromatography-mass spectrometry (GC-MS) to determine the types of biomolecules involved in the reducing and capping processes that result in ZnONP formation. After that, UV-Vis spectrophotometry, scanning electron microscopy, energy dispersive X-ray analysis, transmission electron microscopy, X-ray diffractometry, and Fourier transform infrared spectroscopy (FTIR) were used to study ZnONP formation, morphological characteristics, elemental composition, shape and size properties, and phase composition. The ZnONPs made with *Chromolaena odorata* leaf extract had a better distribution of spherical and hexagonal forms, with an average particle size of 42.35 nm. The ZnONPs made with *Manihot esculenta* leaf as a reductant had a particle size of 14.71 nm on average and were more agglomerated with poor particle distribution. Phytosterols were shown to be the most important biomolecules in the reduction and capping reactions, according to GC-MS and FTIR analyses. In this study, we created a cost-effective technique for the synthesis of eco-friendly ZnONPs for diverse applications, particularly in Africa, using *Chromolaena odorata* and *Manihot esculenta* leaves.

**Significance:**

- This study could provide useful information on how the phytochemicals embedded in *Chromolaena odorata* and *Manihot esculenta* could influence the properties of the ZnONPs obtained from them.
- Differences in morphology and formation yield of ZnONPs are obtainable from aqueous leaf extracts of *Chromolaena odorata* and *Manihot esculenta*.
- *Chromolaena odorata* and *Manihot esculenta* could serve as dependable raw materials for the green synthesis of ZnONPs in Africa.

## Introduction

Due to their unique features as compared to bulk materials, nanostructured materials with dimensions of 1–100 nm have attracted a lot of research in recent decades.<sup>1</sup> Nanomaterials such as nanoparticles, nanolayers, powders, optoelectronics, mechanical nanodevices, and nanostructured biological materials have all been created using nanoscience. Metal oxide nanoparticles have been used as antibacterial and anticancer drug/gene delivery vehicles, and in cell imaging and biosensing materials, among other biomedical uses.<sup>2</sup> Furthermore, metal oxide nanoparticles are important in the field of catalysis.<sup>3</sup>

Zinc oxide nanoparticles (ZnONPs) are a type of metal oxide nanoparticle that has good ultraviolet (UV) light-absorbing characteristics as well as visible light transparency, making them ideal as sunscreen agents.<sup>4</sup> Furthermore, because of their capacity to produce reactive oxygen species and induce apoptosis, they are being studied as antibacterial and anticancer drugs. The US Food and Drug Administration has designated bulk ZnO as 'a generally recognised as safe' chemical, making ZnONPs appealing for drug administration.<sup>5</sup> As a result, ZnONPs are thought to be superior to other metal oxide nanoparticles like iron oxide nanoparticles, which have anticancer, antibacterial, and UV-absorbing capabilities. A report<sup>6</sup> on the safety of ZnONPs demonstrates that they do not interact with the majority of pharmaceutically accessible compounds.

Several methods have been used to prepare ZnONPs with a key focus on developing stable and uniform nanosized particles. Some examples of these methods are precipitation, wet chemical synthesis and solid-state pyrolysis. A reaction between a zinc precursor and a precipitating reagent is used in the precipitation method. When ZnO is calcined at a high temperature, an intermediate Zn product is generated.<sup>7</sup> The precipitation process has been modified to create the wet chemical synthesis method. An additive is employed in this method to stabilise the nanoparticles that are generated.<sup>8</sup> The solid-state pyrolytic method is a straightforward, quick, and cost-effective process that involves combining zinc acetate and sodium bicarbonate, then pyrolysing the combination.<sup>9</sup> ZnONPs are formed from zinc acetate, while sodium bicarbonate produces sodium acetate. The pyrolytic temperature can be adjusted to control the particle size of the nanoparticles. The pH-dependent sol-gel method of manufacturing ZnONPs, first developed by Spanhel and Anderson<sup>10</sup> and later refined by Meulenkamp<sup>11</sup>, involves solvation, hydrolysis, polymerisation, and transformation with zinc acetate dihydrate as the precursor.

The potential toxic effects of the reagents and side-products of the aforementioned chemical synthesis methods to humans and the environment, render them unattractive for synthesising ZnONPs. These shortcomings have resulted

in a paradigm shift to the plant-mediated route of synthesising ZnONPs. Plant extracts are typically used as reducing and stabilising agents in the formation of ZnONPs. The benefits of this method are simplicity of the process, biocompatibility, eco-friendliness, extensive antimicrobial activity of the obtained nanoparticles, and, most importantly, cost-effectiveness.<sup>12</sup>

Plant extracts have been used to synthesise ZnONPs in several studies. Using *Andrographis paniculata* leaf extract, Rajakumar et al.<sup>13</sup> produced ZnONPs of spherical and hexagonal forms in the size ranges of 98–115 nm and 57 nm, respectively, with strong antioxidant, anti-diabetic, and anti-inflammatory effects. Nagajyothi et al.<sup>14</sup> produced ZnONPs from a *Polygala tenuifolia* root extract. Apart from demonstrating antioxidant activity by scavenging 45.47% 2,2-diphenyl-1-picrylhydrazyl (DPPH) at 1 mg/mL, the ZnONPs also showed remarkable dose-dependent anti-inflammatory action by reducing iNOS, COX-2, IL-1 $\beta$ , IL-6, and TNF- $\alpha$  mRNA and protein expressions. The green synthesis approach was then used to generate ZnONPs using a reducing agent extracted from the *Jacaranda mimosifolia* flower.<sup>15</sup> The results revealed ZnONPs with a size range of 2–4 nm that were cytotoxic against Gram-negative *Escherichia coli* and Gram-positive *Enterococcus faecium* bacteria.

Using the leaf extracts of *Chromolaena odorata* and *Manihot esculenta*, the current study offers yet another intriguing opportunity to extend the green synthesis of ZnONPs. Previous studies showed that *Chromolaena odorata*, a fast-growing perennial and invasive weed, possesses therapeutic effects against diarrhoea, hypertension, and inflammation.<sup>16</sup> The pharmacological potency is no doubt the result of important phytochemicals inherent in the plant. In Africa, *Manihot esculenta* is widely grown as an annual crop. The tubers (cassava) are a primary carbohydrate source. Vitamins A, B1, calcium, calories, phosphorus, protein, fat, carbohydrate, and iron are all found in the leaf, which is often discarded during harvest. It can be used to treat measles, smallpox, chickenpox, skin rashes, fevers and headaches, colds, constipation, ringworm, tumours, conjunctivitis, sores and abscesses.<sup>17</sup> Furthermore, chlorophyll in the leaves serves as an antioxidant and anti-cancer agent. Again, the pharmacological potency of these plants is no doubt the result of important phytochemicals inherent in them.

The goal of this study was to assess the phytochemicals found in aqueous leaf extracts of *Chromolaena odorata* and *Manihot esculenta*, as well as to use them to make ZnONPs and investigate their qualities. To our knowledge, there have been no previous studies in which the synthesis of ZnONPs was jointly performed using *Chromolaena odorata* and *Manihot esculenta* to evaluate the effect of phytochemicals on the properties of the obtained ZnONPs.

## Materials and methods

### Materials

The *Chromolaena odorata* and *Manihot esculenta* leaves utilised in this study were obtained from a bush near Bells University of Technology in Ota, Ogun State, Nigeria, and their identities were confirmed at the University of Lagos' Botany Department. Sigma-Aldrich (Gillingham, UK) provided the reagents utilised, which included Zn(NO<sub>3</sub>)<sub>2</sub>·6H<sub>2</sub>O and absolute ethanol.

### Preparation of the aqueous leaf extracts

Dust and particle contaminants were removed from the leaves of *Chromolaena odorata* and *Manihot esculenta* by washing them first with tap water and then with deionised water to prepare the extracts. They were then dried in the sun and ground into fine granules to speed up the extraction process. Each powdered sample (24 g) was combined separately with 250 mL deionised water, sealed, and heated in a water bath for 15 min. The combinations were then cooled to ambient temperature and filtered to yield the aqueous extracts, which were then stored at 5–10 °C in the refrigerator for later use.

### Synthesis of ZnONPs

The *Chromolaena odorata* and *Manihot esculenta* aqueous leaf extracts (250 mL) were added in drops to a 0.1-M solution of Zn(NO<sub>3</sub>)<sub>2</sub>·6H<sub>2</sub>O

(50 mL) in a conical flask under a continual stirring condition using a magnetic stirrer to make ZnONPs. The 12-h addition time resulted in the production of solid-liquid dispersion mixtures, which were centrifuged for 15 min at 3835 g force. The supernatants were then removed, and the residues were rinsed with deionised water to remove any remaining Zn(NO<sub>3</sub>)<sub>2</sub>·6H<sub>2</sub>O and organic compounds. For drying, the remnants were placed in a 70 °C oven for 2 h. After that, ZnONPs were obtained by calcination in a muffle furnace at 500 °C for 3 h. To improve the dispersion of the ZnONPs, they were sonicated in ethanol at 40 °C for 1 h in an ultrasonic cleaner. ZnONPs from *Chromolaena odorata* were designated ZnO\_CNPs, while those from *Manihot esculenta* were designated ZnO\_MNPs.

### Characterisation

The phytochemicals in the *Chromolaena odorata* and *Manihot esculenta* aqueous leaf extracts were determined using a gas chromatograph–mass spectrometer (GC-MS; Shimadzu QP2010SE, Markham, Ontario, Canada). Before injection into the GC-MS, ethanol was added to the crude aqueous extracts to obtain an ethanolic solution of the extracts at a mixture ratio of 1:1. From the retention times, fragmentation patterns and peak areas, the various phytochemicals present in the extracts and their concentrations were determined. The formation of ZnONPs was validated using a UV-Vis absorption spectrophotometer to measure the wavelengths of absorption of the mixture obtained during the reaction between Zn(NO<sub>3</sub>)<sub>2</sub>·6H<sub>2</sub>O and the *Chromolaena odorata* and *Manihot esculenta* leaf extracts, which ranged from 300 nm to 800 nm (Uniscop SM 7504).

In a scanning electron microscope (SEM) equipped with an energy dispersive X-ray analyser (EDX) unit (JEOL JSM 7660F), the microstructure and elemental composition of the ZnONPs were assessed to evaluate particle distribution and support the presence of ZnO in the samples. An accelerating voltage of 15 kV was used to evaluate the material.

The samples were analysed using a transmission electron microscope (TEM; JEM-ARM200F-G) running at a 200-kV accelerating voltage to determine the particle size and shape of the ZnONPs. The average particle size of each sample was then calculated using ImageJ software from the TEM micrographs.

To establish the type of phases present and analyse the crystalline nature of the ZnONPs, the diffraction patterns of the samples were obtained using an X-ray diffractometer (XRD; Rigaku D/Max-IIIC).

Fourier transform infrared (FTIR) spectroscopy (Nicolet iS10) with a wavenumber in the range of 350–4000 cm<sup>-1</sup> was used to determine the type of bonds present in the ZnONPs to complement the results of the GC-MS, UV-Vis, and XRD.

## Results and discussion

### UV-visible spectrophotometry

Nanoparticles are known to absorb visible to near-infrared radiation depending on their size and shape. This phenomenon is known as surface plasmon resonance (SPR) and is linked to the collective oscillation of surface electrons of nanoparticles. Dispersion of plasmonic nanoparticles produces one or more peaks that can be exploited to obtain relevant information on shape, size, and size distribution due to the SPR property of nanoparticles. The UV-Vis analysis gave a significant UV absorption band at 373 nm, as seen in the UV-Vis spectrum of the reaction mixture of the *Chromolaena odorata* extract and Zn(NO<sub>3</sub>)<sub>2</sub>·6H<sub>2</sub>O (Figure 1a). The band is due to the excitation of the valence electrons of ZnO present in the nanoparticles (nanocrystal/nanosphere) generated by the reaction of the *Chromolaena odorata* extract and Zn(NO<sub>3</sub>)<sub>2</sub>·6H<sub>2</sub>O. There are no extra absorption bands visible, indicating that the ZnONPs are extremely pure. Figure 1b shows the UV-Vis spectrum of the reaction mixture of the *Manihot esculenta* extract and Zn(NO<sub>3</sub>)<sub>2</sub>·6H<sub>2</sub>O. A prominent UV absorption band may be seen near 379 nm. The smoothness of the curve, in addition to the shift in absorption band, demonstrates the purity of the ZnONPs derived from the *Manihot esculenta* leaf. The ZnO UV absorption area is reported to range between 300 nm and 500 nm.<sup>18</sup>



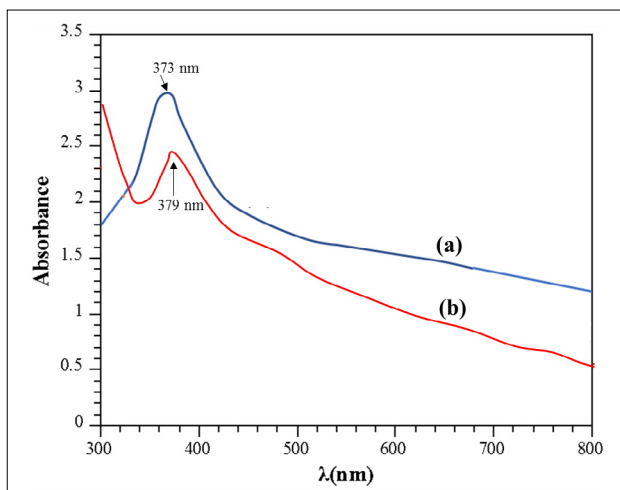


**Figure 1:** Ultraviolet-visible absorption spectra of the mixture of  $Zn(NO_3)_2 \cdot 6H_2O$  with extracts of (a) *Chromolaena odorata* and (b) *Manihot esculenta* stirred for 12 h, indicating the formation of ZnONPs observed at 373 nm and 379 nm, respectively.

Previous research found that ZnO has UV absorption peaks at 372 nm<sup>19</sup>, 375 nm<sup>18</sup>, and in the region of 358–375 nm<sup>20</sup>. The symmetry of the bands suggests that a larger proportion of the particle is spherically shaped. This result also indicates the high bio-reducing ability of the phytochemicals present in the extract.

Furthermore, the surface SPR peak of the produced ZnONPs was 327 nm. Using Equation 1, the bandgap energy of the resultant SPR was calculated:

$$E = hc/\lambda, \quad \text{Equation 1}$$

where  $h$  stands for Planck's constant ( $6.626 \times 10^{-34}$  J.s),  $c$  for light velocity ( $3.0 \times 10^8$  m/s), and  $\lambda$  for the wavelength. A bandgap of 3.79457 eV was discovered, indicating the occurrence of a blue shift.<sup>21</sup>

### Morphological characteristics and elemental composition of ZnONPs

The morphologies of the ZnONPs are depicted in Figure 2. As observed in Figure 2a, the microstructure of ZnO\_CNPs are spherical and hexagonal with some degree of agglomeration. Even so, the particles are well distributed to present a high surface area. The result from a previous study<sup>22</sup> which obtained a similar morphology from plant-mediated synthesis using *Andrographis paniculata* leaf extract indicated that the obtained ZnONPs exhibited strong antioxidant, anti-diabetic, and anti-inflammatory potentials. Similarly, ZnONPs prepared using an aqueous extract of *Aloe vera*<sup>23</sup> not only presented a microstructure resembling the one obtained in this study, but also gave good antibacterial activity against *E. coli* and *Staphylococcus aureus*.

In contrast, ZnO\_MNPs exhibited spherical, hexagonal and rod-like shapes but appeared less agglomerated than those of ZnO\_CNPs, nonetheless showing lower particle distribution and limited surface area.

The presence of Zn and O in the sample at high intensity and 1:1 atomic ratio, as found in pure ZnO, verifies the synthesis of ZnONPs in ZnO\_CNPs (Figure 3a) and ZnO\_MNPs (Figure 3b), respectively. The spectra show carbon atom peaks from several biomolecules in the plant extract that served as reducing and capping agents during the process that resulted in the creation of ZnONPs.

### Particle size and shape

The TEM images of the ZnONPs are presented in Figure 4. The micrograph of ZnO\_CNPs indicates that the particles were different shapes, some spherical and others oval or hexagonal (Figure 4a), in agreement with the SEM result (Figure 2a). The TEM revealed an average particle size of 42.35 nm. The particles appeared agglomerated, as observed earlier in the SEM micrograph (Figure 2a). Those of ZnO\_MNPs (Figure 4b)

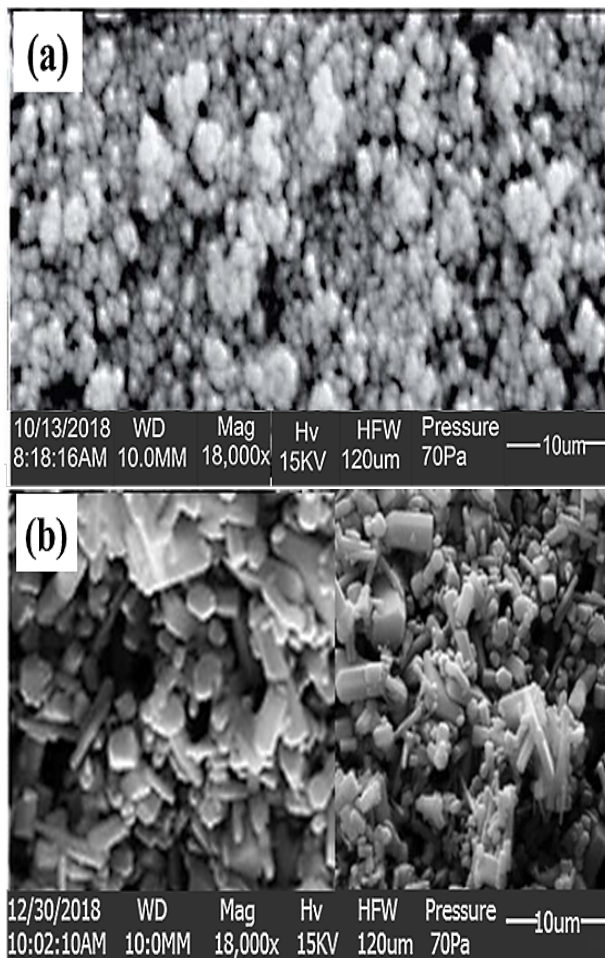


**Figure 2:** Scanning electron micrographs of (a) ZnO\_CNPs and (b) ZnO\_MNPs.

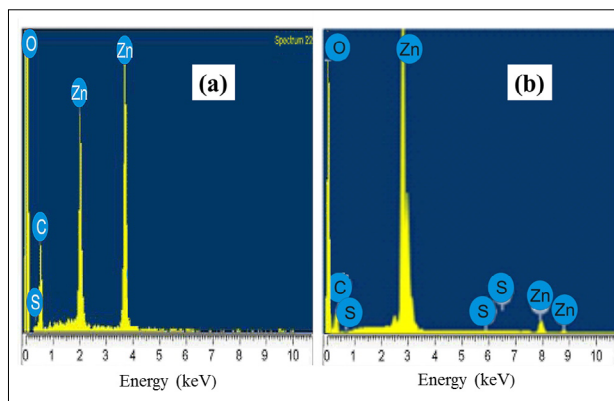


**Figure 3:** Energy dispersive X-ray analyser spectra of (a) ZnO\_CNPs and (b) ZnO\_MNPs showing a 1:1 atomic ratio of Zn and O.

were much smaller, with an average size of 14.71 nm, most of which were hexagonal and less agglomerated, as observed previously in the SEM result (Figure 2b). The agglomeration observed in the particles is the result of high surface energy, usually associated with synthesis occurring in an aqueous medium.<sup>13</sup> The disparity in the degree of particle dispersion and size in ZnO\_CNPs and ZnO\_MNPs could be attributed to the different types of biomolecules present in the extracts and the extent to which they were involved in the capping reactions.

Equation 2<sup>24</sup> was used to calculate the average number of Zn atoms ( $N$ ) in each kind of nanosphere:

$$N = \frac{\pi \rho D^3}{M} N_A, \quad \text{Equation 2}$$

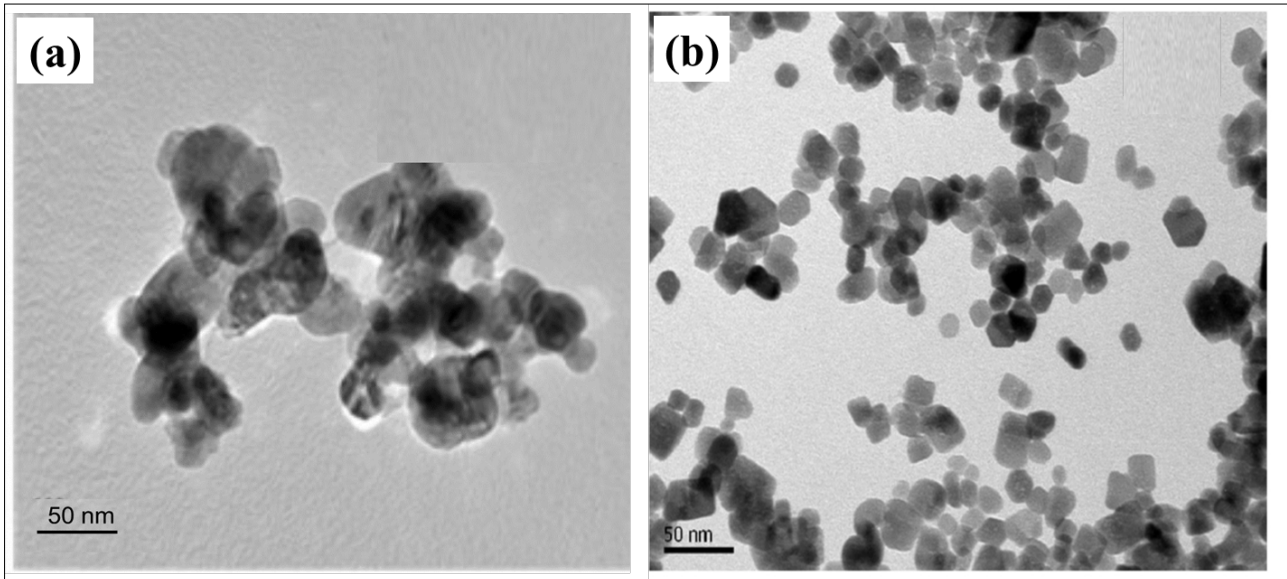


**Figure 4:** Transmission electron micrographs of the ZnONPs: (a) ZnO\_CNPs and (b) ZnO\_MNPs.

Where  $\rho$  is the density for hcp unit cell lattice of Zn ( $7.13 \text{ g/cm}^3 = 7.13 \times 10^{-21} \text{ g/nm}^3$ ),  $D$  is the particle size in nm,  $M$  represents the atomic weight of Zn ( $63.3800 \text{ g/mol}$ ) and  $N_A$  is Avogadro's constant ( $6.023 \times 10^{23}$  atoms/mol). By applying Equation 2, the average number of Zn atoms per synthesised nanoparticles in ZnO\_CNPs was 2 695 040 atoms, but was 676 251 atoms in ZnO\_MNPs. This result is indicative of the number of Zn atoms present on the surface of the samples. Therefore, ZnO\_CNPs contained more Zn surface atoms than did ZnO\_MNPs, which validates the SEM results presented in Figure 2.

### Diffraction patterns

The XRD patterns of the ZnONPs are shown in Figure 5. For ZnO\_CNPs (Figure 5a), the peaks gave hkl reflection plane reflections at 100, 002, 101, 110 and 201, corresponding to hexagonal wurtzite ZnO, when indexed using the standard diffraction reference file (JCPDS36-1451) in both angular location and intensity.<sup>13</sup> In ZnO\_MNPs (Figure 5b), the peaks corresponded to 100, 002, 101, 102, 110, 103 and 112 ZnO crystal planes. The sharp nature of diffraction peaks indicates that the ZnONPs possessed crystalline structure, especially ZnO\_MNPs. Interestingly, no additional peaks due to the presence of metallic impurities are seen on the diffractograms, suggesting the absence of impurities of other metal oxides in the samples.

The Scherrer equation<sup>13</sup> (Equation 3) was also used to estimate the crystallite size of the ZnONPs to compare with those obtained from the

TEM data, where  $k = 0.9$  is the shape factor,  $\lambda$  is the X-ray wavelength of CuK $\alpha$  radiation ( $1.54 \text{ \AA}$ ),  $\theta$  is the Bragg diffraction angle, and  $\beta$  is the full width at half maximum of the most prominent diffraction peak. The crystallite sizes obtained from the Scherrer calculation were 44.50 nm and 16.32 nm, respectively, for ZnO\_CNPs and ZnO\_MNPs. These values were close to the 42.35 nm and 14.71 nm obtained for ZnO\_CNPs and ZnO\_MNPs, respectively, using TEM, which thus validates the TEM results.

$$D = k\lambda/\beta\cos\theta$$

Equation 3

### GC-MS analyses

The compounds identified in the GC-MS analyses of the aqueous leaf extracts of *Chromolaena odorata* and *Manihot esculenta* are depicted in Table 1 and Table 2, respectively. The data analysis of the *Chromolaena odorata* aqueous leaf extract (Table 1) revealed the presence of four major compounds based on their percentage peak area, namely: 7-oxabicyclo[4.1.0]heptan-2-ol (10.89%), beta-sitosterol (37.97%), methanesulfonic acid (4.92%), 1,6-dideoxydulcitol (4.09%), [(6R)-6-[(8R,9S,10S,13R,14S,17R)-10,13-dimethyl-2,3,4,5,6,7,8,9,11,12,14,15,16,17-tetradecahydro-1H-cyclopenta[a]phenanthren-17-yl]-2-methylhepta-1,3-dienyl] benzoate (7.80%), and kauran-18-al, 17-(acetyloxy-, (4.beta.)) (7.33%) and beta-sitosterol (36.97%).

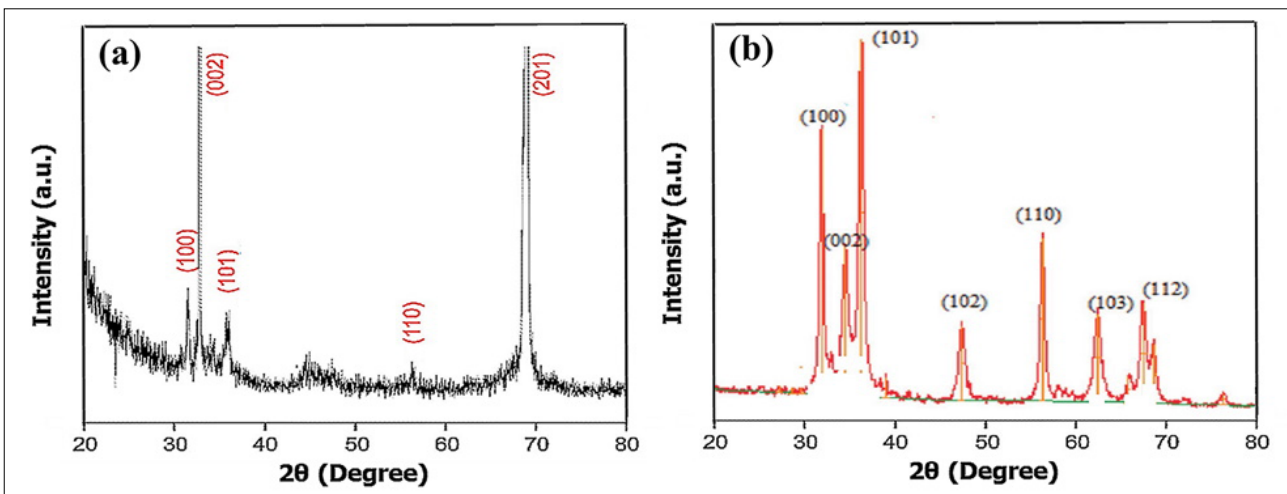


**Figure 5:** X-ray diffractometer pattern of the ZnONPs – (a) ZnO\_CNPs and (b) ZnO\_MNPs – showing the presence of pure ZnO crystalline phase.

**Table 1:** Gas chromatography–mass spectrometry results showing the phytochemicals, along with their corresponding peak areas, found in the *Chromolaena odorata* aqueous leaf extract

Peak	Retention time (min)	Peak area (%)	Name of compound	Molecular weight	Molecular formula
1	7.564	1.55	Glycerin	92.094	C <sub>3</sub> H <sub>8</sub> O <sub>3</sub>
2	9.587	0.53	Trans-1,4-cyclohexanediol	116.158	C <sub>6</sub> H <sub>12</sub> O <sub>2</sub>
3	10.357	0.34	Benzoic acid, ethyl ester	150.17	C <sub>9</sub> H <sub>10</sub> O <sub>2</sub>
4	11.099	0.90	2,2,3,3-Tetraethyloxirane	156.269	C <sub>10</sub> H <sub>20</sub> O
5	12.131	10.89	7-Oxabicyclo[4.1.0]heptan-2-ol	114.144	C <sub>6</sub> H <sub>10</sub> O <sub>2</sub>
6	12.294	4.09	1,6-Dideoxydulcitol	150.174	C <sub>6</sub> H <sub>14</sub> O <sub>4</sub>
7	13.745	0.95	1,4,2,5-Cyclohexanetetrol	148.16	C <sub>6</sub> H <sub>12</sub> O <sub>2</sub>
8	15.313	1.83	1-Methyl-6-(3-methylbuta-1,3-dienyl)-7-oxabicyclo[4.1.0]heptane	178.27	C <sub>12</sub> H <sub>18</sub> O
9	15.550	2.50	Stevioside	804.88	C <sub>38</sub> H <sub>60</sub> O <sub>18</sub>
10	15.735	1.63	1,7,7-Trimethylbicyclo[2.2.1]heptane-2,5-diol	170.252	C <sub>10</sub> H <sub>18</sub> O <sub>2</sub>
11	15.941	1.37	cis-Z- $\alpha$ -Bisabolene epoxide	220.356	C <sub>15</sub> H <sub>24</sub> O
12	16.153	1.14	cis-Z- $\alpha$ -Bisabolene epoxide	220.356	C <sub>15</sub> H <sub>24</sub> O
13	16.920	1.23	1-Heptadec-1-ynyl-cyclopentanol	320.361	C <sub>22</sub> H <sub>40</sub> O
14	17.086	3.27	1-Heptatriacotanol	357	C <sub>37</sub> H <sub>76</sub> O
15	18.051	15.91	Beta-Sitosterol	414.718	C <sub>29</sub> H <sub>50</sub> O
16	18.120	13.37	Beta-Sitosterol	414.718	C <sub>29</sub> H <sub>50</sub> O
17	18.201	8.69	Beta-Sitosterol	414.718	C <sub>29</sub> H <sub>50</sub> O
18	19.012	4.92	Methanesulfonic acid	96.1	CH <sub>3</sub> O <sub>3</sub> S
19	19.324	7.80	[(6R)-6-[(8R,9S,10S,13R,14S,17R)-10,13-Dimethyl-2,3,4,5,6,7,8,9,11,12,14,15,16,17-tetradecahydro-1H-cyclopenta[a]phenanthren-17-yl]-2-methylhepta-1,3-dienyl] benzoate	488.74	C <sub>34</sub> H <sub>48</sub> O <sub>2</sub>
20	19.529	2.79	(1-(Naphthalen-1-yl)propan-1-ol	186.104	C <sub>13</sub> H <sub>14</sub> O
21	19.625	7.33	Kauran-18- $\alpha$ , 17-(acetyloxy-, (4. $\beta$ .)-	346.511	C <sub>22</sub> H <sub>34</sub> O <sub>3</sub>
22	20.024	3.39	1-Naphthalenepropanol, $\alpha$ -ethenyldecahydro-3-hydroxy- $\alpha$ ,5,5,8a-tetramethyl-2-methylene-	306.4828	C <sub>20</sub> H <sub>34</sub> O <sub>2</sub>
23	20.274	2.86	2H-3,9a-Methano-1-benzoxepin, octahydro-2,2,5a,9-tetramethyl-, [3R-(3 $\alpha$ ,5 $\alpha$ ,9 $\alpha$ ,9 $\alpha$ )]-	222.366	C <sub>15</sub> H <sub>26</sub> O
24	20.906	0.71	2H-3,9a-Methano-1-benzoxepin, octahydro-2,2,5a,9-tetramethyl-, [3R-(3 $\alpha$ ,5 $\alpha$ ,9 $\alpha$ ,9 $\alpha$ )]-	222.366	C <sub>15</sub> H <sub>26</sub> O

The biomolecules identified in high concentration from the GC-MS analysis of *Manihot esculenta* aqueous leaf extract included glycerin (10.31%), d-mannitol (8.55%) 2-deoxy-D-galactose (3.90%), 11-(2-Cyclopentene-1-yl)undecanoic acid (4.04%), [1,1'-bicyclopropyl]-2-octanoic acid (3.99%), 9,9-dimethoxybicyclo [3.3.1]nona-2,4-dione (8.47%), 2-methoxy-4-vinylphenol (3.39%),  $\beta$ -sitosterol (12.22%) and cholest-5-en-3-ol (7.48%). These biomolecules (including phytosterols) contain  $\text{C}-\text{O}-\text{C}$ ,  $\text{C}-\text{O}-$ ,  $\text{C}=\text{C}-$ ,  $\text{C}\equiv\text{C}-$ , and  $\text{C}=\text{O}$  functions which are known to act as reducing agents in plant-based synthesis.<sup>25</sup>

Two phytochemicals – glycerin and beta-sitosterol – were present in both extracts in significant amounts and could have played dominant roles in the formation of the ZnONPs. Glycerin, in particular, has been found to play various roles in the synthesis of metal and metal oxide nanoparticles. It has been used in the hydrothermal reduction of nitrates of manganese, cobalt, copper, iron, nickel, and silver to their corresponding metals and metal oxides.<sup>26</sup> Janković et al.<sup>27</sup> synthesised ZnONPs by combining the Zn(NO<sub>3</sub>)<sub>2</sub>·6H<sub>2</sub>O starting material with glycerin without using a solvent, wherein the glycerol served as the dispersant.

The result obtained showed that the ZnONPs were well dispersed, with an average size of 2.06 nm. Furthermore, ZnONPs were prepared starting from aqueous ZnCl<sub>2</sub> solution and aqueous hydroxide solution. In this reaction, glycerin was added as a stabiliser at room temperature.<sup>28</sup> It was reported in this study<sup>28</sup> that the shape of the ZnONPs obtained depended on the concentration of the ZnCl<sub>2</sub> and the molar ratio of the glycerin to Zn<sup>2+</sup> in the mixture. The role of beta-sitosterol in extracts was also profound. Previous studies<sup>29,30</sup> have attributed the reducing and capping reactions of nanoparticles formation to phytosterols.

#### FTIR confirmation of ZnONPs formation

The FTIR spectra of the ZnONPs are presented in Figure 6. The spectrum of ZnO\_CNPs (Figure 6a) gave a broad band centred at 3415.64 cm<sup>-1</sup> considered to be the stretching vibrational mode of OH groups, with a bending mode around 1619.13 cm<sup>-1</sup> resulting from the phytochemicals involved in the capping reactions to form ZnO\_CNPs.<sup>18</sup> Other peaks attributed to the presence of the phytochemicals are those at 2929.13, 2345.59, 1619.13 and 1568.13 cm<sup>-1</sup> which are the stretching vibrational



**Table 2:** Gas chromatography–mass spectrometry results showing the phytochemicals, along with their corresponding peak areas, found in the *Manihot esculenta* aqueous leaf extract

Peak	Retention time (min)	Peak area (%)	Name of compound	Molecular weight	Molecular formula
1	6.727	0.26	2,5-Hexanediol	118	C <sub>6</sub> H <sub>14</sub> O <sub>2</sub>
2	8.149	10.31	Glycerin	92	C <sub>3</sub> H <sub>8</sub> O <sub>3</sub>
3	8.502	1.95	Methyl 2-O-benzyl-d-arabinofuranoside	254	C <sub>13</sub> H <sub>18</sub> O <sub>5</sub>
4	8.707	1.05	Methoxyacetic acid, heptyl ester	188	C <sub>10</sub> H <sub>20</sub> O <sub>3</sub>
5	9.036	1.12	Hexane, 1,1'-oxybis-	186	C <sub>12</sub> H <sub>26</sub> O
6	10.068	0.56	1,3-Dioxolane, 2,4,5-trimethyl-	116	C <sub>6</sub> H <sub>12</sub> O <sub>2</sub>
7	10.496	0.58	Oxirane, octyl-	156	C <sub>10</sub> H <sub>20</sub> O
8	10.860	0.50	Hydroquinone	110	C <sub>6</sub> H <sub>6</sub> O <sub>2</sub>
9	10.875	1.25	Hydroquinone	110	C <sub>6</sub> H <sub>6</sub> O <sub>2</sub>
10	11.092	3.49	d-Mannitol, 1,4-anhydro-	164	C <sub>6</sub> H <sub>12</sub> O <sub>5</sub>
11	11.452	1.63	cis1-Deoxy-d-mannitol-Z-alpha-Bisabolene epoxide	166	C <sub>8</sub> H <sub>14</sub> O <sub>5</sub>
12	12.122	5.06	d-Mannitol, 1,4-anhydro-	64	C <sub>6</sub> H <sub>12</sub> O <sub>5</sub>
13	12.180	3.18	1-Deoxy-d-altritol	166	C <sub>6</sub> H <sub>14</sub> O <sub>5</sub>
14	12.317	3.39	2-Methoxy-4-vinylphenol	150	C <sub>9</sub> H <sub>10</sub> O <sub>2</sub>
15	12.408	0.92	2-Methyl-9-.beta.-d-ribofuranosylhypoxanthine	282	C <sub>11</sub> H <sub>14</sub> N <sub>4</sub> O <sub>5</sub>
16	12.760	1.53	2-Deoxy-D-galactose	164	C <sub>6</sub> H <sub>12</sub> O <sub>5</sub>
17	13.564	1.12	2-Azatricyclo[4.3.1.1(4,8)]undecane	151	C <sub>10</sub> H <sub>17</sub> N
18	13.653	0.67	2,7-Dioxatricyclo[4.3.1.0(3,8)]dec-4-ene	138	C <sub>8</sub> H <sub>10</sub> O <sub>2</sub>
19	14.529	3.90	2-Deoxy-D-galactose	164	C <sub>6</sub> H <sub>12</sub> O <sub>5</sub>
20	15.198	4.04	11-(2-Cyclopenten-1-yl)undecanoic acid, (+)-	252	C <sub>16</sub> H <sub>28</sub> O <sub>2</sub>
21	15.627	4.27	9,9-Dimethoxybicyclo[3.3.1]nona-2,4-dione	212	C <sub>11</sub> H <sub>16</sub> O <sub>4</sub>
22	16.204	3.99	[1,1'-Bicyclopropyl]-2-octanoic acid, 2'-hexyl-, methyl ester	322	C <sub>21</sub> H <sub>38</sub> O <sub>2</sub>
23	16.862	1.26	cis-Z-.alpha.-Bisabolene epoxide	220	C <sub>15</sub> H <sub>24</sub> O
24	16.924	2.82	2,6,8-Trimethylbicyclo[4.2.0]oct-2-ene-1,8-diol	182	C <sub>11</sub> H <sub>18</sub> O <sub>2</sub>
25	17.085	0.94	1,2-15,16-Diepoxyhexadecane	254	C <sub>16</sub> H <sub>30</sub> O <sub>2</sub>
26	17.398	0.73	8-Tetradecyn-1-ol	210	C <sub>14</sub> H <sub>26</sub> O
27	17.474	0.26	cis-Z-.alpha.-Bisabolene epoxide	220	C <sub>15</sub> H <sub>24</sub> O
28	17.993	4.20	9,9-Dimethoxybicyclo[3.3.1]nona-2,4-dione	212	C <sub>11</sub> H <sub>16</sub> O <sub>4</sub>
29	18.060	7.48	Cholest-5-en-3-ol, 4,4-dimethyl-, (3.beta.)-	414	C <sub>29</sub> H <sub>50</sub> O
30	18.120	12.22	beta.-Sitosterol	414	C <sub>29</sub> H <sub>50</sub> O
31	18.558	1.85	cis-Z-.alpha.-Bisabolene epoxide	536	C <sub>37</sub> H <sub>76</sub> O
32	18.838	0.88	cis-Z-.alpha.-Bisabolene epoxide	220	C <sub>15</sub> H <sub>24</sub> O
33	19.269	1.08	1-Heptadec-1-ynyl-cyclopentanol	320	C <sub>22</sub> H <sub>40</sub> O
34	19.410	1.03	9,12,15-Octadecatrienoic acid, 2-[(trimethylsilyloxy)-1-[(trimethylsilyl)	496	C <sub>27</sub> H <sub>52</sub> O <sub>4</sub> Si <sub>2</sub>
35	19.532	2.52	1-Heptatriacotanol	536	C <sub>37</sub> H <sub>76</sub> O
36	19.627	3.12	Kauran-18-al, 17-(acetyloxy)-, (4.beta.)-	346	C <sub>22</sub> H <sub>34</sub> O <sub>3</sub>
37	19.877	1.70	9,10-Secocholesta-5,7,10(19)-triene-1,3-diol, 25-[(trimethylsilyl)	488	C <sub>30</sub> H <sub>52</sub> O <sub>3</sub> Si
38	20.027	2.14	1-Naphthalenepropanol, .alpha.-ethyldecahydro-5-(hydroxymethyl)-	308	C <sub>20</sub> H <sub>36</sub> O <sub>2</sub>
39	20.278	1.00	9,12,15-Octadecatrienoic acid, 2-[(trimethylsilyloxy)-1-[(trimethylsilyl)	496	C <sub>27</sub> H <sub>52</sub> O <sub>4</sub> Si <sub>2</sub>



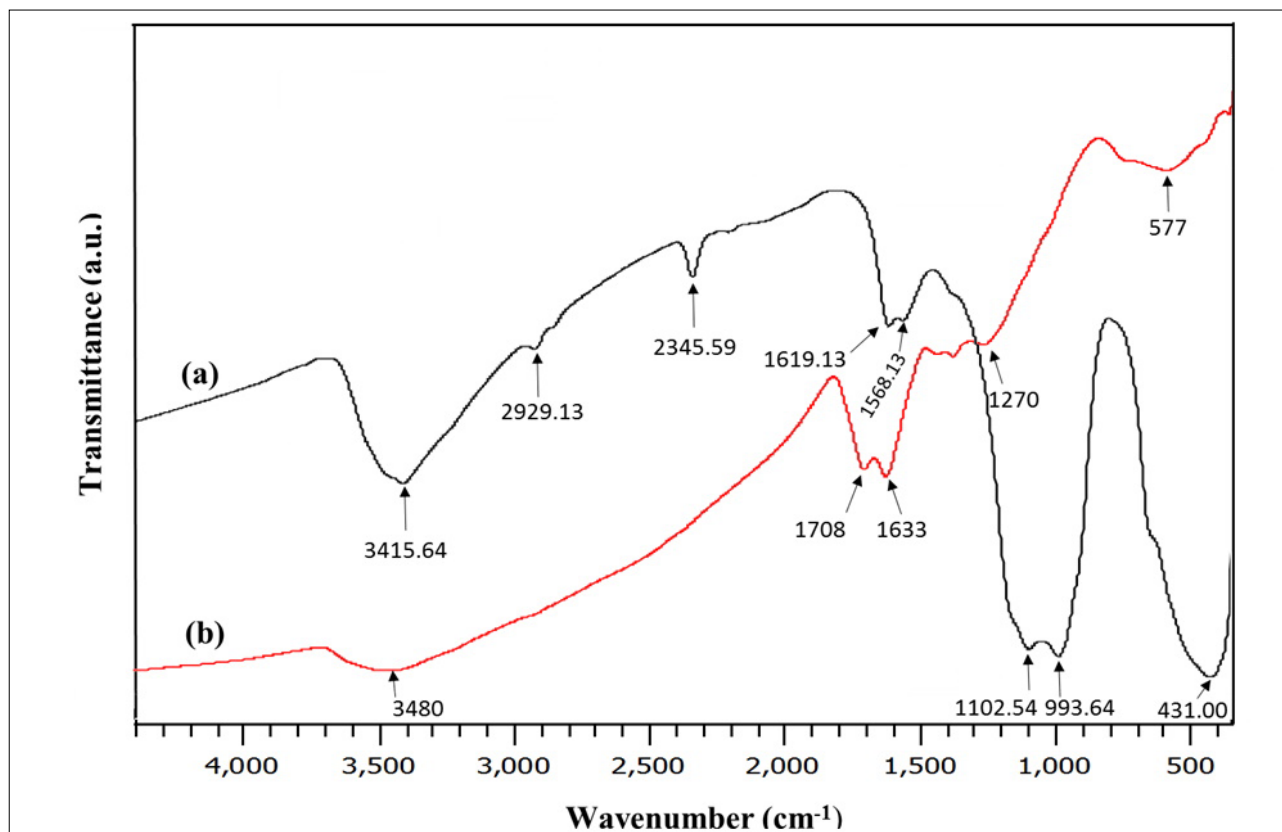


**Figure 6:** Fourier transform infrared spectra showing the vibrational modes of the bonds present in (a) ZnO\_CNPs and (b) ZnO\_MNPs.

frequencies of C–H, O–H in  $\text{SO}_3\text{H}^{31}$  and C=C in benzene, respectively. The presence of ZnONPs is observed as a broad band centred at  $577\text{ cm}^{-1}$ . The spectrum of ZnO\_MNPs showed peaks due to the presence of capping biomolecules at  $3480$ ,  $1708$ ,  $1633$ ,  $1102.54$  and  $993.64\text{ cm}^{-1}$ . The broad band centred at  $3480\text{ cm}^{-1}$  is associated with the stretching vibrations of O–H, the one at  $1708\text{ cm}^{-1}$  is considered as C=O stretch, while those at  $1102.54\text{ cm}^{-1}$  and  $993.64\text{ cm}^{-1}$  are due to the presence of C–O diagnostic stretching vibration.<sup>32</sup> The peak for the Zn–O bond in ZnO\_MNPs is observed at  $431\text{ cm}^{-1}$ .<sup>33-35</sup>

In conclusion, our results validate the biological synthesis of ZnONPs using *Chromolaena odorata* and *Manihot esculenta* aqueous leaf extracts. GC-MS analysis identified 24 phytochemicals in the aqueous extract of *Chromolaena odorata* leaf and 33 in that for *Manihot esculenta*, mostly phytosterols which, in synergy with other phytochemicals, acted as reducing, capping and stabilising agents to form the ZnONPs. The capping and stabilising roles performed by these biomolecules were confirmed by the appearance of a carbon peak in the EDX spectra of the ZnONPs and the presence of bonds related to the biomolecules when examined through FTIR. This method offers an interesting alternative approach for synthesising ZnONPs which precludes the use of harsh conditions, such as high temperature, pressure, high energy demand, and toxic chemicals usually associated with conventional techniques. Even more interesting is that, while *Chromolaena odorata* is a ravaging weed, after harvesting the tubers, the leaves of *Manihot esculenta* are discarded as waste. We also found that the properties of the ZnONPs were influenced by the type of phytochemicals inherent in the plants. Therefore, the current plants' parts, being abundant in most parts of Africa, could serve as raw materials for the large-scale synthesis of ZnONPs.

## Acknowledgements

We thank the Department of Chemical and Food Sciences at Bells University of Technology in Ota, Nigeria, for supplying materials and equipment for this study.

## Competing interests

We have no competing interests to declare.

## Authors' contributions

E.R.E.: Conceptualisation; student supervision; writing. V.N.A.: Project management; funding acquisition. D.O.N.: Project leadership; writing – initial draft. E.A.: Methodology; data collection. F.T.O.: Sample analysis; data analysis; validation.

## References

1. Laurent S, Forge D, Port M, Roch A, Robic C, Vander LE, et al. Magnetic iron oxide nanoparticles: Synthesis, stabilization, vectorization, physicochemical characterizations, and biological applications. *Chem Rev*. 2010;110(4), Art. #2574. <https://doi.org/10.1021/cr900197g>
2. Mishra PK, Mishra H, Ekielski A, Talegaonkar S, Vaidya B. Zinc oxide nanoparticles: A promising nanomaterial for biomedical applications. *Drug Discov Today*. 2017;22:1825–1834. <https://doi.org/10.1016/j.drudis.2017.08.006>
3. Navalón S, García H. Nanoparticles for catalysis. *Nanomaterials*. 2016;6, Art. #123. <https://doi.org/10.3390/nano6070123>
4. Sruthi S, Millot N, Mohanan PV. Zinc oxide nanoparticles mediated cytotoxicity, mitochondrial membrane potential and level of antioxidants in presence of melatonin. *Int J Biol Macromol*. 2017;103:808–818. <https://doi.org/10.1016/j.ijbiomac.2017.05.088>
5. Hanley C, Layne J, Punnoose A, Reddy KM, Coombs I, Coombs A, et al. Preferential killing of cancer cells and activated human T cells using ZnO nanoparticles. *Nanotechnology*. 2008;19, Art. #295103. <https://doi.org/10.1088/0957-4484/19/29/295103>
6. Sahdev P, Podaralla S, Kaushik RS, Perumal O. Calcium phosphate nanoparticles for transcutaneous vaccine delivery. *J Biomed Nanotechnol*. 2013;9:132–141. <https://doi.org/10.1166/jbn.2013.1545>
7. Sabir S, Arshad M, Chaudhari SK. Zinc oxide nanoparticles for revolutionizing agriculture: Synthesis and applications. *Sci World J*. 2014;2014, Art. #925494. <https://doi.org/10.1155/2014/925494>



8. Yadav A, Prasad V, Kathe AA, Raj S, Yadav D, Sundaramoorthy C, et al. Functional finishing in cotton fabrics using zinc oxide nanoparticles. *Bull Mater Sci*. 2006;29:641–645. <https://doi.org/10.1007/s12034-006-0017-y>
9. Wang ZJ, Zhang HM, Zhang LG, Yuan JS, Yan SG, Wang CY. Low-temperature synthesis of ZnO nanoparticles by solid-state pyrolytic reaction. *Nanotechnology*. 2003;14:11–15. <https://doi.org/10.1088/0957-4484/14/1/303>
10. Spanhel L, Anderson MA. Semiconductor clusters in the sol-gel process: Quantized aggregation, gelation, and crystal growth in concentrated zinc oxide colloids. *J Am Chem Soc*. 1991;113:2826–2833. <https://doi.org/10.1021/ja00008a004>
11. Meulenkamp EA. Synthesis and growth of ZnO nanoparticles. *J Phys Chem B*. 1998;102:5566–5572. <https://doi.org/10.1021/jp980730h>
12. Gunalan S, Sivaraj R, Rajendran V. Green synthesized ZnO nanoparticles against bacterial and fungal pathogens. *Prog Natl Sci Mater Int J*. 2012;22:693–700. <https://doi.org/10.1016/j.pnsc.2012.11.015>
13. Rajakumar G, Thiruvengadam M, Mydhili G, Gomathi T, Chung III M. Green approach for synthesis of zinc oxide nanoparticles from *Andrographis paniculata* leaf extract and evaluation of their antioxidant, anti-diabetic, and anti-inflammatory activities. *Bioprocess Biosyst Eng*. 2018;41:21–30. <https://doi.org/10.1007/s00449-017-1840-9>
14. Nagajyothi PC, Cha SJ, Yang IJ, Sreekanth TVM, Kim KJ, Shin HM. Antioxidant and anti-inflammatory activities of zinc oxide nanoparticles synthesized using *Polygala tenuifolia* root extract. *J Photochem Photobiol B Biol*. 2015;146:10–17. <https://doi.org/10.1016/j.jphotobiol.2015.02.008>
15. Sharma D, Sabelaa MI, Kanchi S, Mdlulia PS, Singh G, Stenström TA, et al. Biosynthesis of ZnO nanoparticles using *Jacaranda mimosifolia* flowers extract: Synergistic antibacterial activity and molecular simulated facet specific adsorption studies. *J Photochem Photobiol B*. 2016;162:199–207. <https://doi.org/10.1016/j.jphotobiol.2016.06.043>
16. Iwu MM, Duncan AR, Okunji CO. New antimicrobials of plant origin. In: Janick J, editor. *Perspectives on new crops and new uses*. Alexandria, VA: ASHS Press; 1999. p. 457–462.
17. Rahalison L, Gupta MP, Santana AI. Screening for antifungal activity of Panamanian plants. *J Pharmacol*. 1993;31:68–76. <https://doi.org/10.3109/13880209309082921>
18. Ali K, Dwivedi S, Azam A, Saquib Q, Al-Said MS, Alkhedhairy AA, et al. Aloe vera extract functionalized zinc oxide nanoparticles as nanoantibiotics against multi-drug resistant clinical bacterial isolates. *J Colloid Interface Sci*. 2016;472:145–156. <https://doi.org/10.1016/j.jcis.2016.03.021>
19. Nagarajan S, Kuppusamy KA. Extracellular synthesis of zinc oxide nanoparticles using seaweeds of gulf of Mannar, India. *J Nanobiotechnol*. 2013;11, Art. #39. <https://doi.org/10.1186/1477-3155-11-39>
20. Sangeetha G, Rajeshwari S, Venckatesh R. Green synthesis of zinc oxide nanoparticles by *Aloe barbadensis* Miller leaf extract: Structure and optical properties. *Mater Res Bull*. 2011;46:2560–2566. <https://doi.org/10.1016/j.materresbull.2011.07.046>
21. Bhuyan T, Mishra K, Khanuja M, Prasad R, Varma A. Biosynthesis of zinc oxide nanoparticles from *Azadirachta indica* for antibacterial and photocatalytic applications. *Mater Sci Semicond Process*. 2015;32:55–61. <https://doi.org/10.1016/j.mssp.2014.12.053>
22. Qian YG, Yao J, Russel M, Chen K, Wang XY. Characterization of green synthesized nano-formulation (ZnO-A. Vera) and their antibacterial activity against pathogens. *Environ Toxicol Pharmacol*. 2015;39:736–746. <https://doi.org/10.1016/j.etap.2015.01.015>
23. Salam HA, Sivaraj R, Venckatesh R. Green synthesis and characterization of zinc oxide nanoparticles from *Ocimum basilicum* L. var. *purpurascens* Benth.-Lamiaceae leaf extract. *Mater Lett*. 2014;131:16–18. <https://doi.org/10.1016/j.matlet.2014.05.033>
24. Liu HL, Dai SA, Fu KY, Hsu SH. Antibacterial properties of silver nanoparticles in three different sizes and their nanocomposites with a new waterborne polyurethane. *Int J Nanomed*. 2010;5:1017–1028. <https://doi.org/10.2147/IJN.S14572>
25. Huang J, Chen C, He N, Hong J, Lu Y, Qingbiao L, et al. Biosynthesis of silver and gold nanoparticles by novel sundried *Cinnamomum camphora* leaf. *Nanotechnol*. 2007;18:105–106. <https://doi.org/10.1088/0957-4484/18/10/105104>
26. Kim M, Son W-S, Ahn KH, Kim DS, Lee H, Lee Y-W. Hydrothermal synthesis of metal nanoparticles using glycerol as a reducing agent. *J Supercrit Fluids*. 2014;90:53–59. <https://doi.org/10.1016/j.supflu.2014.02.022>
27. Janković S, Milisavić D, Okolić T, Jelić D. Preparation and characterization of ZnO nanoparticles by solvent free method. *Contemp Mater*. 2018;IX:1:48–52. <https://doi.org/10.7251/COMEN1801048J>
28. Wang Z, Li H, Tang F, Ma J, Zhou X. A facile approach for the preparation of nano-size zinc oxide in water/glycerol with extremely concentrated zinc sources. *Nanoscale Res Lett*. 2018;13:1–9. <https://doi.org/10.1186/s11671-018-2616-0>
29. Cu TS, Cao VD, Nguyen CK, Tran NQ. Preparation of silver core-chitosan shell nanoparticles using catechol-functionalized chitosan and antibacterial studies. *Macromol Res*. 2014;22:418–423. <https://doi.org/10.1007/s13233-014-2054-5>
30. Doan P, Cao VD, Nguyen DH, Tran NQ. Metallic nanoparticles: Potential ecofungicide for controlling growth of plant-pathogenic fungi. *J Chem Soc Pak*. 2018;40:664–675. [https://inis.iaea.org/search/search.aspx?orig\\_q=RN:49089054](https://inis.iaea.org/search/search.aspx?orig_q=RN:49089054)
31. Vijayalekshmi V, Khastgir D. Eco-friendly methanesulfonic acid and sodium salt of dodecylbenzene sulfonic acid doped cross-linked chitosan based green polymer electrolyte membranes for fuel cell applications. *J Membrane Sci*. 2016;523:45–59. <https://doi.org/10.1016/j.memsci.2016.09.058>
32. Somanathan T, Krishna VM, Saravanan V, Kumar R, Kumar R. MgO nanoparticles for effective uptake and release of doxorubicin drug: pH sensitive controlled drug release. *J Nanosci Nanotechnol*. 2016;16:9421–9431. <https://doi.org/10.1166/jnn.2016.12164>
33. Kwon YJ, Kim KH, Lim CS, Shim KB. Characterization of ZnO nanopowders synthesized by the polymerized complex method via an organo chemical route. *J Ceram Proc Res*. 2002;3:146–149.
34. Silva RF, Zaniquelli MED. Morphology of nanometric size particulate aluminium doped zinc oxide films. *Colloids Surf A Physicochem Eng Asp*. 2002;198:551–558. [https://doi.org/10.1016/S0927-7757\(01\)00959-1](https://doi.org/10.1016/S0927-7757(01)00959-1)
35. Li H, Wang J, Liu H, Yang C, Xu H, Li X, et al. Sol-gel preparation of transparent zinc oxide films with highly preferential crystal orientation. *Vacuum*. 2004;77:57–62. <https://doi.org/10.1016/j.vacuum.2004.08.003>



Check for updates

**AUTHORS:**

Ahmed Y. El Gamal<sup>1</sup>   
Mahmoud M. Atia<sup>2</sup>  
Tarek El Sayed<sup>1</sup>  
Mohamed I. Abou-Zaid<sup>2</sup>   
Mohamed R. Tohamy<sup>2</sup>

**AFFILIATIONS:**

<sup>1</sup>Virus and Phytoplasma Research Department, Plant Pathology Research Institute, Agricultural Research Center, Giza, Egypt  
<sup>2</sup>Plant Pathology Department, Zagazig University, Zagazig, Egypt

**CORRESPONDENCE TO:**

Ahmed El Gamal

**EMAIL:**

ahmedvnp1@yahoo.com

**DATES:**

**Received:** 09 Apr. 2021

**Revised:** 21 July 2021

**Accepted:** 28 July 2021

**Published:** 27 Jan. 2022

**HOW TO CITE:**

El Gamal AY, Atia MM, El Sayed T, Abou-Zaid MI, Tohamy MR. Antiviral activity of chitosan nanoparticles for controlling plant-infecting viruses. *S Afr J Sci.* 2022;118(1/2), Art. #10693. <https://doi.org/10.17159/sajs.2022/10693>

**ARTICLE INCLUDES:**

- Peer review
- Supplementary material

**DATA AVAILABILITY:**

- Open data set
- All data included
- On request from author(s)
- Not available
- Not applicable

**EDITOR:**

Teresa Coutinho

**KEYWORDS:**

chitosan nanoparticles, *Bean yellow mosaic virus* (BYMV), antiviral, faba bean, PR-1 gene regulation

**FUNDING:**

None

# Antiviral activity of chitosan nanoparticles for controlling plant-infecting viruses

Chitosan nanoparticles (ChiNPs) are a potentially effective means for controlling numerous plant diseases. This study firstly describes the antiviral capabilities of ChiNPs to control plant viral diseases compared to its bulk form. *Bean yellow mosaic virus* (BYMV) was used as a model plant virus affecting faba bean plants and many other legumes. The antiviral effectiveness of ChiNPs and chitosan were evaluated as a curative application method, using six dosage rates (50, 100, 200, 250, 300 and 400 mg/L). Results indicated that ChiNPs curatively applied 48 h post virus inoculation entirely inhibit the disease infectivity and viral accumulation content at 300 mg/L and 400 mg/L. The virus titre was greatly alleviated within the plant tissues by 7.71% up to 100% depending on ChiNP dosage rates. However, chitosan used in its bulk-based material form revealed a relatively low to an intermediate reduction in virus infectivity by 6.67% up to 48.86%. Interestingly, ChiNPs affect the virus particle's integrity by producing defective and incomplete BYMV viral particles, defeating their replication and accumulation content within the plant tissues. Simultaneously, ChiNP applications were appreciably shown to promote the pathogenesis-related (PR-1) gene and other defence-related factors. The mRNA of the PR-1 gene was markedly accumulated in treated plants, reaching its maximum at 400 mg/L with 16.22-fold relative expression change over the untreated control. Further, the total phenol dynamic curve was remarkably promoted for 30 days in response to ChiNP application, as compared to the untreated control. Our results provide the first report that chitosan-based nanomaterials have a superior effect in controlling plant viruses as an antiviral curing agent, suggesting that they may feasibly be involved in viral disease management strategies under field conditions without serious health concerns and environmental costs.

**Significance:**

- Our findings show that chitosan nanoparticles have a powerful curing antiviral activity against BYMV disease. These findings open the door for the use of eco-friendly nano-based tools in controlling numerous plant viruses. The use of eco-friendly nano-based materials could result in a successful integrative control strategy for plant viruses under field conditions, negating the need for the conventional measure used to control most of the insect-transmitted plant viruses, that is insecticide application against vector insects.

## Introduction

Plant viruses are destructive diseases that cause serious concerns for the agroecosystem and global food security due to their ability to infect many plant species that are grown for both food and feed production.<sup>1</sup> Faba bean (*Vicia faba* L.) is a legume crop cultivated mainly for its edible seeds. Due to their high protein content, faba beans are widely used as a cheap and high-quality protein source for poor consumers in many developing countries.<sup>2</sup> *Bean yellow mosaic virus* (BYMV) belongs to the *Potyvirus* genus (Family: *Potyviridae*) and is a devastating viral disease for many crop legumes and ornamental plants throughout the world.<sup>3</sup> BYMV disease poses a significant threat for faba bean production, with losses of 30–50%.<sup>4</sup> However, under severe epidemic conditions, the disease can cause a total crop failure.<sup>5</sup> The virus is naturally transmitted by over 20 species of aphids, resulting in a high rate of viral infections for faba bean and other host species.<sup>6</sup> BYMV and most plant viruses are conventionally managed by pesticide applications against insect vectors.<sup>7</sup> However, from a sustainability point of view, the extensive use of pesticides tremendously affects the environment and the whole ecosystem. According to the World Health Organization, thousands of agricultural workers in developing countries die each year from severe poisoning by pesticides.<sup>8</sup> Therefore, new strategic technologies are urgently needed to avoid pesticide treadmills.

Nanotechnology-based tools have provided great hope for scientific revolutions in the near-future in many applications.<sup>9</sup> The engineered nanoparticles have superior chemical and physical features compared to their bulk materials, allowing them to be used in many different sectors.<sup>10</sup> Chitosan (poly (1,4)-2-amino-2-deoxy-β-D glucose) is a glucosamine polymer obtained by alkaline deacetylation of chitin extracted from the exoskeleton of crustaceans.<sup>11</sup> From an ecological point of view, chitosan has received considerable interest due to its potential wide applications in plant protection and growth promotion because of its excellent biodegradability, non-toxicity and bioactivity.<sup>12,13</sup> Moreover, chitosan has unique antimicrobial properties and it can additionally be used as an elicitor molecule against different plant pathogens and viral infections when used preventatively before inoculation.<sup>14-17</sup> In limited previous studies, the partial antiviral potential of chitosan bulk material in controlling some plant viruses has been investigated for use of chitosan as a protective agent involved in the stimulation of plant defence systems against virus invasion.<sup>18,19</sup>

In addition to the capability of the chitosan polymer for use preventatively as a plant defence enhancer against pathogen attacks, it has since been found that this capability is further enhanced by using it in the form of nanoparticles.<sup>20</sup> This study was performed to evaluate the antiviral capability of the nanoparticle-based form of chitosan against plant virus infectivity in comparison with that of the chitosan bulk polymer. We also investigated

© 2022. The Author(s). Published under a Creative Commons Attribution Licence.

their effects on some defence-related parameters involved in plant immunity mechanisms when curatively applied after a viral challenge in faba bean plants.

## Materials and methods

### Virus isolation and propagation

Faba bean plant samples with *Bean yellow mosaic virus*-like symptoms were collected from local faba bean fields in the Giza governorate, Egypt, during the 2017/2018 growing season. Leaf samples were initially tested using the double antibody sandwich enzyme-linked immunosorbent assay (DAS-ELISA) technique as described by Clark and Adams<sup>21</sup> using specific polyclonal antibodies against BYMV (EPHYRA Bioscience Inc., Ontario, Canada). The reactions were assessed at 405 nm in a microplate reader (Bio-Tek, USA). Samples that tested positive against BYMV were used as sources of virus inoculum. The virus was isolated through single local lesion inoculations on *Chenopodium amaranticolor* indicator plants.<sup>22</sup> Ten-day-old plants were mechanically inoculated with the BYMV crude sap using 0.01 M phosphate buffer pH 7.1, (1:10), 0.01% Na<sub>2</sub>SO<sub>3</sub> and carborundum (600 mesh) and kept under insect-proof greenhouse conditions until symptoms developed. The isolated source was propagated on 10-day-old faba bean plants (cv. Giza 843) and was used as inoculum for further studies.

### Molecular identification of the isolated virus

Total RNA was isolated from both healthy and symptomatic faba bean leaves using RNeasy Plant Mini Kit (Qiagen, Germany) according to the manufacturer's instructions. Reverse transcription (RT)-PCR reaction was optimised using the One-Step RT-PCR system (Thermo Fisher, USA). A specific primer pair, BYMV-CPU (5' GTCGATTCAATCCGAACAAG 3') and BYMV-CPD (5' GGAGGTGAAACCTCAATAAC 3'), was used to target the CP gene region to amplify a 907-bp fragment of the BYMV genome.<sup>23</sup> The one-step RT-PCR reaction was performed by combining 25  $\mu$ L One-Step PCR Master Mix, 1  $\mu$ L of each primer pair (200 nM), 2.5  $\mu$ L of RT-enzyme enhancer, 1  $\mu$ L verso enzyme mix, and 3 ng of RNA template, and the mixture was made up to 50  $\mu$ L using nuclease-free water. The amplification reaction was automated in a T-Gradient thermal cycler (Biometra, Germany) with an initial reverse transcription process at 50 °C for 15 min, followed by 35 cycles of denaturation at 94 °C for 1 min, annealing at 50 °C for 1 min and extension at 72 °C for 2 min, with a final additional extension step for 10 min at 72 °C. The PCR products were electrophoresed on 1% agarose gel in 0.5 x TAE buffer, then visualised with a Gel Doc system (2000, Bio-Rad, USA).

### Preparation of chitosan nanoparticles

A chitosan nanoparticle solution was chemically prepared by reduction of low molecular weight chitosan (Sigma, Egypt) based on the ion-gelation method using sodium tripolyphosphate as a reducing agent.<sup>24</sup> Chitosan powder (0.5 mg/mL) was dissolved in 1% acetic acid in deionised distilled water and left under vigorous stirring for 30 min. Sodium tripolyphosphate was dissolved separately in deionised distilled water (0.7 mg/mL). Chitosan nanoparticles were formed by mixing 500 mL of chitosan with increasing amounts of sodium tripolyphosphate solution (160 mL) under continuous stirring for 1 h. The synthesised chitosan nanoparticles (ChiNPs) were subjected to further physicochemical characterisation.

### Physicochemical characterisation of ChiNPs

#### Dynamic light scattering analysis

The particle size distribution and zeta potential of constructed ChiNPs were assessed using a Zetasizer (Malvern, ZS Nano, UK). The colloidal chitosan nanoparticle solution was diluted with distilled water and put into a disposable cuvette for analysis.

#### X-ray diffraction

The physicochemical crystalline nature of ChiNPs was confirmed using an X-ray diffractometer (X'pert PRO, PAN analytical, Netherlands) operated with a CuK radiation tube (= 1.54 Å) at 40 kV. The ChiNP solution was centrifuged at 20 000 x g for 30 min at 4 °C for powder

phase yield, the precipitated ChiNPs were dried, then bombarded by X-ray for phase analysis.<sup>25</sup>

### Surface morphology

Particle size and the actual shape of ChiNPs were determined by high-resolution transmission electron microscope (Tecnai G2, FEI, Netherlands) under an accelerating voltage of 200 kV.

### Effect of ChiNPs on virus infectivity

#### Treatments

Foliar applications were carried out under an insect-proof greenhouse using six concentrations of chitosan and ChiNPs (50, 100, 200, 250, 300 and 400 mg/L). Ten-day-old faba bean plants (five plants/pot) were mechanically inoculated with BYMV- infected plant sap. The inoculated plants were uniformly sprayed until runoff with all tested dosage rates (48 h post-viral challenge). Water-treated plants served as a comparable control. Each experimental group had four replicates.

#### Disease assessment

Virus infectivity was determined 3 weeks post-inoculation on all treated and untreated faba bean plants using the assessment of disease incidence and severity response. Disease severity and symptom response were also assessed using a numerical scale of grades 0–4, where 0=no visible symptom apparent; 1=mild chlorotic patterns; 2=mosaic patterns and dark green vein banding; 3=mosaic patterns, leaf distortion, and reduction in leaf size; 4=severe mosaic and stunting of the whole plant. Values of disease severity were estimated by the following formula<sup>26</sup>:

$$\text{Viral disease severity (\%)} = \frac{\sum \text{disease grade} \times \text{number of plants in each grade}}{\text{total number of plants} \times \text{highest disease grade}} \times 100 \quad \text{Equation 1}$$

The inhibition index in virus infectivity was calculated using the following formula:

$$\text{Reduction index in virus infectivity (\%)} = \frac{C-T}{C} \times 100 \quad \text{Equation 2}$$

where C is the mean average of virus incidence values in untreated control plants; and T is the average value in each treatment.

### Transmission electron microscope

For electron microscopic examination of virus particles, the leaf-dip preparation method was performed on the faba bean plants treated with 400 mg/L of ChiNPs and untreated controls 5 days post-treatment. Briefly, the leaf samples of both treated and untreated plants were washed, a small disc was prepared (1.5 cm in diameter) and resuspended in deionised water to remove any surface-ChiNPs attached to the leaf samples. The samples were ground in a drop of phosphate buffer pH 7.5 and 0.01% Na<sub>2</sub>SO<sub>3</sub>. Leaf extracts (10  $\mu$ L) were individually loaded on carbon-coated grids for 5 min, washed with distilled water and negatively stained with 2% uranyl acetate.<sup>27</sup> The grids were examined using a JEOL JEM1400 transmission electron microscope (JEOL Co., Tokyo, Japan).

### Determination of virus accumulation content

Newly emerged small leaves were collected 30 days post-inoculation to detect the BYMV accumulation and to further confirm the virus replication inhibition rate using the DAS-ELISA method.<sup>21</sup> The virus titre reactions were quantified at 405 nm in a microplate reader (BioTek, USA). Samples were considered positive when optical density (OD)-405 values were two times higher than the mean of the healthy control. The reduction percentage in virus accumulation was measured as follows:

$$\text{Inhibition index in virus accumulation content (\%)} = \frac{V_{t,A} - V_{t,B}}{V_{t,A}} \times 100 \quad \text{Equation 3}$$



where  $Vt.A$  is the mean average of virus titre OD values in positive untreated control plants and  $Vt.B$  is the average virus titre OD value in each ChiNP treatment.

### Enzyme activity assays

Fresh leaves (0.2 g) from all treated and untreated plants were collected at 0, 24, 48, 72, 96, 120, and 144 h post-ChiNP spraying. The polyphenol oxidase antioxidant enzyme activity was determined using the methods described by Kar and Mishra.<sup>28</sup> Change in activity was expressed as nmol of guaiacol per mg protein per min. Phenylalanine ammonia lyase activity was measured according to Lisker et al.<sup>29</sup> Values are expressed as nmol of cinnamic acid/gfw/s. All experiments were performed in triplicate.

### Pathogenesis-related (PR-1) gene expression analysis

#### Total RNA isolation

Leaf samples from ChiNP-treated and untreated control plants were collected 48 h post-treatment for total RNA isolation. The total RNA was extracted using the RNeasy Plant Mini Kit (Qiagen) protocol.

#### cDNA synthesis

The harvested RNA (2  $\mu$ g) was primed with Oligo (dT) and converted into the first-strand cDNA using COSMO cDNA synthesis kit (Willowfort, UK) according to the manufacturer's protocol. The cDNA synthesis reaction was performed in a T-Gradient thermal cycler with initial annealing at 25 °C for 10 min, followed by an extension phase at 45 °C for 15 min.

#### Primers used

Gene-specific primers encoding pathogenesis-related protein 1 (PR-1 forward 5'-GGGCAGTGGTGACATAACAGGAA-3') upstream and (PR-1 reverse 5'-CATCCAACCCGAACCGAAT-3') downstream were designed.<sup>30</sup> A specific primer pair of the elongation factor 1-alpha gene *ELF1A*/forward (5'-GTGAAGCCCGTATGCTTGT-3') and *ELF1A*/reverse (5'-CTTGAGATCCTTGACTGCAA CATT-3') was used as an endogenous reference gene.

#### qRT-PCR analysis

The HERA SYBR Green qPCR kit (Willowfort, UK) was used for qRT-PCR analysis with a 20- $\mu$ L reaction mixture consisting of 10  $\mu$ L SYBR green master mix, nuclease-free water (7.2  $\mu$ L), diluted cDNA template (2  $\mu$ L) and 0.5  $\mu$ L of each primer pair. The qRT-PCR programme was as follows: 95 °C for 2 min, followed by 40 cycles at 95 °C for 1 min and 60 °C for 30 s. The reaction was normalised with melting curve analysis at 65 °C for 10 s for 61 cycles. The changes in gene expression were calculated based on the internal reference gene using the  $2^{-\Delta\Delta Ct}$  method.<sup>31</sup> Each experiment was conducted in triplicate.

### Determination of total phenolic content

The total polyphenol dynamic curve was determined following the Folin–Ciocalteu's reagent according to the methods described by Lin and Tang<sup>32</sup> with slight modifications. Briefly, the collected leaf samples (0.5 g) were vigorously homogenised in 10 mL absolute ethanol. The leaf extract solution (100  $\mu$ L) was transferred in a test tube containing 4 mL distilled water and 1 mL of Folin–Ciocalteu's reagent. After 5 min, 1 mL of sodium bicarbonate (10%) and 1 mL of ethanolamine were added to the mixture. The tubes were shaken and left for 1 h in the dark at room temperature. The samples were electro-optically measured at 740 nm. A standard calibration curve for total phenol was established using gallic acid (0–200 ppm). The results were expressed as mg of gallic acid equivalents/gram fresh weight (gfw).

### Effects on plant growth and vegetation parameters

Vegetation and growth parameters (i.e. leaf area, shoot length and chlorophyll content) of treated and untreated faba bean plants were determined at the end of the experiment. Leaf area was estimated following the estimation model proposed by Chahit<sup>33</sup>. For each tested concentration, 20 leaflets of all treated plants were measured. The maximum length of the leaflet was excised from petiole to the tip along

the mid-vein, while the width was obtained by measuring the area between two leaflet margins perpendicular to the mid-vein. The leaf area was estimated by:

$$LA \text{ (cm}^2\text{)} = -1.6923 + (L \times 0.0161) + (W \times 0.0929) + (0.062 \times L \times W)$$

where LA is leaf area in  $\text{cm}^2$ , L is leaflet length (cm), and W is the leaflet width (cm).

Changes in chlorophyll content were automatically assessed using a portable chlorophyll meter (SPAD-502 Plus, Minolta UK) and the obtained results were expressed as a chlorophyll content index. Leaflets from all treated and untreated plants were assessed and chlorophyll index values were obtained for all tested concentrations. Finally, shoot length (in cm) was also measured for all treated and untreated plants from the soil line to the top of the plant using a one-metre tape measure.

### Statistical analysis

Data were statistically analysed using a completely randomised design for analysis of variance (ANOVA). Statistical analysis of the data was performed with the Assisat-Statistics Software (version 7.7 beta).<sup>34</sup> The significant differences in each treatment group were determined at  $p = 0.05$ . Each experiment was performed in triplicate.

## Results

### Virus isolation and characterisation

The biologically isolated source produced mosaic symptoms typical of BYMV disease and similar to those observed in the field (Figure 1a). BYMV isolate was confirmed by DAS-ELISA in mechanically inoculated plants and all tested samples were positive for BYMV. The virus titre was 1.113 OD in faba bean, compared with 0.230 OD for negative control plants. All tested samples failed to react with antiserum specific for other viruses affecting faba bean plants. The RT-PCR products for the CP gene of BYMV were confirmed with 1% agarose gel electrophoresis. Two clear bands of 907 bp, the expected amplicon size, were produced from BYMV-infected samples. However, no PCR products were achieved from healthy faba bean plants used as a negative control (Figure 1b).

### Characterisation of ChiNPs

The synthesised ChiNPs showed an average hydrodynamic size distribution of 37.84 nm (ranging between 20.68 nm and 60.74 nm) with a polydispersity index of 0.423 (Figure 2a). The zeta potential of ChiNPs indicates a positive surface area charge of 25.4 mV (Figure 2b). The amorphous fingerprint nature of ChiNPs is represented on the X-ray diffraction system by the formation of a hump shape from 10 to 30  $2\theta$  angle (Figure 3a). The transmission electron micrograph illustrates

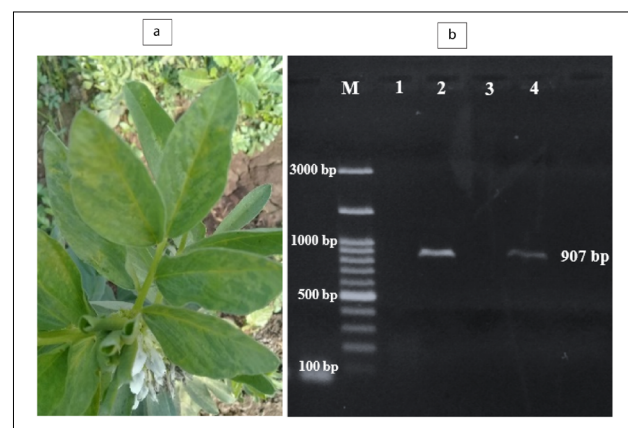


**Figure 1:** (a) *Bean yellow mosaic virus* (BYMV) phenotypic symptoms. (b) Gel electrophoresis image of the RT-PCR test conducted to identify BYMV: Lanes 1 & 3: healthy plant controls; Lanes 2 & 4: BYMV-infected faba bean plants; Lane M: 100-bp DNA ladder.

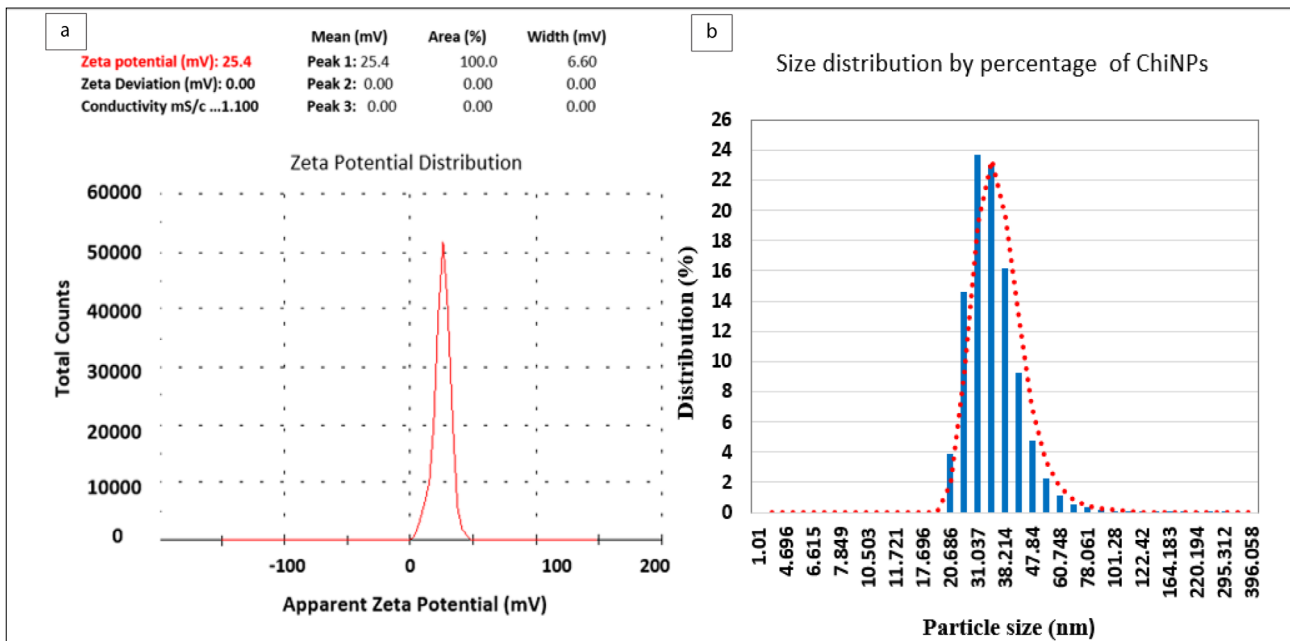


**Figure 2:** Physicochemical characterisation of synthesised chitosan nanoparticles (ChiNPs). (a) Zeta potential measurement showing a positive surface charge with 25.4 mV. (b) Particle size distribution histogram with an average size of 37.84 nm.

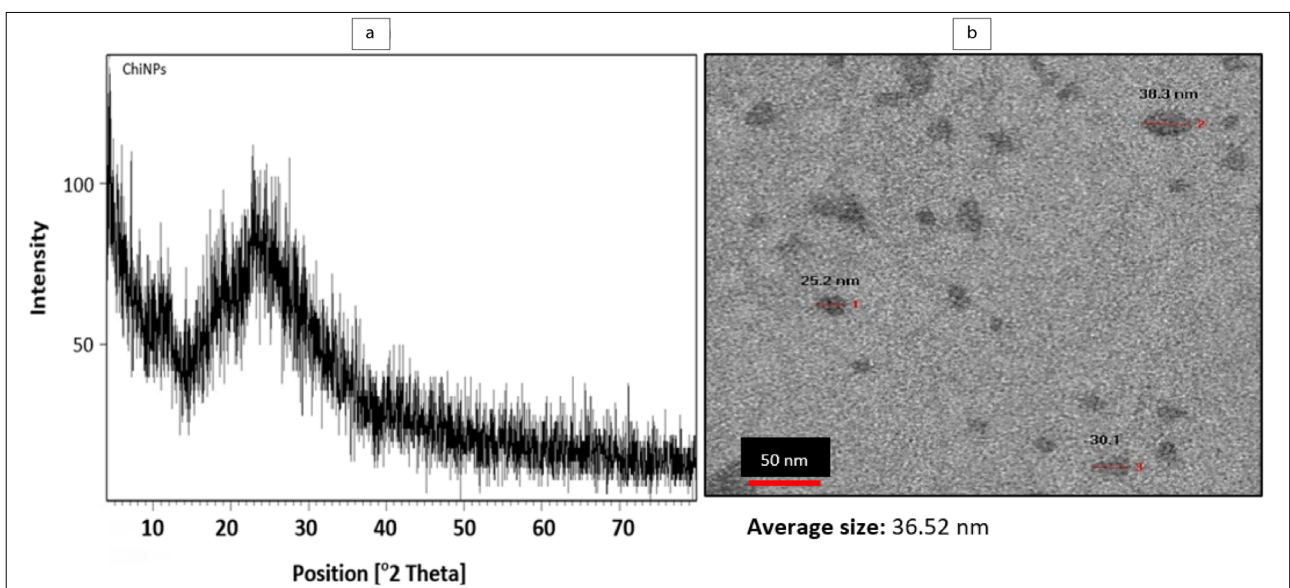


**Figure 3:** (a) X-ray diffraction pattern displaying amorphism nature of chitosan nanoparticles with the formation of a hump shape from 10 to 30  $2\theta$  angle. (b) Transmission electron micrograph illustrating the pseudospherical to spherical shape of chitosan nanoparticles (ChiNPs) with an average size of 36.52 nm.

a pseudospherical shape for the synthesised ChiNPs and the average particle size was estimated to be about 36.52 nm (Figure 3b).

### Virucidal activity of ChiNPs on BYMV infectivity

ChiNPs suppressed BYMV replication on faba bean plants when compared to the bulk chitosan polymer form (Figure 4a,c). Untreated control plants infected with BYMV showed severe mosaic and stunting symptoms. Interestingly, symptoms were not observed with plants treated with 300 mg/L and 400 mg/L ChiNPs, with a complete reduction of the disease response 48 h post virus inoculation. Faba bean plants treated with 100, 200 and 250 mg/L ChiNPs revealed different levels of protection against BYMV occurrence of 47.67%, 43.34% and 75.40%, respectively. However, a low to moderate reduction in virus infectivity was obtained in bulk chitosan-treated plants – 21.11% and 48.86%, respectively – compared with the untreated control plants (Figure 4b,d).

In this respect, transmission electron micrographs illustrate that ChiNP applications resulted in defective and incomplete particles compared to the untreated control (Figure 5). The viral particles obtained from the ChiNP-treated plants were clearly found to be lower than 300 nm in length (Figure 5b,c,d). Contrastingly, the normal well-developed virus particles in untreated control plants were estimated to be 715–730 nm in length (Figure 5a).

### Effect of ChiNPs on virus accumulation content

ChiNPs appreciably decreased virus accumulation in treated faba bean plants to varying levels depending on the ChiNP dosage rate. All tested concentrations of ChiNPs, except for 50 mg/L and 100 mg/L, significantly reduced virus accumulation in the treated plants when applied 48 h post-inoculation (Table 1). The highest activity was obtained when the plants were sprayed with 300 mg/L and 400 mg/L in which a negative ELISA

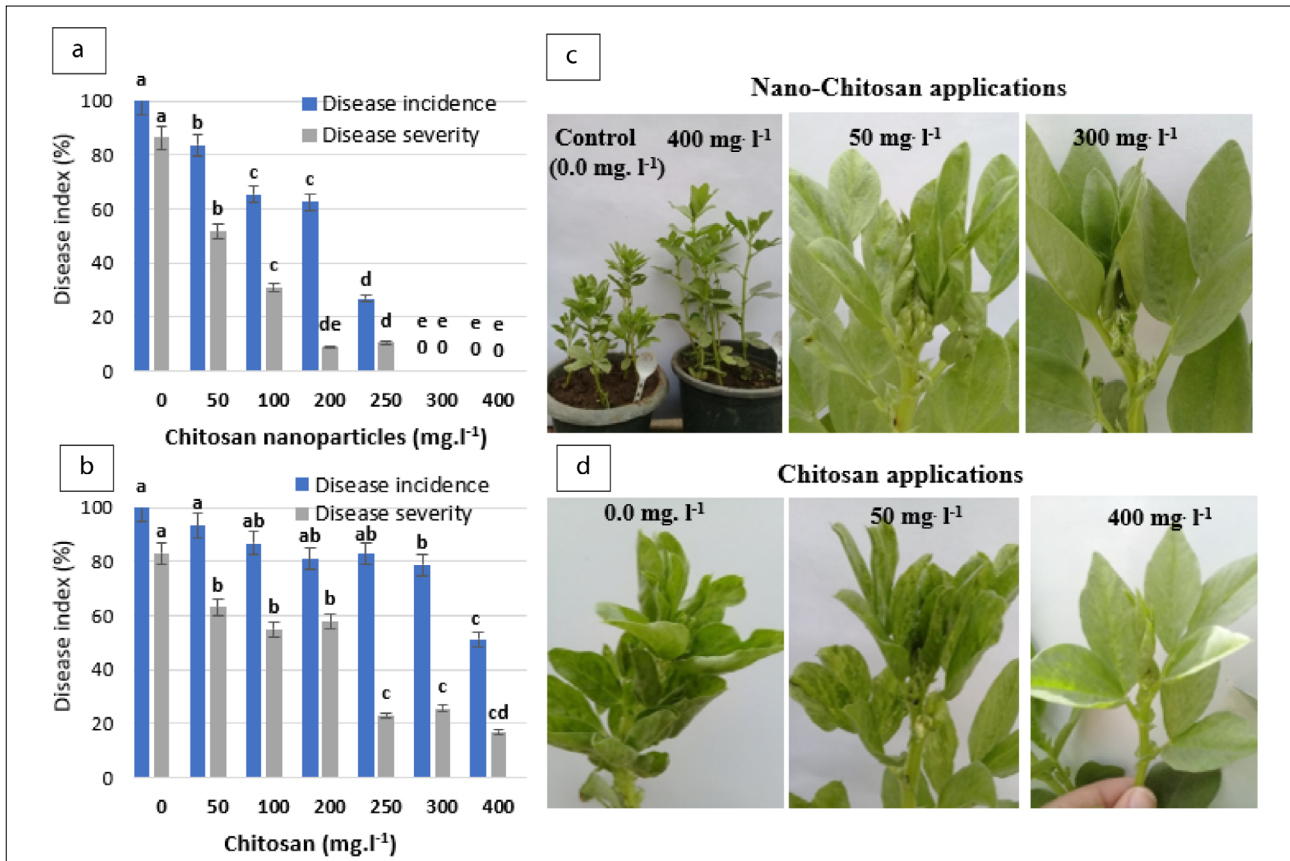


**Figure 4:** Virucidal activity of (a) chitosan nanoparticles compared to (b) chitosan bulk polymers against *Bean yellow mosaic virus* disease infectivity on faba bean plants treated with six concentrations compared to untreated control. Disease response scored on foliar treated plants compared to untreated control (c & d). Values with the same letters for each experiment are not significantly different ( $p \leq 0.05$ ).

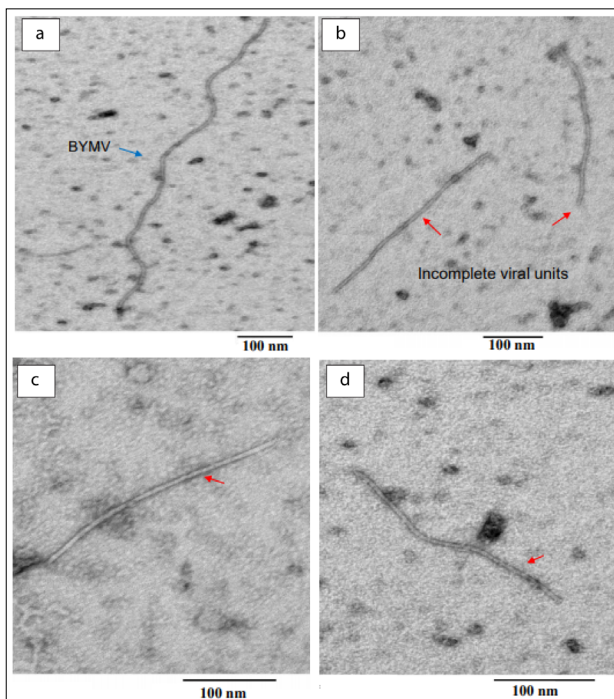


**Figure 5:** Transmission electron micrograph of *Bean yellow mosaic virus* (BYMV) particle unit obtained from chitosan nanoparticle (ChiNP)-treated plants (b, c, d) and untreated control (a). Red arrows indicate the defective viral particles in ChiNP-treated plants. Photos were captured under direct magnification of 100 000 x with scale of 100 nm, HV=80.0 kV.

reaction was observed with no significant difference compared to the negative control. A significant difference was recorded after treatment with 200 mg/L and 250 mg/L ChiNPs, with the virus content significantly decreased by 44.95% (0.915 OD) and 60.18% (0.649 OD), respectively, compared to the untreated control. However, bulk chitosan application showed that the BYMV accumulation content did not change significantly from all tested concentrations, only from 300 mg/L and 400 mg/L and the virus titre was significantly reduced by 36.12% (0.945 OD) and 42.66% (0.880 OD), respectively, as compared with the untreated control (1.244 OD).

#### Modulations in enzyme activity

Phenylalanine ammonia lyase activity was considerably increased by 1.00-fold in all ChiNP-treated plants at 24 h post spraying. The maximum increase in phenylalanine ammonia lyase activity was noted in 400 mg/L treated plants. The peak activity continually increased to reach its maximum level at 144 h with a 3.14-fold increase, while the activity increased only 0.93-fold in untreated control plants (Figure 6a). The maximum *polyphenol oxidase* activity was recorded in plants treated with 400, 300 and 250 mg/L ChiNPs in which the increase in polyphenol oxidase activity was found to be considerably higher than in untreated controls. However, a slight increase in polyphenol oxidase activity was generated after the virus treatment, with a 0.28-fold increase at 72 h post-treatment, reaching a maximum of 1.11-fold at 144 h (Figure 6b).

#### Changes in gene expression level

ChiNP foliar spraying was found to modulate the plant defence machinery by upregulating the PR-1 gene (Figure 7a). The gene transcriptome was strongly promoted with all tested applications of ChiNPs compared to untreated control plants. The relative expression increased as the ChiNP concentration increased. The maximum upregulating expression level of a 16.22-fold change was attained with 400 mg/L. Simultaneously, the mRNA accumulation of the PR-1 gene in 200- and 300 mg/L treated



**Table 1:** Effect of chitosan nanoparticles and chitosan bulk form on virus concentration and accumulation contents in treated plants at six tested concentrations compared to healthy and infected untreated controls using ELISA reaction

Concentration (mg/L)	Virus titre (optical density (OD) at 405 nm)					
	Chitosan nanoparticles			Chitosan bulk polymer		
	OD	+/-	%	OD	+/-	%
Positive untreated control	1.411±0.087 <sup>a</sup>	(+)	–	1.204±0.093 <sup>a</sup>	(+)	–
50	1.132±0.042 <sup>ab</sup>	+	7.17	1.292±0.018 <sup>a</sup>	+	0.00
100	1.364±0.063 <sup>a</sup>	+	22.34	1.367±0.098 <sup>a</sup>	+	0.00
200	0.915±0.078 <sup>bc</sup>	+	44.95	1.290±0.015 <sup>a</sup>	+	0.00
250	0.649±0.053 <sup>c</sup>	+	69.18	1.301±0.049 <sup>a</sup>	+	0.00
300	0.286±0.037 <sup>d</sup>	–	100.00	0.945±0.138 <sup>b</sup>	+	36.12
400	0.311±0.009 <sup>d</sup>	–	100.00	0.880±0.275 <sup>b</sup>	+	42.66
Negative healthy control	0.309±0.012 <sup>d</sup>	(–)	–	0.294±0.023 <sup>c</sup>	(–)	–
$p \leq 0.05$	0.305	–	0.163		–	

(%): Efficiency index in reducing virus concentration over the positive control in samples reacting positively (+) with tested BYMV antibodies. The proportion of reduction in each negative sample was considered with a value of 100%. Values with the same letters in each experiment were not significantly different. Values are means of three repeats ±s.e. ( $p \leq 0.05$ ).

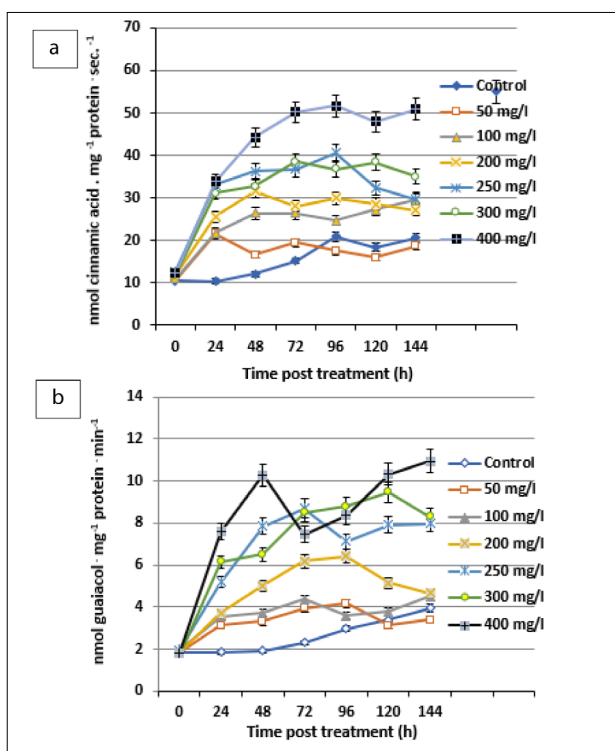


**Figure 6:** (a) Phenylalanine ammonia lyase and (b) polyphenol oxidase time course of modulation activities in chitosan nanoparticle treated plants compared to untreated control plants. Values are mean ±s.e. of three repeats ( $p \leq 0.05$ ).

plants was high, with 10.26- and 9.56-relative expression fold increases, respectively, over the untreated control plants.

### Changes in total phenolic content

Total phenolic content was relatively affected in faba bean plants treated with the tested ChiNP concentrations (Figure 7b). Among all tested concentrations of ChiNPs, only the 400 mg/L dosage rate increased the

total phenolic content curve significantly over untreated controls until 30 days post-application, while 300 mg/L significantly increased the total phenolic content for 20 days compared to controls.

### Effects of ChiNPs on plant vegetation and growth parameters

Foliar application of ChiNPs significantly affected plant growth, leaf area and chlorophyll content parameters compared to untreated infected controls. Moreover, 400 mg/L ChiNPs not only produced a significant increase in shoot length in comparison to the untreated infected controls, but also increased plant growth more than that of the untreated healthy control plants (Table 2).

### Discussion

The nanotechnology approach has recently emerged as a new potential means of control for a wide array of plant diseases.<sup>35</sup> However, the use of nanotechnology in plant protection management has not been broadly introduced on large scales as yet, and is still under research at a small scale of production and application.<sup>36,37</sup> The current study shows the antiviral activity of ChiNPs against BYMV and its accumulation within the plant tissues as compared to the bulk form of chitosan. To our knowledge, this is the first comprehensive study to investigate the antiviral ability of ChiNPs against plant viruses. However, previous reports have confirmed that ChiNPs increased the antiviral capabilities against human viruses such as hepatitis C virus<sup>38</sup> and HIV<sup>39</sup>. Furthermore, very limited reports have also shown the partial effectiveness of bulk chitosan polymers against plant viruses.<sup>40</sup>

The mechanisms underlying the effectiveness of ChiNPs in controlling plant viruses and other plant diseases have not as yet been investigated. Nanoparticles, ranging from 1 nm to 100 nm in size, provide superior chemical and physical features when compared to their bulk materials due to their large surface area to volume ratios.<sup>9,10</sup> Because all plant viruses are biological nano-size particles, it is reasonable to argue that chitosan in nano-based form could facilitate antiviral activity by targeting the virus particles and the replication process within the host tissues. Further, our findings show that ChiNPs altered the virus integrity by producing incomplete and defective viral particles. A potential reason for this may be that the synthesised ChiNPs have a surface area with positive charges and positively charged amino gatherings on chitosan glucosamine polymer chains. These facts support the suggestion



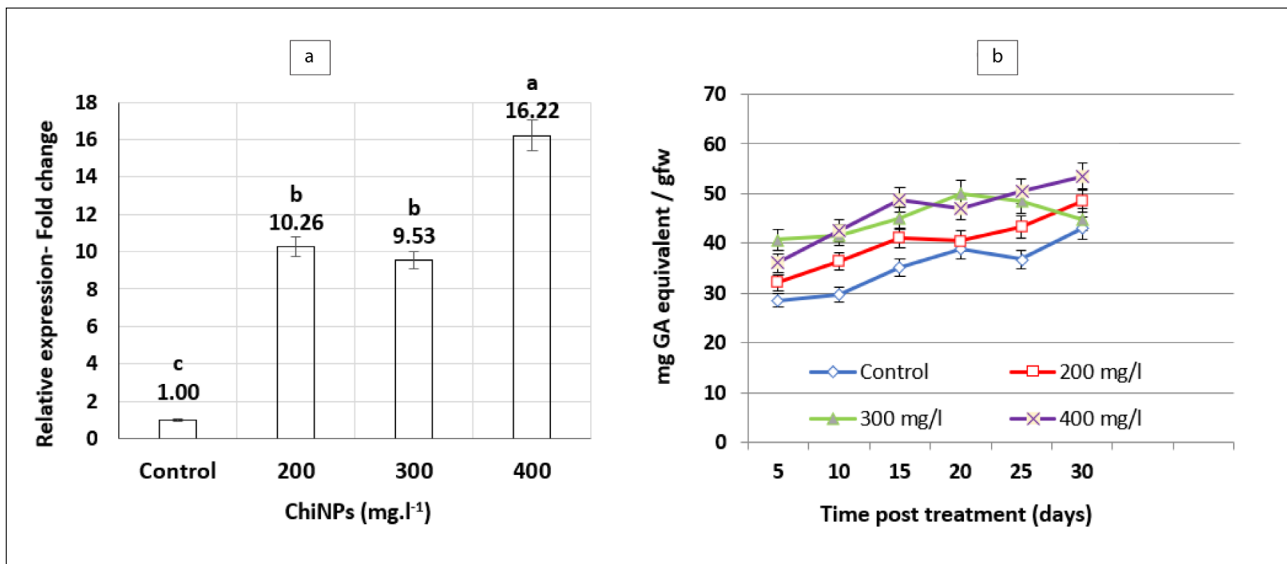


**Figure 7:** (a) Expression pattern analysis of pathogenesis-related gene 1 (PR-1) in response to three tested concentrations of chitosan nanoparticles (ChiNPs) and an untreated control. Values with the same letters are not significantly different ( $p \leq 0.05$ ). (b) Phenolic dynamic curve in faba plants treated with three tested concentrations compared to the untreated control faba bean plants.

**Table 2:** Vegetation parameters of faba bean plants treated with chitosan nanoparticles and chitosan bulk polymer at six tested concentrations compared to untreated healthy and infected control plants

Concentration (mg/L)	Chitosan nanoparticles			Chitosan bulk polymer		
	Shoot length (cm)	Leaf area (cm <sup>2</sup> )	Chlorophyll index	Shoot length (cm)	Leaf area (cm <sup>2</sup> )	Chlorophyll index
Untreated infected control (0.00)	27.31 ± 1.44 <sup>e</sup>	9.73 ± 0.65 <sup>b</sup>	20.83 ± 1.24 <sup>c</sup>	30.75 ± 0.651 <sup>b</sup>	11.02 ± 1.35 <sup>b</sup>	23.66 ± 1.09 <sup>e</sup>
Untreated healthy control (0.00)	38.90 ± 0.355 <sup>b,c</sup>	14.45 ± 1.44 <sup>a</sup>	42.53 ± 1.00 <sup>a</sup>	38.41 ± 0.924 <sup>a</sup>	14.45 ± 1.29 <sup>a</sup>	42.54 ± 0.634 <sup>a</sup>
50	35.55 ± 1.52 <sup>cd</sup>	13.13 ± 1.86 <sup>ab</sup>	31.60 ± 1.65 <sup>b</sup>	32.11 ± 1.85 <sup>b</sup>	12.76 ± 1.43 <sup>ab</sup>	28.1 ± 2.65 <sup>d</sup>
100	40.16 ± 1.27 <sup>ab</sup>	12.28 ± 0.66 <sup>ab</sup>	30.16 ± 2.20 <sup>b</sup>	31.79 ± 1.06 <sup>ab</sup>	11.57 ± 0.962 <sup>ab</sup>	31.5 ± 2.75 <sup>cd</sup>
200	37.46 ± 0.971 <sup>bc</sup>	14.54 ± 1.28 <sup>a</sup>	33.90 ± 1.88 <sup>b</sup>	36.16 ± 2.43 <sup>a</sup>	13.49 ± 0.712 <sup>a</sup>	32.6 ± 1.55 <sup>cd</sup>
250	34.23 ± 0.710 <sup>d</sup>	13.93 ± 1.68 <sup>a</sup>	40.83 ± 1.31 <sup>a</sup>	33.20 ± 0.78 <sup>ab</sup>	14.44 ± 1.39 <sup>a</sup>	36.13 ± 1.42 <sup>bc</sup>
300	36.19 ± 0.557 <sup>bc</sup>	16.34 ± 1.85 <sup>a</sup>	43.60 ± 1.19 <sup>a</sup>	38.61 ± 1.34 <sup>a</sup>	13.24 ± 0.77 <sup>a</sup>	37.40 ± 1.08 <sup>abc</sup>
400	42.08 ± 0.530 <sup>a</sup>	14.41 ± 2.17 <sup>a</sup>	44.86 ± 2.16 <sup>a</sup>	38.56 ± 0.520 <sup>a</sup>	13.36 ± 1.02 <sup>a</sup>	39.23 ± 1.55 <sup>ab</sup>
$p \leq 0.05$	4.204	3.892	5.882	3.737	2.369	6.022

Values are mean ± s.e. and those with the same letter are not significantly different.

that ChiNPs might have high bio-reactivity to attract viral RNA which contains negatively charged phosphate groups in its primary chain,<sup>41,42</sup> and thereby suppresses virus replication and disease progression. Furthermore, as all viral proteins have negatively charged clusters of glycol proteins, it is assumed that the positively charged nanoparticles could also target the virus coat protein.<sup>43</sup> This supports our suggestion that the role of ChiNPs in controlling the plant viruses might be strongly governed by their nano physicochemical properties, particle chemical nature and bio-reactivity, in which the chitosan in nano-size seems to be critical for its antiviral properties.

In parallel with these findings, our research also suggests that the ChiNPs promote the plant defence mechanism against virus invasion by promoting expression of the PR-1 gene and some defence-related enzymes (phenylalanine ammonia lyase, polyphenol oxidase) and increasing the total phenolic content. The initiation of plant defence boosters in treated plants may be attributable to the ability of chitosan

to modulate salicylic acid phytohormone pathways which include the synthesis of phenylalanine ammonia lyase and pathogenesis-related proteins.<sup>44</sup> This supports the results of Chandra et al.<sup>20</sup> who investigated the role of ChiNPs as a natural biopolymer in the immunomodulatory response. Chitosan was found to enhance anti-oxidising enzymes and total phenolic content that are involved in the plant defence response. Moreover, Jia et al.<sup>45</sup> found that chitosan oligosaccharide spraying boosted the innate immunity system in treated plants by upregulating the PR-1 defence-related gene and increased the level of salicylic acid in treated plants. Further, Jia et al.<sup>45</sup> investigated how to reduce the virus accumulation content and symptom development by activating plant hormone signalling pathways. The increase in total phenolic contents may strongly be associated with increasing phenylalanine ammonia lyase activity, which is the first key enzyme for producing phenolics and other secondary metabolites involved in the plant defence system against pathogen attacks.<sup>46</sup>



Our data suggest that chitosan nano applications have a dual role in controlling plant viral infection and disease expression. Our data demonstrate that ChiNP application prevented the stunting of the plant usually caused by the virus, by reducing the virus infectivity, and thereby increasing growth parameters even above those of the non-infected untreated controls. The role of the chitosan polymer in promoting plant growth and yield has been documented in numerous crops.<sup>47-50</sup> Furthermore, chitosan nanoparticles have been investigated as plant growth enhancers.<sup>51</sup> The mode of action underlying the role of chitosan in enhancing plant growth was proposed to be its ability to induce many physiological processes including nutrient uptake, photosynthesis, and cell division as well as plant hormones.<sup>52</sup> Thus, it is reasonable to assume that chitosan in its nano-based form could be curatively used to alleviate viral infections.

## Conclusion

In conclusion, the current findings provide an indication of the potency of chitosan nano-based materials against plant viruses. ChiNPs showed a powerful antiviral activity against BYMV infectivity, virus replication and accumulation in treated plants. This might offer a new alternative strategy to manage plant viral diseases without the use of pesticides. However, further research to support this initial study is needed to explore the mechanisms underlying the role of ChiNPs against plant viruses.

## Acknowledgements

We thank Dr Khaled Y. Farroh, Head of the Central Laboratory of Nanotechnology & Advanced Materials, Agricultural Research Center (Giza, Egypt), for providing laboratory facilities for the characterisation of chitosan nanoparticles. We also thank Dr Yosra Ahmed, Head of the Plant Quarantine Pathogens Laboratory, Plant Pathology Research Institute, Agricultural Research Center (Giza, Egypt) for providing chemical reagents and consumables for the PR-1 gene expression experiment.

## Competing interests

We have no competing interests to declare.

## Authors' contributions

A.Y.E.: Conceptualisation, methodology, data collection, data analysis, writing – the initial draft. M.M.A.: Validation, supervision, writing – revisions. T.E.: Methodology, data analysis. M.I.A.: Supervision, review and editing. M.R.T.: Supervision, writing – revisions. All authors revised the initial draft of the manuscript and approved the final draft.

## References

- Bos L. Hundred years of virology: From vitalism via molecular biology to genetic engineering. *Trends Microbiol.* 2000;8:82–104. [https://doi.org/10.1016/S0966-842X\(99\)01678-9](https://doi.org/10.1016/S0966-842X(99)01678-9)
- Singh AK, Bharati RC, Manibhushan NC, Pedpati A. An assessment of faba bean (*Vicia faba* L.) current status and future prospects. *Afr J Agric Res.* 2013;8(50):6634–6641. [https://academicjournals.org/article/article1387443711\\_Singh%20et%20al.pdf](https://academicjournals.org/article/article1387443711_Singh%20et%20al.pdf)
- Sharma PN, Sharma V, Anuradha S, Rajput K, Sharma SK. Identification and molecular characterization of *Bean yellow mosaic virus* infecting French bean in Himachal Pradesh. *Virus Diseases.* 2015;26(4):315–318. <https://doi.org/10.1007/s13337-015-0270-z>
- Khalil SA, Erskine W. Combating disease problems of grain legumes in Egypt. *Grain Legumes.* 2001;32:24–26.
- Latham LJ, Jones RA. Incidence of virus infection in experimental plots, commercial plots, and seed stocks of cool-season crop legumes. *Aust J Agric Res.* 2001;52:397–413. <https://doi.org/10.1071/AR00079>
- Hampton RO, Jensen A, Hagel GT. Attributes of Bean yellow mosaic potyvirus transmission from clover to snap beans by four species of aphids (*Homoptera: Aphididae*). *J Econ Entomol.* 2005;98(6):1816–1823. <https://doi.org/10.1603/0022-0493-98.6.1816>
- Jones RA. Trends in plant virus epidemiology: Opportunities from new improved technologies. *Virus Res.* 2014;186:3–19. <https://doi.org/10.1016/j.virusres.2013.11.003>

- Miller G. *Sustaining the earth.* 6th edition. Pacific Grove, CA: Thompson Learning; 2004.
- Osuwa JC, Anusionwu PC. Some advances and prospects in nanotechnology: A review. *Asian J Inform Technol.* 2011;10(2):96–100. <https://doi.org/10.3923/ajit.2011.96.100>
- Bakshi M, Singh HB, Abhilash PC. The unseen impact of nanoparticles: More or less? *Current Sci.* 2014;106(3):350–352.
- Hadwiger LA, Beckman JM. Chitosan as a component of pea-*Fusarium solani* interactions. *J Plant Physiol.* 1980;66:205–211. <https://doi.org/10.1104/pp.66.2.205>
- Wu T, Zivanovic S, Draughon FA, Conway WS, Sams CE. Physicochemical properties and bioactivity of fungal chitin and chitosan. *Agric Food Chem.* 2005;53:3888–3894. <https://doi.org/10.1021/jf048202s>
- Xing K, Zhu X, Peng X, Qin S. Chitosan antimicrobial and eliciting properties for pest control in agriculture. *Rev Agron Sustain Dev.* 2015;35:569–588. <https://doi.org/10.1007/s13593-014-0252-3>
- Chirkov S. The antiviral activity of chitosan (review). *Appl Biochem Microbiol.* 2002;38:1–8. <https://doi.org/10.1023/A:1013206517442>
- Chirkov S, Il'ina A, Surgucheva N, Letunova E, Varitsev Y, Tatarinova N, et al. Effect of chitosan on systemic viral infection and some defense responses in potato plants. *Russian J Plant Physiol.* 2001;48:774–779. <https://doi.org/10.1023/A:1012508625017>
- Atia MM, Buchenauer H, Aly AZ, Abou-Zaid MI. Antifungal activity of chitosan against *Phytophthora infestans* and activation of defence mechanisms in tomato to late blight. *Biol Agric Hortic.* 2005;23(2):175–197. <https://doi.org/10.1080/01448765.2005.9755319>
- El Gamal AYS, Zayed MA, El-Nashar FK, Atia MM. The potential ability of some abiotic agents to control barley net blotch disease. *Zagazig J Agric Res.* 2016;43(4):1215–1232. <https://doi.org/10.21608/zjar.2016.100490>
- Mishra S, Jagadeesh KS, Krishnaraj PU, Prem S. Biocontrol of *tomato leaf curl virus* (TLCV) in tomato with chitosan supplemented formulations of *Pseudomonas* sp. under field conditions. *Aus J Crop Sci.* 2017;8:347–355.
- Firmansyah D, Hidayat S, Widodo W. Chitosan and plant growth-promoting rhizobacteria application to control squash mosaic virus on cucumber plants. *Asian J Plant Pathol.* 2017;11:148–155. <https://doi.org/10.3923/ajppaj.2017.148.155>
- Chandra S, Chakraborty N, Dasgupta A, Sarkar J, Panda K, Acharya K. Chitosan nanoparticles: A positive modulator of innate immune responses in plants. *Sci Rep.* 2015;5:1–13. <https://doi.org/10.1038/srep15195>
- Clark MF, Adams AN. Characteristics of the microplate method of enzyme-linked immunosorbent assay for the detection of plant viruses. *J Gen Virol.* 1977;34:475–483. <https://doi.org/10.1099/0022-1317-34-3-475>
- Kuhn CW. Separation of cowpea virus mixtures. *Phytopathology.* 1964;54:739–740. <https://doi.org/10.1016/j.jviromet.2008.07.023>
- 23 AL-Khalifa M, Kumari SG, Kasem A, Makkouk KM, Shalaby AA, AL-Chaabi SA. Molecular characterization of a *Bean yellow mosaic virus* isolate from Syria. *Phytopathol Mediterr.* 2008;47:282–285. [https://doi.org/10.14601/Phytopathol\\_Mediterr-2734](https://doi.org/10.14601/Phytopathol_Mediterr-2734)
- Masarudin MJ, Cutts SM, Evison BJ, Phillips DR, Pigram PJ. Factors determining the stability, size distribution, and cellular accumulation of small, monodisperse chitosan nanoparticles as candidate vectors for anticancer drug delivery: Application to the passive encapsulation of [14 C]-doxorubicin. *Nanotechnol Sci Appl.* 2015;8:67–80. <https://doi.org/10.2147/NSA.S91785>
- Zhang H, Wu F, Li Y, Yang X, Huang J, Lv T, et al. Chitosan-based nanoparticles for improved anticancer efficacy and bioavailability of mifepristone. *Beilstein J Nanotechnol.* 2016;7:1861–1870. <https://doi.org/10.3762/bjnano.7.178>
- Yang X, Liangyi K, Tien P. Resistance of tomato infected with cucumber mosaic virus satellite RNA to potato spindle tuber viroid. *Ann Appl Biol.* 1996;129:543–551. <https://doi.org/10.1111/j.1744-7348.1996.tb05775.x>
- Campos RE, Bejerman N, Nome C, Laguna IG, Pardina PR. *Bean Yellow Mosaic Virus* in Soybean from Argentina. *J Phytopathol.* 2013;162:322–325. <https://doi.org/10.1111/jph.12185>
- Kar M, Mishra D. Catalase, peroxidase, and polyphenol oxidase activities during rice leaf senescence. *Plant Physiol.* 1976;57:315–319. <https://doi.org/10.1104/pp.57.2.315>



29. Lisker N, Coren L, Chalutz E, Fucus Y. Fungal infections suppress ethylene-induced phenylalanine ammonia-lyase activity in grape fruits. *Physiol Plant Pathol.* 1983;22:331–338. [https://doi.org/10.1016/S0048-4059\(83\)81020-0](https://doi.org/10.1016/S0048-4059(83)81020-0)
30. Cheng Y, Zhang H, Yao J, Wang X, Xu J, Han Q, et al. Characterization of non-host resistance in broad bean to the wheat stripe rust pathogen. *BMC Plant Biol.* 2012;12:96. <https://doi.org/10.1186/1471-2229-12-96>
31. Pfaffl MW. A new mathematical model for relative quantification in real-time RT-PCR. *Nucleic Acids Res.* 2001;29(9):1–45. <https://doi.org/10.1093/nar/29.9.e45>
32. Lin JY, Tang CY. Determination of total phenolic and flavonoid contents in selected fruits and vegetables, as well as their stimulatory effects on mouse splenocyte proliferation. *Food Chem.* 2007;101(1):140–147. <https://doi.org/10.1016/j.foodchem.2006.01.014>
33. Chahit D. A leaf area estimation model for faba bean (*Vicia faba* L.) grown in the Mediterranean type of climate. *Agric J SDU.* 2012;7(1):58–63.
34. Siliva FDA, Azevedo CA. Principal components analysis in the software Assitstat-statistical attendance. In: *World Congress on Computers in Agriculture*. Reno, NV: American Society of Agricultural and Biological Engineers; 2009. [https://www.scirp.org/\(S\(i43dyn45teexjx455qlt3d2q\)\)](https://www.scirp.org/(S(i43dyn45teexjx455qlt3d2q)))
35. Singh S, Singh BK, Ydava SM, Gupta AK. Applications of nanotechnology in agriculture and their role in disease management. *Res J Nanosci Nanotechnol.* 2015;5(1):1–5. <https://doi.org/10.3923/rjnn.2015.1.5>
36. Prasad R, Bhattacharyya A, Nguyen QD. Nanotechnology in sustainable agriculture: Recent developments, challenges, and perspectives. *Front Microbiol.* 2017;8:1014. <https://doi.org/10.3389/fmicb.2017.01014>
37. Luca M. Nanotechnology in agriculture: New opportunities and perspectives. *New Visions in Plant Science*. IntechOpen; 2018. <https://doi.org/10.5772/intechopen.74425>
38. Loutfy S, Elberry M, Farroh K, Mohamed H, Mohamed A, Mohamed E, et al. Antiviral activity of chitosan nanoparticles encapsulating curcumin against Hepatitis C Virus genotype 4a in human hepatoma cell lines. *Int J Nanomed.* 2020;15:2699–2715. <https://doi.org/10.2147/IJN.S241702>
39. Ramana LN, Sharma S, Sethuraman S, Ranga U, Krishnan UM. Evaluation of chitosan nanoformulations as potent anti-HIV therapeutic systems. *Biochim Biophys Acta.* 2014;1840(1):476–484. <https://doi.org/10.1016/j.bbagen.2013.10.002>
40. Iriti M, Sironi M, Gomarasca S, Casazza AP, Soave C, Faoro F. Cell death-mediated antiviral effect of chitosan in tobacco. *Plant Physiol Biochem.* 2006;44:893–900. <https://doi.org/10.1016/j.plaphy.2006.10.009>
41. Xing K, Chen XG, Liu CS, Cha DS, Park HJ. Oleoyl-chitosan nanoparticles inhibit *Escherichia coli* and *Staphylococcus aureus* by damaging the cell membrane and putative binding to extracellular or intracellular targets. *Int J Food Microbiol.* 2009;132:127–133. <https://doi.org/10.1016/j.ijfoodmicro.2009.04.013>
42. Mansilla AY, Albertengo L, Rodríguez MS, Debbaudt A, Zúñiga A, Casalongué CA. Evidence on antimicrobial properties and mode of action of a chitosan obtained from crustacean exoskeletons on *Pseudomonas syringae* pv. *tomato* DC3000. *Appl Microbiol Biotechnol.* 2013;97:6957–6966. <https://doi.org/10.1007/s00253-013-4993-8>
43. Karlin S, Brendel V. Charge configurations in viral proteins. *Proc Natl Acad Sci USA.* 1988;85(24):9396–9400. <https://doi.org/10.1073/pnas.85.24.9396>
44. Siddaiah S, Prashanth H, Satyanarayana N, Mudili V, Gupta V, Kalagatur N, et al. Chitosan nanoparticles having higher degree of acetylation induce resistance against pearl millet downy mildew through nitric oxide generation. *Sci Rep.* 2019;8:101–116. <https://doi.org/10.1038/s41598-017-19016-z>
45. Jia X, Meng Q, Zeng H, Wang W, Yin H. Chitosan oligosaccharide induces resistance to Tobacco mosaic virus in Arabidopsis via the salicylic acid-mediated signaling pathway. *Sci Rep.* 2016;6:26144. <https://doi.org/10.1038/srep26144>
46. Dogbo DO, Gogbeu SJ, Zuel B, Yao NK, Zohouri GP, Mamybekov-Abekro JA, et al. Comparative activities of phenylalanine ammonia-lyase and tyrosine ammonia-lyase and phenolic compounds accumulated in cassava elicited cell. *Afr Crop Sci.* 2012;20(2):85–94.
47. Lee YS, Kim YH, Kim SB. Changes in the respiration, growth, and vitamin C content of soybean sprouts in response to chitosan of different molecular weights. *Hortic Sci.* 2005;40:1333–1335. <https://doi.org/10.21273/HORTSCI.40.5.1333>
48. Mondal MMA, Malek MA, Puteh AB, Ismail MR, Ashrafuzzaman M, Naher L. Effect of foliar application of chitosan on growth and yield in okra. *Aust J Crop Sci.* 2012;6(64):918–921.
49. Sultana S, Islam M, Khatun MA, Hassain MA, Huque R. Effect of foliar application of oligo-chitosan on growth, yield and quality of tomato and eggplant. *Asian J Agric Res.* 2017;11:36–42. <https://doi.org/10.3923/ajar.2017.36.42>
50. Akter J, Jannat R, Hossain MM, Ahmed JU, Rubayet MT. Chitosan for plant growth promotion and disease suppression against anthracnose in chili. *Int J Agric Environ Biotechnol.* 2018;3:806–817. <https://doi.org/10.22161/ijeab/3.3.13>
51. Choudhary RC, Kumaraswamy RV, Kumari S, Sharma SS, Pal A, Raliya R, et al. Cu-chitosan nanoparticle boost defense responses and plant growth in maize (*Zea mays* L.). *Sci Rep.* 2017;7:9754–9765. <https://doi.org/10.1038/s41598-017-08571-0>
52. Chakraborty M, Hasanuzzaman M, Rahman M, Khan M, Bhowmik P, Mahmud N, et al. Mechanism of plant growth promotion and disease suppression by chitosan biopolymer. *Agriculture.* 2020;10:624. <https://doi.org/10.3390/agriculture10120624>

**AUTHORS:**

Esperance D. Codjia<sup>1,2</sup>   
 Bunmi Olasanmi<sup>1,3</sup>   
 Paterne A. Agre<sup>2</sup>  
 Ruth Uwugiaren<sup>2</sup>  
 Adenike D. Ige<sup>1,2</sup>  
 Ismail Y. Rabbi<sup>2</sup>

**AFFILIATIONS:**

<sup>1</sup>Pan African University Life and Earth Sciences Institute (including Health and Agriculture), University of Ibadan, Ibadan, Nigeria  
<sup>2</sup>International Institute of Tropical Agriculture (IITA), Ibadan, Nigeria  
<sup>3</sup>Department of Agronomy, University of Ibadan, Ibadan, Nigeria

**CORRESPONDENCE TO:**

Bunmi Olasanmi

**EMAIL:**

bunminadeco@yahoo.com

**DATES:**

**Received:** 29 June 2021

**Revised:** 11 Sep. 2021

**Accepted:** 13 Sep. 2021

**Published:** 27 Jan. 2022

**HOW TO CITE:**

Codjia ED, Olasanmi B, Agre PA, Uwugiaren R, Ige AD, Rabbi IY. Selection for resistance to cassava mosaic disease in African cassava germplasm using single nucleotide polymorphism markers. *S Afr J Sci.* 2022;118(1/2), Art. #11607. <https://doi.org/10.17159/sajs.2022/11607>

**ARTICLE INCLUDES:**

- Peer review
- [Supplementary material](#)

**DATA AVAILABILITY:**

- Open data set
- All data included
- On request from author(s)
- Not available
- Not applicable

**EDITOR:**

Teresa Coutinho

**KEYWORDS:**

CMD resistance, SNP markers, KASP genotyping, prediction accuracy, marker-assisted selection

**FUNDING:**

African Union Commission



# Selection for resistance to cassava mosaic disease in African cassava germplasm using single nucleotide polymorphism markers

Cassava mosaic disease (CMD) is one of the main constraints that hamper cassava production. Breeding for varieties that are CMD resistant is a major aim in cassava breeding programmes. However, the use of the conventional approach has its limitations, including a lengthy growth cycle and a low multiplication rate of planting materials. To increase breeding efficiency as well as genetic gain of traits, SNP markers can be used to screen and identify resistant genotypes. The objective of this study was to predict the performance of 145 cassava genotypes from open-pollinated crosses for CMD resistance using molecular markers. Two SNP markers (S12\_7926132 and S14\_4626854), previously converted into Kompetitive allele-specific PCR (KASP) assays, as well as CMD incidence and severity scores, were used for selection. About 76% of the genotypes were revealed to be resistant to CMD based on phenotypic scores, while over 24% of the total population were found to be susceptible. Significant effects were observed for alleles associated with marker S12\_7926132 while the other marker had non-significant effects. The predictive accuracy (true positives and true negatives) of the major *CMD2* locus on chromosome 12 was 77% in the population used in this study. Our study provides insight into the potential use of marker-assisted selection for CMD resistance in cassava breeding programmes.

**Significance:**

- With an aim towards reducing the food insecurity rate in Africa, we report on the use of genetic tools for a fast and efficient release of new cassava varieties to benefit breeders, farmers and consumers, given the food and industrial importance of this staple crop.
- This study adds tremendous knowledge to phenotypic and molecular screening for CMD resistance. The outcome will encourage breeders in various cassava breeding programmes to accelerate genetic gains as well as increase breeding accuracy and efficiency for CMD resistance.

**Introduction**

Cassava is one of the staple crops in Africa. The importance of this crop lies in the high starch content of its storage roots, which provides a cheap source of calories in developing countries where malnutrition and calorie deficiency are widespread.<sup>1</sup> In 2019, Africa accounted for 63% of the 303 million metric tons produced globally, with Nigeria being the highest producer.<sup>2</sup> Cassava leaves and delicate shoots are eaten as vegetables in many parts of Africa.<sup>1</sup> Cassava is also used to make cassava starch, which is used as a raw material in the food, textile, paper, and glue industries.<sup>3</sup>

Despite the economic importance of the crop, a large number of constraints hinder cassava production in Africa, especially in Nigeria where a high incidence of pests and diseases, unavailability of agrochemicals and insecticides, and degradation of soil fertility as a result of erosion and urbanisation have been reported.<sup>4</sup>

Cassava mosaic disease (CMD) is one of the most devastating viral plant diseases in Africa. It can cause yield losses ranging from 12% to 82% depending on infection type and cassava variety.<sup>5</sup> These translate into an annual reduction of more than 30 million tons of fresh root yield.<sup>6</sup> The disease is caused by cassava mosaic geminivirus of the family *Geminiviridae* and genus *Begomovirus*<sup>7</sup> and the symptoms vary from irregular yellow to yellow-green chlorotic areas on the leaves, leading to leaf distortion and plant stunted growth.

The deployment of host plant resistance and the application of cultural treatments, particularly phytosanitation, are the most extensively utilised approaches in reducing the negative impacts of CMD.<sup>8</sup> However, the use of resistant varieties is the most sustainable solution because it decreases disease-related production losses as well as the inoculum source for whitefly (*Bemisia tabaci*) which is known to be the disease vector.<sup>9</sup>

Genetic mapping studies have identified three sources of CMD resistance: *CMD1* (recessive and polygenic), *CMD2* (monogenic and dominant), and *CMD3* (quantitative trait locus or QTL for CMD resistance)<sup>9,10</sup>, but *CMD2* remains the most commonly employed<sup>11</sup>. *CMD1*, known as the polygenic source of resistance, was derived from the wild species *Manihot glaziovii*.<sup>12</sup> The *CMD2*, which is monogenic, was discovered in some West African cassava landraces (tropical *Manihot esculenta*).<sup>12,13</sup> The complementary effect between the *CMD2* locus and a newly identified QTL confers *CMD3* source of resistance.<sup>14</sup>

A traditional cassava breeding programme relies on phenotypic characterisation of mature plants<sup>15</sup>, which makes it last for about a decade, leading to a delay in releasing a new variety. The low multiplication rate of planting material needed for phenotypic screening across multi-environments, and variation in performance of the plants due to the physiological status of the cuttings, are some of the several factors that reduce breeding efficiency in cassava programmes<sup>16</sup> thus resulting in a low rate of genetic gain. To overcome the aforementioned limitations, molecular markers such as single nucleotide polymorphisms (SNPs) can be incorporated in cassava breeding programmes





for rapid genetic improvement of traits of interest through marker-assisted selection. Marker-assisted selection is a technique that involves establishing a link between a molecular marker and the chromosomal location of the QTL that controls the desired trait.<sup>17</sup>

Understanding the genetic architecture is necessary for the development of molecular tools to speed up the transfer of beneficial genes into farmer-preferred cultivars.<sup>18</sup> Significant loci linked to some important traits including CMD resistance were identified through a genome-wide association study which was conducted at the International Institute of Tropical Agriculture, Nigeria.<sup>18</sup> The favourable alleles at the most significant markers associated with CMD resistance, S12\_7926132 (allele G/T) and S14\_4626854 (A/G), were T and A, respectively.<sup>18</sup> SNPs tagging major loci could be useful for screening and identifying individuals with favourable alleles during the early stages of selection if allele-specific high-throughput SNP tests are developed. Before large-scale implementation, a validation study of these loci is required to guarantee their relevance across environments and populations.<sup>18</sup>

The major objective of this work was to predict the performance of cassava genotypes for CMD resistance using SNP molecular markers and phenotypic data.

## Materials and methods

### Field experiment and CMD evaluation

A population comprising 145 cassava genotypes was evaluated for CMD incidence and severity at the Teaching and Research Field of the Department of Agronomy, University of Ibadan, Nigeria, during two cropping seasons (2019/2020 and 2020/2021). The seeds of the genotypes were derived from open-pollinated crosses and were collected from five female parents (IITA-TMS011368; IITA-TMS011371; IITA-TMS011412; IITA-TMS070593 and IITA-TMS070539).

To minimise experimental error related to the large experimental field size, the genotypes were divided into four sets. The trial was laid out using a randomised complete block design with two replications per set. The experimental site was cleared and ridges were made with a row spacing of 3 m between sets. A total of 20 cuttings (25–30 cm long) from matured stems of each genotype were planted in a plot size of 20 m<sup>2</sup> at a spacing of 1 m x 1 m. The experimental location was chosen because of the high disease pressure by cassava mosaic virus.<sup>9</sup> Moreover, the early stage (first 6 months) of the plants corresponded with the period of high whitefly activity, resulting in a significant risk of disease exposure. Variety IITA-TMS-IBA070593 was included as a resistant control while IITA-TMS-IBA30572 and IITA-TMS-IBA30555 were used as susceptible controls.

Data on CMD incidence and severity scores were collected at 1, 3, and 5 months after planting. The incidence was recorded as the ratio of the number of plants with symptoms to the total number of plants per plot. The severity of CMD was measured on a scale of 1 to 5, with 1 denoting no symptoms, 2 denoting mild chlorotic areas on most leaves, with the remaining parts of the leaves and leaflets appearing green and healthy, 3 denoting a pronounced mosaic pattern on most leaves, with distortion of the lower one-third of most leaves, 4 denoting severe mosaic pattern on most leaves, and 5 denoting very severe mosaic symptoms on all leaves, often accompanied by stunting of the plant.<sup>1,19</sup>

### DNA extraction

A modified Dellaporta approach was used to extract genomic DNA from freeze-dried leaf samples.<sup>20</sup> The DNA quantification and purity were checked using a NanoDrop spectrophotometer (ND-8000, Thermo Fisher Scientific, USA). The absorbance at a wavelength of 260/280 nm ranging from 1.80 to 2.0 indicates that the DNA solution was free of contaminants. The quality of the DNA samples was checked on 1% agarose gel (Sunrise 96, Biometra, Göttingen, Germany) and bands were viewed on a gel documentation system (Labnet ENDURO GDS Gel Documentation System Aplegen) incorporated with an ultraviolet transilluminator.

### Kompetitive allele-specific PCR genotyping

Markers S12\_7926132 and S14\_4626854 derived from Rabbi et al.<sup>18</sup> were used to screen the cassava genotypes for resistant and susceptible alleles. The sequences of the specific forward and common reverse primers used for the Kompetitive allele-specific PCR (KASP) genotyping were extracted from Ige et al.<sup>21</sup> and are presented in Table 1. A positive (IITA-TMS-IBA070593) and two negative (IITA-TMS-IBA30572 and IITA-TMS-IBA30555) control varieties were included in the genotyping as well as a no-template control of 5 µL of distilled water. The KASP reaction mix consisted of 5 µL of DNA at a concentration of 50 ng and 5 µL of the prepared genotyping mix [5 µL (2 × KASP master mix) and 0.14 µL primer mix]. The PCR cycling was performed as follows: hot-start activation at 94 °C for 15 min followed by 10 touchdown cycles (20 s at 94 °C; touchdown at 61 °C to 55 °C initially and dropping by 0.6 °C per cycle for 60 s), followed by 26 additional cycles (20 s at 94 °C; 55 °C for 20 s). The KASP genotyping reactions were run on the Roche Light Cycler 480-II at the Biosciences Unit, International Institute of Tropical Agriculture (IITA), Ibadan, Nigeria.

The SNPs were called using KlusterCaller software (LGC, Biosearch Technologies, USA) and visualised based on the fluorescence signal using the SNPviewer software (LGC, Biosearch Technologies), where data on SNP allele calls were visualised graphically. Fluorophores FAM and HEX plotted on the x- and y-axes, respectively, allowed the distinction of the assayed genotypes.

### Statistical analysis

#### Phenotypic data analysis

The mean cassava mosaic disease severity scores (CMDSS) were subjected to a combined analysis of variance across the two years of experimentation to assess the genotypes, year, and block effects on the expression of the disease using aov function in Agricolae R package.<sup>22</sup> The disease progress curve for the average CMDSS across the three periods of observation was plotted using Agricolae package in R software. To obtain the BLUE (best linear unbiased estimator) value for each genotype, a linear mixed model was fitted using the lme4 R package to estimate the performance of each genotype independent of the season, block, and replication. The year, block, and replications were treated as random variables while the genotypes and checks were considered fixed. The statistical model for randomised complete block design<sup>23</sup> used with few adaptations is as follows:

$$y_{ij} = \mu + \beta_i + \tau_j + \gamma_k + \varepsilon \quad \text{Equation 1}$$

**Table 1:** Kompetitive allele-specific PCR primers for single nucleotide polymorphism (SNP) markers associated with cassava mosaic disease resistance

SNP	Favourable allele 1	Alternative allele 2	Forward primers Allele 1 and allele 2	Common reverse primer
S12_7926132	T	G	Allele 1: TTCCATGTTCCACCCTCAAATGG; Allele 2: TTCCATGTTCCACCCTCAAATGT	GGAGTACAAGAATCTTGCTTCTGTGATA
S14_4626854	A	G	Allele 1: GCACGCTGCACCTCTTCATTA; Allele 2: GCACGCTGCACCTCTTCATTG	CAAAGGTGGGATGCAATGAGCGAT

where  $y_{ij}$  is the phenotypic value,  $\mu$  is the overall average (shared by all observations),  $\beta_i$  is the effect of block  $i$ ,  $\tau_j$  is the specific effect to genotype  $j$ ,  $\gamma_k$  is the specific effect to year  $k$  and  $\varepsilon_{ij}$  is an effect specific to each experimental unit (combination block and genotype).

Least significant difference was used to compare the genotypes' BLUEs for CMDSS at 5%. Broad-sense heritability for CMDSS was determined as described by Ige et al.<sup>21</sup> according to Equation 2:

$$H^2 = \frac{v_g}{v_g + v_e} \quad \text{Equation 2}$$

where  $H^2$  stands for broad-sense heritability,  $v_g$  for genotypic variance and  $v_e$  for residual variance.

### Marker data analysis

Polymorphism information content (PIC) and favourable allele frequency were calculated using R base package<sup>22</sup> and Tassel software jointly.<sup>24</sup> The `lm` function from the `lm4` package was used to compute the analysis of variance of the markers. Boxplots were plotted using the `ggpubr` R package to assess the discriminative power of each marker allele combination. The correlation analysis between the two markers was performed using the `cor.test` function in `stats` package.

### Breeding metrics determination

For evaluation of the marker's accuracy, two main groups of genotypes were constituted, following Lokko et al.<sup>25</sup>'s classification method: resistant group (comprising individuals with CMDSS of 1 to 2) and susceptible group (comprising individuals with CMDSS of 2.1 to 5). Thereafter, a confusion matrix was generated as described by Olanmi et al.<sup>26</sup> which enabled the estimation of false positive and false negative individuals. Breeding metrics such as accuracy, precision, and misclassification were calculated as follows:

$$\text{Accuracy} = \frac{TP+TN}{TP+FP+TN+FN} \quad \text{Equation 3}$$

$$\text{Misclassification} = 1 - \text{accuracy} \quad \text{Equation 4}$$

$$\text{Precision} = \text{Predictive positive value} = \frac{TP}{TP+FP} \quad \text{Equation 5}$$

where TN is true negative, TP is true positive, FP is false positive, and FN is false negative. The FP refers to the number of genotypes predicted to be resistant by the marker and were susceptible in the field while the FN are the individuals that had unfavourable alleles at the marker but were resistant based on field screening.

### Logistic regression analysis

To assess the probability of markers in predicting resistance or susceptibility, a binary logistic regression analysis was performed. The entire data were used to fit the model using the `glm` function in `tidymodels` packages in R software. CMD severity BLUE value was used as a dependent variable while marker data were considered independent variables (predictor). Individuals with CMDSS of 1–2.0 were considered as unaffected while those with CMDSS 2.1–5 were categorised as affected according to Lokko et al.<sup>25</sup>

The mathematical formula used as described by Ige et al.<sup>21</sup> is:

$$\log \left[ \frac{\pi}{1-\pi} \right] = \beta_0 + \beta_1 x_1 \quad \text{Equation 6}$$

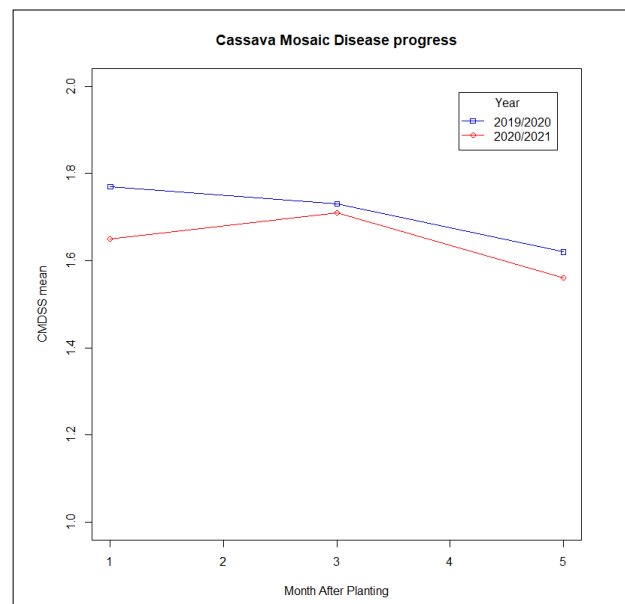
where  $\pi$  indicates the probability that a genotype is resistant or susceptible,  $\beta_0$  is the intercept constant, and  $\beta_1$  is the regression coefficient associated with the  $x_1$  explanatory variable (S12\_7926132). The logistic regression model fitted was validated on a bootstrapped sample ( $n=10$ ).

## Results

### Phenotypic evaluation of genotypes for cassava mosaic disease

The evaluation of the disease progress over time revealed that the average CMD severity score recorded during the first year of the experiment (2019/2020) was 1.71 while that of the 2020/2021 season was 1.64 (Figure 1). A decrease in disease severity was observed after the first 3 months of planting during the two years of experimentation (Figure 1).

The frequency distribution of the mean CMDSS across the two years was observed to be bimodal. However, the majority of the genotypes were within the first peak with a severity score of 1 (Figure 2). The combined analysis of variance across the 2 years revealed significant effects for year, genotypes, and genotype x year for CMD severity with a coefficient of variation of 16.68% (Table 2). There was a significant variability at 5% among the genotypes as revealed by the least significant difference test (Supplementary table 1). Based on the severity scores, about 76% of the genotypes evaluated were resistant to CMD while the remaining were susceptible (Figure 2). The broad-sense heritability of cassava mosaic disease was 0.97 in the African cassava population.



CMDSS, cassava mosaic disease severity scores

Figure 1: Cassava mosaic disease progression over time.

### Marker informativeness and allelic effects on CMD resistance

In the study population, the frequencies of the favourable alleles at marker S12\_7926132 (T) and marker S14\_4626854 (A) were 0.65 and 0.22, respectively. The two markers had polymorphism information content (PIC) values of 0.36 (S14\_4626854) and 0.46 (S12\_7926132).

The markers were shown to have a high call rate (>98%) as revealed by the KASP genotyping results. For each marker, three distinct clusters (favourable homozygous genotypes, unfavourable homozygous genotypes, and heterozygotes) were observed (Figure 3).

Boxplots showed that only the marker on chromosome 12 was able to discriminate favourable allele (T) from susceptible allele (G) for both CMDSS and mean incidence (Figure 4). The majority of the genotypes carrying at least a copy of allele T had a CMDSS of 1 (resistant) while individuals with two copies of the allele G had a mean CMDSS of 3.42 (susceptible). Similarly, for mean incidence, most of the genotypes with allele copies TT and TG had a mean incidence of 0%, whereas 76.67 was recorded for marker genotype GG (Figure 4). Also, a non-significant correlation ( $r=0.16$ ;  $p>0.05$ ) was observed between the two markers.



**Table 2:** Analysis of variance of cassava genotypes and other components under cassava mosaic disease pressure

Source of variation	d.f.	Sum of squares	Mean square	F value	Pr(>F)
Genotypes	144	758.5	5.268	65.057	< 2E-16***
Block	1	0.0	0.013	0.163	0.68742
Year	1	0.6	0.583	7.202	0.00828**
Genotypes*year	139	17.0	0.123	1.514	0.00958**
Genotypes*bloc	143	23.5	0.165	2.033	3.27 E-05***
Residuals	123	10.0	0.081		
Coefficient of variation			16.86%		

\*\*p<0.01; \*\*\*p<0.001

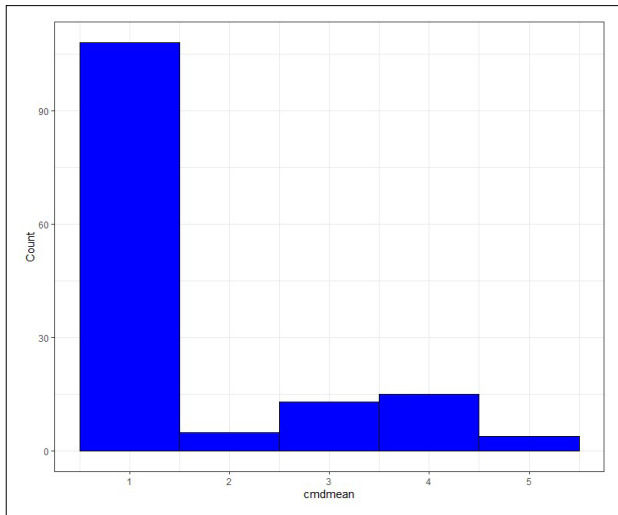


**Figure 2:** Frequency distribution of genotypes for cassava mosaic disease severity scores (1–5).

### Marker-trait association and prediction of genotype response to CMD

The analysis of variance based on the marker and phenotypic data revealed a significant ( $p < 0.01$ ) association between S12\_7926132 and the genotypes' response to CMD while S14\_4626854 was not significantly associated (Table 3). It was observed that the interaction between the two markers was significant ( $p < 0.01$ ) on the mean CMDSS (Table 3). For mean incidence, a similar trend was observed (Table 4). These findings suggest that the newly identified locus associated with S14\_4626854 could be polygenic with additive effects.

Discriminating marker S12\_7926132 was used as an independent variable in a binary logistic regression model. The effects of allele combinations TT and TG associated with the explanatory variable were

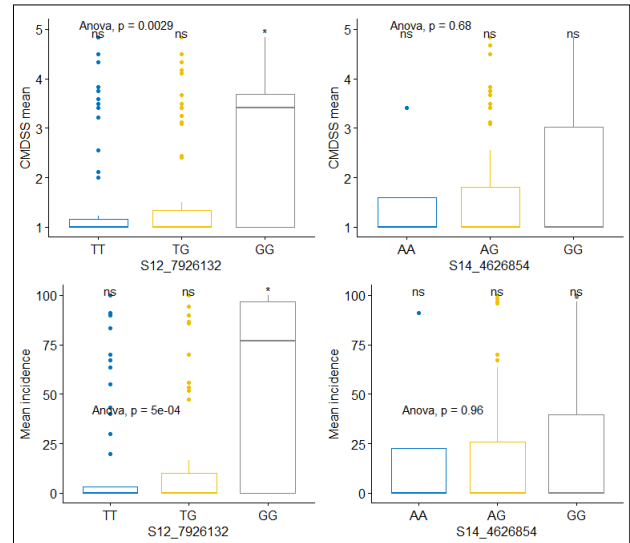
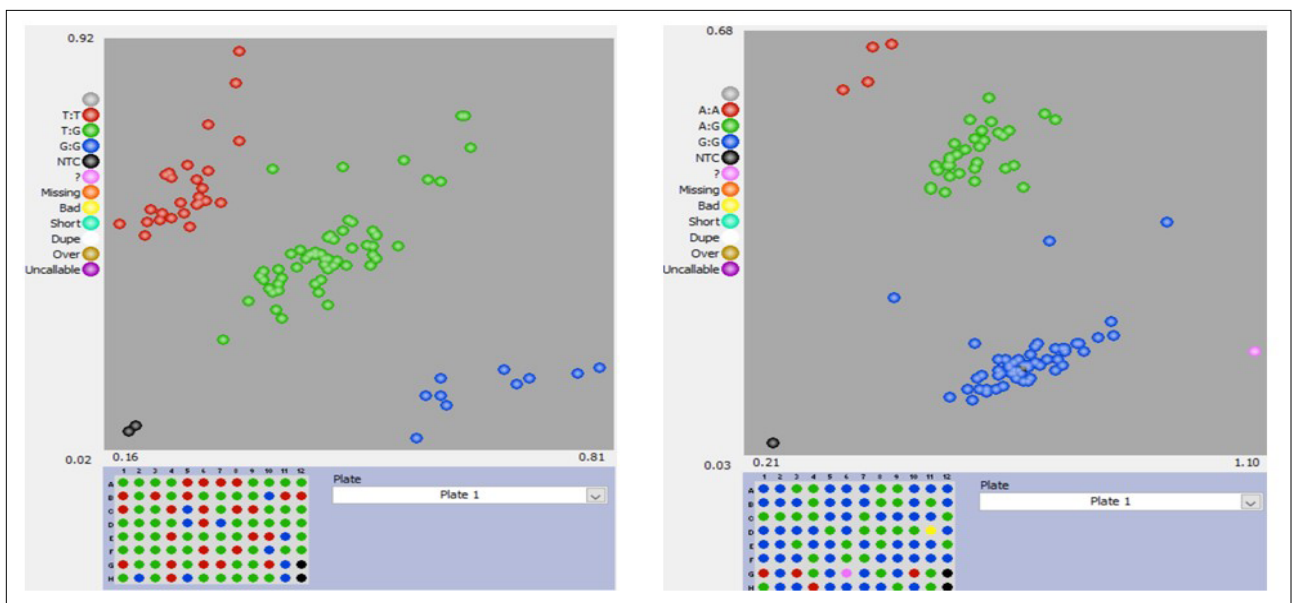


**Figure 4:** Boxplot for distribution of cassava mosaic disease severity scores (CMDSS) and mean incidence among cassava genotypes using the single nucleotide polymorphism markers S12\_7926132 and S14\_4626854: (left) marker S12\_7926132 with TT=homozygote resistant, TG= heterozygote, GG=homozygote susceptible, and (right) marker S14\_4626854 with AA=homozygote resistant, AG=heterozygote, GG=homozygote susceptible.



Red spots = homozygote resistant genotypes; green spots = heterozygotes; and blue spots = homozygote susceptible genotypes

**Figure 3:** Polymorphism patterns of the two single nucleotide polymorphism markers after Kompetitive allele-specific PCR genotyping assays.

significant in predicting genotypes' CMDSS (Table 5). This observation corroborates the results presented in Figure 4 which further highlights the crucial role of the T allele in conferring resistance to CMD. The model's area under curve (AUC) value was 0.61 and the probability that the marker would predict resistance and susceptibility is 0.20 and 0.56, respectively, with an accuracy of 0.77. Bootstrapped samples used for model validation resulted in accuracy values ranging from 0.72 to 0.83 with a mean of 0.77 and AUC values between 0.54 and 0.68 with an average of 0.61 (Supplementary table 2).

**Table 3:** Analysis of variance output for cassava mosaic disease severity scores

Source of variation	d.f.	Sum of square	Mean square	F-value	Pr(>F)
S12_7926132	2	15.001	7.5007	5.8111	0.0038**
S14_4626854	2	0.281	0.1403	0.1087	0.8970
S12_7926132*S14_4626854	3	11.645	3.8816	3.0073	0.0326*
Residuals	132	170.379	1.2907		

\*p<0.05; \*\*p<0.01

**Table 4:** Analysis of variance based marker output for mean incidence of cassava mosaic disease

Source of variation	d.f.	Sum of square	Mean square	F-value	Pr(>F)
S12_7926132	2	17337	8668.6	8.0556	0.0005***
S14_4626854	2	178	88.8	0.0825	0.9208
S12_7926132:S14_4626854	3	16839	5612.9	5.2160	0.0020**
Residuals	123	132360	1076.1		

\*\*p<0.01; \*\*\*p<0.001

### Breeding metrics for marker S12\_7926132 in predicting response to CMD

Of the 145 assayed genotypes, 103 were true positives and 9 were true negatives (Table 6), resulting in an accuracy of 77%. Thus, the misclassification (1-accuracy) was 23%, of which 26 genotypes were false positives and 7 were false negatives.

**Table 5:** A prediction model for CMDSS using binary logistic regression

	Estimate	Standard error	z-value	Pr(> z )
Intercept	0.25	0.504	0.499	0.61800
S12_7926132(TG)	-1.56	0.581	-2.696	0.00701**
S12_7926132(TT)	-1.70	0.605	-2.815	0.00487**

\*\*p<0.01

## Discussion

The highest peak of the average disease severity observed at 1 month after planting in the first year of the field evaluation might be due to an increase in the whitefly (*Bemisia tabaci*) population. Time et al.<sup>27</sup> observed a peak in the whitefly population during the early plant growth stage of cassava (first 30 days after planting) and a decline thereafter during the period of slow cassava growth due to maturity. The observation could also be due to the vector's preference for the succulent nature of plants

**Table 6:** Confusion matrix and derived metrics for mosaic disease severity among cassava genotypes evaluated in Ibadan in two seasons

Prediction by the marker S12_7926132	Prediction in the field	
	Resistant (1.0–2.0)	Susceptible (2.1–5.0)
Resistant	103 TP	26 FP
Susceptible	7 FN	9 TN
Total	145	
Accuracy	Misclassification	Precision
0.77	0.23	0.80

TP=true positive; FP=false positive; FN=false negative; TN=true negative

in their young stages.<sup>27</sup> The slight decrease in the average CMD severity observed in the 2020/2021 cropping season could be as a result of the recovery of some genotypes from CMD infestation or reduced whitefly population. The high broad-sense heritability for CMDSS in the African cassava population suggests that CMD resistance is highly influenced by genetic components. Ige et al.<sup>21</sup> reported a broad-sense heritability of 0.90 in a breeding population of cassava derived from IITA's elite genotype crosses at the clonal evaluation trial stage in 2018.

Three major categories of metrics are usually considered when studying the ability of a marker in a population for the absence or presence of QTLs linked to a trait.<sup>28</sup> These include technical metrics which evaluate the performance of the marker in the genotyping assay, the biological metrics which describe the association of the marker with the QTL/gene/allele, and breeding metrics that check the accuracy of a marker in a particular breeding programme.<sup>28</sup> In our study, there were more false positives than false negatives. This result is consistent with the findings of Javid et al.<sup>29</sup> who validated marker *PsM10* on a set of 171 field pea genotypes for powdery mildew disease resistance and boron tolerance. The low false negative rate observed indicated that the natural exposure method to cassava mosaic geminivirus for phenotypic CMD screening was efficient and Ibadan remains a confirmed area of high disease pressure. The absence of symptoms as observed by the low false negative rate in the field does not reflect genetic resistance to the virus infection; instead, it could suggest a lack of virus infection.<sup>25,30</sup> Symptomless plants could be CMD-free (escapes) or they could have been extremely tolerant.<sup>31,32</sup> Therefore, in combination with field evaluation for CMD, polymerase chain reaction (PCR) detection methods using cassava mosaic geminivirus strain-specific primers is an alternative method that could give more precision about the presence or absence of the virus coat protein in the assayed genotypes.<sup>25,30</sup>

According to Platten et al.<sup>28</sup>, the ideal genetic distance between a marker and its associated QTL/gene should be 0 cM. Rabbi et al.<sup>9</sup> reported that marker S12\_7926132 is about 45 kbp away from the two candidate peroxidase genes, *Manes.12G076300* and *Manes.12G076200*, for CMD resistance. Possible recombination between the marker and the locus, the presence of a marker haplotype indistinguishable from the expected allele size, or possibly another available source of CMD resistance that can be exploited in new breeding programmes might have resulted in the false positives and false negatives.<sup>29</sup>

False positives and false negatives are usually high when a marker is applied to a small breeding population, as in this current study.<sup>28</sup> Many QTL-linked markers discovered might be informative in the mapping population but will perform poorly in other independent populations when used for marker-assisted selection.<sup>28</sup> This usually happens when the marker is used in a population in which at least one parent's QTL status is unknown.<sup>28</sup> This could have also explained the observed false positive and false negative rates as the genotypes screened in this study were derived from open-pollinated crosses. Thus, as the male parents' resistance status are unknown, the resistance allele may not be associated with the *CMD2* locus. The level of accuracy reported in this study is similar to the value (79%) reported for marker *PsM10* for its





association with powdery mildew resistance and the boron tolerance trait across a set of pea germplasm by Javid et al.<sup>29</sup> In a recent study by Ige et al.,<sup>21</sup> similar accuracy values of 80% and 78% were reported in pre-breeding and breeding cassava populations, respectively. On the other hand, the accuracy values reported by Olasanmi et al.<sup>26</sup>, who used simple-sequence repeats to screen five cassava populations at the seedling nursery stage, were lower (61% to 74%) than the value found in the present study. The marker on chromosome 12 was more accurate in predicting susceptibility (56%) than resistance (20%) in our cassava population, which is in contrast with the findings reported by Ige et al.<sup>21</sup> This could be attributed to the higher number of false positive genotypes recorded compared to that of false negatives.

Our study also confirmed the role of the dominant T allele which confers resistance at the *CMD2* locus on chromosome 12 as previously reported by Akano et al.<sup>12</sup> and Rabbi et al.<sup>9</sup> The introgression of this locus into susceptible elite varieties is relatively easy because of its qualitative nature of inheritance.<sup>33</sup> However, vertical resistance is strain-specific and non-durable compared to horizontal resistance which protects the host plant against a wide spectrum of strains with an intermediate level of resistance.<sup>33</sup> Marker-assisted selection has been revealed to be efficient in increasing the selection accuracy, and hence decreasing the rigours of genotype screening across seasons and locations.<sup>26</sup> However, its combination with genomic selection for the selection of genotypes with horizontal resistance would also be recommended for sustainable breeding for CMD resistance.

## Conclusion

We investigated the use of SNP markers S12\_7926132 and S14\_4626854 in predicting resistance to CMD. Marker S12\_7926132 was efficient in detecting the *CMD2* locus in the study population with an accuracy of 77%; hence, the marker could be deployed for marker-assisted selection in African cassava genetic backgrounds. However, its efficiency might be tested on other cassava breeding populations across the globe to expand its deployment for marker-assisted selection. Also, the 103 resistant genotypes identified and selected based on phenotypic scores and marker data could be used as potential parents in breeding programmes targeting CMD resistance on the continent and should also be tested for agronomic traits stability in multi-environments.

## Acknowledgements

We thank the Cassava Improvement Programme of the University of Ibadan, Nigeria, for providing the plant material and the facilities for phenotyping. We acknowledge support from the International Institute of Tropical Agriculture for the genotyping platform and training provided. We also thank Stephen Adiga for his assistance during the establishment of the experiment and field screening for cassava mosaic disease. We are grateful to the African Union Commission for a PhD scholarship granted to E.D.C. to complete a PhD programme in plant breeding at PAULESI, Ibadan, Nigeria.

## Competing interests

We have no competing interests to declare.

## Authors' contributions

E.D.C., B.O. and I.Y.R. conceptualised the study; E.D.C. and B.O. screened the populations in the field for response to CMD; B.O. input and collated the phenotypic data; I.Y.R. developed the SNP markers; R.U. and E.D.C. carried out the genotyping work and collated the molecular data; E.D.C., B.O., P.A., and A.D.I. carried out the statistical analysis; E.D.C. wrote the paper with input and supervision from O.B. and I.Y.R.

## References

1. International Institute of Tropical Agriculture (IITA). Cassava in tropical Africa: A reference manual. Ibadan: IITA; 1990. Available from: [https://www.iita.org/wp-content/uploads/2016/06/Cassava\\_in\\_tropical\\_Africa\\_a\\_reference\\_manual\\_1990.pdf](https://www.iita.org/wp-content/uploads/2016/06/Cassava_in_tropical_Africa_a_reference_manual_1990.pdf)

2. FAOSTAT. Crops and livestock products [webpage on the Internet]. c2019 [cited 2021 May 30]. Available from: <https://www.fao.org/faostat/en/#data/QCL>
3. Nassar NM, Ortiz R. Cassava improvement: Challenges and impacts. *J Agric Sci.* 2007;145(2):163–171. <https://doi.org/10.1017/S0021859606006575>
4. Akinagbe OM. Constraints and strategies towards improving cassava production and processing in Enugu North Agricultural Zone of Enugu State, Nigeria. *Bangladesh J Agric Res.* 2010;35(3):387–394. <https://doi.org/10.3329/bjar.v35i3.6445>
5. Owor B, Legg JP, Okao-Okuja G, Obonyo R, Ogenga-Latigo MW. The effect of cassava mosaic geminiviruses on symptom severity, growth and root yield of a cassava mosaic virus disease-susceptible cultivar in Uganda. *Ann Appl Biol.* 2004;145(3):331–337. <https://doi.org/10.1111/j.1744-7348.2004.tb00390.x>
6. Legg JP, Owor B, Sseruwagi P, Ndunguru J. Cassava mosaic virus disease in East and Central Africa: Epidemiology and management of a regional pandemic. *Adv Virus Res.* 2006;67:355–418. [https://doi.org/10.1016/S0065-3527\(06\)67010-3](https://doi.org/10.1016/S0065-3527(06)67010-3)
7. Patil BL, Fauquet CM. Cassava mosaic geminiviruses: Actual knowledge and perspectives. *Mol Plant Pathol.* 2009;10(5):685–701. <https://doi.org/10.1111/j.1364-3703.2009.00559.x>
8. Legg JP. African cassava mosaic disease. In: Mahy BWJ, Van Regenmortel MHV, editors. *Encyclopedia of virology*. 3rd ed. Cambridge, MA: Academic Press; 2008. p. 30–36. <https://doi.org/10.1016/B978-012374410-4.00693-2>
9. Rabbi IY, Hamblin MT, Kumar PL, Gedil MA, Ikpan AS, Jannink JL, Kulakow PA. High-resolution mapping of resistance to cassava mosaic geminiviruses in cassava using genotyping-by-sequencing and its implications for breeding. *Virus Res.* 2014;186:87–96. <https://doi.org/10.1016/j.virusres.2013.12.028>
10. Houngue JA, Zandjanakou-Tachin M, Ngalle HB, Pita JS, Cacaoi GH, Ngatet SE, et al. Evaluation of resistance to cassava mosaic disease in selected African cassava cultivars using combined molecular and greenhouse grafting tools. *Physiol Mol Plant Pathol.* 2019;105:47–53. <https://doi.org/10.1016/j.pmpp.2018.07.003>
11. Kuria P, Ilyas M, Ateka E, Miano D, Onguso J, Carrington JC, Taylor NJ. Differential response of cassava genotypes to infection by cassava mosaic geminiviruses. *Virus Res.* 2017;227:69–81. <https://doi.org/10.1016/j.virusres.2016.09.022>
12. Akano AO, Dixon AG, Mba C, Barrera E, Fregene M. Genetic mapping of a dominant gene conferring resistance to cassava mosaic disease. *Theor Appl Genet.* 2002;105(4):521–525. <https://doi.org/10.1007/s00122-002-0891-7>
13. Fondong VN. The search for resistance to cassava mosaic geminiviruses: How much we have accomplished, and what lies ahead. *Front Plant Sci.* 2017;8:408. <https://doi.org/10.3389/fpls.2017.00408>
14. Okogbenin E, Egesi CN, Olasanmi B, Ogundapo O, Kahya S, Hurtado P, et al. Molecular marker analysis and validation of resistance to cassava mosaic disease in elite cassava genotypes in Nigeria. *Crop Sci.* 2012;52(6):2576–2586. <https://doi.org/10.2135/cropsci2011.11.0586>
15. Wolfe MD, Del Carpio DP, Alabi O, Ezenwaka LC, Ikeogu UN, Kayondo IS, et al. Prospects for genomic selection in cassava breeding. *Plant Genome.* 2017;10(3):19. <https://doi.org/10.3835/plantgenome2017.03.0015>
16. Ceballos H, Kulakow P, Hershey C. Cassava breeding: Current status, bottlenecks and the potential of biotechnology tools. *Trop Plant Biol.* 2012;5(1):73–87. <https://doi.org/10.1007/s12042-012-9094-9>
17. Talukdar D. Leguminosae. In: Maloy S, Hughes K, editors. *Brenner's encyclopedia of genetics*. 2nd ed. Cambridge, MA: Academic Press; 2013. p. 212–216. <https://doi.org/10.1016/B978-0-12-374984-0.00854-8>
18. Rabbi IY, Kayondo SI, Bauchet G, Yusuf M, Aghoghho CI, Ogunpaimo K, et al. Genome-wide association analysis reveals new insights into the genetic architecture of defensive, agro-morphological and quality-related traits in cassava. *Plant Mol Biol.* 2020, 19 pages. <https://doi.org/10.1007/s11103-020-01038-3>
19. Mukiibi DR, Alicai T, Kawuki R, Okao-Okuja G, Tairo F, Sseruwagi P, et al. Resistance of advanced cassava breeding clones to infection by major viruses in Uganda. *Crop Protect.* 2019;115:104–112. <https://doi.org/10.1016/j.cropro.2018.09.015>



20. Dellaporta SL, Wood J, Hicks JB. A plant DNA miniprep: Version II. *Plant Mol Biol Rep*. 1983;1(4):19–21. <https://doi.org/10.1007/BF02712670>
21. Ige AD, Olasanmi B, Nkouaya Mbanjo EG, Kayondo IS, Parkes EY, Kulakow P, et al. Conversion and validation of uniplex SNP markers for selection of resistance to cassava mosaic disease in cassava breeding programs. *Agronomy*. 2021;11(3):420. <https://doi.org/10.3390/agronomy11030420>
22. R Core Team. R: A language and environment for statistical computing. Vienna: R Foundation for Statistical Computing; 2020. Available from: <http://www.r-project.org/index.html>
23. Dixon P. Should blocks be fixed or random? In: Proceedings of the 28th annual Conference on Applied Statistics in Agriculture; 2016 May 01–03; Manhattan, KS, USA. Manhattan, KS: New Prairie Press; 2016. p. 23–39. <https://doi.org/10.4148/2475-7772.1474>
24. Bradbury PJ, Zhang Z, Kroon DE, Casstevens TM, Ramdoss Y, Buckler ES. TASSEL: Software for association mapping of complex traits in diverse samples. *Bioinformatics*. 2007;23(19):2633–2635. <https://doi.org/10.1093/bioinformatics/btm308>
25. Lokko Y, Danquah EY, Offei SK, Dixon AG, Gedil MA. Molecular markers associated with a new source of resistance to the cassava mosaic disease. *Afr J Biotechnol*. 2005;4(9):873–881. <https://www.ajol.info/index.php/ajol/search?query=doi>
26. Olasanmi B, Kyallo M, Yao N. Marker-assisted selection complements phenotypic screening at seedling stage to identify cassava mosaic disease-resistant genotypes in African cassava populations. *Sci Rep*. 2021;11(1):1–8. <https://doi.org/10.1038/s41598-021-82360-8>
27. Time I, Okoroafor E, Nwogwugwu JO, Batcho AA. Evaluation of whitefly population and weather effect of cassava mosaic incidence on commonly grown cassava in Benue State, Nigeria. *J Appl Sci Environ Manag*. 2020;24(10):1839–1846. <https://doi.org/10.4314/jasem.v24i10.20>
28. Platten JD, Cobb JN, Zantua RE. Criteria for evaluating molecular markers: comprehensive quality metrics to improve marker-assisted selection. *PLoS ONE*. 2019;14(1), e0210529. <https://doi.org/10.1371/journal.pone.0210529>
29. Javid M, Rosewarne GM, Sudheesh S, Kant P, Leonforte A, Lombardi M, et al. Validation of molecular markers associated with boron tolerance, powdery mildew resistance and salinity tolerance in field peas. *Front Plant Sci*. 2015;6:917. <https://doi.org/10.3389/fpls.2015.00917>
30. Ogbé FO. Survey of cassava begomoviruses in Nigeria and the response of resistant cassava genotypes to African cassava mosaic begomovirus infection [PhD thesis]. Ibadan: University of Ibadan; 2001.
31. Thresh JM, Cooter RJ. Strategies for controlling cassava mosaic virus disease in Africa. *Plant Pathol*. 2005;54(5):587–614. <https://doi.org/10.1111/j.1365-3059.2005.01282.x>
32. Asare PA, Galyuon IK, Asare-Bediako E, Sarfo JK, Tetteh JP. Phenotypic and molecular screening of cassava (*Manihot esculentum* Crantz) genotypes for resistance to cassava mosaic disease. *J Gen Mol Virol*. 2014;6(2):6–18. <https://doi.org/10.5897/JGMV2014.0056>
33. Acquaah G. Principles of plant genetics and breeding. Chichester: John Wiley & Sons; 2009. p. 367–383. <https://gtu.ge/Agro-Lib/Principles%20of%20Plant%20Genetics%20and%20Breeding.pdf>

**AUTHORS:**

Annette M. Amakali<sup>1</sup>   
 Ali Halajian<sup>2</sup>   
 Margit R. Wilhelm<sup>1</sup>   
 Martin Tjipute<sup>1</sup>  
 Richard Heckmann<sup>3</sup>  
 Wilmien Luus-Powell<sup>2</sup>

**AFFILIATIONS:**

<sup>1</sup>Department of Fisheries and Aquatic Sciences, University of Namibia, Henties Bay, Namibia  
<sup>2</sup>DSI-NRF SARChI Chair (Ecosystem Health), Department of Biodiversity, University of Limpopo, Polokwane, South Africa  
<sup>3</sup>Department of Biology, Brigham Young University, Provo, Utah, USA

**CORRESPONDENCE TO:**

Ali Halajian

**EMAIL:**

ali\_hal572002@yahoo.com

**DATES:**

**Received:** 31 Oct. 2020

**Revised:** 29 July 2021

**Accepted:** 01 Oct. 2021

**Published:** 27 Jan. 2022

**HOW TO CITE:**

Amakali AM, Halajian A, Wilhelm MR, Tjipute M, Heckmann R, Luus-Powell W. Selected parasites of silver kob (*Argyrosomus inodorus*) (Actinopterygii: Sciaenidae) from northern Namibia. S Afr J Sci. 2022;118(1/2), Art. #9139. <https://doi.org/10.17159/sajs.2022/9139>

**ARTICLE INCLUDES:**

- Peer review
- Supplementary material

**DATA AVAILABILITY:**

- Open data set
- All data included
- On request from author(s)
- Not available
- Not applicable

**EDITORS:**

Bettine van Vuuren   
 Sydney Moyo

**KEYWORDS:**

Monogenea, Acanthocephala, mariculture, Atlantic Ocean, fish parasites

**FUNDING:**

University of Namibia; DSI-NRF SARChI (grant no. 101054)



© 2022. The Author(s). Published under a Creative Commons Attribution Licence.

# Selected parasites of silver kob (*Argyrosomus inodorus*) (Actinopterygii: Sciaenidae) from northern Namibia

The present study reports five metazoan parasites recorded from silver kob (*Argyrosomus inodorus*). Five fish were collected monthly ( $n=55$ ) for 11 months in 2017–2018 (excluding July 2017) using conventional angling gear in Toscanini, Mile 108 and Henties Bay, northern Namibia. Fish were examined individually for ecto- and endo-parasites. Photomicrographs, drawings and measurements of parasites were made using a camera lucida and calibrated eyepiece of an Olympus (BX50) compound microscope and/or a Zeiss (Discovery V8) camera calibrated on a Leica dissecting microscope. Amongst species found, monogeneans including *Diplectanum sciaenae* van Beneden & Hesse, 1863, two species of *Calceostoma* van Beneden, 1858, one species of *Sciaenacotyle* Mamaev, 1989 and one acanthocephalan *Corynosoma australe* Johnston, 1937 were found and are reported here. This is the first study of parasites found from silver kob of the Atlantic Ocean. Silver kob has potential to be used as a mariculture species. In addition to mariculture, information obtained from this study may also be used as a baseline for stock structure and biological tagging.

**Significance:**

- Silver kob has potential to be used as a mariculture species. Information obtained from this study will therefore form awareness to future mariculture silver kob farmers in terms of parasites that can infest and infect silver kob, hence making it possible to apply specific prevention and control measures. In addition to mariculture, results obtained from this study may be used as a baseline for biological tagging for stock structure assessment using parasites.

**Introduction**

Silver kob, *Argyrosomus inodorus* Griffiths & Heemstra, 1995, Actinopterygii, Perciformes, Sciaenidae, commonly known as kabeljou in southern Africa, has a short history of culture in southern Africa.<sup>1,2</sup> Its congeners, *A. hololepidotus* Lacepède, 1801 (Madagascar meagre), *A. japonicus* Temminck & Schlegel, 1843 (dusty kob/mulloway) and *A. regius* Asso, 1801 (meagre) have been cultured successfully for many years throughout the world, including in South Africa.<sup>3–10</sup> The Namibian marine aquaculture (mariculture) is dominated by shellfish (oyster and abalone). There is need to diversify the sector to ensure wide specialisation and make it more economically viable (stable). There are ongoing investigations into the aquaculture of some important finfish species (of which kob is one species of interest). Studies are looking into the captive propagation, larval rearing, feeding and disease (including parasites) aspects of the kob species. Currently in Namibia, silver kob is one of the most important species caught by shore anglers and ski-boat anglers in water shallower than 20 m.<sup>11</sup>

Characteristics of silver kob – such as its robust growth, ability to spawn in captivity as well as its market value – make it one of the fish species suitable for mariculture.<sup>5,6,12</sup> However, various diseases, including parasitic infections, pose a threat to fish cultivation, to the success of mariculture, as well as to the people that depend on it for a basic income. In many instances, fish health is not prioritised until extreme impacts are observed, which means the opportunity to manage and control parasites and diseases at the source is missed. Most farmers tend to react to large outbreaks rather than preventing or managing infections, most likely because of insufficient information on the ecology of pathogenic parasites, their prevention and control.<sup>13</sup> The diseases and specific identity of the parasites that are infecting cultured fish are rarely known and very few parasite species, classified only to their genera, are recorded.<sup>14</sup>

External and internal clinical signs triggered by pathogens depend on the host species, fish age and stage of the disease.<sup>15</sup> Parasites generally do not kill their hosts, but some severely stress fish to the point of biological and economical concern.<sup>16</sup> High intensities of ecto-parasites cause excess mucus secretion, loose scales, dermis injuries such as haemorrhages, open sores, ulcers exposing connective and muscle tissues, and osmotic problems affecting respiratory functions.<sup>16</sup> Consequently, damaged skin and gills make the fish host more susceptible to secondary infections, possibly from viruses, bacteria and other microorganisms that may also contribute to mortalities.<sup>17</sup> Martins et al.<sup>18</sup> and Kotob et al.<sup>19</sup> reviewed impacts of different secondary infections, also called co-infections, on fish species.

In the wild, parasites have been used as a biotic force capable of determining the biodiversity of fish communities.<sup>20</sup> Parasites can regulate the population size of some fish species based on their susceptibility. If the host is the predator, parasite infestation causes lack of appetite, thereafter increasing the number of prey and, as most prey are herbivores, further decreasing the plant community. In addition, parasites can indirectly modify the functional importance of the host species by altering the host's phenotype (morphology, colouration and behaviour) which may influence the availability and scarcity of resources for other species. This could make the host, or part of the host's body, available as a resource to other organisms.<sup>20</sup>

The culture of kob is being considered in Namibia and therefore parasites that infect it are being investigated.

## Known parasites of kob

### *Diplectanum* Diesing, 1858

*Diplectanum*, a genus of monopisthocotylean monogeneans, is the largest genus in the Diplectanidae and consists of over 80 species.<sup>21,22</sup> In nature, species of *Diplectanum* are not highly pathogenic parasites; under adverse conditions, however, they can multiply and have detrimental effects on their hosts.<sup>9</sup> There have been several reports associating monogeneans with increased fish mortalities in aquaculture, mostly because cultured fish are grown in high densities and handling procedures result in fish stress.

### *Calceostoma* van Beneden, 1858

Species in the genus *Calceostoma* have been reported from the gills and skin of fish all over the world, including Australia and southern Africa.<sup>3,21</sup> The genus comprises eight species of which only two described were available for use in the present study: *Calceostoma herculeana* Euzet & Vala, 1975 and *Calceostoma glandulosum* Johnston & Tiegss, 1922, synonym *Calceostoma calceostoma* Wagener, 1857 by Williams<sup>3</sup>. They are not highly pathogenic in nature, but can cause haemorrhages if they intensify in a mariculture set-up.

### *Sciaenacotyle* Mamaev, 1989

Mycrocotylids are recognisable by their possession of large numbers of clamps that are relatively simple and lack accessory sclerites.<sup>5</sup> To date, the genus *Sciaenacotyle* consists of only two documented species: *Sciaenacotyle panceri* Sonsino, 1891 and *Sciaenacotyle sciaenacola* Murray, 1932. There have been reports of these blood-feeding species affecting the gills of sciaenids shi drum (*Umbrina cirrosa* Linnaeus, 1758) in Tunisia<sup>23</sup>, congeners meagre, *Argyrosomus regius* in Sardinia<sup>6</sup> and mullet, *Argyrosomus japonicus* in Australia<sup>7</sup>. They are predominantly characterised by the nature of the genital armature. Their lengths may vary depending on the state of the contraction of the body during fixation or observation and the size of the host, as parasites on larger hosts grow faster than those infesting smaller hosts.<sup>5</sup> In addition, temperature may also impact length and clamp size.

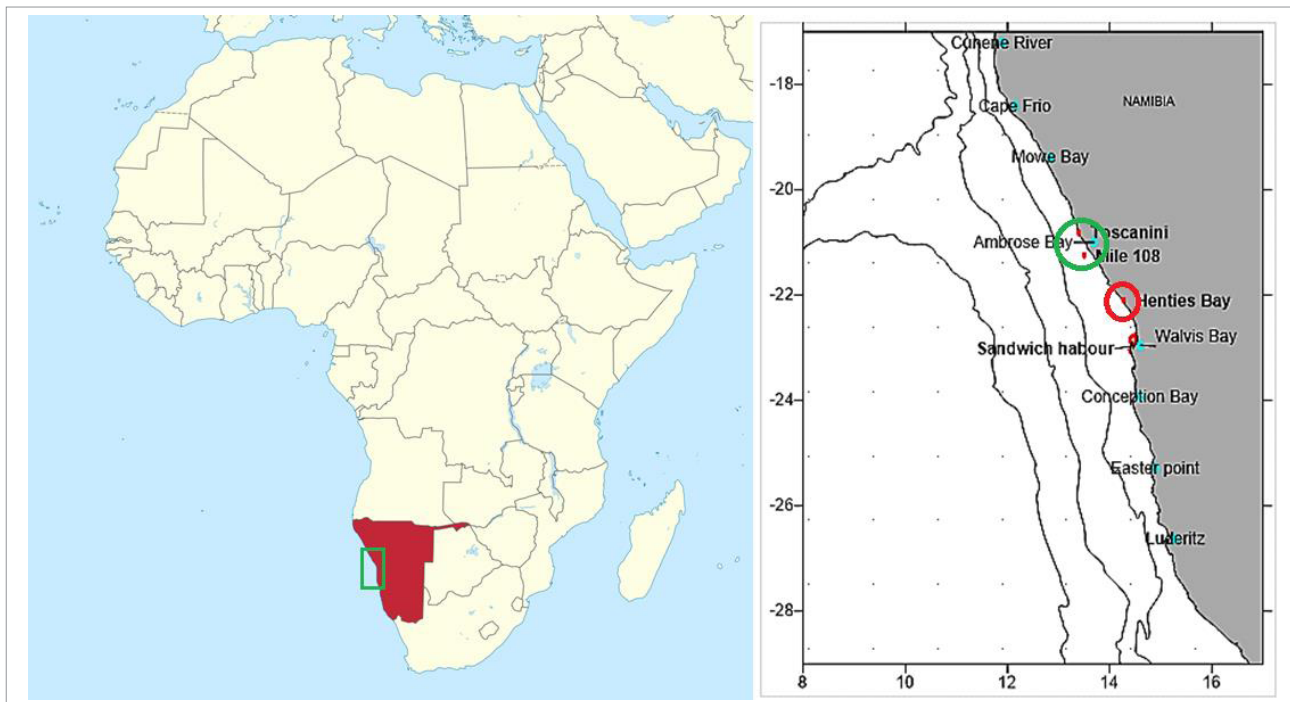
The parasites collected during the current study slightly differ from these two *Sciaenacotyle* species and are briefly described here.

### *Corynosoma* Lühe, 1904

Acanthocephala is a phylum that is closely associated with the Cestoda phylum.<sup>24</sup> They are an integral component of the parasite fauna of pinnipeds. *Corynosoma* Lühe, 1904 consist of numerous species that use cetaceans and fish as intermediate hosts, and pinnipeds and fish-eating birds as definitive hosts.<sup>24-26</sup> Acanthocephalans are characterised by a thorny anterior termed 'proboscis' that serves as an attachment organ and 'drills' firmly into the walls of the intestine and stomach of the host. The proboscis drilling causes damage and changes to the tissues, exposing the tissues to other secondary infections and increasing the host's susceptibility to diseases and infection.<sup>27</sup> Acanthocephalans lack a mouth and digestive tract. They absorb their nutrients directly through their body surface. Adult acanthocephalans usually live in the lumen of the digestive tract only, but sometimes they bore through the walls of the digestive tract and come to lie in the abdominal cavity.<sup>28</sup>

Parasites have also been used as biological tags in stock identification in marine fish according to the principle explained by MacKenzie et al.<sup>29</sup> Fish become infected or infested with a particular parasite only when they come within the endemic area of that parasite – the endemic area being the geographical region in which transmission of the parasite can take place. If infected fish are found outside the endemic area, it is inferred that these fish had been within that area at some time in their past history. Parasite communities differ substantially among fish hosts even in the same geographical area.<sup>30</sup> Parasites, especially monogeneans, are host specific, and this specificity can be so strict that one parasite species may be restricted to only one fish species or genus.<sup>17</sup> The information on the life span of the parasite in that particular host will allow the researcher to estimate the maximum time since the fish could have become infected, that is, the maximum time since it left the endemic area.

Information on parasites infecting silver kob is scarce. Stewart<sup>21</sup> and Christison et al.<sup>31</sup> also reported on *Calceostoma* sp. and *Diplectanum* sp. from the gills of *A. inodorus* in South Africa. Kotungondo has found species of the monogenean *Sciaenacotyle panceri* Sonsino, 1891 on the gills of the Namibian silver kob, *Argyrosomus inodorus* (Kotungondo BCC 2014, written communication, November 24). To the best of our knowledge, there is no previous documented study on parasites of silver



Source: Map on the left: [https://commons.wikimedia.org/wiki/File:Namibia\\_in\\_Africa\\_\(-mini\\_map\\_-rivers\).svg](https://commons.wikimedia.org/wiki/File:Namibia_in_Africa_(-mini_map_-rivers).svg)

**Figure 1:** Sampling area (Toscanini and Mile 108 on the Namibian coast) of silver kob indicated by the green circle and secondary sampling area indicated by the red circle.



kob in Namibia, although there have been a few reports on parasites from its congeners globally. We report on metazoan parasites from silver kob caught in northern Namibia.

## Materials and methods

A total of 55 silver kob were collected over 11 months (June 2017, and August 2017 to May 2018), with 5 fish sampled and examined each month. Of these, 49 silver kob were caught using conventional angling gear at Toscanini and Mile 108, both sites within the Skeleton Coast Park, at about 20°50'S, 13°25'E and 21°49'S, 13°25'E, respectively (Figure 1). Six silver kob were caught by local anglers in Henties Bay (22.1°S and 14.3°E) (Figure 1).

Fish were sacrificed by a single cut through the spinal cord. The skin, fins, eyes and gastrointestinal organs were examined for parasites according to the procedure of Noga<sup>32</sup>. All parasites were identified and counted. In total, 28 species were identified<sup>33</sup>, but for the present study only 5 species are listed and described. Whole mount preparations were made for monogeneans using glycerine ammonium picrate solution on microscope slides and some were preserved in vials with 70% ethanol. Nail varnish was used to seal the whole mounts.

Photomicrographs, drawings and measurements of parasites were made using a camera lucida and calibrated eyepiece of an Olympus (BX50) compound microscope or a Zeiss (Discovery V8) camera calibrated on a Leica dissecting microscope. All measurements are in micrometres ( $\mu\text{m}$ ) unless otherwise indicated. In the descriptions, the initial number is the mean measurement followed by the minimum and maximum measurements (range) in parentheses and finally the number of specimens measured for that particular category ( $n=x$ ).

For scanning electron microscopy, specimens were dehydrated through a series of ethanol (70, 80, 90, 100, and 100%) for 1 h each, followed by immersion in hexamethyldisilazane. After complete evaporation of hexamethyldisilazane, the specimens were sputter coated with gold-palladium in a Polaron SC7640 sputter coater. Specimens were then kept in a fume cupboard so that no dust fell on them while waiting for evaporation of hexamethyldisilazane. The specimens were examined using a LEO VP 1540 microscope at 10 kV.

## Ethics approval

The study was approved by the University of Namibia's Research and Publication Committee.

## Results

During this study, we analysed five helminths identified from silver kob (*A. inodorus*). Some effects of these parasites on their hosts were obvious and profound (damage causing secondary infections, decreased fish quality, reduced growth, etc.) (Table 1).

**Table 1:** Five parasite species found on Namibian silver kob collected from Toscanini, Mile 108 and Henties Bay from June 2017 to May 2018 and their possible pathogenicity

Class	Genus/Order	Species	Pathogenicity
<b>Ecto-parasites</b>			
<b>Monogenea</b>	<i>Diplectanum</i> Diesing, 1858	<i>D. sciaenae</i> van Beneden & Hesse, 1863	Not pathogenic but can have effects on fish quality. Could also act as vectors of viruses and bacteria.
	<i>Calceostoma</i> van Beneden, 1858	<i>C. glandulosum</i> Johnston & Tiegs, 1922	
	<i>Sciaenacotyle</i> Mamaev, 1989	<i>Sciaenacotyle</i> sp.	
<b>Endo-parasites</b>			
<b>Monogenea</b>	<i>Calceostoma</i> van Beneden, 1858	<i>Calceostoma</i> sp.	Unknown
<b>Palaeacanthocephala</b>	<i>Corynosoma</i> Lühe, 1904	<i>C. australe</i> Johnston, 1937	Damage to fish host, causes secondary infections

## Monogeneans

### *Diplectanum sciaenae* van Beneden and Hesse, 1863

Host: *Argyrosomus inodorus* Griffiths and Heemstra, 1995

Site: Skin, gills

Locality: Henties Bay, Mile 108 and Toscanini, Namibia

Description:

Eight whole-mount adult specimens were measured (Diplectanidae; *Diplectanum sciaenae*; Figure 2). Long and slender with total body length measuring 735  $\mu\text{m}$  (436–943) ( $n=8$ ) and mid-body width of 185  $\mu\text{m}$  (117–250) ( $n=8$ ) (Figure 2a). The haptor (Figure 2b), which measured 252  $\mu\text{m}$  (198–310) ( $n=8$ ) total length, consists of a lip-shaped median bar (Figure 2c), which measured 107  $\mu\text{m}$  (97–134) ( $n=8$ ) total length, 23  $\mu\text{m}$  (20–27) ( $n=8$ ) maximum width (i) and 15  $\mu\text{m}$  (12–17) ( $n=8$ ) minimum width (ii) at centre. The haptor has two transverse bars (Figure 2d) on either side of the median bar with total length of 95  $\mu\text{m}$  (81–122) ( $n=8$ ) that mostly meet midway from each side of the median bar, but do not overlap each other. In rare cases, the transverse bars were shifted 1/4<sup>th</sup> from the median bars toward the ends. At the end of each transverse bar lies a pair of curved-in hamuli consisting of a ventral (Figure 2e) and dorsal (Figure 2f) hamulus. The ventral hamulus has a long deep root and a short superficial root with the following dimensions: length (i) 70  $\mu\text{m}$  (64–74) ( $n=8$ ); length (ii) 65  $\mu\text{m}$  (59–67) ( $n=8$ ); length (iii) 37  $\mu\text{m}$  (35–40) ( $n=8$ ), length (iv) 28  $\mu\text{m}$  (25–33) ( $n=8$ ). The dorsal hamulus has a long deep-root and a poorly developed superficial root: length (i) 62  $\mu\text{m}$  (55–65) ( $n=8$ ) and length (ii) 57  $\mu\text{m}$  (52–60) ( $n=8$ ). Just below the median bar, the squamodiscs (Figure 2b) measure 161  $\mu\text{m}$  (124–222) ( $n=8$ ) total length and 140  $\mu\text{m}$  (109–187) ( $n=8$ ) maximum width with 36  $\mu\text{m}$  (32–38) ( $n=8$ ) concentric divergent rows.

The male copulatory organ (MCO) (Figure 2g) is small with 55  $\mu\text{m}$  (50–76) ( $n=8$ ) total length. The MCO widens at the base and has a spiral end encircling the tip end. The sclerotised canal (Figure 2h) at the conspicuous prostatic reservoir measures 29  $\mu\text{m}$  (26–40) ( $n=8$ ) total length and 9  $\mu\text{m}$  (6–12) ( $n=8$ ) maximum width. The sclerotised canal is sharply curved as described for *D. sciaenae* previously.<sup>8,9</sup>

### *Calceostoma glandulosum* Johnston and Tiegs, 1922

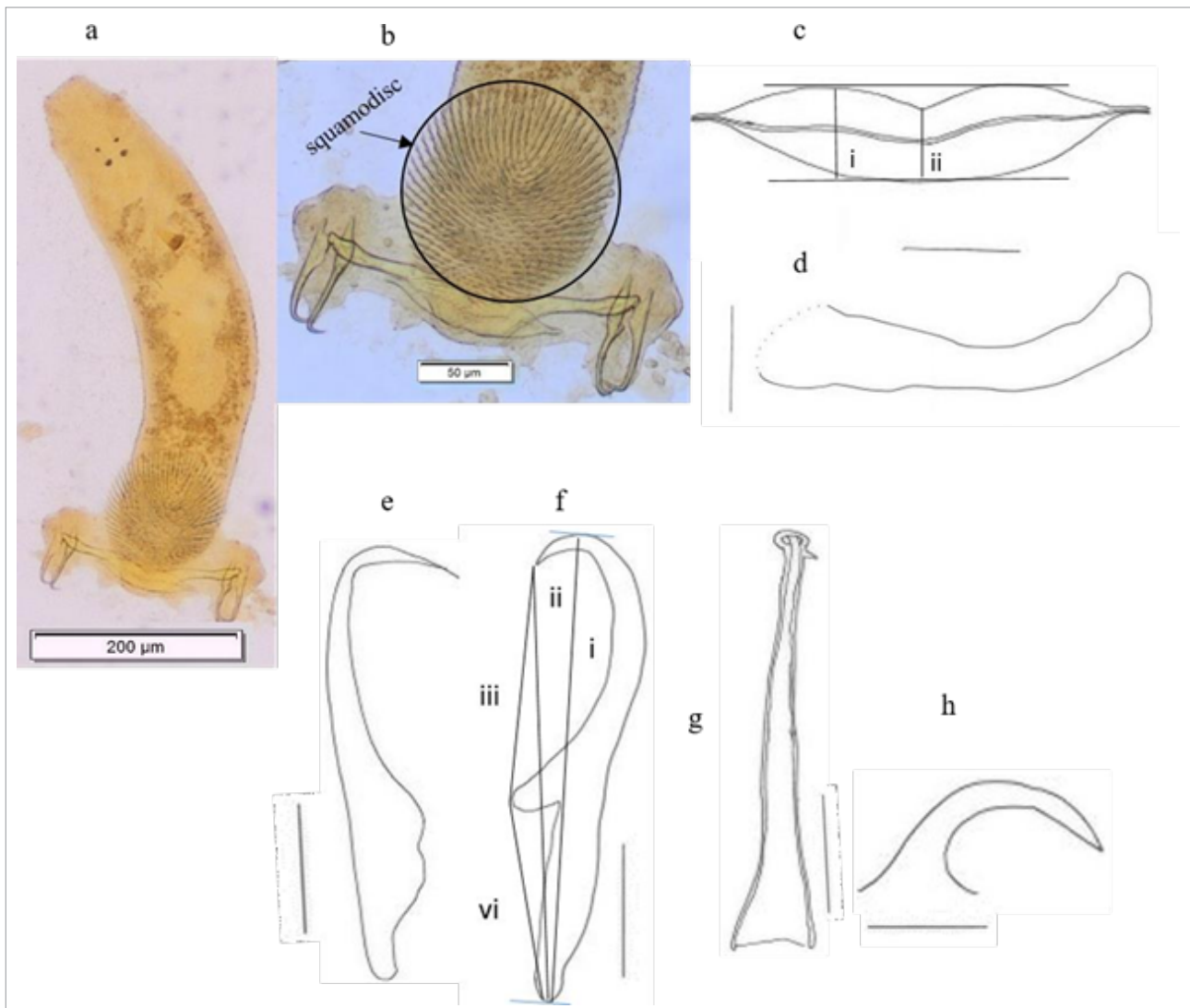
Host: *Argyrosomus inodorus* Griffiths and Heemstra, 1995

Site: Gills, skin

Locality: Henties Bay, Mile 108 and Toscanini, Namibia

Description:

Four whole-mount adult specimens were measured. Body elongated, total body length measures 6250  $\mu\text{m}$  (4200–8000) ( $n=4$ ) and maximum body width 1000  $\mu\text{m}$  (900–1100) (Figure 3). Hood-like lappet (Figure 3e) with irregular margins at anterior end measuring 1225  $\mu\text{m}$  (200–1900) ( $n=4$ ) maximum width. Two pairs of small conspicuous eyespots just anterior to the pharynx. The pharynx (Figure 3e) measures 290  $\mu\text{m}$  (234–322) ( $n=4$ ) total length and 271  $\mu\text{m}$  (227–342) ( $n=4$ ) maximum width. The haptor consists of a median bar with t-shaped



Scale bars: 20  $\mu\text{m}$  (c–h)

**Figure 2:** *Diplectanum sciaenae* van Beneden & Hesse, 1863 from the gills of silver kob. (a) *Diplectanum sciaenae* whole mount. (b) Haptor with squamodiscs and hamuli. (c) Median bar (lengths (i) and (ii)). (d) Transverse bar. (e) Ventral bar/hamulus. (f) Dorsal bar/hamulus with measurements (lengths i–iv). (g) Male copulatory organ. (h) Sclerotised canal.

posterior end and a paddle-shaped anterior end, which is associated with a pair of hamuli (Figure 3a–c). The haptor measures 225  $\mu\text{m}$  (220–233) ( $n=4$ ) and 50  $\mu\text{m}$  (44–53) ( $n=4$ ) anterior end ‘T’ width. The hamulus (Figure 3c) measures 200  $\mu\text{m}$  (188–213) ( $n=4$ ). The MCO (Figure 3d) has a total length (i) of 189  $\mu\text{m}$  (179–195) ( $n=4$ ); length (ii) of 165  $\mu\text{m}$  (159–171) ( $n=4$ ) and width of 24  $\mu\text{m}$  (21–26) ( $n=4$ ).

### ***Calceostoma* sp.**

Host: *Argyrosomus inodorus* Griffiths and Heemstra, 1995

Site: Stomach

Locality: Henties Bay, Mile 108 and Toscanini, Namibia

Description:

These species were found in nine *A. inodorus* hosts throughout the study and from all three study areas. Each host had either one or two *Calceostoma* sp. parasites. They were mostly found attached at the threshold walls of the stomach rather than in the middle of the stomach itself. Three whole-mount specimens were measured. Body slimmer and darker in colour compared to *C. glandulosum*. Total body length 4633  $\mu\text{m}$  (2900–6900) ( $n=3$ ) and 567  $\mu\text{m}$  (400–800) ( $n=3$ ) maximum body width (Figure 4). Lappet not hood-like but less developed (2000  $\mu\text{m}$ ) ( $n=1$ ). This could be an adaptation mechanism to allow it to attach

properly to the host stomach walls. Pharynx (see Figure 3e) length 303  $\mu\text{m}$  (294–312) ( $n=2$ ) and 276  $\mu\text{m}$  (261–292) ( $n=2$ ) pharynx maximum width. The median bar (Figure 4e) measures 147  $\mu\text{m}$  (133–172) ( $n=3$ ) length, 36  $\mu\text{m}$  (33–39) ( $n=3$ ) anterior end ‘V’ width and 144  $\mu\text{m}$  (129–159) ( $n=3$ ) hamulus length, slightly curved in at the tips (Figure 4c). The MCO (Figure 4b) has a coiled anterior end and a thin posterior end and measures 184  $\mu\text{m}$  (173–202) ( $n=3$ ) length (i), 139  $\mu\text{m}$  (125–153) ( $n=3$ ) length (ii) and 13  $\mu\text{m}$  (12–13) ( $n=3$ ) width.

### ***Sciaenacotyle* sp. Mamaev, 1989**

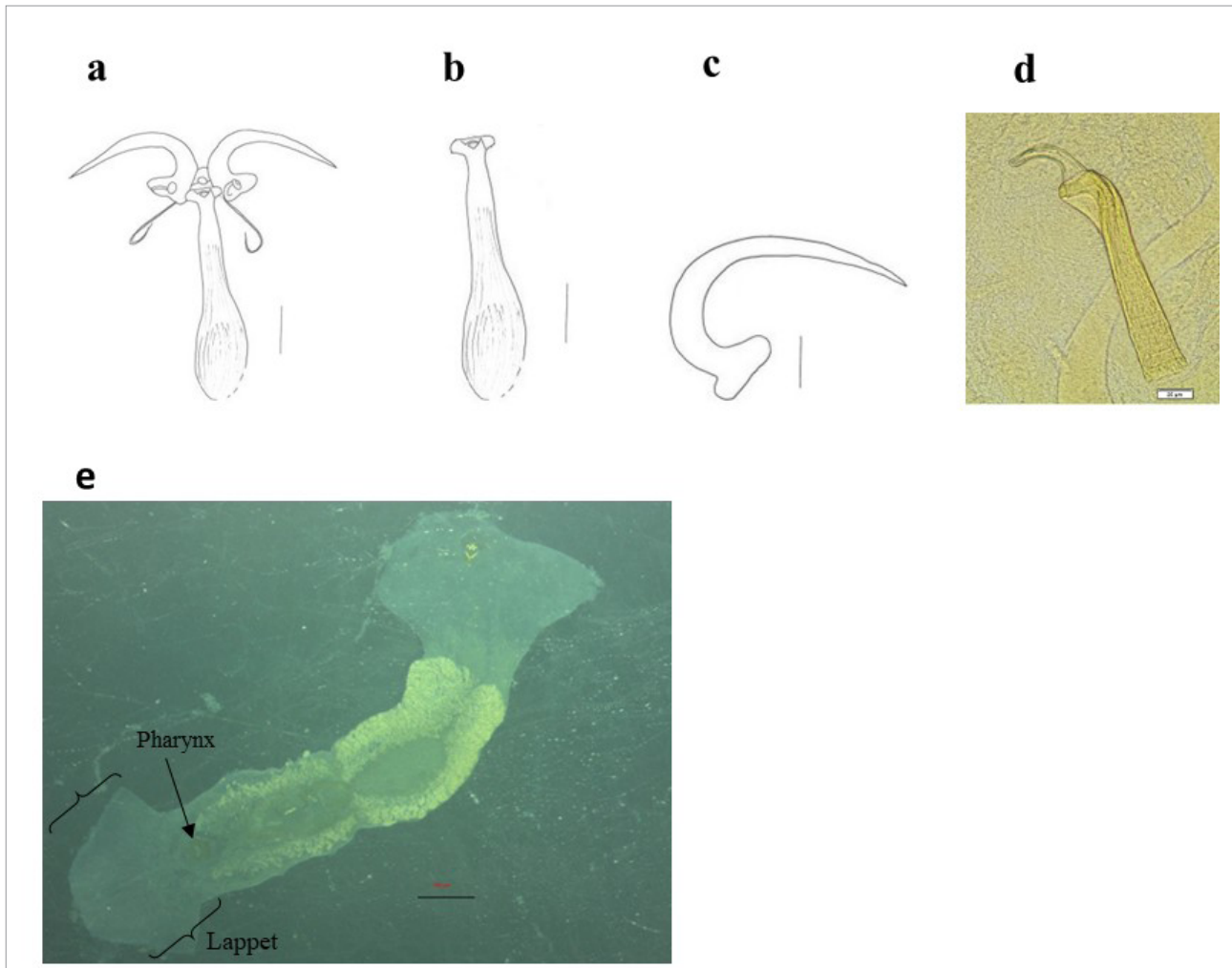
Host: *Argyrosomus inodorus* Griffiths and Heemstra, 1995

Site: Gills

Locality: Henties Bay, Mile 108 and Toscanini, Namibia

Description:

Thirteen whole-mount specimens were measured. Elongated body measures 8123  $\mu\text{m}$  (4000–11 400) ( $n=13$ ) total body length and 1208  $\mu\text{m}$  (500–1800) ( $n=13$ ) maximum body width (Figure 5). Possesses a triangular posterior haver that occupies about a third of the total body with numerous clamps (Figure 5f). The haver measures 4000  $\mu\text{m}$  (1600–5400) ( $n=13$ ). The genital atrium (Figure 5a) opens ventrally, is formed by two globular muscular masses, and consists of



Scale bars: 20  $\mu\text{m}$  (a–d); 2.5 mm (e)

**Figure 3:** *Calceostoma glandulosum* Johnston & Tiegs, 1922 collected from gills of silver kob. (a) Haptor with median bar and hamuli. (b) Median bar. (c) Hamulus. (d) Male copulatory organ. (e) Whole mount.

two symmetrical continuous genital hamuliform spine rows (instead of three as described in the other two *Sciaenacotyle* species), parallel to each other (Figure 5a). These spinal rows of the genital atrium (Figure 5a and 5c) interchange where they bend anteriorly with the longer outer spinal row coiling outwards at the anterior end and the shorter spinal row coiling inwards at the anterior end as they continue in a parallel manner. The genital hamuliform spines of the outer spiral rows increase toward the end of the row (Figure 5b). The hamuliform spine counts were 139 (131–154) ( $n=5$ ) in total number and measure length at posterior end 11  $\mu\text{m}$  (6–16) ( $n=5$ ) (Figure 5d); mid-length 21  $\mu\text{m}$  (14–28) ( $n=5$ ) (Figure 5c) and length at anterior end 8  $\mu\text{m}$  (3–11) ( $n=5$ ) (Figure 5b). Spines at the anterior end slightly curved compared to the spines at the posterior end, which are straight and also sharper. Spines at the middle of the row have a hook that is curved and a blade that is curved at almost 90° (Figure 5c).

### Acanthocephalan

#### *Corynosoma australe* Johnston, 1937

Host: *Argyrosomus inodorus* Griffiths and Heemstra, 1995

Site: Body cavity

Locality: Henties Bay, Mile 108 and Toscanini, Namibia

Description:

The measurements of *C. australe* in this study are not described separately for female and male individuals due to the small number of specimens measured, but, generally, males had more and longer genital

spines than females. Measurements were done in relation to Sardella et al.<sup>25</sup> Six whole-mount specimens were measured (3 males, 3 females). Total body length 3331  $\mu\text{m}$  (2867–3647) ( $n=5$ ) and maximum body width 1076  $\mu\text{m}$  (943–1211) ( $n=6$ ) (Figure 6). Females possessed a relatively wider maximum body width than males. The spiny proboscis measures 556  $\mu\text{m}$  (356–712) ( $n=6$ ) total length and 269  $\mu\text{m}$  (238–290) ( $n=6$ ) maximum width. Proboscis receptacle 1194  $\mu\text{m}$  (936–1339) ( $n=5$ ) total length and 276  $\mu\text{m}$  (227–331) ( $n=5$ ) width. The neck, wider than long, total length 258  $\mu\text{m}$  (236–273) ( $n=5$ ) and maximum neck width 424  $\mu\text{m}$  (400–448) ( $n=5$ ). Trunk length measures 2448  $\mu\text{m}$  (2063–2617) ( $n=5$ ) and is relatively longer in males than in females. The genital spines have a length of 32  $\mu\text{m}$  (18–45) ( $n=6$ ) and mid-width of 14  $\mu\text{m}$  (7–21) ( $n=6$ ). Only one of the three males had testes visible enough to make accurate measurement: right testes length 117  $\mu\text{m}$ ; right testes width 85  $\mu\text{m}$ ; left testes length 112  $\mu\text{m}$ ; and left testes width 88  $\mu\text{m}$ .

### Discussion

We have reported five parasite species from silver kob (*A. inodorus*): *Diplectanum sciaenae*, *Calceostoma glandulosum*, *Calceostoma* sp., *Sciaenacotyle* sp. and *Corynosoma australe*.

The morphological characteristics and measurements of *D. sciaenae* correspond with those described previously<sup>9,34</sup> (Table 2). Diplectanids have been reported several times in aquaculture from all over the world, with increasing mortality in sciaenids, but they are not highly pathogenic parasites in nature.<sup>9</sup>

**Table 2:** Measurements ( $\mu\text{m}$ ) of *Diplectanum* Diesing, 1858 species from *Argyrosomus hololepidotus*, *Argyrosomus regius* and *Argyrosomus inodorus*

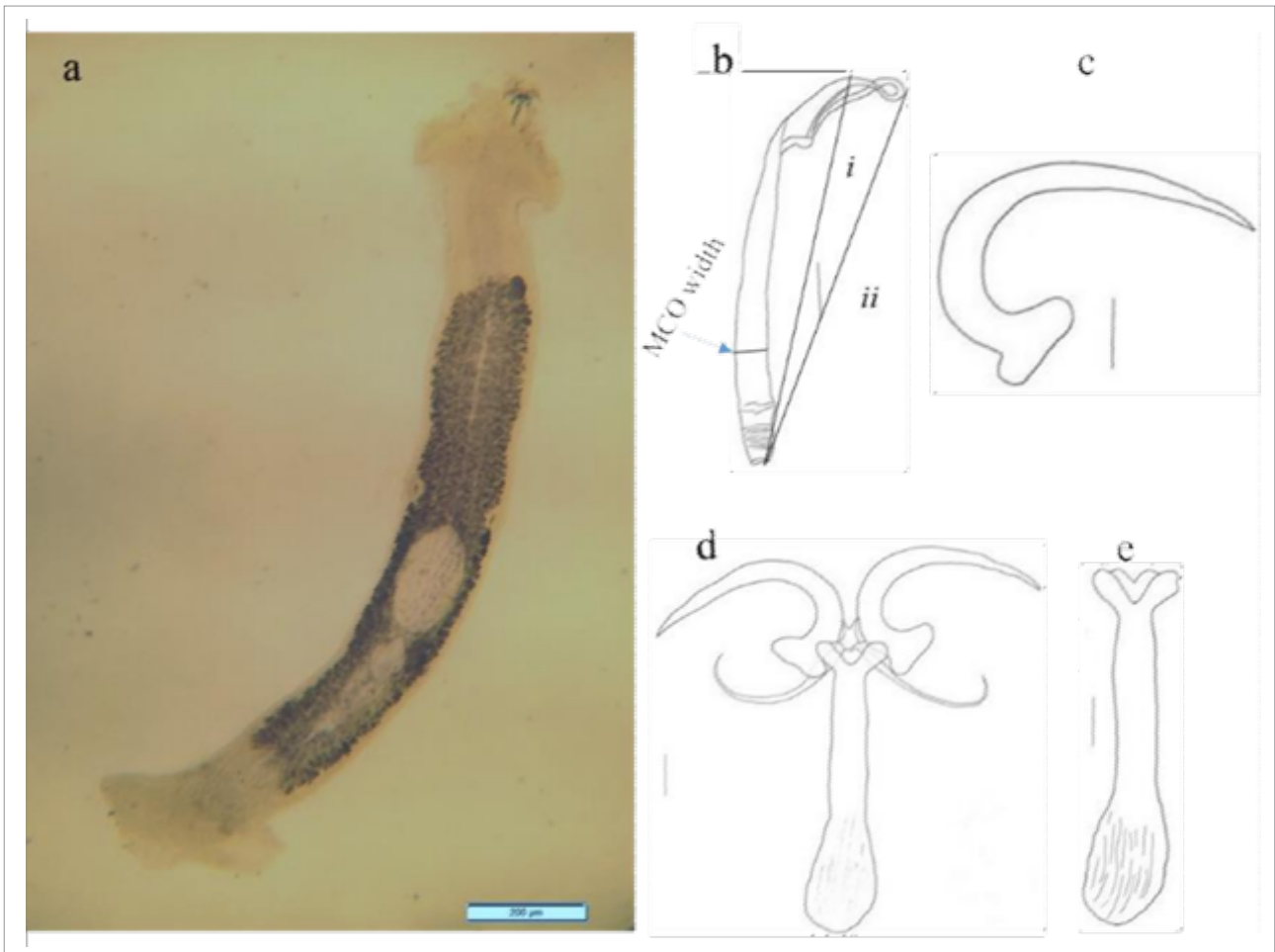
Character	<i>D. oliveri</i> <sup>a</sup>	<i>D. glandulosum</i> <sup>a</sup>	<i>D. dollfus</i> <sup>b</sup>	<i>D. bocqueti</i> <sup>b</sup>	<i>D. sciaenae</i> <sup>b</sup>	<i>D. sciaenae</i> <sup>c</sup>
Host	<i>A. hololepidotus</i>	<i>A. hololepidotus</i>	<i>A. regius</i>	<i>A. regius</i>	<i>A. regius</i>	<i>A. inodorus</i>
Body length	909 – 1139	499 – 640	660 – 1370	800 – 1230	500 – 1160	751 (436–1066)
Body width	166 – 224	128 – 154	160 – 370	240 – 370	140 – 400	165 (79–250)
Haptor width	224 – 275	243 – 269	230 – 480	120 – 400	260 – 380	252 (198–310)
Penis length	166 – 179	51 – 66	57 – 78	90 – 123	51 – 94	63 (49–76)
Canal length	–	–	–	–	–	29 (26–40)
Canal width	–	–	–	–	–	9 (5–12)
Squamodisc length	–	–	–	–	–	173(124–222)
Squamodisc width	166 – 189	99 – 106	144 – 160	120 – 160	144 – 170	148 (109–187)
Concentric rows	–	–	32 – 38	26 – 32	31 – 41	35 (32–38)
Median bar length	128 – 158	117 – 153	108 – 159	102 – 132	95 – 150	107 (97–134)
Median bar width	–	–	–	–	–	23 (19–27)
Median bar 1/2 width	–	–	–	–	–	15 (12–17)
Transverse bar length	96 – 110	90 – 117	92 – 146	88 – 100	88 – 100	94 (81–122)
Ventral hamulus (a)	67 – 77	72 – 77	87– 94	58 – 67	69 – 79	70 (64–74)
Ventral hamulus (b)	–	65 – 69	78 – 86	52 – 63	63 – 73	65 (59–67)
Ventral hamulus (c)	32 – 34	34	43 – 50	27 – 32	33 – 41	37 (34–40)
Ventral hamulus (d)	30 – 32	30 – 32	33 – 39	25 – 32	26 – 35	28 (25–33)
Dorsal hamulus (a)	66 – 70	64 – 67	83 – 89	57 – 62	62 – 68	62 (55–65)
Dorsal hamulus (b)	61 – 64	59 – 64	62 – 135	51 – 56	59 – 64	57 (52–60)

<sup>a</sup>Williams<sup>3</sup>; <sup>b</sup>Oliver<sup>24</sup>; <sup>c</sup>present study

**Table 3:** Measurements ( $\mu\text{m}$ ) of *Calceostoma glandulosum* Johnston & Tiegs, 1922, *Calceostoma calceostoma* Wagener, 1857 and *Calceostoma* sp. from *Argyrosomus hololepidotus*, *Argyrosomus regius* and *Argyrosomus inodorus*

Character	<i>C. glandulosum</i>	<i>C. calceostoma</i>	<i>C. calceostoma</i>	<i>C. glandulosum</i>	<i>Calceostoma</i> sp.
Host	<i>A. hololepidotus</i> (Western Australia)	<i>A. regius</i> (Tunis)	<i>A. regius</i> (Gulf of Gascoigne)	<i>A. inodorus</i> (northern Namibia)	<i>A. inodorus</i> (northern Namibia)
Total length	2724 (1848–4176)	3295 (2875–4002)	6302	6250 (4200–8000)	46332900–6900
Max body width	748 (592–960)	632 (598–644)	759–1012	1000 (900–1100)	566 (400–800)
Lappet max width	794 (504–1296)	776 (644–897)	943	1225 (200–1900)	2000
Pharynx length	210 (157–272)	202 (179–216)	273 (255–291)	289 (236–322)	303 (293–312)
Pharynx width	168 (132–208)	164 (156–179)	–	270 (226–342)	276 (260–292)
Median length	238 (243–236)	178 (154–207)	239 (230–251)	225 (219–233)	146 (132–172)
Median max width	–	–	–	50 (44–53)	36 (32–39)
Hamulus length	129 (112–139)	94 (71–106)	135 (124–147)	199 (188–213)	143. (128–159)
Penis length (a)	182	134 (124–152)	189 (179–209)	188 (178–195)	183 (172–202)
Penis length (b)	–	–	–	165 (159–171)	138 (124–153)
Penis width	23	14 (12–14)	19 (14–23)	24 (21–26)	12 (11–13)
Study	Williams <sup>3</sup>	Williams <sup>3</sup>	Williams <sup>3</sup>	This study	This study





Scale bars: 20  $\mu\text{m}$  (a–d). 2.5 mm (e)

**Figure 4:** *Calceostoma* sp. collected from stomach of silver kob. (a) Whole mount. (b) Male copulatory organ. (c) Hamulus. (d) Haptor with median bar and hamuli. (e) Median bar.

*Calceostoma glandulosum* in the present study was longer and wider than described by Williams<sup>3</sup> (Table 3). The reason could be due to stretching of the parasites during mounting on the slides, as monogeneans were fixed without coverslip pressure. Williams<sup>3</sup> also found that *Calceostoma calceostoma* in *Argyrosomus regius* from Tunis differed in size (were smaller) compared to *Calceostoma calceostoma* Wagener, 1857 in *Argyrosomus regius* from the Gulf of Gascogne. This means that *Calceostoma* species may vary according to their geographical distribution with different physical and chemical environmental parameters.

A calceostomatid *Calceostoma* sp., possessing morphological characteristics almost similar to an undescribed *Calceostoma* sp. found by Stewart<sup>21</sup> from the gills of *Argyrosomus inodorus*, was found in the stomach of *A. inodorus*. Stomach dactylogyrid monogeneans such as *Enterogyrus* Paperna, 1963 have been documented on freshwater fish by Bayoumy and El-Monem<sup>35</sup> and others, but they possess different haptor and copulatory characteristics that enable them to adapt to the internal environment of their fish hosts. This is the first case of a calceostomatid in the gastrointestinal organs of marine species and more studies are necessary to understand the differences and/or similarities between these two species as well as their parasitic behaviours and pathogenic characteristics.

It could be assumed that because these *A. inodorus* feed on small pelagic fish (mostly sardine based on their gut content), the monogenean parasites could have survived from the gills of sardine (*Sardinops* sp.) into the stomach of *A. inodorus* during ingestion. To test this hypothesis, the inspection of sardine gills is required to confirm whether *Calceostoma* sp. infest the gills of sardine. Only one or two individual *Calceostoma* sp.

were found in every infected *A. inodorus* host. These may have been individuals that 'luckily' managed to survive the new environment of the stomach, despite being morphologically adapted to live and reproduce on the gills. The life cycle of a monogenean involves a free-living ciliated larva, called oncomiracidium.<sup>34,36</sup> Chances are that a few parasites of *Calceostoma* sp. accumulated from the aquatic environment when fish were feeding and very few individuals managed to survive at the

**Table 4:** Measurements ( $\mu\text{m}$ ) of *Sciaenacotyle* sp. from *Argyrosomus inodorus* from northern Namibia

Character	Mean	Minimum	Maximum
Body length	8123	4000	11 400
Body width	1208	500	1800
Tail length	4000	1600	5400
Genital spine rows	2	2	2
No. of hamuliform spines			
Row 1	139	131	154
Row 2	154	148	163
Length at posterior end	11	6	16
Mid-length	21	14	28
Length at anterior end	8	3	11

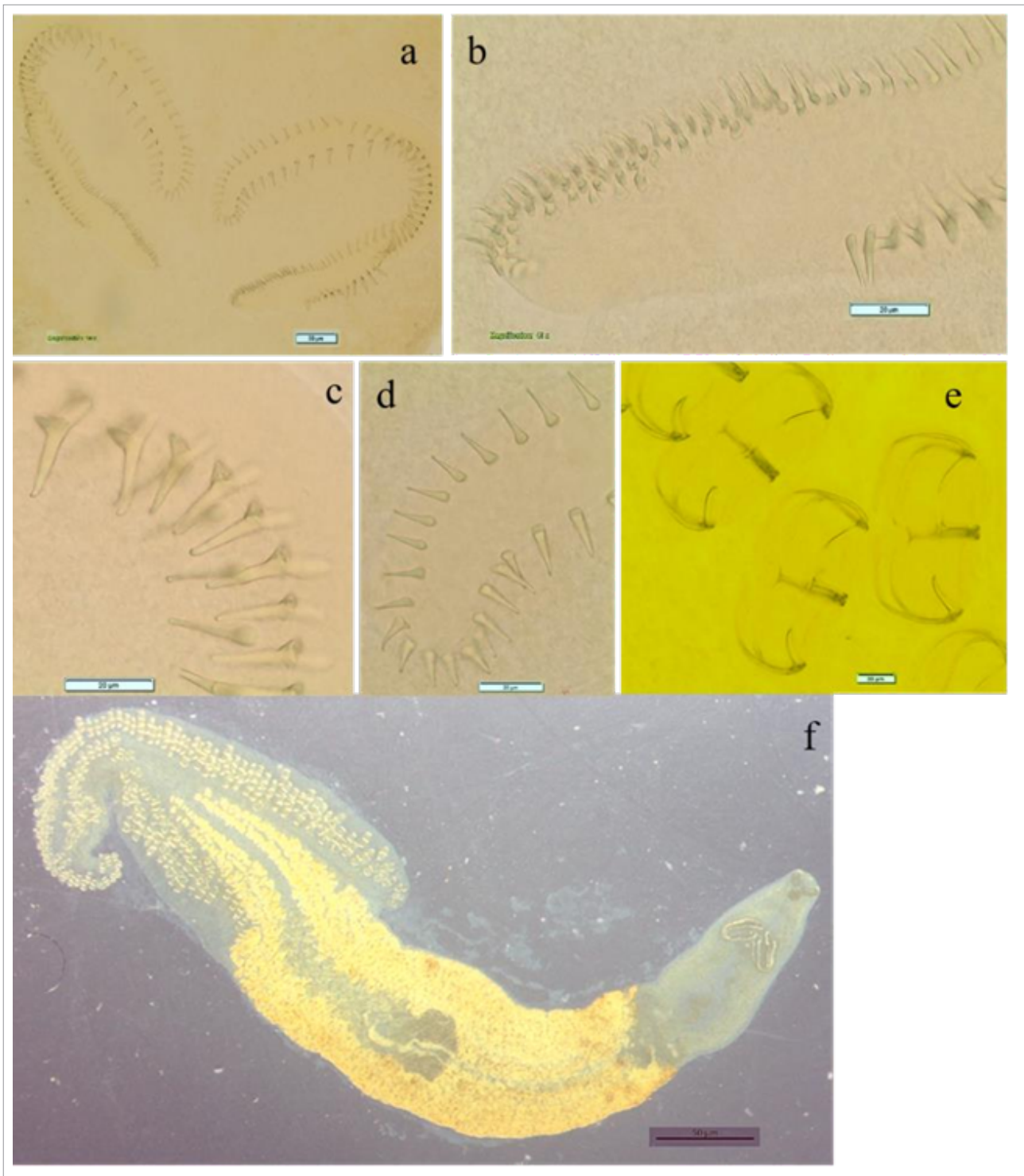


**Figure 5:** *Sciaenacotyle* sp. collected from the gills of silver kob. (a) Genital atrium. (b) Genital anterior end hamuliform spines. (c) Genital mid hamuliform spines. (d) Genital posterior end hamuliform spines. (e) Clamps. (f) Whole mount.

threshold of the stomach walls, where all these parasites were recovered. More studies, including molecular work on *Calceostoma* species from the gills, previously described<sup>33</sup>, and *Calceostoma* sp. from the stomach, are therefore required to supplement the similarities described in this study, explain the survival of this parasite and understand the unusual adaptive mechanism of this gill monogenean parasite, which allows it to survive in the stomach of its *A. inodorus* host.

The microcotylid *Sciaenacotyle* sp. in the present study differed in makeup of their genital atrium from the other two *Sciaenacotyle* species, *S. sciaenicola*<sup>5</sup> and *S. pancer*<sup>6,23</sup>, previously described. The two species

possess a genital atrium consisting of three genital spine rows. However, the microcotylid in the present study possessed a genital atrium consisting of two genital spine rows. In addition, *Sciaenacotyle* sp. has more genital spines with a smaller minimum length than those described for the two previously described species (Table 4).

Sardella et al.<sup>25</sup> showed that adult *C. australe* differed in size from different hosts (seal *Arctocephalus australis* and fish hosts *Corynoscion quatuorcupa*). *Corynosoma australe* from the present study were larger than those formerly described.<sup>14</sup> They also possessed longer proboscis, neck and truck lengths (Table 5).

**Table 5:** Measurements ( $\mu\text{m}$ ) of *Corynosoma australe* Johnston, 1937 from *Arctocephalus australis*, *Cynoscion guatucupa* and *Arygosomus inodorus*

Host	<i>A. australis</i> <sup>a</sup>	<i>C. guatucupa</i> <sup>a</sup>	<i>A. inodorus</i> <sup>b</sup>
Body L (length)	4200–5500	2560–3180	3331 (2867–3647)
Body W (width)	1300–1620	760–1140	1076 (943–1211)
Proboscis L	580–740	580–740	556 (356–712)
Proboscis W	210–250	180–280	269 (238–290)
Neck L	160–260	19–270	258 (236–273)
Neck max W	360–500	260–420	424 (400–448)
Trunk L	3420–4660	1640–2180	2448 (2063–2617)
Genital spines L	25–48	31–48	32 (24–39)
Genital spines W	8.0–29	8.0–27	14 (9–17)
Proboscis receptacle L	740–1040	860–1300	1194 (936–1390)
Proboscis receptacle W	140–200	140–280	276 (227–331)
Right testes L	440–700	100–140	117
Right testes W	260–420	80–120	85
Left testes L	400–660	110–140	112
Left testes W	280–420	80–120	88

<sup>a</sup>Sardella et al.<sup>25</sup>; <sup>b</sup>present study

This is the first descriptive study of parasites of *A. inodorus* in Namibia. More studies are required to complement the findings. The presence of parasites from *A. inodorus* hosts highlights the need for further surveillance of the health of fish, especially when used in an aquaculture set-up.<sup>5</sup>

Results from this study are also a significant tool towards stock identification, which is a key component for the management of economically important fish species. They will contribute to and improve the understanding of the vulnerability of unequally exploited subpopulations within the *A. inodorus* species range and thus help with the implementation of sustainable fisheries practices.<sup>37</sup> Biological tags used for stock identification is significant research given the rise in global fisheries as more species are being targeted and commercially exploited to keep up with the increasing demand.<sup>38</sup> Many natural tags have been used in population structure studies but parasites as biological tags have gained wide acceptance in recent decades as they can provide a reliable guide to understanding the biology of the hosts.<sup>39</sup> Parasites as biological tags for stock identification have not been used in Namibia, but they have been used successfully in South Africa to identify between two hake species (*Merluccius capensis* Castelnau, 1861 and *Merluccius paradoxus* Franca, 1960)<sup>40</sup> and recently for sardine species (*Sardinops sagax* Jenyns, 1842)<sup>41</sup>. This study will significantly add to that resource and create a threshold for more studies on *A. inodorus* and other marine fish species.

### Acknowledgements

We acknowledge a NAMSOV fellowship from the University of Namibia for funding the study. This work was supported by the South African Research Chairs Initiative (SARChI) of the Department of Science and Innovation and National Research Foundation of South Africa. Any opinion, finding and conclusion or recommendation expressed in this material is that of the authors and the NRF does not accept any liability in this regard.

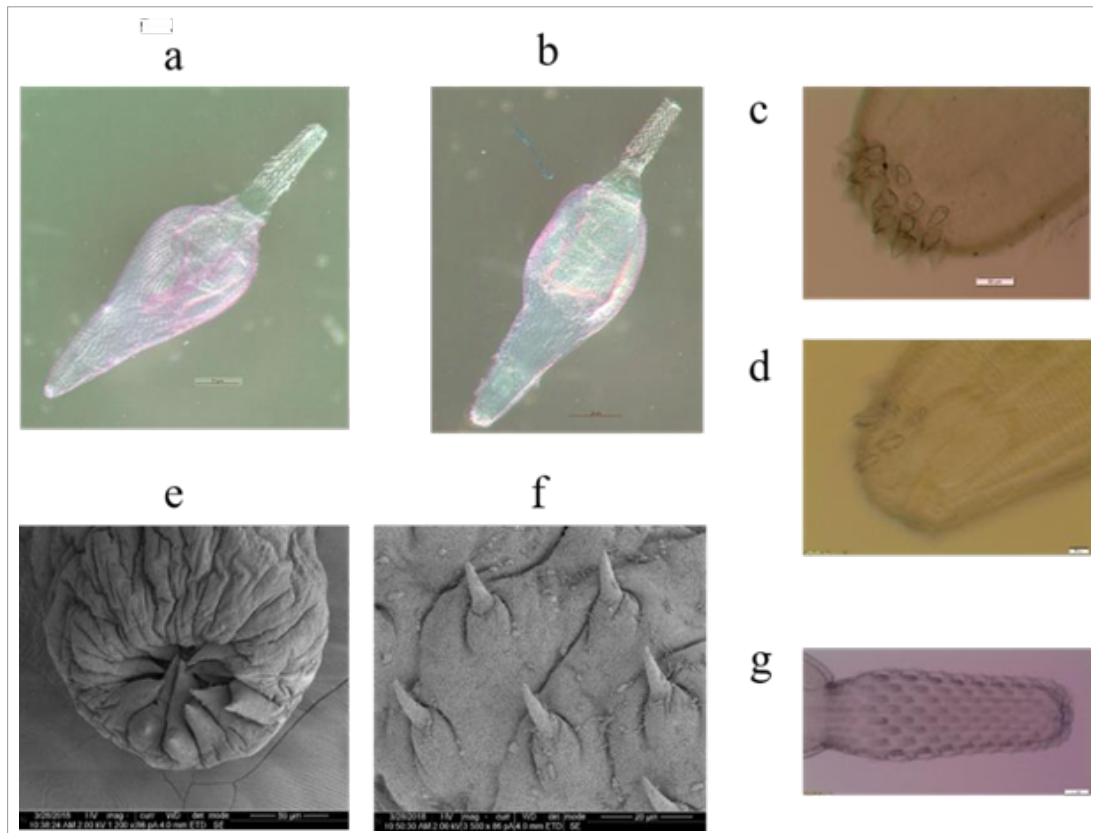


**Figure 6:** *Corynosoma australe* Johnston, 1937 collected from the body cavity of silver kob. (a) Female and (b) male. (c) Male and (d) female genital spines of adult *C. australe*. (e) Scanning electron micrograph (SEM) of spines at the folded in neck of *C. australe*. (f) SEM of spines. (g) Proboscis of adult *C. australe*, notice hooks.





## Competing interests

We have no competing interests to declare.

## Authors' contributions

A.M.A.: Methodology, data collection, data analysis, writing – the initial draft, writing – revisions. A.H.: Student supervision, project leadership, validation. M.J.W.: Student supervision, project leadership, validation. M.T.: Student supervision, methodology, data collection. R.H.: Validation. W.L.-P.: Student supervision, funding acquisition, validation.

## References

- Griffiths MH. The taxonomy and life-history of *Argyrosomus japonicus* and *A. inodorus*, two important sciaenids off the South African coast [PhD thesis]. Makhanda: Rhodes University; 1995.
- Griffiths MH. The life history and stock separation of silver kob, *Argyrosomus inodorus*, in South African waters. *Oceanogr Lit Rev.* 1997;11(44):1358–1359.
- Williams A. Some monogenean parasites of the genera *Calceostoma* van Beneden, 1852 and *Diplectanum* Diesing, 1858 from *Argyrosomus hololepidotus* (Lacepède, 1802) (Sciaenidae: Teleostei) in Western Australia. *Syst Parasitol.* 1989;14(3):187–201. <https://doi.org/10.1007/bf02187053>
- Grab DJ. Parasitological Society of Southern Africa. *J S Afr Vet Assoc.* 2005;76(3):172–183. <https://doi.org/10.4102/jsva.v76i3.421>
- Hayward CJ, Bott NJ, Itoh N, Iwashita M, Okihiro M, Nowak BF. Three species of parasites emerging on the gills of mulloway, *Argyrosomus japonicus* (Temminck and Schlegel, 1843), cultured in Australia. *Aquaculture.* 2007;265(1–4):27–40. <https://doi.org/10.1016/j.aquaculture.2007.04.080>
- Merella P, Cherchi S, Garippa G, Fioravanti ML, Gustinelli A, Salati F. Outbreak of *Sciaenacotyle panceri* (Monogenea) on cage-reared meagre *Argyrosomus regius* (Osteichthyes) from the western Mediterranean Sea. *Dis Aquat Org.* 2009;86(2):169–173. <https://doi.org/10.3354/dao02115>
- Hutson KS, Catalano SR, Whittington ID. Metazoan parasite survey of selected macro-inshore fish of southeastern Australia, including species of commercial importance. No. 2007/225. Townsville: James Cook University; 2011.
- Oliva ME, Valdivia IM, Chavez RA, Molina H, Cárdenas L. Molecular and morphological evidence demonstrating two species of *Helicometrina* Linton 1910 (Digenea: Opecoelidae) in Northern Chile. *J Parasitol.* 2015;101(6):694–700. <https://doi.org/10.1645/14–523>
- Andree KB, Roque A, Duncan N, Gisbert E, Estevez A, Tsertou MI, et al. *Diplectanum sciaenae* (Van Beneden & Hesse, 1863) (Monogenea) infecting meagre, *Argyrosomus regius* (Asso, 1801) broodstock in Catalonia, Spain. A case report. *Vet Parasitol Reg Stud Reports.* 2015;1:75–79. <https://doi.org/10.1016/j.vprsr.2016.02.006>
- Costa JZ, McCarthy Ú, Perez O, Ramos E, Rodríguez M, Monterroso O, et al. Occurrence of *Photobacterium damsela* subsp. *Piscicida* in sea-cage farmed meagre (*Argyrosomus regius*) in Tenerife, Canary Islands, Spain. *Int J Mar Sci.* 2017;33(1):65–71. <https://doi.org/10.1007/s41208–017–0022–5>
- Kirchner CH, Stage J. An economic comparison of the commercial and recreational line fisheries in Namibia (No. 71). Windhoek: Directorate of Environmental Affairs, Ministry of Environment and Tourism; 2005.
- Tjipute M. Feasibility study for mass production of the silver kob, *Argyrosomus inodorus*, in Namibia. Reykjavik: United Nations University – Fisheries Training Programme; 2011.
- Iwanowicz DD. Overview on the effects of parasites on fish health. In: Proceedings of the Third Bilateral Conference between Russia and the United States: Bridging America and Russia with shared perspectives on aquatic animal health. Landover, MD: Khaled bin Sultan Living Oceans Foundation; 2011. p. 176–184.
- Woo PT, Gregory DWB, editors. Diseases and disorders of finfish in cage culture. Wallingford: CAB; 2014. <https://doi.org/10.1079/9781780642079.0000>
- Labella A, Berbel C, Machado M, Castro D, Borrego JJ. *Photobacterium damsela* subsp. *damsela*, an emerging pathogen affecting new cultured marine fish species in southern Spain. In Recent advances in fish farms. Malaga: Institution of Technology; 2011. <https://doi.org/10.5772/26795>
- Bruno DW, Noguera PA, Poppe TT. A colour atlas of salmonid diseases. Vol. 91. Aberdeen: Springer Science & Business Media; 2013. <https://doi.org/10.1007/978-94-007-2010-7>
- Rohde K, Rohde PP. The ecological niches of parasites. In: Rohde K, editor. Marine Parasitology. Wallingford: CAB; 2005. p. 286–293. <https://doi.org/10.1079/9780643090255.0000>
- Martins ML, Cardoso L, Marchiori N, Benites de Pádua S. Protozoan infections in farmed fish from Brazil: Diagnosis and pathogenesis. *Rev Bras DE Parasitol Vet.* 2015;24(1):1–20. <https://doi.org/10.1590/s1984–29612015013>
- Kotob MH, Menanteau-Ledouble S, Kumar G, Abdelzاهر M, El-Matbouli M. The impact of co-infections on fish: A review. *Vet Res.* 2017;47(1):98. <https://doi.org/10.1186/s13567–016–0383–4>
- Poulin R. The functional importance of parasites in animal communities: Many roles at many levels? *Int J Parasitol.* 1999;29(6):903–914. [https://doi.org/10.1016/s0020–7519\(99\)00045–4](https://doi.org/10.1016/s0020–7519(99)00045–4)
- Stewart KA. Embryonation and efficacy of treatments on monogenean gill flukes infecting silver kob (*Argyrosomus inodorus*) [PhD thesis]. Cape Town: University of Cape Town; 2005.
- Gibson DI, Bray RA. *Diplectanum* Diesing, 1858. In: Tyler S, Artois T, Schilling S, Hooge M, Bush LF, editors. World list of plathyhelminthes [webpage on the Internet]. c2010 [cited 2018 Oct 13]. Available from: <http://www.marinespecies.org/aphia.php?p=taxdetails&id=119291>
- Ktari MH. *Microcotyle panceri* Sonsino, 1891 (Monogenea – Microcotylidae) parasite of *Umbrina cirrhosa* L. dans le golfe de Tunis [*Microcotyle panceri* Sonsino, 1891 (Monogenea – Microcotylidae) parasite of *Umbrina cirrhosa* L. in the Gulf of Tunis]. *Bull Inst Natl Sci Tech Océanogr Pêche Salammbô.* 1970;1:169–180. French.
- Amin OM. Classification of the Acanthocephala. *Folia Parasitologica.* 2013;60(4):273–305. <https://doi.org/10.14411/fp.2013.031>
- Sardella NH, Mattiucci S, Timi JT, Bastida RO, Rodríguez DH, Nascetti G. *Corynosoma australe* Johnston, 1937 and *C. cetaceum* Johnston & Best, 1942 (Acanthocephala: Polymorphidae) from marine mammals and fishes in Argentinian waters: Allozyme markers and taxonomic status. *Syst Parasitol.* 2005;61(2):143–156. <https://doi.org/10.1007/s11230–005–3131–0>
- Ironia M, Varela MG, Lyons ET, Spraker TR, Tolliver SC. Hookworms (*Uncinaria lucasi*) and acanthocephalans (*Corynosoma* spp. and *Bolbosoma* spp.) found in dead northern fur seals (*Callorhinus ursinus*) on St. Paul Island, Alaska in 2007. *Parasitol Res.* 2008;103(5):1025. <https://doi.org/10.1007/s00436–008–1087–0>
- Silva RZ, Pereira J, Cousin JCB. Histological patterns of the intestinal attachment of *Corynosoma australe* (Acanthocephala: Polymorphidae) in *Arctocephalus australis* (Mammalia: Pinnipedia). *J Parasit Dis.* 2014;38(4):410–416. <https://doi.org/10.1007/s12639–013–0250–4>
- Hayunga EG. Morphological adaptations of intestinal helminths. *J Parasitol.* 1991;77(6):865–873. <https://doi.org/10.1007/s12639–013–0250–4>
- MacKenzie K, Abaunza P, Campbell N. The use of parasites as biological tags in multidisciplinary stock identification studies of small pelagic fish. Aberdeen: School of Biological Sciences (Zoology), University of Aberdeen; 2005.
- Marcogliese DJ. Food webs and the transmission of parasites to marine fish. *Parasitology.* 2002;124(7):83–99. <https://doi.org/10.1017/s003118200200149x>
- Christison KW, Ottob H, Moutonc A. Screening of 4 anthelmintics for their efficacy against the gill-parasitising monogeneans *Calceostoma* sp. and *Diplectanum* sp. from the silver kob, *Argyrosomus inodorus*. (Abstract). *Tydskr S Afr Vet Ver.* 2005;76(3):172–183.
- Noga EJ. Fish disease: Diagnosis and treatment. Raleigh, NC: John Wiley & Sons; 2010. <https://doi.org/10.1002/9781118786758>
- Amakali AM. Ecto- and endo-parasites of silver kob (*Argyrosomus inodorus*) from northern Namibia (21°–24°S) [thesis]. Windhoek: University of Namibia; 2019.
- Oliver G. Les Diplectanidae Bychowsky, 1957 (Monogenea, Monopisthocotylea) parasites des Sciaenidae (Pisces, Perciformes) du Golfe de Gascogne [(Diplectanidae Bychowsky, 1957 (Monogenea, Monopisthocotylea) parasites of the Sciaenidae (Pisces, Perciformes) of the Bay of Biscay)]. *Bull Mus natl hist nat Écol gén.* 1980;3:669–689. French. <https://doi.org/10.1111/j.1463–6409.1984.tb00035.x>





35. Bayoumy EM, El-Monem SA. Functional adaptation of branchial and stomach dactylogyrid monogenean: *Cichlidogyrus* and *Enterogyrus* isolated from *Oreochromis niloticus*. In: Proceedings of the 5th Global Fisheries and Aquaculture Research Conference; 2012 October 1–3; Giza, Egypt. p. 353–360.
  36. Whittington ID, Chisholm LA, Rohde K. The larvae of Monogenea (Platyhelminthes). *Adv Parasitol.* 1999;44:139–232. [https://doi.org/10.1016/s0065-308x\(08\)60232-8](https://doi.org/10.1016/s0065-308x(08)60232-8)
  37. Whittington ID, Kearn GC. Hatching strategies in monogenean (Platyhelminth) parasites that facilitate host infection. *Integr Comp Biol.* 2011;51(1):91–99. <https://doi.org/10.1093/icb/icr003>
  38. Klapper R, Kochmann J, O'Hara RB, Karl H, Kuhn T. Parasites as biological tags for stock discrimination of beaked redfish (*Sebastes mentella*): Parasite infra-communities vs. limited resolution of cytochrome markers. *PLoS ONE.* 2016;11(4), e0153964. <https://doi.org/10.1371/journal.pone.0153964>
  39. Catalano SR, Whittington ID, Donnellan SC, Gillanders BM. Parasites as biological tags to assess host population structure: Guidelines, recent genetic advances and comments on a holistic approach. *Int J Parasitol Parasites Wildl.* 2014;3(2):220–226. <https://doi.org/10.1016/j.ijppaw.2013.11.001>
  40. Botha L. Major endoparasites of the Cape hakes *Merluccius capensis* and *M. paradoxus*, with brief notes on some conspicuous ectoparasites. *Afr J Mar Sci.* 1986;4(1):45–49. <https://doi.org/10.1016/j.ijppaw.2013.11.001>
  41. Reed C, MacKenzie K, Van der Lingen CD. Parasites of South African sardines, *Sardinops sagax*, and an assessment of their potential as biological tags. *Bull Eur Assoc Fish Pathol.* 2012;32(2):41–48.
-

**AUTHORS:**J. Francis Thackeray<sup>1</sup>   
Ottmar Kullmer<sup>2,3</sup> **AFFILIATIONS:**<sup>1</sup>Evolutionary Studies Institute,  
University of the Witwatersrand,  
Johannesburg, South Africa<sup>2</sup>Department of Palaeoanthropology,  
Senckenberg Research Institute and  
Natural History Museum Frankfurt,  
Frankfurt, Germany<sup>3</sup>Department of Palaeobiology and  
Environment, Institute of Ecology,  
Evolution, and Diversity, Goethe  
University, Frankfurt, Germany**CORRESPONDENCE TO:**

Francis Thackeray

**EMAIL:**

mrsples@global.co.za

**DATES:****Received:** 21 May 2021**Revised:** 12 Oct. 2021**Accepted:** 21 Oct. 2021**Published:** 27 Jan. 2022**HOW TO CITE:**Thackeray JF, Kullmer O. The use of  
Z-scores to facilitate morphometric  
comparisons between African  
Plio-Pleistocene hominin fossils:  
An example of method. *S Afr J Sci.*  
2022;118(1/2), Art. #11182. <https://doi.org/10.17159/sajs.2022/11182>**ARTICLE INCLUDES:**

- 
- Peer review
- 
- 
- Supplementary material

**DATA AVAILABILITY:**

- 
- Open data set
- 
- 
- All data included
- 
- 
- On request from author(s)
- 
- 
- Not available
- 
- 
- Not applicable

**EDITOR:**Margaret Avery   
Jemma Finch **KEYWORDS:**morphometrics, hominin, Plio-  
Pleistocene, *Australopithecus*, *Homo*  
*habilis***FUNDING:**National Research Foundation  
(South Africa)

# The use of Z-scores to facilitate morphometric comparisons between African Plio-Pleistocene hominin fossils: An example of method

South Africa and East Africa each have a rich palaeoanthropological heritage, but the taxonomy of fossil hominins from these regions is controversial. In this study, two morphometric methods related to the quantification of variability in morphology have been applied to pairwise comparisons of linear measurements of hominoid crania and mandibles. The log-transformed standard error of the m-coefficient ('log sem') is calculated from linear regressions. Like Procrustes Distances (PD), log sem statistics can serve to quantify variation in the shape of a cranium or mandible in the context of a constellation of landmarks. In this study, PD and log sem statistics are integrated and standardised using Z-scores, and applied probabilistically to Plio-Pleistocene hominins. As a test case, OH 7 and OH 24 as reference specimens of *Homo habilis* are compared to fossils representing other taxa. There is a wide spectrum of variation in Z-scores for specimens attributed to early *Homo* dated within the period between circa 1.8 Ma and 2 Ma. In terms of morphometric variation predating 1.8 Ma, Z-scores ( $Z < 2$ ) for *Australopithecus afarensis*, *A. africanus* and *Homo habilis* display a small range of variability. This study serves as a demonstration of a method whereby log sem and PD can be used together to facilitate an objective assessment of morphological variability, applicable in palaeontological contexts.

**Significance:**

- Using a probabilistic approach, two morphometric methods are integrated to quantify morphological variability in Plio-Pleistocene African hominin mandibles and crania.
- Two Tanzanian specimens of *Homo habilis* (the OH 7 mandible of the holotype specimen, and the OH 24 skull) can be used as reference material for morphometric comparisons with other fossils (mandibles or crania) attributed to *Australopithecus africanus*, *A. afarensis*, *H. erectus* and *H. rudolfensis*.
- The results of these comparisons are expressed as standardised probabilistic Z-scores such that these statistics for skulls and mandibles can be expressed on a common scale.

## Introduction

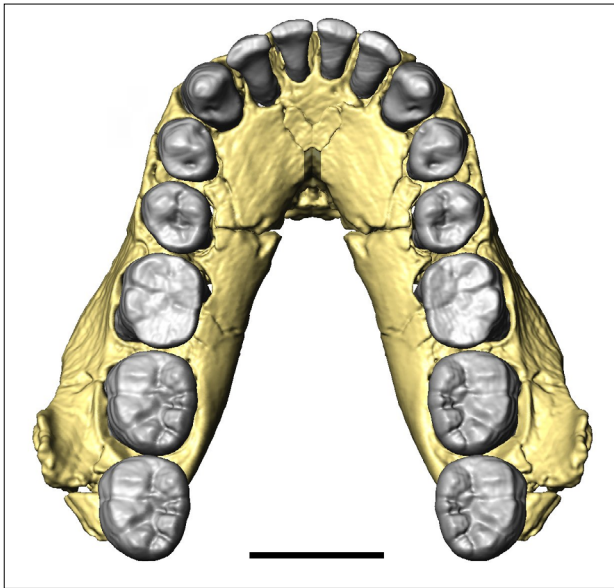
The taxonomy of fossil hominins appears increasingly more complex given recent discoveries and announcements of new species.<sup>1</sup> This is true for early hominins, with new *Australopithecus* species recently named, and also with respect to questions about the emergence of the genus *Homo* and of modern humans. Taxonomic attributions and affiliations are therefore one of the major issues in palaeoanthropology, including, for example, the debate between Tobias and Robinson regarding specimens attributed to *Australopithecus* or early *Homo*.<sup>2-5</sup> By 1992, Tobias<sup>6</sup> triumphantly declared that *Homo habilis* was 'widely accepted as a good taxon'. However, just a few years later, Wood and Collard<sup>7</sup> suggested that *H. habilis* as well as *H. rudolfensis* should be placed within *Australopithecus*. The development of analytical and statistical tools is required to help clarify the complex picture such as this (as an example), notably for fossil specimens that cannot be sampled for DNA analyses.

In this study, our aim was to present a methodological approach combining two morphometric methods to quantitatively assess the degree of variability among individuals and provide a probabilistic reference that can be applied to the hominin fossil record for clarification of taxonomic attribution. This approach has the potential to add value for taxonomic debates. As a test case, it is applied to specimens attributed to *H. habilis* and other Plio-Pleistocene taxa. The primary objective of our current morphometric analyses was to demonstrate the novel approach without as yet attempting to resolve particular problems of taxonomy.

## Materials

A hominin mandible catalogued as OH 7 (virtual reconstruction<sup>8</sup> shown in Figure 1), attributed to *H. habilis* (the holotype), was discovered at Olduvai Gorge (Bed I) in Tanzania from deposits dated at 1.8 Million years ago (Ma).<sup>9</sup> OH 24 is a contemporaneous skull of the same species from the same site.<sup>10,11</sup> The two specimens can be used as reference material for morphometric comparisons with other fossils (mandibles or crania) attributed to *Australopithecus africanus*, *A. afarensis*, *H. erectus* and *H. rudolfensis*.

The materials used in this study (Table 1) relate primarily to fossils from three general time periods: firstly, specimens attributed to *A. afarensis*, circa 3 million years ago; secondly, specimens attributed to *A. africanus*, circa 2.5 Ma; and, thirdly, specimens attributed to early *Homo*, between circa 1.8 Ma and 2 Ma. *A. afarensis* mandibles from Ethiopia<sup>12-14</sup> include AL 288-1 ('Lucy'), AL 200, AL 822 and AL 400-1. A mandible of *A. africanus* from Sterkfontein in South Africa is Sts 52b, while Sts 5 (the skull of 'Mrs Ples') from the same site also represents the latter species.<sup>15</sup> Sts 71 (a partial skull) from Sterkfontein was originally attributed to *A. africanus* but has also been referred to as *A. prometheus*.<sup>16-18</sup> AL 666-1 is a maxilla (*Homo* sp.) from Hadar in Ethiopia, circa 2.3 Ma.<sup>19,20</sup> KNM-ER 1482 (mandible), KNM-ER 60000 (mandible) and KNM-ER 62000 (maxilla) are Kenyan specimens attributed to *H. rudolfensis* from the Turkana Basin, dated between 1.8 Ma and 2.0 Ma.<sup>21-23</sup> OH 65 (maxilla) is a specimen of early *Homo* from Olduvai, circa 1.8 Ma.<sup>24</sup> Early *Homo* specimens from Dmanisi in Georgia (including mandibles



Scale = 2 cm

**Figure 1:** Virtual reconstruction of the mandible of OH 7, holotype of *Homo habilis*. Reconstruction from Spoor et al.<sup>8</sup> with permission.

D 211, D 2600 and D 2735), circa 1.8 Ma, have been attributed to *H. erectus* or *H. georgicus*.<sup>25,26</sup> East African specimens considered to represent *H. habilis* include the KNM-ER 1813 skull and possibly the KNM-ER 1802 mandible as part of the hominin assemblage from the Turkana Basin<sup>23,27</sup> as well as OH 13 (mandible and maxilla) as part of the hominin assemblage from Olduvai.<sup>11,28</sup> OH 7 is a reference specimen in this study, but for purposes of the record (Table 1), we include OH 7 MAX which is a virtual representation of the maxilla, as reconstructed by Spoor et al.<sup>8</sup> using a technique whereby mandibular morphology can facilitate the reconstruction of a maxilla, and vice versa.

## Methods

In a morphometric approach based on pairwise comparisons, Thackeray and Odes<sup>29</sup> calculated 'log sem' statistics associated with regression analyses to compare OH 24 with other crania, based on measurements from original specimens published by Wood.<sup>23</sup> The log sem results reflect variability in skull shape. In the case of the comparison between OH 24 and Sts 5 (almost complete skulls), 54 measurements are in common. In the instance of OH 24 and Sts 71 (partial skull), 44 measurements are common to both specimens.

A log sem value was obtained from a comparison between our measurements of OH 7 and Sts 52b mandibles, using landmarks based mainly on points associated with mesiodistal and bucco-lingual diameters (excluding third lower molars because the specimens do not represent fully adult individuals). Forty measurements per specimen

**Table 1:** Specimen numbers, taxonomic nomenclature, approximate date, skeletal element (mandible or cranium) and Z-score

Specimen	Species	Age (Ma)	Skeletal element	Z-score
AL 288-1	<i>Australopithecus afarensis</i>	Ca. 3 Ma	Mandible	1.43
AL 400-1	<i>Australopithecus afarensis</i>	Ca. 3 Ma	Mandible	0.71
AL 822	<i>Australopithecus afarensis</i>	Ca. 3 Ma	Mandible	0.47
AL 200	<i>Australopithecus afarensis</i>	Ca. 3 Ma	Mandible	0.71
Sts 5	<i>Australopithecus africanus</i>	Ca. 2.5 Ma	Cranium	1.00
Sts 71	<i>Australopithecus africanus</i> or <i>A. prometheus</i>	Ca. 2.5 Ma	Cranium	0.10
Sts 52b	<i>Australopithecus africanus</i>	Ca. 2.5 Ma	Mandible	1.60
AL 666-1	<i>Homo</i> sp.	2.3 Ma	Maxilla	3.86
OH 7	<i>Homo habilis</i>	1.8 Ma	Mandible	-
OH 7 MAX	<i>Homo habilis</i>	1.8 Ma	Maxilla (virtual)	-0.90
OH 24	<i>Homo habilis</i>	1.8 Ma	Cranium	-
OH 13	<i>Homo habilis</i>	1.8 Ma	Mandible	0.33
KNM ER 1813	<i>Homo habilis</i>	1.9 Ma	Cranium	1.95
KNM ER 1802	<i>Homo rudolfensis</i> or <i>H. habilis</i>	1.9 Ma	Mandible	-0.90
KNM ER 60000	<i>Homo rudolfensis</i>	1.9 Ma	Mandible	2.90
KNM ER 1482	<i>Homo rudolfensis</i>	2.0 Ma	Mandible	4.33
KNM ER 62000	<i>Homo rudolfensis</i>	2.0 Ma	Partial face	5.29
OH 65	<i>Homo rudolfensis?</i>	1.8 Ma	Maxilla	4.81
D 211	<i>Homo erectus</i>	1.8 Ma	Mandible	1.95
D 2600	<i>Homo erectus</i>	1.8 Ma	Mandible	2.90
D 2735	<i>Homo erectus</i>	1.8 Ma	Mandible	2.43

were taken from virtual reconstructions of OH 7 and Sts 52b by Spoor et al.<sup>8</sup> and Benazzi et al.<sup>30</sup> respectively. Sts 52b was selected for comparison in this study because of an apparent degree of morphological similarity with OH 7, as discussed by Tattersall.<sup>31</sup>

Using Procrustes Distances (PD), Spoor et al.<sup>8</sup> compared Plio-Pleistocene hominin specimens with a focus on OH 7, based on more than 50 landmarks. For purposes of our study, we used PD data made available through Spoor and Gunz (personal communication to JFT, 2020). Here we integrate the two kinds of shape-related statistics (PD and log sem) by expressing them as standardised Z-scores in relation to data obtained from humans and extant great apes.

The AL 400-1 mandible of *A. afarensis* has been compared with OH 7 on the basis of the PD method. AL 400-1 has also been compared with OH 7 using the log sem statistic. The difference between Z-scores is expected to be relatively small if the approaches yield consistent results.

### Log sem statistics for crania

The log sem statistic has been previously used in analyses of linear measurements obtained from crania of modern specimens in natural history museums<sup>32-34</sup> and Plio-Pleistocene hominins.<sup>29,32,34</sup> In this method, measurements are subjected to pairwise comparisons, using least squares linear regression to generate an equation of the form  $y = mx + c$ , where  $m$  is the slope and  $c$  is the intercept. In an initial study of pairs of specimens of the same (extant) species in 1997, Thackeray et al.<sup>32</sup> reported central tendency of the log-transformed standard error of the  $m$ -coefficient, known as 'log sem' which is a measure of the degree of scatter around the regression line, reflecting variability in shape. Central tendency of log sem was also discovered using larger samples, associated with a mean log sem value of -1.61 reported in 2007 by Thackeray.<sup>33</sup> At least for hominoids, the mean log sem value of  $-1.61 \pm 0.1$  was recognised in 2016 as a typical degree of intraspecific morphological variation in extant species.<sup>34</sup>

In response to views expressed by Gordon and Wood,<sup>35</sup> Thackeray and Dykes<sup>34</sup> emphasised the need to make pairwise comparisons with specimen A on the  $x$ -axis and specimen B on the  $y$ -axis, and vice versa. Two log sem values are obtained. The absolute difference between these values is termed 'delta log sem'. The mean delta log sem is small (generally  $\leq 0.03$ ) when pairs of specimens of the same species are compared. By contrast, delta log sem values are large (generally  $\gg 0.03$ ) when specimens of different species are compared.<sup>34</sup> Thackeray and Dykes<sup>34</sup> stated that the number of measurable dimensions ( $k$ ) obtained from pairs of specimens should be maximised as far as possible to ensure robusticity of the log sem statistic. When this is done, with the number of measurements for pairwise comparisons being

greater than 20, there is a tendency for the mean log sem to stabilise around a value of circa -1.6.<sup>34,35</sup>

In their analyses of cranial measurements of *Pan troglodytes*, *P. paniscus*, *Gorilla gorilla* and *H. sapiens* (using more than 20 measurable dimensions as published by Gordon and Wood<sup>35</sup>), Thackeray and Dykes<sup>34</sup> obtained the following results from pairwise comparisons:

1. Mean log sem =  $-1.612 \pm 0.129$  ( $n=8072$  pairwise regressions) reflects what is considered to be a typical degree of *intraspecific variation* within hominoids.
2. Mean log sem =  $-1.063 \pm 0.126$  ( $n=26\ 780$  regressions), reflecting the degree of variability from *interspecific comparisons*.

These results, based on a very large number of regressions, clearly show that there is indeed a significant difference between the log sem values calculated for intraspecific and interspecific comparisons, which is related to similarity (or dissimilarity) in shape.

A criticism that has been levelled against the log sem approach relates to which variables are being measured. Remarkable as it may seem, the degree of intraspecific variability reflected by a mean log sem value of *circa*  $-1.61 \pm 0.1$  has been obtained, not only from cranial variables, but also from measurements from teeth.<sup>34</sup>

### Procrustes Distances for mandibles

Bookstein<sup>36</sup> and Duta<sup>37</sup> have described the method whereby PD are calculated, reflecting differences in shape between objects (in this case, mandibles). PD statistics serve to quantify the difference between landmarks by using the square root of the sum of squared differences in positions of those landmarks.

Spoor et al.<sup>8</sup> calculated PD values from pairwise comparisons of OH 7 and other hominins, using landmarks indicated in their Fig. 2f and 2g. PD were also calculated for purposes of comparisons with *H. sapiens*, *P. troglodytes* and *G. gorilla*. The mean PD for the extant hominoids, based on data obtained by Spoor and Gunz (personal communication to JFT, 2020), provides a 'within group' (conspecific) frame of reference.

### Z-scores

The mean and standard deviation for PD for pairwise comparisons of extant hominoids ( $0.089 \pm 0.021$ ) are analogous to the mean and standard deviation for log sem values for extant hominoids ( $-1.61 \pm 0.1$ ). These two means can both be related to probabilistic Z-scores, where the Z value of 0 corresponds to the mean value of 0.089 (PD) and also to the mean log sem value of -1.61. One standard deviation above or below the mean is circa 1 and -1, respectively. Likewise, two standard deviations above or below a mean Z-value of 0 correspond to Z-score values of

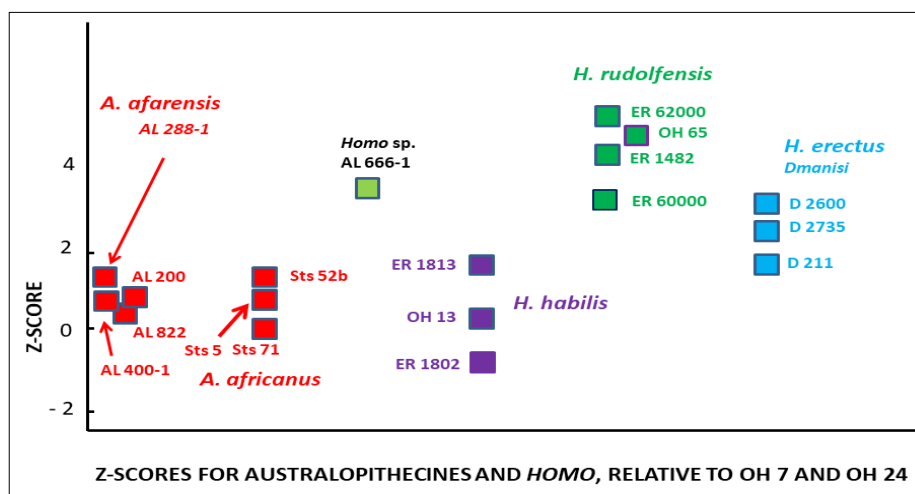


**Figure 2:** Visualisation of Z-scores for hominins based on data in Table 1. OH 7 and OH 24 are the reference specimens for pairwise comparisons with other hominins.



circa 2 and -2, respectively. In this way, log sem statistics (including those calculated for a comparison between OH 24 and skulls of other hominins) and PD values (including those calculated for comparisons between OH 7 and other hominin mandibles) can be expressed on a common (Z) scale.

## Results

Results from this study are presented in Table 1. Figure 2 is a visualisation of the results without a time scale.

The AL 400-1 mandible of *A. afarensis* has a Z-value of 0.71 when it is compared with OH 7 using the PD statistical method. A Z-value of 1.0 is obtained when AL 400-1 is compared to OH 7 using the log sem statistical method. The difference of only 0.29 is relatively small, reflecting consistency.

As indicated in Table 1 and Figure 2, the Z-score for the Sts 52b jaw (compared to the OH 7 mandible) is similar to that which has been obtained for the Sts 5 skull (compared to the OH 24 cranium), and similar also to the Z-score for the Sts 71 skull (also compared to OH 24).

In Figure 2 there is a clear separation between specimens attributed to *H. habilis* (including KNM-ER 1813 and OH 13) and others attributed to *H. rudolfensis* (e.g. KNM-ER 62K and KNM-ER 1482). In terms of Z-scores, specimens from Dmanisi attributed to *H. erectus* are intermediate between *H. habilis* and *H. rudolfensis*.

## Discussion and conclusions

We integrated two statistics (PD and log sem) by expressing them as standardised Z-scores. As the important type specimen of *H. habilis*, the OH 7 mandible has been used as a frame of reference for quantifying PD between it and other hominin mandibles. The contemporary OH 24 skull has been used for purposes of calculating log sem statistics in the context of pairwise comparisons between it and other hominin skulls (notably Sts 5 and Sts 71) from South Africa. With OH 7 and OH 24 representing the same species, measurements of mandibles and skulls have been used to obtain PD and log sem statistics, respectively, expressed on a common Z-score scale relative to values for conspecific extant hominoids.

There is a wide spectrum of variation in Z-scores for Tanzanian and Kenyan specimens attributed to early *Homo* dated within the period between circa 1.8 Ma and 2 Ma. By contrast, in terms of variation through time predating 1.8 Ma, Z-scores for *A. afarensis*, *A. africanus* and *H. habilis* display a relatively small range of variability. Put another way, the Sterkfontein specimens are a similar morphological distance to the Olduvai hominins using Z-score measurements. The Z-scores of the specimens from Hadar fall within the range of those determined for specimens from Sterkfontein (0.10–1.60).

We do not intend to say that all specimens attributed to *A. afarensis*, *A. africanus*, and *H. habilis* are necessarily conspecific. The Z-scores serve to quantify the degree of morphological distance between specimens in relation to OH 7 (mandibles) and OH 24 (cranium). We note, however, the suggestion raised by Wood and Collard<sup>7</sup> that specimens attributed to *H. habilis* could be referred to *A. habilis*. If this were to be the case, a Z-score of approximately 2 would at least potentially constitute a 'fuzzy boundary' between specimens attributed to *Australopithecus* and *Homo*. In addition, we note Thackeray's<sup>38</sup> suggestion that the transition between *A. africanus* and *H. habilis* (*A. habilis*) might constitute a chronospecies,

We recognise that our study is based on data derived from only a few specimens within the hypodigms of certain taxa (especially with respect to the two *Australopithecus* species). In addition, we are including only data from the cranium and mandible, and, more narrowly, the mandibular data only reflect the shape of the dental arcade in the context of a constellation of landmarks. However, we have demonstrated a method whereby Z-scores allow us to integrate data from mandibles such as OH 7, Sts 52b and AL 288-1 ('Lucy') and skulls such as OH 24, Sts 71 and Sts 5 ('Mrs Ples'), in a probabilistic context.

Ideally, probabilistic approaches (as in the use of Z-scores) can be used to support one potential taxonomic attribution over another, as examples of sigma taxonomy,<sup>39</sup> defined as 'the classification of taxa in terms of probabilities of conspecificity, without assuming distinct boundaries between species', whereas alpha taxonomy generally does assume clear limits.<sup>39,40</sup> The probabilistic method of the kind presented in this study can supplement alpha taxonomy by providing an objective assessment of morphological variability, applicable in palaeontological contexts. One of the limitations relates to the fact that fossils are often fragmentary such that the number of measurable dimensions (*k*) is relatively small. Ideally log sem and PD values should be calculated from complete and undistorted specimens. Despite these limitations, we recommend that our approach using Z-scores should be explored further in the context of additional cases, to include assessment of the transition between *Australopithecus* and *Homo*.

## Acknowledgements

This research was supported by the National Research Foundation (South Africa). Philipp Gunz and Fred Spoor kindly made Procrustes Distance data available for this study, based on results obtained from their reconstruction of OH 7 compared to other hominins. We are grateful to Leslie Aiello, José Braga, Marine Cazenave, the late Sue Dykes, Jean-Michel Loubes, Caitlin Schrein, Clément Zanolli and anonymous referees for encouragement and advice in the course of preparation of this article.

## Competing interests

We have no competing interests to declare.

## Authors' contributions

J.F.T.: Conceptualisation, methodology, writing and data analysis. O.K.: Writing and revision.

## References

1. McNulty KP. Hominin taxonomy and phylogeny: What's in a name? *Nature Education Knowledge*. 2016;7(1):2
2. Tobias PV. The Olduvai Bed I Hominine with special reference to its cranial capacity. *Nature*. 1964;202:3–7. <https://doi.org/10.1038/202003a0>
3. Tobias PV. The distinctiveness of *Homo habilis*. *Nature*. 1966;209:953–957. <https://doi.org/10.1038/209953a0>
4. Robinson JT. *Homo habilis* and the australopithecines. *Nature*. 1965;205:121–124. <https://doi.org/10.1038/205121a0>
5. Robinson JT. The distinctiveness of *Homo habilis*. *Nature*. 1966;209:957–960. <https://doi.org/10.1038/209957a0>
6. Tobias PV. The species *Homo habilis*: Example of a premature discovery. *Ann Zool Fenn*. 1992;28:371–380.
7. Wood BA, Collard M. The changing face of the genus *Homo*. *Evol Anthropol*. 1999;8:195–207. [https://doi.org/10.1002/\(SICI\)1520-6505\(1999\)8:6<195::AID-EVAN1>3.0.CO;2-2](https://doi.org/10.1002/(SICI)1520-6505(1999)8:6<195::AID-EVAN1>3.0.CO;2-2)
8. Spoor F, Gunz P, Neubauer S, Stellzer S, Scott N, Kwekason A, et al. Reconstructed *Homo habilis* type OH 7 suggests deep-rooted species diversity in early *Homo*. *Nature*. 2015;519:83–86. <https://doi.org/10.1038/nature14224>
9. Leakey LSB, Tobias PV, Napier JR. A new species of the genus *Homo* from Olduvai Gorge. *Nature*. 1964;202:7–9. <https://doi.org/10.1038/202007a0>
10. Leakey MD, Clarke RJ, Leakey LSB. New hominid skull from Bed I, Olduvai Gorge, Tanzania. *Nature*. 1971;232:308–312. <https://doi.org/10.1038/232308a0>
11. Tobias PV. The skulls, endocasts and teeth of *Homo habilis*: Volume 4 of Olduvai Gorge. Cambridge, UK: Cambridge University Press; 1991.
12. Johanson DC, White TD, Coppens Y. A new species of the genus *Australopithecus* (Primates: Hominidae) from the Pliocene of eastern Africa. *Kirtlandia*. 1978;28(2):1–14.
13. White TD, Johanson DC. Pliocene hominid mandibles from the Hadar Formation, Ethiopia: 1974–1977 Collections. *Am J Phys Anthropol*. 1982;57:501–544. <https://doi.org/10.1002/ajpa.1330570405>



14. Kimbel WH, Rak Y, Johanson DC. The skull of *Australopithecus afarensis*. Oxford: Oxford University Press; 2004.
15. Brain CK. The hunters or the hunted? An introduction to African cave taphonomy. Chicago, IL: The University of Chicago Press; 1981.
16. Clarke RJ. Latest information on Sterkfontein's *Australopithecus* skeleton and a new look at *Australopithecus*. *S Afr J Sci*. 2008;104:443–449.
17. Clarke RJ. *Australopithecus* from Sterkfontein Caves, South Africa. In: Reed K, Fleagle J, Leakey R, editors. The paleobiology of *Australopithecus*. New York: Springer; 2013. p. 105–123.
18. Clarke RJ, Kuman K. The skull of StW 573, a 3.67 My old *Australopithecus prometheus* skeleton from Sterkfontein Caves. *J Hum Evol*. 2019;134:102634. <https://doi.org/10.1016/j.jhevol.2019.06.005>
19. Kimbel W, Walter RC, Johanson D, Reed K, Aronson JL, Assefa Z, et al. Late Pliocene *Homo* and Oldowan tools from the Hadar Formation (Kada Hadar member), Ethiopia. *J Hum Evol*. 1996;31(6):549–561. <https://doi.org/10.1006/jhevol.1996.0079>
20. Kimbel WH, Johanson DC, Rak Y. Systematic assessment of a maxilla of *Homo* from Hadar, Ethiopia. *Am J Phys Anthropol*. 1998;103:235–262. [https://doi.org/10.1002/\(SICI\)1096-8644\(199706\)103:2<235::AID-AJPA8>3.0.CO;2-S](https://doi.org/10.1002/(SICI)1096-8644(199706)103:2<235::AID-AJPA8>3.0.CO;2-S)
21. Leakey RE. Evidence for an advanced Plio-Pleistocene hominid from East Rudolf, Kenya. *Nature*. 1973;242:447–450. <https://doi.org/10.1038/24247a0>
22. Leakey M, Spoor F, Dean MC, Feibel CS, Antón S, Kiarie C, et al. New fossils from Koobi Fora in northern Kenya confirm taxonomic diversity in early *Homo*. *Nature*. 2012;488:201–204. <https://doi.org/10.1038/nature11322>
23. Wood BA. Koobi Fora Research Project. Volume 4: Hominid cranial remains. Oxford: Clarendon Press; 1991.
24. Blumenschine R, Peters CR, Masao FT, Clarke RJ, Deino AL, Hay RL, et al. Late Pliocene *Homo* and hominid land use from western Olduvai Gorge, Tanzania. *Science*. 2003;299:1217–1221. <https://doi.org/10.1126/science.1075374>
25. Lordkipanidze D, Ponce de León MS, Margvelashvili A, Rak Y, Rightmire GP, Vekua A, et al. A complete skull from Dmanisi, Georgia, and the evolutionary biology of early *Homo*. *Science*. 2013;342:326–331. <https://doi.org/10.1126/science.1238484>
26. Gabunia L, Vekua A, Lordkipanidze D, Swisher CC 3rd, Ferring R, Justus A, et al. Earliest Pleistocene hominid cranial remains from Dmanisi, Republic of Georgia: Taxonomy, geological setting, and age. *Science*. 2000;288(5468):1019–1025. <https://doi.org/10.1126/science.288.5468.1019>
27. Andrews P. B. Wood 1991. Koobi Fora Research Project volume 4. Hominid cranial remains. *Geological Magazine*. 1993;130(3):395–396.
28. Tattersall I. Olduvai Gorge, volume 4: The skulls, endocasts and teeth of *Homo habilis*. *Int J Primatol*. 1992;13:349–352. <https://doi.org/10.1007/BF02547820>
29. Thackeray JF, Odes E. Morphometric analysis of early Pleistocene African hominid crania in the context of a statistical (probabilistic) definition of a species. *Antiquity*. 2013;87. <http://antiquity.ac.uk/projgall/thackeray335/>
30. Benazzi S, Kullmer O, Schulz D, Gruppioni G, Weber GW. Technical note: Individual tooth macrowear pattern guides the reconstruction of Sts 52 (*Australopithecus africanus*) dental arches. *Am J Phys Anthropol*. 2013;150:324–329. <https://doi.org/10.1002/ajpa.22225>
31. Tattersall I. Defining and recognizing the genus *Homo*. *Gortania*. 2014;36:5–22.
32. Thackeray JF, Bellamy CL, Bellars D, Bronner G, Bronner L, Chimimba C, et al. Probabilities of conspecificity: Application of a morphometric technique to modern taxa and fossil specimens attributed to *Australopithecus* and *Homo*. *S Afr J Sci*. 1997;93:195–196.
33. Thackeray JF. Approximation of a biological species constant? *S Afr J Sci*. 2007;103:489. <https://sajs.co.za/article/view/4033>
34. Thackeray JF, Dykes S. Morphometric analyses of hominoid crania, probabilities of conspecificity and an approximation of a biological species constant. *HOMO J Comp Hum Biol*. 2016;67(1):1–10. <http://dx.doi.org/10.1016/j.jchb.2015.09.003>
35. Gordon AD, Wood BA. Evaluating the use of pairwise dissimilarity metrics in paleoanthropology. *J Hum Evol*. 2013;65:465–477. <http://dx.doi.org/10.1016/j.jhevol.2013.08.002>
36. Bookstein FL. Morphometric tools for landmark data. Cambridge, UK: Cambridge University Press; 1991.
37. Duta N. Procrustes shape distance. In: Li SZ, Jain AK, editors. Encyclopedia of biometrics. Boston, MA: Springer; 2015. [https://doi.org/10.1007/978-1-4899-7488-4\\_864](https://doi.org/10.1007/978-1-4899-7488-4_864)
38. Thackeray JF. *Homo habilis* and *Australopithecus africanus* in the context of a chronospecies and climatic change. In: Runge R, editor. Changing climates, ecosystems and environments within arid southern Africa and adjoining regions. Palaeoecology of Africa 33. Leiden: CRC Press; 2015. p. 53–58.
39. Thackeray JF, Schrein CM. A probabilistic definition of a species, fuzzy boundaries and 'sigma taxonomy'. *S Afr J Sci*. 2017;113(5/6), Art. #a0206. <http://dx.doi.org/10.17159/sajs.2017/a0206>
40. Mayr E, Linsley EG, Usinger RL. Methods and principles of systematic zoology. New York: McGraw-Hill; 1953.



Check for updates

**AUTHORS:**

Charles W. Helm<sup>1</sup>   
Hayley C. Cawthra<sup>1,2</sup>   
Jan C. De Vynck<sup>1</sup>   
Rudolf Hattingh<sup>3</sup>   
Martin G. Lockley<sup>4</sup>

**AFFILIATIONS:**

<sup>1</sup>African Centre for Coastal Palaeoscience, Nelson Mandela University, Port Elizabeth, South Africa  
<sup>2</sup>Geophysics and Remote Sensing Unit, Council for Geoscience, Cape Town, South Africa  
<sup>3</sup>South African Spelaeological Association (SASA), Cape Town, South Africa  
<sup>4</sup>Dinosaur Trackers Research Group, University of Colorado Denver, Denver, Colorado, USA

**CORRESPONDENCE TO:**

Charles Helm

**EMAIL:**

helm.c.w@gmail.com

**DATES:**

Received: 24 July 2021

Revised: 31 Oct. 2021

Accepted: 03 Nov. 2021

Published: 27 Jan. 2022

**HOW TO CITE:**

Helm CW, Cawthra HC, De Vynck JC, Hattingh R, Lockley MG. Possible Pleistocene hominin tracks from South Africa's west coast. *S Afr J Sci.* 2022;118(1/2), Art. #11842. <https://doi.org/10.17159/sajs.2022/11842>

**ARTICLE INCLUDES:**

- Peer review
- Supplementary material

**DATA AVAILABILITY:**

- Open data set
- All data included
- On request from author(s)
- Not available
- Not applicable

**EDITORS:**

Margaret Avery   
Jemma Finch

**KEYWORDS:**

Langebaan, hominin, fossil tracks, aeolianites, Pleistocene

**FUNDING:**

None

© 2022. The Author(s). Published under a Creative Commons Attribution Licence.

# Possible Pleistocene hominin tracks from South Africa's west coast

Two probable tracks have been identified on the ceiling of a small overhang in the Pleistocene Langebaan Formation on South Africa's west coast. They may have been made by a hominin trackmaker. They appear to have been registered at walking speed on a level, sandy dune substrate. Three tracks, attributed to *Homo sapiens*, were previously identified near Langebaan in 1995, and were popularly labelled 'Eve's Footprints'. The new identification of possible hominin tracks near Langebaan is the second from South Africa's west coast. This discovery adds to the sparse but growing global record of possible hominin tracks preserved in aeolianites.

**Significance:**

- Two probable fossil tracks have been identified on the ceiling of an overhang near Langebaan.
- The tracks may have been made by a human walking on a level dune surface during the Pleistocene.
- This discovery is the second of its kind on the west coast, and complements the 1995 identification near Langebaan of Pleistocene fossil tracks attributed to humans.

## Introduction

The presence of fossil vertebrate tracks in Cenozoic aeolianites on South Africa's west coast is well established, since a 1976 report of a carnivore trackway at Kraalbaai, near Langebaan.<sup>1</sup> In the 1990s this trackway could not be located, but further tracks were identified nearby in 1995, and attributed to a hyaena, and a purported hominin trackway, containing three tracks, was dated to ~117 ka<sup>2</sup> and described in detail<sup>3</sup>. The tracks all occurred in the Late Pleistocene Langebaan Formation of the Sandveld Group.<sup>4</sup>

The announcement of the discovery of hominin tracks created considerable interest, and they became popularly known as 'Eve's footprints'.<sup>5</sup> A trackway replica is exhibited at Geelbek Visitor Centre in the West Coast National Park. International acceptance of their hominin nature was more muted. Lockley et al.<sup>6</sup> described them as 'rather poorly preserved' and 'less well-defined'. Bennett and Morse<sup>7</sup> indicated that they were not unequivocally human, had 'relatively poor anatomical form', and stated that 'not all authorities are convinced that they are in fact human tracks'. However, the hominin interpretation was not contested; for example, the tracks were mentioned in a study on the morphological affinity of hominin footprints.<sup>8</sup>

No further fossil tracks have been reported in the subsequent quarter-century, although there have been a number of Cape south coast hominin tracksite discoveries.<sup>9,10</sup> Unfortunately, modern graffiti on aeolianite surfaces in the Langebaan area occurs in abundance, and such graffiti abutted the trackway identified by Roberts<sup>3</sup>. A possible hominin tracksite on the Cape south coast was defaced and compromised by graffiti before it could be properly assessed.<sup>11</sup> The prevalence of graffiti may in part account for the absence of further reports of fossil tracks from the west coast. This, combined with the lack of international consensus with regard to the attribution of 'Eve's footprints', means that the identification of possible further hominin tracks at sites free of graffiti is potentially of interest.

A new site was recently discovered by one of us (RH) on an aeolianite surface in the Langebaan Formation (Figure 1). Two probable tracks (referred to herein as 'tracks'), which can possibly be attributed to a Pleistocene hominin trackmaker, occur in hyporelief on the ceiling of an overhang. The purpose of this article is to describe this site and discuss its implications.

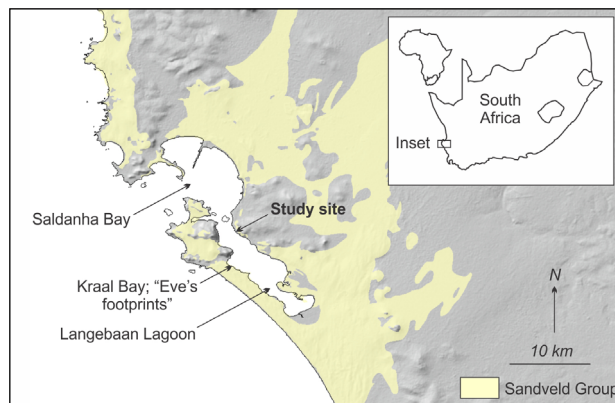


**Figure 1:** Locality map showing Sandveld Group sediments in the Langebaan region of South Africa's west coast, and the study site in relation to 'Eve's footprints'.



## Methods

GPS readings were taken and elevation was obtained using a hand-held Garmin 60 device. Locality data were reposit with the African Centre for Coastal Palaeoscience at Nelson Mandela University, to be made available to researchers upon request. The rock overhang dimensions were measured. Maximum track length (from the most proximal to most distal margins of the track, in the longitudinal axis of the track), track width, track depth, and pace length (from the most proximal portion of the first track to the most proximal portion of the second track) were measured. Results were recorded in centimetres. The trackway bearing was determined.

Photographs were taken, including images for photogrammetry.<sup>12</sup> Photogrammetry 3D models were generated with Agisoft MetaShape Professional (v. 1.0.4) using an Olympus TG-4 camera (focal length 4 mm; resolution 314 dpi; pixel size 4608 x 3456  $\mu\text{m}$ ). Final images were rendered using CloudCompare v2.6.3.beta.

## Results

The aeolianite deposits form part of the Kraal Bay Member of the Langebaan Formation. They unconformably overlie intrusive rocks of the Palaeozoic Saldanha Batholith (Hoedjiespunt Granite) of the Cape Granite Suite, that fringe the Langebaan Lagoon. The site is situated on a level surface 18 m above sea level. The relatively coarse-grained (medium to coarse sand) aeolianite forms a massive outcrop, with homogeneous beds reaching several metres in thickness with no foresets visible. Vertically orientated solution pipes are evident (Figure 2a).

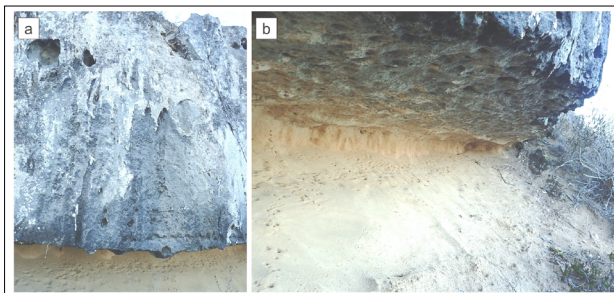


**Figure 2:** (a) The massive aeolianite outcrop above the overhang, facing east, showing homogeneous beds and solution pipes. (b) View of the overhang facing southeast, showing track-bearing ceiling and rear wall composed of a palaeosol.

The overhang is 6.6 m long and 1.5 m deep. It has a lens shape, pinching out at the lateral edges. Maximum ceiling-to-floor height of the lagoon-facing overhang is 1.2 m. It has a sandy floor, a friable aeolianite ceiling, and a rear wall composed of a palaeosol into which the overhang has incised (Figure 2b). There is no evidence of graffiti.

Many protrusions are present on this overhang surface, representing the infill of depressions in the (now absent) original dune surface. They are interpreted here as natural casts of probable vertebrate tracks, although in most cases their amorphous nature, poor preservation and lack of morphological detail preclude identification to trackmaker group, and imply that a non-biogenic origin for these features cannot be completely excluded. The two largest of these features, interpreted here as probable tracks, exhibit some definable morphological characteristics, and approximately similar orientations, suggesting a trackway segment (Figure 3a), with a bearing of 355° (heading towards the rear wall). The southern feature is referred to as Track 1, and the northern feature as Track 2, consistent with the inferred direction of travel. Track 2 exhibits better morphological detail.

Track margins are not crisply defined, and the possibility that measured track lengths may include infill of heel-drag impressions cannot be excluded, reminiscent of the phenomenon noted at a hominin tracksite by Helm et al. (Fig. 5)<sup>10</sup> on the Cape south coast. Track 1 (Figure 3b) is

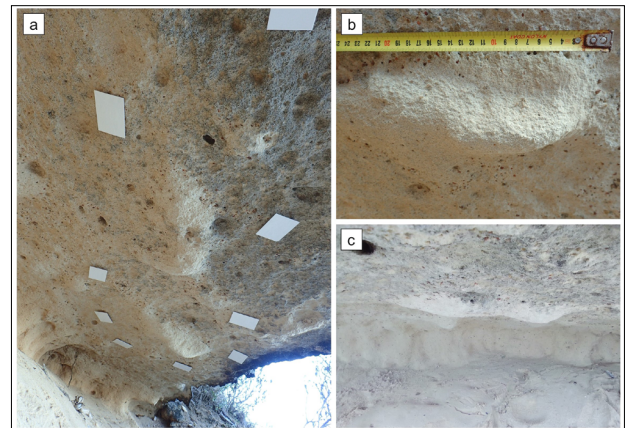


**Figure 3:** (a) Tracks on overhang ceiling, viewed facing south. (b) Track 1 in profile. (c) Track 2 in profile.

28 cm in maximum length, and 14 cm in maximum width. Maximum depth of the anterior portion is 3 cm, and the posterior portion is 4 cm. Track 2 (Figure 3c) is 29 cm in maximum length, and 13 cm in maximum width. Maximum depth of the anterior portion is 3.5 cm, and the posterior portion is 4 cm.

Pace length is 49 cm. Both features exhibit an outward convexity, more evident in Track 2, with the medial margin in particular being curved (Figure 4a). When only two tracks are present, the approximate trackway direction can be inferred by bisecting the two footprint long axes, assuming equal rotation from the midline. In this case, each track is aligned  $\sim 18^\circ$  to the outside of the bisector (Figure 4b). No definite evidence of digit traces or displacement rims is evident, although a faint hallux trace may be present at the anterior end of Track 2 (Figure 4b).

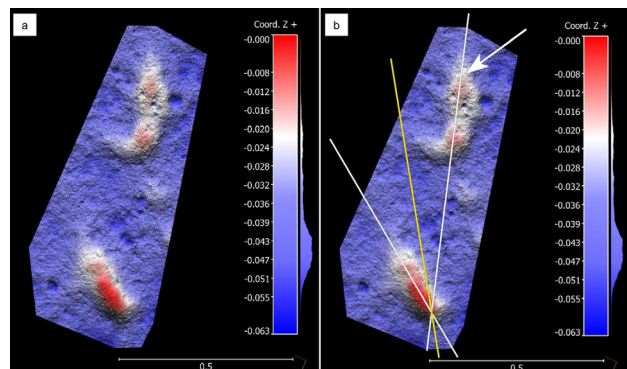


**Figure 4:** (a) Photogrammetry colour mesh of possible hominin tracks, using 64 images. Photos were taken an average 27.1 cm from the surface. The reprojection error is 0.731 pix. Vertical and horizontal scales are in metres. (b) Identical image to (a), with the addition of white lines to indicate footprint long axes, and the yellow line as a bisector; the arrow indicates faint possible hallux trace at the anterior end of Track 2.

## Discussion

The identification of fossil hominin tracks has been addressed<sup>7,13</sup>, and the hominin track record has been reviewed in detail: tracks registered in aeolianites are a global rarity, and the southern African tracksites therefore represent an exception.<sup>6,7</sup> An approach to the identification of southern African hominin tracks has been developed and refined.<sup>9,14</sup> Applying these principles to the features described here facilitates their evaluation, while recognising that they apply more to well-preserved tracks in suitable substrates than to the tracks described here.



Dimensions and pace length are broadly consistent with a hominin trackmaker<sup>7,15</sup>, especially considering the possible length overestimate due to heel-drag impressions as noted above. The true tracks may therefore not have been as gracile (elongate) as they appear. Moreover, the friable nature of the ceiling and tracks, indicating that they are vulnerable even to light touch, suggests that more detail might have been evident if they had been discovered earlier. In addition, a longer trackway, or more definite evidence of digit impressions, would allow for more confident trackmaker identification. Nonetheless, a possible right-left footfall pattern can be inferred from the outward convexity of each track (providing possible evidence of a medial longitudinal arch). This pattern of outward convexity would be unlikely to be registered by any contemporary trackmakers, including overstepping equids.<sup>14</sup> In such a scenario, Track 1 would be a right track and Track 2 a left track. The different orientation of the two tracks is consistent with an eversion gait pattern or a direction change. The recorded pace length is broadly consistent with a walking gait.<sup>7,15</sup> A profile view of Track 2 (Figure 3c) is similar to that of hominin tracks at Brenton-on-Sea, although at the latter site the rocks are well cemented and the tracks exhibit better preservation.<sup>10</sup> The finding of moderately deep tracks without much morphological detail suggests they were made in a non-cohesive substrate such as dry sand.<sup>15</sup> On the basis of track outlines, dimensions, pace length, profile view, possible hallux trace, and the suggestion that the trackmaker may have had a medial longitudinal arch, we contend that these are likely hominin tracks, while acknowledging that more rigorous identification criteria cannot be met and that this contention cannot be asserted with certainty. Nonetheless, similarity to natural cast hominin tracks on the Cape south coast is apparent.<sup>9</sup>

The Langebaan tracks identified by Roberts in 1995 ('Eve's footprints') were recovered and are housed in the Iziko South Africa Museum, Cape Town.<sup>3</sup> Roberts described three natural mould tracks, in a right-left-right sequence, with displacement rims, and attributed them to *Homo sapiens*.<sup>3</sup> The trackway was interpreted as descending diagonally down a dune, and involving a direction change. A track length of 22.8 cm and pace length of 50.0 cm were recorded.<sup>3</sup> Evidence of a medial longitudinal arch was reported in one track, along with poorly preserved digit impressions. Roberts<sup>3</sup> used a formula<sup>16</sup> to estimate trackmaker stature, giving a height estimate of 152 cm. Roberts reportedly excavated the adjacent area, exposing additional tracks. However, these were in a softer substrate, and were described as 'ephemeral'. They were left in situ and covered (Avery G, personal communication, September 2018).

The aeolianite horizon at the newly identified site, 18 m above sea level, is higher than the horizon of 'Eve's footprints'. Nonetheless, the identification of further inferred hominin tracks, free of graffiti and within kilometres of those previously reported, suggests support for Roberts<sup>3</sup> conclusion of a hominin trackmaker. The quality of preservation and lack of morphological detail are consistent with many other Pleistocene tracksites on the Cape coast, where tracks were registered on unconsolidated dune substrates.<sup>9</sup> Dedicated exploration of aeolianite surfaces (preferably free of graffiti) in the area, in search of tracks of unequivocal hominin origin, would be valuable.

While the track-bearing surface has not been dated, we can speculate that if the tracks were registered during a higher-than-present sea level, the lagoon would likely have appeared different to its present-day configuration. Parts of the coastal ridge may not yet have accreted; extensive dunefields may have existed, and the western and eastern shores of the lagoon may conceivably have been linked in places by these dunes, if the extent of the lagoon was more limited.

## Conclusions

The identification of two new possible hominin tracks near Langebaan adds to the sparse record of putative hominin tracks from South Africa's west coast. Although not unequivocally attributed to a hominin trackmaker, they lend credence to the purported hominin origin of the tracks identified nearby in 1995, known as 'Eve's footprints'. The newly identified tracks were probably made in a soft, sandy dune substrate by an individual moving at a walking speed.

## Acknowledgements

We are grateful for the assistance of Jack Carrigan and Carina Helm. We thank Julian Paterson for field assistance in documenting the site.

## Competing interests

We have no competing interests to declare.

## Authors' contributions

C.W.H.: Conceptualisation, data analysis, project leadership, photogrammetry. H.C.C.: Data collection and analysis, site analysis, field stratigraphy, review of drafts and revisions. J.C.D.V.: Conceptualisation, track analysis, review of drafts and revisions. R.H.: Area exploration and site discovery, conceptualisation, review of drafts and revisions. M.G.L.: Conceptualisation, data analysis, review of drafts and revisions.

## References

1. Tankard AJ. Pleistocene history and coastal morphology of the Ysterfontein-Elands Bay area, Cape Province. *Ann S Afr Mus.* 1976;69:73–119.
2. Roberts D, Berger LR. Last Interglacial (c. 117 kyr) human footprints from South Africa. *S Afr J Sci.* 1997;93(8):349–350.
3. Roberts DL. Last Interglacial hominid and associated vertebrate fossil trackways in coastal aeolianites, South Africa. *Ichnos.* 2008;15(3):190–207. <http://dx.doi.org/10.1080/10420940802470482>
4. Roberts DL, Botha GA, Maud RR, Pether J. Coastal Cenozoic deposits. In: Johnson MR, Annhauser CR, Thomas RJ, editors. *The geology of South Africa.* Johannesburg: Geological Society of South Africa/Council for Geoscience; 2006. p. 605–628.
5. Berger LR, Hilton-Barber B. *In the footsteps of Eve: The mystery of human origins.* Washington DC: National Geographic Society; 2000.
6. Lockley M, Roberts G, Kim JY. In the footprints of our ancestors: An overview of the hominid track record. *Ichnos.* 2008;15(3–4):106–125. <http://dx.doi.org/10.1080/10420940802467835>
7. Bennett MR, Morse SA. *Human footprints: Fossilised locomotion?* Cham: Springer; 2014. <https://doi.org/10.1007/978-3-319-08572-2>
8. Wiseman ALA, Stringer CB, Ashton NM, Hatala KG, Bennett MR, O'Brien T, et al. The morphological affinity of the Early Pleistocene footprints from Happisburgh, England, with other footprints of Pliocene, Pleistocene, and Holocene age. *J Hum Evol.* 2020;144, 102776. <https://doi.org/10.1016/j.jhevol.2020.102776>
9. Helm CW, Lockley MG, Cawthra HC, De Vynck JC, Dixon MG, Helm CJZ, et al. Newly identified hominin trackways from the Cape south coast of South Africa. *S Afr J Sci.* 2020;116(9/10), Art. #8156. <https://doi.org/10.17159/sajs.2020/8156>
10. Helm CW, McCrea RT, Cawthra HC, Cowling RM, Lockley MG, Marean CW, et al. A new Pleistocene hominin tracksite from the Cape south coast, South Africa. *Sci Rep.* 2018;8, Art. #3772. <http://dx.doi.org/10.1038/s41598-018-22059-5>
11. Helm CW, Cawthra HC, Cowling RM, De Vynck JC, Lockley MG, Marean CW, et al. Protecting and preserving South African aeolianite surfaces from graffiti. *Koedoe.* 2021;63(1), a1656. <https://doi.org/10.4102/koedoe.v63i1.1656>
12. Matthews NA, Noble TA, Breithaupt BH. Close-range photogrammetry for 3-D ichnology: The basics of photogrammetric ichnology. In: Falkingham PL, Marty D, Richter A, editors. *Dinosaur tracks: The next steps.* Bloomington, IN: Indiana University Press; 2016. p. 28–55.
13. Tuttle RH. Footprint clues in hominid evolution and forensics: Lessons and limitations. *Ichnos.* 2008;15:158–165. <https://doi.org/10.1080/10420940802467892>
14. Helm CW, Lockley MG, Cole K, Noakes TD, McCrea RT. Hominin tracks in southern Africa: A review and an approach to identification. *Palaeont Afr.* 2019;53:81–96.
15. Morse SA, Bennett MR, Liutkus-Pierce C, Thackeray F, McClymont J, Savage R, et al. Holocene footprints in Namibia: The influence of substrate on footprint variability. *Am J Phys Anthropol.* 2013;151:265–279. <https://doi.org/10.1002/ajpa.22276>
16. Mietto P, Avanzini M, Rolandi G. Palaeontology: Human footprints in Pleistocene volcanic ash. *Nature.* 2003;422:133. <https://doi.org/10.1038/422133a>

# Corrigendum

[Original article] Bergstrom K, Lawrence AB, Pelissero AJ, Hammond LJ, Maro E, Bunn HT, Musiba CM. Aerial map demonstrates erosional patterns and changing topography at Isimila, Tanzania. *S Afr J Sci.* 2019;115(7/8), Art. #5911. <https://doi.org/10.17159/sajs.2019/5911>

## HOW TO CITE:

Corrigendum: Aerial map demonstrates erosional patterns and changing topography at Isimila, Tanzania [*S Afr J Sci.* 2019;115(7/8), Art. #5911]. *S Afr J Sci.* 2022;118(1/2), Art. #5911C. <https://doi.org/10.17159/sajs.2022/5911C>

Due to an error in the reference plane, the elevation range shown for the digital elevation model (DEM) in Figure 5a (Page 3) is incorrect. The correct elevation range is 1629.41–1679.64 m. The DEM and orthomosaic map data were reprocessed using Agisoft Metashape 1.7.4. Processing parameters for the corrected DEM and orthomosaic differ slightly from those in Supplementary table 1 as a result of correcting the reference plane and differences in technical specifications of the computers used to process data. The corrected DEM, orthomosaic, and processing parameters are available for download at: <https://doi.org/10.5281/zenodo.4592344>. The corrected Figure 5 and Supplementary table 1 appear below. The error does not affect the interpretation of data in the original article.

We thank Rebecca Bateman and Richard Bates for bringing the error to our attention and for sharing their data, as well as Pastory Bushozi and Philbert Katto for sharing their field data.

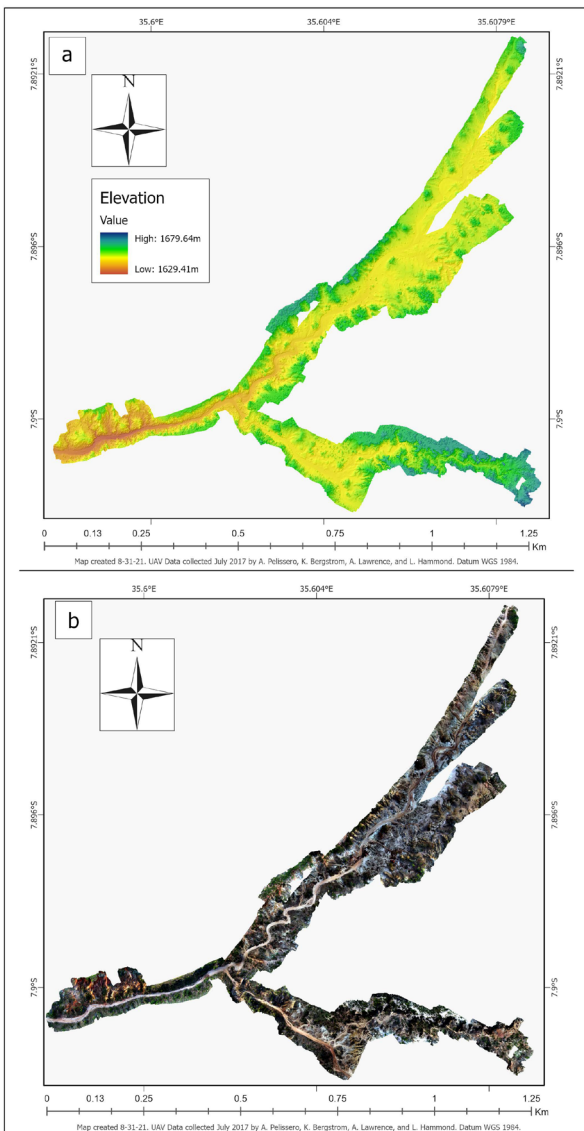


**Figure 5:** (a) Digital elevation map of Isimila. (b) Orthomosaic map of Isimila.

**Supplementary table 1:** Agisoft Metashape processing parameters for Isimila map

General	
Aligned cameras	4220 of 4419
Camera pixel size	0.0025
Coordinate system	WGS* 84 (EPSG**4326)
Rotation angles	yaw, pitch, roll
UAV camera specifications	
Sensor size (mm)	13.2 x 8 mm
Focal length (mm)	8.8 mm/24 mm (35 mm equivalent)
Field of view	84°
Image size (pixels)	4096 x 2160
Effective pixels	20 megapixels
Image data capture parameters	
Flight altitude	40 m
Average flight velocity	4 m/s
Ground sample distance	1.6 cm / pixel
Image footprint	60 x 31 m
Total surface	1.533 km <sup>2</sup>
Alignment parameters	
Alignment accuracy	High
Pair pre-selection	Generic, reference
Key point limit	40 000
Tie point limit	0 (no limit)
Exclude stationary tie points	No
Guided image matching	No
Adaptive camera model fitting	Yes
Matching time	1 h, 56 min
Alignment time	15 h, 34 min
Sparse point cloud	
Points	13 963 537 of 15 221 034
RMS reprojection error	0.150504 (0.709835 pix)
Max reprojection error	0.599607 (44.886 pix)
Mean key point size	4.13703 pix
Average tie point multiplicity	4.07828
Dense point cloud and depth maps	
Quality	High
Depth filtering	Aggressive
Depth map count	4220
Points	821 513 074
Depth map processing time	2 h, 56 min
Dense cloud generation time	5 h, 46 min
Digital elevation model	
Size	86 103 x 84 329
Pixel size	2.39 cm/pixel
Source data	Dense cloud
Interpolation	Enabled
Processing time	1 h, 8 min
Orthomosaic	
Size	104 582 x 102 432
Pixel size	1.19 cm/pixel
Channels	3, uint8
Coordinate system	WGS 84 (EPSG:4326)
Blending mode	Mosaic
Enable colour correction	No
Enable hole filling	Yes
Processing time	2 h, 38 min
Software	
Version	1.7.4.12950
Platform	Windows 10 x 64

\*World Geodetic System 1984

\*\*European Petroleum Parameter System



## Corrigendum

[Original article] Bopape M-JM, Sebege E, Ndarana T, Maseko B, Netshilema M, Gijben M, et al. Evaluating South African Weather Service information on Idai tropical cyclone and KwaZulu-Natal flood events. *S Afr J Sci.* 2021;117(3/4), Art. #7911. <https://doi.org/10.17159/sajs.2021/7911>

### HOW TO CITE:

Corrigendum: Evaluating South African Weather Service information on Idai tropical cyclone and KwaZulu-Natal flood events [S Afr J Sci. 2021;117(3/4), Art. #7911]. *S Afr J Sci.* 2022;118(1/2), Art. #7911C. <https://doi.org/10.17159/sajs.2022/7911C>

The authors' employment at the South African Weather Service (SAWS) was inadvertently omitted from the Competing Interests statement in the original article. All but one of the authors are employees of SAWS and were involved in the forecasting process or were in the section responsible for observations during the forecasting and observations of the weather events reported on.

The responsibilities of the authors in their respective roles are as follows:

- Mary-Jane M. Bopape: Chief Scientist: Weather Research – oversees the running of numerical weather prediction models and nowcasting products
- Ezekiel Sebege: Manager: Disaster Risk Reduction – oversees the forecasting process
- Bathobile Maseko: Scientist: Satellite Meteorology – responsible for satellite products
- Masindi Netshilema: Senior Manager: Channel Management – responsible for the community radio stations project to increase reach of SAWS products
- Morne Gijben: Lead Scientist: Remote Sensing – responsible for satellite and radar products
- Stephanie Landman: Lead Scientist: Postprocessing – responsible for operational running of the Unified Model
- Elelwani Phaduli: Scientist: Postprocessing – responsible for model verification
- Gift Rambuwani: Scientist: Model Development – responsible for running of the Unified Model
- Louis van Hemert: Senior Scientist: Postprocessing – responsible for model maintenance
- Musa Mkhwanazi: Senior Scientist: Climate Services – responsible for issuing of ground observations data